Immunogenität von Hautkrebszellen und dem Modellprotein Ovalbumin nach einer Kaltplasma-Behandlung

Inauguraldissertation

zur

Erlangung des akademischen Grades eines

Doktors der Naturwissenschaften (Dr. rer. nat.)

der

Mathematisch-Naturwissenschaftlichen Fakultät

der

Universität Greifswald

vorgelegt von

Ramona Clemen

Greifswald, den 30.11.2021

Dekan: Prof. Dr. Gerald Kerth

1. Gutachter: Prof. Dr. Michael Lalk

2. Gutachterin: Prof. Dr. Barbara Bröker

3. Gutachterin: Prof. Dr. Brigitte Vollmar

4. Gutachter: Prof. Dr. Ingo Stoffels

Tag der Promotion: 31.05.2022

Inhaltsverzeichnis

Zusammenfassung

Eine Behandlung von Tumoren mit physikalischem Kaltplasma zeigt eine erhöhte Toxizität und ein reduziertes Tumorwachstum. Zeitgleich werden während einer Behandlung mit Plasma eine Vielzahl an reaktiven Sauerstoff- und Stickstoffspezies (RONS) generiert, welche Immunzellen stimulieren können. Viele neue Therapieansätze bestreben nicht nur eine Tumortoxizität, sondern auch eine Förderung der körpereigenen, da diese häufig durch Mechanismen der Tumorzellen unterdrückt wird. Zu solchen Therapien zählen *checkpoint inhibitoren*, Vakzinierungen oder ein adaptiver Zelltransfer mit transgenen oder vor-stimulierten Zellen. Die dadurch geförderte Antitumor-Immunantwort basiert grundlegend auf einem mehrphasigen Prozess. Dieser beginnt mit einer Antigen-unspezifischen frühen Phase, in der das innate Immunsystem aktiviert wird und zu einer Vermehrung und Differenzierung von Antigen-spezifischen $CD4^+$ und $CD8^+$ T-Zellen führt. Da während einer Entzündungsreaktion viele RONS gebildet werden, um Fremdkörper zu eliminieren und Immunzellen zu rekrutieren, ist eine Therapie mit RONS naheliegend. Durch die Anwendung von Kaltplasma können die gebildeten RONS zum Entzündungsgeschehen beitragen und Zellen des innaten und adaptiven Immunsystems stimulieren. Eine veränderte Immunogenität von Tumorzellen sowie eine daraus resultierende direkte Aktivierung von Immunzellen im Kontext einer Antitumor-Immunantwort wurden nach einer Behandlung mit Jet-Plasmen bislang nicht untersucht.

In der vorliegenden Arbeit wurde die Kaltplasma-Behandlung von Hautkrebszellen und eines Modellantigens unter Berücksichtigung einer Antitumor-Immunantwort durch natürliche Killerzellen des innaten Immunsystems sowie adaptive Immunzellen *in vitro* und *in vivo* untersucht. Es konnte gezeigt werden, dass eine Behandlung mit Kaltplasma zu einer erhöhten Tumortoxizität führt und das Repertoire der Oberflächenmoleküle auf Tumorzellen verändert. *In vivo* wurde eine vermehrte Infiltration von Immunzellen in das Tumormikromilieu beobachtet, welche mit einer erhöhten Aktivierung von Lymphozyten und Konzentrationen immunstimulatorischer Zytokine einherging. Durch die zeitgleich reduzierten Tumorgrößen, ist eine durch Immunzellen vermittelte Tumortoxizität als Erklärung naheliegend. In zwei Vakzinierungsstudien konnte die Immunogenität von Plasma-behandelter Tumorzellen und einem Tumorassoziierten Modellantigen bestätigt werden.

Glossar

Alle für diese Doktorarbeit relevanten Termini sind wie folgt definiert:

A375	A375 ist eine humane Zelllinie des malignen Melanoms.
A431	A431 ist eine humane Zelllinie des Plattenepithelkarzinoms.
B16F10	B16F10 ist eine murine Zelllinie des stark metastasierenden Melanoms.
B16F10-Ova	B16F10-Ova ist eine murine, transgene Zelllinie des stark metastasierenden Melanoms, welches Ovalbumin exprimiert.
Adaptive Immunantwort	Während der adaptiven Immunantwort erkennen Antigen-spezifische T-Zellen ihr entsprechendes Antigen auf der Zelloberfläche und können weitere Immunzellen rekrutieren und Tumorzellen eliminieren.
Adjuvans	Adjuvanzien sind nicht-biologische Hilfsstoffe (z.B. Lösungen mit Aluminiumverbindungen, Emulsionen) um die Wirkung einer Substanz zu verstärken und/oder eine Immunantwort zu unterstützen.
Antigen	Ein Antigen ist eine Substanz (z.B. Protein oder Peptid), welches extrazellulär vorliegt oder auf der Zelloberfläche (auch Epitop genannt) präsentiert wird.
Antigenität	Die Antigenität beschreibt die Fähigkeit einer Substanz mit einem Antikörper oder durch die Bindung an MHC mit einem T-Zell-Rezeptor zu interagieren.
Antigen-präsentierende Zelle	Antigen-präsentierende Zellen nehmen extrazelluläre Antigene auf, spalten sie enzymatisch zu kleineren Peptiden und präsentieren sie an der Zelloberfläche.
$CD4^+$ T-Zellen	$CD4^+$ T-Helferzellen interagieren über spezifischer Rezeptoren (TCR) mit Antigenen, welche auf Antigen-präsentierenden Zellen präsentiert werden, um weitere Immunzellen zu rekrutieren.
$CD8^+$ T-Zellen	$CD8^+$ T-Zellen erkennen mit Hilfe ihres TCR Antigene auf der Zelloberfläche und können zytotoxische Moleküle sezernieren, um körperfremde Zellen wie z.B. Tumorzellen zu eliminieren.

Gedächtniszellen (*memory cells*)	Gedächtniszellen besitzen spezifische Rezeptoren die gegen ein Antigen gerichtet sind und können bei einer wiederholten Infektion sofort eine Immunantwort auslösen.
HaCat	HaCat sind humane, nicht-maligne Zelllinie (immortale Kerationzyten).
Immunogenität	Die Immunogenität beschreibt die Fähigkeit einer Zelle oder eines Proteins eine Immunzellantwort zu induzieren.
MHC-Komplex	Die an den *major histocompatibility complex* (MHC) gebundenen Antigene (pMHC), auch Epitop genannt, ermöglichen eine Interaktion mit TCR tragenden T-Zellen.
Natürliche Killerzellen (NK-Zellen)	NK-Zellen sind Teil des angeborenen Immunsystems (*innat*), können Tumorzellen eliminieren und weitere Immunzellen rekrutieren.
OT-II	Transgener Mausstamm, dessen Mäuse $CD4^+$ T-Zellen mit einem spezifischen TCR für Ovalbumin besitzen und durch die Interaktion mit $Ova_{323-339}$ Epitope beladenen MHC-II aktiviert werden.
Plasma	Als (physikalisches) „Plasma“ wird ein energetisches, ionisiertes Gas bezeichnet, das unter anderem durch eine hohe Produktion reaktiver Spezies gekennzeichnet ist. Im Kontext dieser Arbeit werden primär molekulare Plasmen einer Ionentemperatur nahe oder bei Raumtemperatur (physikalische Kaltplasmen) behandelt.
RONS	Reaktive Sauerstoff- (ROS) und Stickstoffspezies (RNS) umfassen eine Vielzahl kurz- und langlebiger Moleküle wie Wasserstoffperoxid (H_2O_2), Hydroxyl-Radikal (HO•), Superoxid Anion (O_2^-•), Hypochlorid (OCl^-), Peroxynitrit ($ONOO^-$), und Stickstoffmonoxid (NO). RNS enthalten reaktiven Sauerstoff und werden daher in aufgeführten Publikationen unter dem Begriff ROS subsumiert.
Tumorantigen	Tumorantigene sind spezifische oder assoziierte Antigene und dienen als Zielstruktur zur Unterscheidung von Krebszellen und normalen Zellen.

1. Einleitung

1.1. Hautkrebs und Therapieoptionen

Nach dem Basalkarzinom ist das Plattenepithelkarzinom (Spinaliom) der zweithäufigste bösartige Hauttumor, da Metastasen zu einer hohen Mortalitätsrate führen [1]. Das Spinaliom entwickelt sich häufig aus der Krebsvorstufe der aktinischen Keratose und entsteht vorrangig in Hautarealen mit starker UV-Exposition wie dem Gesicht, den Händen, Schultern, Armen sowie im Übergangsbereich von der Haut zur Schleimhaut. Weitere prädisponierende Faktoren sind Gifte wie Teer, Arsen, Ruß und chronischer Alkohol- oder Tabakkonsum. Neben dem Plattenepithelkarzinom ist ein weiterer bösartiger Hauttumor das maligne Melanom, welches von Melanozyten ausgeht. Dieser bereits frühzeitig metastasierende Tumor betrifft vor allem hellhäutige Menschen und korreliert mit schweren Sonnenbränden vor dem 20. Lebensjahr, sowie mit angeborenen oder erworbenen Dysplasien der Haut (Nävi). Melanome entstehen zu 30% aus Nävuszellnävi, die restlichen aus normaler Haut.

Während das Plattenepithelkarzinom nur selten Fernmetastasen bildet, ist das Metastasierungsrisiko beim malignen Melanom sehr hoch. Dennoch ist eine hohe Überlebensrate von etwa 80% beim Melanom vor allem durch die medizinische Früherkennung und weniger durch erfolgreiche Therapieoptionen begründet. Bei fortgeschrittenem Krankheitsverlauf zeigen nur wenige Therapien Erfolg (non-responder) [2]. Zudem sind die häufig lokal angewandten Therapien, wie Exzision, bei Metastasen wirkungslos. In diesen Fällen ist eine Kombinationstherapie erforderlich, z.B. durch die zusätzliche Behandlung mit systemisch-wirkenden Agenzien. Therapieoptionen neben der operativen Resektion sind beim fortgeschrittenen Plattenepithelkarzinom und malignen Melanom die Chemotherapie und Bestrahlung. Sie haben jedoch starke Nebenwirkungen und verbessern die Prognose nur marginal [3, 4]. Bei dem malignen Melanom werden aufgrund einer häufig auftretenden Mutation und Fehlfunktion der Serin–Threonin-Proteinkinase Therapien mit Proteinkinaseinhibitoren angewendet. Diese Therapien zeigen jedoch nur eine bedingte Tumorremission, gehen häufig mit Nebenwirkungen einher und haben meist keinen Effekt auf Metastasen [5, 6]. Eine weitere Therapieoption ist die Gabe von körpereigenen

Botenstoffen, wie z.B. mit Interferon Alpha. Die Behandlung zeigte in geringer Konzentration keinerlei Effekte auf Tumorzellen [7] und eine Gabe mit erhöhter Konzentration Tumortoxisch wirkte, führte diese Therapie zu einem vermehrten Auftreten von Autoimmunerkrankungen [8-10].

Ein vielversprechender Therapieansatz ist die Stimulation der körpereigenen Immunantwort. Bereits 1950 beschrieb Frank Macfarlane Burnet die Idee der immunologischen Tumorüberwachung (*tumor surveillance*), bei der Immunzellen den Organismus überwachen, um entartete Zellen zu töten oder ihr Wachstum zu begrenzen. Zu den immunologisch wirkenden Therapieoptionen gehören z.B. monoklonale Antikörper, die an Oberflächenmoleküle auf Immunzellen oder Tumorzellen binden. Tumorzellen haben verschiedene Mechanismen entwickelt um sich der Erkennung von Immunzellen zu entziehen. Zu diesen Mechanismen zählt die Veränderung der Oberflächenmarker und die immunsuppressive Eigenschaft des Tumormikromilieus. Das Versagen des Immunsystems bösartige Zellen zu erkennen und zu eliminieren, spielt eine wichtige Rolle bei der Pathogenese von Krebs. Daher ist das Ziel einer Immuntherapie die Intensivierung der Immunzellaktivität des Wirts, um eine erfolgreiche Antitumor-Wirkung zu erzielen. 2018 wurde der Medizin-Nobelpreis für die Forschung an Checkpoint-Inhibitoren an James P. Allison (USA) und Tasuku Honjo (Japan) verliehen. Diese Inhibitoren binden Rezeptoren an der Zelloberfläche von Immunzellen (z.B. PD-1 und CTLA 4) oder Liganden von Tumorzellen (z.B. PD-L1) um die Toleranz von anergischen, supprimierten Lymphozyten zu durchbrechen. Durch die Blockade der inhibitorisch-wirkenden Moleküle wird eine Rezeptor-Ligand Interaktion verhindert. Nachfolgend wird die Aktivität von Lymphozyten gefördert, wodurch zytotoxisch wirkende Moleküle sekretiert werden, um Tumorzellen zu töten. Trotz des vielversprechendes Ansatzes gibt es *non-responder*, da nicht alle Tumorzellen die entsprechenden Liganden auf der Zelloberfläche präsentieren [11, 12].

Neben den Checkpoint-inhibitoren ist die therapeutische Vakzinierung eine weitere immunologische Behandlungsoption. Als Vakzin werden Tumor-spezifische Moleküle, Antigene, oder Antigen-codierende Gensequenzen (mRNA) verabreicht, damit Antigen-spezifische T-Zellen ausdifferenzieren und den Tumor spezifisch bekämpfen. Antigene sind Aminosäuresequenzen aus intrazellulär abgebauten Proteinen, welche für T-Zellen auf der Zelloberfläche präsentiert werden. In Tumorzellen

können aufgrund von Mutationen und Fehlfunktionen tumorspezifische Antigene (TA) entstehen, die sich gänzlich von Antigenen auf gesunden Zellen unterscheiden [13]. Im Melanom wurden bereits in den 1990er Jahren verschiedene TA identifiziert (z.B. MAGE, TRP2, PMEL, MART), welche adaptive, Antigen-spezifische T-Zellen stimulieren [14, 15]. Tumorspezifische Proteine können aufgrund verschiedener fehlregulierter Prozesse entstehen, die eine Tumorzelle von einer gesunden Zelle unterscheidet, und eine Gruppierung ermöglicht. Dazu zählen TA z.B. aus unnatürlich stark exprimierten Proteinen, oder jene die einem bestimmten Expressionmuster eines anderen Zelltyps zugeordnet sind (Differenzierungsantigen). Außerdem kann eine onkogene Virusinfektion (Onkovirale Antigene), Mutationenen (Neoantigene), oder epigenetische Dysregulation (Keimbahnantigene) spezifische Proteine hervorrufen. Durch ihre hohe Spezifität gilt die Vakzinierung mit TA als personalisierte Therapieoption und einige Studien belegen bereits die erfolgreiche Anwendung [16-18]. Ähnlich zu der therapeutischen Immunisierung, kann eine präventive Vakzinierung ebenfalls eine adaptive Immunantwort initialisieren. Solche Immunisierungen werden durch die Vakzinierung von Antigenen induziert und z.B. bei Virus-assoziierten Tumoren, zur Prävention des Gebärmutterhalskrebses, bereits angewendet.

Einen immunologischen Effekt zur Stärkung der eigenen Immunantwort zeigt auch die photodynamische Therapie (PDT) [19, 20]. Durch die Gabe von Photosensibilisatoren, welche bei einer Wellenlänge zwischen 630 und 635nm lokal angeregt werden, wird oxidativer Stress in Tumorzellen hervorgerufen und eine Entzündungsreaktion ausgelöst. Mechanistisch erfolgt dies über die Generierung von reaktiven Spezies durch den im Gewebe angereicherten Sauerstoff. Daher ist eine sauerstoffreiche Tumorumgebung erforderlich, was jedoch durch das überwiegend hypoxisch vorliegende Tumormikromilieu häufig nicht gegeben ist [21, 22]. In einem optimierten System oder mit Hilfe einer kombinatorischen Therapie könnte ein erhöhter Sauerstoffgehalt erzielt werden, wodurch die PDT in Tumorzellen zu einem durch oxidativen Stress vermittelten Zelltod führt. Da während des Zelluntergangs der Tumorzelle immunzellstimulierende Moleküle sekretiert und an der Zelloberfläche präsentiert werden, fördert PDT eine Immunantwort. Ähnlich zur PDT, induziert die Behandlung mit physikalischem Kaltplasma einen oxidativen Stress in Tumorzellen. Dies geschieht durch die Bildung von kurzlebigen und langlebigen reaktiven Sauerstoff- und

Stickstoffspezies (RONS). Für den klinischen Einsatz sind seit 2013 vier Geräte zertifiziert: kINPen MED (Neoplas Tools GmbH, Deutschland), SteriPlas (ADTEC, UK), PlasmaDerm (CINOGY GmbH, Deutschland) und Plasma Care (terraplasma medical GmbH, Deutschland) [23]. Eine lokale Anwendung von Kaltplasma zeigt *in vitro* und *in vivo* eine erhöhte Tumortoxizität und ein reduziertes Tumorwachstum des malignen Melanoms [24-26] und des Plattenepithelkarzinoms [27, 28]. Zudem wurde in einer erst kürzlich veröffentlichten Studie eine systemische Tumorreduktion nach einer lokalen Tumor-Behandlung mit Kaltplasma, eine sogenannte abskopale Wirkung, gezeigt [29, 30]. Eine hierfür erforderliche Aktivität von Immunzellen verdeutlicht die verschiedenen Wirkparameter des Multi-Komponenten Systems. Nachdem das Plasma auf das Gewebe trifft, sorgen kurzlebige Spezies für primär biochemische Prozesse, wie zum Beispiel Veränderungen an Biomolekülen und Modifikationen an Strukturen. Nachfolgend sorgen körpereigene Signale der regulären Zellbiologie für sekundäre biologische Prozesse. Dazu zählen abhängig vom Zelltyp u.a. Redox-Stress, Zelltod, Aktivierung, Veränderung von Oberflächenmarkern und Ausschüttung von Chemokinen und Zytokinen [31-35]. Diese wiederum führen zu einer Veränderung der Interaktion zwischen Tumorzelle und Immunzelle, sowie einer Veränderung des Tumormikromilieus, welches die körpereigene Immunabwehr fördert.

1.2. Kaltplasma generierte RONS als Therapie

Als „Plasma“ wird ein energetisch angereichertes quasi-neutrales Gas bezeichnet. Durch die zugeführte Energie werden Elektronen aus der Elektronenhülle von Atomen oder Molekülen entfernt, sodass ein Gebilde (altgriechisch πλάσμα plásma) aus leichten Molekülen, Atomen, Radikalen, Ionen und ungebundenen Elektronen entsteht. Plasma wird auch als vierter Aggregatzustand beschrieben, wenn nach dem Übergang von flüssig zu fest, zu gasförmig weitere Energie zugegeben wird (Abb.1A).

Beispiele für verschiedene Arten von Plasma sind im Zusammenhang mit astrophysikalischen und atmosphärischen Erscheinungen (Sterne, Blitze, Polarlichtern) oder auch mit industriellen Prozessen (Plasmaschweißen) zu finden. Solche Plasmen sind durch ein thermisches Gleichgewicht mit hoher Wärmeerzeugung charakterisiert, sodass Elektronen und Ionen dieselbe Temperatur aufweisen. Für die Ionisierung eines Gases ist es möglich, Plasmen im Bereich der Raumtemperatur zu erzeugen. Dazu erfolgt

beispielsweise eine Stoßionisation durch eine Elektronenbeschleunigung in einem elektrischen Feld [36]. Bei nieder-energetischen „nicht-thermischen Plasmen“, auch Kaltplasmen genannt, besitzen Elektronen eine viel höhere Temperatur als die Ionen. Zudem liegt die Ionen- bzw. Neutralteilchentemperatur nahe oder bei Raumtemperatur (Abb. 1B). Daher ermöglicht die Nutzung von Kaltplasma eine Behandlung von temperaturempfindlichen Oberflächen und findet, neben anderen Anwendungsbereichen, Verwendung als medizinische Technologie [37]. Im medizinischen Bereich ist besonders die Eigenschaft der RONS-Produktion hervorzuheben, welche in der Gasphase sowie durch die Interaktion mit Oberflächen und Flüssigkeiten entstehen [38-42] (Abb. 1C). „RONS“ bezeichnet eine heterogene Gruppe von Molekülen und Verbindungen wie z.B. Wasserstoffperoxid (H_2O_2), das Hydroxyl-Radikal (OH•), das Superoxid Anion (O_2^-•) und Hypochlorid (OCl^-). Da die meisten reaktiven Stickstoffspezies ebenfalls reaktiven Sauerstoff enthalten, werden diese in den aufgeführten Publikationen unter dem Begriff ROS subsumiert (Siehe Kapitel 6).

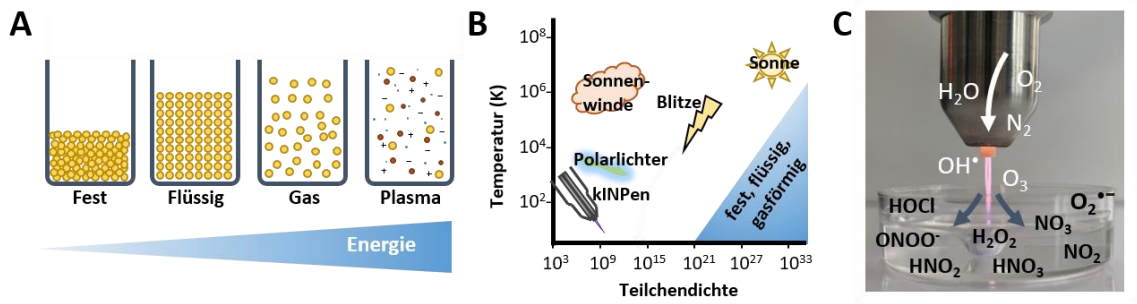

Abbildung 1: Kaltplasma generiert reaktive Sauerstoff- und Stickstoffspezies. (**A**) Durch die sukzessive Energiezufuhr kann ein Aggregatzustand von fest, zu flüssig, zu gasförmig, zu Plasma wechseln. (**B**) Verhältnis zwischen Neutralteilchentemperatur und Teilchendichte mit Beispielen von natürlich auftretenden Plasmen und dem Kaltplasmajet (kINPen). (**C**) Das im kINPen gezündete Plasma trifft als Effluent auf eine Flüssigkeit. Neben geladenen Teilchen werden reaktive Spezies gebildet, welche mit Oberflächen und Flüssigkeiten reagieren.

Die Zusammensetzung der entstehenden RONS in der Gas- und Flüssigphase kann durch eine Modulation der Plasmaerzeugung beeinflusst werden [43]. Zu den Simulationsparametern gehören beispielsweise das elektrische Feld und dessen Frequenz sowie Amplitude. Zudem kann die Verwendung verschiedener Einzelgase, Gasgemische, sowie Änderungen der Distanz, Durchflussrate und Behandlungsdauer zu

qualitativen und quantitativen Veränderungen der RONS-Zusammensetzung führen. Dieses variable Multi-Komponenten-System macht die Verwendung von Kaltplasma in der Medizin einzigartig und schafft Synergien zu biologischen Abläufen wie nachfolgend erläutert.

In biologischen Systemen sind exogene und endogene reaktive Spezies von großer Relevanz, da sie molekulare Prozesse regulieren und abhängig vom ihrer Konzentration zu Eustress oder Distress führen [44]. Geringere Konzentrationen fördern verschiedene zelluläre Abläufe, wie Proliferation, Migration oder Angiogenese. Eine erhöhte RONS Konzentration hingegen löst eine zunächst harmlose Stressantwort aus, die mit zunehmender Konzentration oxidativen Stress auslöst. Letzteres ist durch Zellschädigung und Zelltod gekennzeichnet. Mit Hilfe von extrazellulären RONS, z.B. durch eine Behandlung mit Kaltplasma, kann das natürliche Gleichgewicht verändert werden, wodurch unterschiedliche Wirkungen erzielt werden [45]. Abhängig von der generierten RONS Konzentration kann Kaltplasma eine Gewebestimulierende Wirkung in der Wundheilung oder eine toxische Wirkung bei der Behandlung von Krebs erzielen [46, 47].

In chronischen Wunden mit Läsionen bleibt eine Wundheilung häufig aus. Obwohl die zellulären und molekularen Mechanismen einer ausbleibenden Gewebereparatur und Heilung noch wenig verstanden sind, liegen schlecht regulierte Reparaturmechanismen, Entzündung, Angiogenese, Matrixablagerung und Zellrekrutierung, sowie mikrobielle Kontaminationen der Pathologie zugrunde [48]. Ein wichtiger sekundärer Botenstoff während der Wundheilung ist Sauerstoff [49]. Sauerstoff dient als Substrat für die Adenosintriphosphat Produktion, welches während der Gewebeerneuerung als Energiequelle benötigt wird. Die durch Kaltplasma generierten RONS dienen als Radikalderivat für Sauerstoff, um die Wundheilungsprozesse zu fördern. Außerdem hat Plasma eine toxische Wirkung auf Bakterien, welche chronische Wunden häufig besiedeln. Diese Effekte wurden in zahlreichen Studien der Vergangenheit untersucht und kürzlich von Bekeschus et al. Zusammengefasst [50]. Neben der desinfizierenden Wirkung zeigte eine Behandlung mit Kaltplasma positive Effekte auf die Wundheilung und auf Läsionen [51-55]. Eine Plasmaexposition führt zu einer Zellvermehrung in Keratinozyten und Fibroblasten [56, 57] und fördert die Migration und Ausbreitung von Hautzellen durch die Veränderung

der Integrin-abhängigen Zell-Adhäsion [58]. Generell beschleunigt Kaltplasma den Wundverschluss [59], wirkt antimikrobiell [60] und fördert Entzündungen sowie die Rekrutierung von Immunzellen [61].

Während der Behandlung von chronischen Wunden spielt der Aspekt der bakteriellen Kontamination eine wichtige Rolle, da sie eine Entzündungseaktion und Immunantwort erschwert. Besonders bei Entzündungsreaktionen ist die natürliche Bildung von RONS ein wesentlicher Bestandteil [62, 63], da sie für den Redox-basierten Energie- und Signaltransport wichtig sind [64, 65]. Während dieser Immunreaktion sind einige Immunzellen wie Neutrophile Granulozyten und Makrophagen in der Lage, durch enzymatisch katalysierte Prozesse reaktive Spezies zu bilden [66]. Diese RONS lösen nicht nur in Bakterien, sondern auch in infizierten und atypischen Körperzellen einen oxidativen Stress aus, wodurch spezielle Moleküle auf der Zelloberfläche präsentiert werden. Immunzellen erkennen die präsentierten Moleküle als *Damage associated pattern* (DAMP), werden aktiviert und tragen zur Rekrutierung weiterer Immunzellen bei [67, 68], um eine adaptive Immunantwort zu induzieren. Da DAMPs auf Immunzellen stimulierend wirken, wird dieser Zelluntergang auch als immunogener Zelltod (*immunogenic cell death*, ICD) bezeichnet [69]. Die durch Neutrophile Granulozyten und Makrophagen sezernierten RONS können nicht nur oxidativen Stress in Tumorzellen auslösen, sondern dienen auch als Signalmoleküle zur Rekrutierung weiterer Immunzellen. Die Behandlung mit Kaltplasma kann eine Entzündungsreaktion fördern, die natürliche Produktion von RONS unterstützen und eine Immunreaktion durch Redox-Stress stimulieren. Letzteres konnte nicht nur während der Wundbehandlung gezeigt werden, sondern wird auch bei der Behandlung von Tumoren vermutet. In vitro Studien bestätigen, dass eine Behandlung mit Kaltplasma zu der Präsentation verschiedener DAMPs an der Zelloberfläche führt [70, 71]. Daher ist ein durch Kaltplasma induzierter ICD und nachfolgend vermittelte Immunantwort naheliegend.

1.3. Die innate und adaptive Antitumor Immunantwort

Um den Körper vor Pathogenen und anderen körperfremden Strukturen zu schützen, besitzen höhere Lebewesen neben dem innaten (angeborenen) ein adaptives (erworbenes) Immunsystem. Zu dem angeborenen Immunsystem gehören natürliche Barrieren (Haut- und Schleimhäute), welche das Eindringen von Pathogenen

erschweren, sowie Zellen zur „Frontlinien“-Verteidigung, um Fremdstoffe und Pathogene zu beseitigen und ihre Ausbreitung zu verhindern. Diese schnelle, jedoch unspezifische Reaktion geht mit einer Entzündungsreaktion einher und induziert durch die Rekrutierung von weiteren Immunzellen eine adaptive Immunantwort [72, 73].

Eine Entzündungsreaktion ist die erste Reaktion für die Induktion einer Immunantwort. Sie ist in erster Hinsicht durch die Entstehung von Wärme, Schmerz, Rötung, Schwellung und funktionelle Beeinträchtigung charakterisiert. Während des Entzündungsgeschehens infiltrieren unter anderem natürliche Killerzellen (NK-Zellen), Monozyten, Granulozyten, Mastzellen, Makrophagen und dendritische Zellen (DCs) das geschädigte Gewebe. NK-Zellen attackieren und töten geschädigte, infizierte Zellen, aber auch Tumorzellen, indem sie ein bestimmtes Expressionsmuster von Oberflächenmolekülen erkennen [74]. Zu diesen Expressionsmustern zählt z.B. eine verstärkte Expression von inhibitorischen Markern, oder eine reduzierte Präsentation von stimulierenden Rezeptoren [75, 76]. Außerdem erkennen sie Zellen, denen diese Moleküle gänzlich fehlen. Nachdem eine Tumorzelle getötet wurde, nehmen Makrophagen, Granulozyten und DCs die verbliebenen Proteine über verschiedene Mechanismen auf. Während der Phagozytose werden Proteine in einem Phagosom aufgenommen, welches mit dem Lysosom zum Phagolysosom verschmilzt. Die aufgenommenen Proteine werden enzymatisch verdaut, sodass Peptide entstehen, welche im endoplasmatischen Retikulum an ungebundenen *Major histocompatibility complex* (MHC)-Moleküle der Klasse I (*cross-presentation*) oder der Klasse II gebunden werden. Die mit Peptid beladenen MHC-Moleküle (pMHC) werden in Vesikeln zur Zellmembran transportiert, um von dort die Antigene mittels MHC-I für $CD8^+$ T-Zellen oder mittels MHC-II für $CD4^+$ T-Zellen zu präsentieren. Neben der phagolysosomalen Aufnahme ins Zellinnere, können extrazelluläre Proteine auch mittels Pinozytose oder Makropinozytose aufgenommen, im Makropinosom verdaut und an der Zelloberfläche präsentiert werden. Nach der MHC-Beladung migrieren die professionellen Antigen-präsentierenden Zellen (APC) zum lymphatischen Gewebe, um eine T-Zell Aktivierung zu ermöglichen. APCs sind durch die Präsentation von Antigenen wichtig für die Induktion der adaptiven Immunantwort. Antigene entstehen jedoch nicht nur aus verdauten, extrazellulären Proteinen, sondern auch durch den Abbau von intrazellulären Proteinen im Proteasom und werden ebenfalls mittels MHC-I präsentiert. Im Vergleich

zu den extrazellulär aufgenommenen Proteinen, handelt es sich hierbei um Peptide von „körpereigenen“ Proteinen und werden auf allen kernhaltigen Zellen mittels MHC-I präsentiert. Da auch Tumorzellen Antigene präsentieren, ist es die Aufgabe von Antigen-spezifischen Lymphozyten die präsentierten Antigene zu erkennen, zu unterscheiden und zu reagieren.

Die adaptive Immunantwort wird durch Antigen-spezifische Lymphozyten vermittelt, welche einen spezifischen T-Zell-Rezeptor (TCR) bzw. B-Zell-Rezeptor (BCR) besitzen. Man unterscheidet auch zwischen der humoralen Immunantwort, welche sich durch Antikörper sezernierende Plasmazellen auszeichnet (in den hier vorliegenden Arbeiten nicht weiter untersucht) und der zellulären Immunantwort, welche durch direkten Zell-Zellkontakt ausgelöst wird. Zu den Antigen-spezifischen T-Zellen gehören $CD8^+$ T-Zellen, welche auch als Effektor-Zellen oder zytotoxischen T-Zellen (CTL) bezeichnet werden, sowie die $CD4^+$ Helferzellen. Diese T-Zellen reifen im Thymus heran (priming) und werden dort selektiert um einen Angriff auf körpereigene Strukturen zu vermeiden [77]. Dann migrieren sie zu lymphatischen Geweben und patrouillieren, bis sie auf eine Zelle treffen, die ein Antigen präsentiert. Naive $CD4^+$ T-Zellen werden in peripheren Lymphorganen durch eine Interaktion zwischen TCR und pMHC-II auf APCs aktiviert, woraufhin sie proliferieren und zu Subpopulationen differenzieren. Eine Aktivierung von zytotoxischen T-Zellen erfolgt durch eine $CD4^+$ vermittelte Rekrutierung, eine Interaktion mit APCs, oder eigenständig durch die Interaktion zwischen TCR und MHC-I auf Tumorzellen. Sobald eine Antigen-spezifische $CD8^+$ T-Zelle ein TA auf der Zelloberfläche erkennt, wird sie aktiviert, um die transformierte Zelle mittels zytotoxischer Enzyme (z.B. Granzym B) zu töten. Im Vergleich zu $CD8^+$ T-Zellen differenzieren $CD4^+$ Helferzellen nach ihrer Aktivierung zu verschiedenen Subtypen, um unter anderem eine zelluläre ($CD8^+$ Rekrutierung) oder humorale (B-Zell Rekrutierung) Immunantwort hervorzurufen. Abhängig von ihrem Subtyp haben verschiedene Aufgaben; sie können zu einer Aktivierung (als T_H1 oder T_H17 Zelle) oder Hemmung (regulatorische T-Zellen, T_{reg}) der zellulären Immunantwort beitragen.

Sobald eine Immunreaktion eingeleitet wird, können Antigen-spezifische T-Zellen differenzieren und die Tumorzelle spezifisch töten. Dieses Zusammenspiel der innaten und adaptiven Immunzellen im Kontext der Immunabwehr gegen Tumorzellen wird auch als Tumorimmunitätszyklus bezeichnet [78] (Abb. 2).

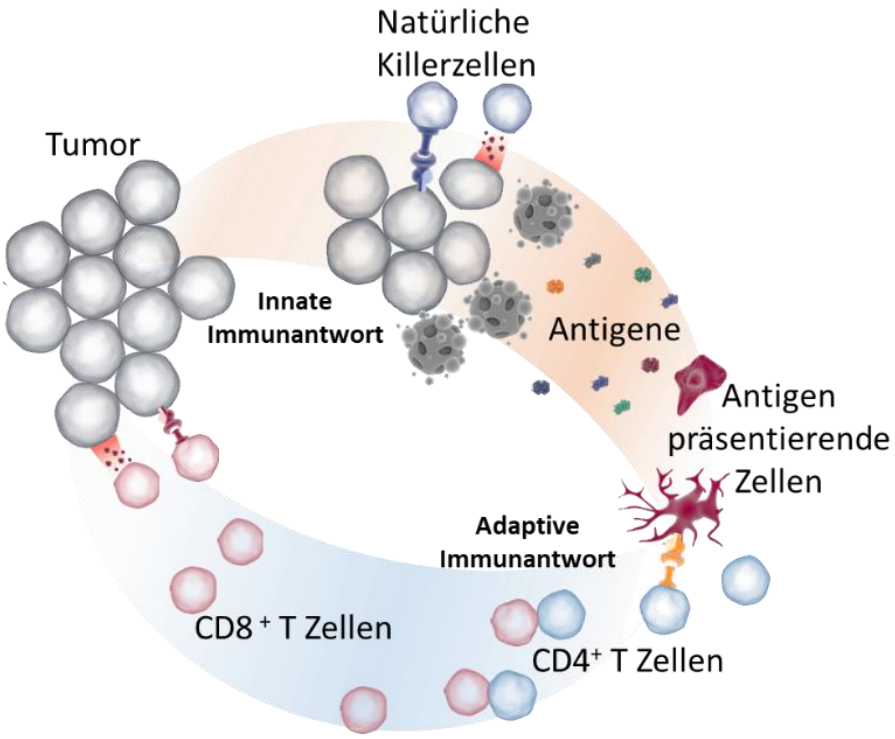

Abbildung 2: Tumorimmunitätszyklus. Die Antitumor-Immunantwort wird durch innate Zellen eingeleitet, um adaptive Immunzellen zu rekrutieren und Tumorzellen zu eliminieren. Natürliche Killerzellen erkennen atypische Zellen mittels einer Rezeptor-Ligand Interaktion und töten solche Tumorzellen. Die durch den Zelltod sekretierten Proteine werden durch dendritische Zellen aufgenommen, degradiert und als Peptide an der Zelloberfläche präsentiert. Eine solche Antigen-präsentierende Zelle interagiert mit $CD8^+$ oder $CD4^+$-Zellen, um eine Antigen-spezifische $CD8^+$ T-Zellantwort einzuleiten. Diese infiltrieren das Tumormikromilieu, interagieren mit Tumorzellen und sezernieren zytotoxische Enzyme.

1.4. Kaltplasma zur Unterstützung der Antitumor-Immunantwort

Vereinzelt vorliegende entartete Zellen können durch Immunzellen meist erfolgreich identifiziert und eliminiert werden, sodass ein Tumor bei immunkompetenten Menschen seltener wächst, als bei immunsupprimierten Patienten. Dennoch entwickeln Tumorzellen aufgrund ihrer hohen Mutationsrate und einer Selektivität unterschiedliche Mechanismen, um einer Immunantwort zu entkommen (*Immune escape*). Zu diesen Mechanismen gehören die Präsentation von Rezeptoren und die Sekretion von Molekülen mit immunsuppressiven Funktionen, sowie eine reduzierte Expression von MHC-I [79, 80]. Durch ihre reduzierte Antigenität und/oder Immunogenität haben sie einen Wachstumsvorteil, da sie der zytotoxischen T-Zell Antwort entgehen. Sobald sich ein Tumorgewebe bildet, schaffen einige Tumore eine Mikroumgebung, die die Produktivität einer Antitumor-Immunantwort zusätzlich beeinflusst.

Der hypothetische Effekt von Kaltplasma auf die Immunogenität von Tumorzellen und auf Immunzellen im Tumormikromilieu wurde bereits in einigen Übersichtsarbeiten zusammengefasst [81-83], jedoch nur geringfügig wissenschaftlich belegt. Eine Behandlung mit Kaltplasma zeigte, ähnlich zu einer PDT-Behandlung [84], in verschiedenen Krebszelllinien eine Erhöhung von ICD-Markern und MHC-I [85-87], sowie einer Reduktion von PDL-1 [88]. Neben Veränderungen des Rezeptorrepertoires, induziert Kaltplasma auch Redox-Stress welcher zum Zelltod führt [89, 90].

Der Effekt von innaten Immunzellen auf Plasma-behandelte Zellen wurde hauptsächlich *in vitro* mit ko-kultivierten DCs oder Makrophagen gezeigt. Zum Beispiel sezernieren DCs und Makrophagen vermehrt entzündungsfördernde Zytokine wie IFNγ und TNFα, wenn sie mit behandelten Pankreas Tumorzellen ko-kultiviert werden [91, 92]. Zudem wirkt eine Behandlung mit Plasma durch ein RONS angereichertes Mikromilieu stimulierend auf DCs und Makrophagen [93-96]. Die Anreicherung an extrazellulären RONS kann dazu beitragen, dass die durch ICD freigesetzten Antigene oxidativ modifiziert werden, wodurch ihre Immunogenität erhöht werden kann. RONS-modifizierte Proteine führen in APCs zu einer veränderten Antigen-Prozessierung und zu einer verstärkten Aktivierung von Immunzellen [97-99]. Die daraus resultierenden oxidierten Epitope können eine veränderte Immunogenität aufweisen, wodurch Antigen-spezifische T-Zellen aktiviert oder inhibiert werden. Einige durch RONS induzierte Modifikationen, wie eine Oxidation, können außerdem zu der Entstehung einiger Krankheiten beitragen und wurden kürzlich zusammengefasst [100]. Außerdem können durch oxidativ modifizierte Antigene neue Erkennungssequenzen für T-Zellen entstehen, wodurch eine Erweiterung des T-Zell Pools möglich ist.

Das adaptive Immunsystem beinhaltet einen großen Pool verschiedener Antigen-spezifischer T-Zellen. Dennoch ist die Aktivierung einer einzelnen T-Zelle nicht ausreichend, um eine Immunantwort zu induzieren, sodass eine minimale Anzahl an Zellen vorliegen muss (*Threshold*) [101-103]. Antigen-spezifische T-Zellen erkennen ihr spezifisches Antigen durch die Interaktion zwischen TCR und beladenem MHC-Komplex. Abhängig von der Bindungsstärke wird eine Aktivierung induziert. Die Bindung kann durch Modifikationen, wie z.B. einen Aminosäureaustausch oder posttranslationelle Modifikationen (PTM) auf Aminosäure- oder Strukturebene, am Peptid verhindert oder verändert werden [104, 105]. Durch eine lokale Behandlung von Tumoren mit

Kaltplasma können reaktive Spezies oxidative Modifikationen an Antigenen von Tumorzellen induzieren, um sie als „körperfremd“ zu markieren. Diese können zu einer verstärkten T-Zellantwort führen. Zusätzlich bewirkt das Plasma-behandelte Mikromilieu, ähnlich zu einer RONS-angereicherte inflammatorischen Umgebung, eine Stimulation von APCs. Dies löst eine verbesserte Antigen-Prozessierung und verstärkte T-Zellaktivierung vermuten.

1.5. Ziele der Arbeit

Seit einigen Jahren wird physikalisches Kaltplasma erfolgreich in der Klinik zur Behandlung von Wunden und infektiös-ulzerierenden Tumoren eingesetzt. Aus zahlreichen *in vitro* und *ex vivo* Studien geht hervor, dass die Behandlung nicht nur eine toxische und direkte tumorreduzierende Wirkung hat, sondern auch eine immunologische Komponente besitzt. Trotz jahrelanger anwendungsorientierter Forschung wurden die Funktionen von innaten und adaptiven Immunzellen in einem Kaltplasma-behandelten Tumormikromilieu wenig untersucht. In dieser Doktorarbeit werden in vier wissenschaftlichen Arbeiten die folgenden Ziele verfolgt:

1. Nachweis einer zytotoxischen Aktivität von NK-Zellen auf Plasma-behandelte Tumorzellen, um den Effekt von angeborenen Immunzellen im Tumormikromilieu als erste Immunantwort zu untersuchen (Kapitel 2.1 und 6.1);

2. Analyse einer immunologischen Komponente der Plasma-Behandlung *in vivo* durch eine verstärkte Rekrutierung und Aktivierung von $CD4^+$, $CD8^+$ und APCs im Tumormikromillieu (Kapitel 2.2 und 6.2);

3. *Ex vivo* und *in vivo* Untersuchung der Immunogenität von Plasma-modifizierten Antigenen unter der Verwendung des Ovalbumin-Modellsystems (Kapitel 2.3 und 6.3);

4. Erläuterung der Verwendung von Kaltplasma zur Modifizierung und Optimierung von Tumor-Vakzinen (Kapitel 2.4 und 6.4).

2. Zusammenfassung und Diskussion

2.1. Kaltplasma-behandelte Tumorzellen stimulieren innate Lymphozyten

Hautkrebszellen und andere Tumore sind in der Lage, körpereigene Abwehrmechanismen zu umgehen und eine immunsupprimierende Umgebung zu schaffen. Dadurch können sie, trotz starker phänotypischer Unterschiede zu nicht-malignen Zellen, die Wahrscheinlichkeit reduzieren, von Immunzellen erkannt und eliminiert zu werden. NK-Zellen beispielsweise migrieren als Lymphozyten des angeborenen Immunsystems durch den Körper, um infizierte Zellen, immunglobulin-markierte Zellen oder entartete Zellen zu identifizieren und zu töten [106]. Wenn Tumorzellen die Expression von immunstimulierenden MHC-Klasse-IB-Kettenproteinen (MIC-A/MIC-B) herunterregulieren, oder die Expression von immunsupprimierenden Markern wie MHC-I steigern, reduziert dies die Aktivität von NK-Zellen: *immune escape* [107-109]. Einige Therapeutika und andere äußere Einflüsse sind in der Lage, das Repertoire der Oberflächenmarker von Tumorzellen so zu verändern, dass NK-Zellen wieder aktiviert werden können [110, 111].

Wir konnten zeigen, dass eine Kaltplasma-Behandlung von Plattenepithelkarzinomzellen (A431) und Melanomzellen (A375) zu einem veränderten Oberflächenmarker-Profil führt (Kapitel 6.1, [112]). Wir beobachteten eine erhöhte Expression der aktivierenden Liganden MIC-A und MIC-B, sowie eine reduzierte Expression von inhibierenden HLA-E-Molekülen in behandelten A431- und/oder A375-Tumorzellen, jedoch nicht in nicht-malignen Zellen (HaCaT Keratinozyten). Bereits zuvor wurde eine durch RONS und Redox-Stress erhöhte Expression von MIC-A,B beschrieben [113, 114], welche relevant für die Aktivierung von NK-Zellen ist.

NK-Zellen tragen keimbahnkodierte Rezeptoren mit inhibitorischer und aktivierender Funktion [115]. Dazu zählen: T-Zell-Immunglobulin-Mucin (TIM), C-Typ-Lektin-Familienrezeptor-Heterodimer (CD94/NKG2), natürliche zytotoxische Rezeptoren (NCR) wie NKp44 und Killerzell-Immunoglobulin-ähnliche Rezeptoren (KIR). Identifizieren NK-Zellen mit Hilfe ihrer Rezeptoren eine Zelle als Bedrohung, werden Oberflächenmarker wie z.B. der Fas-Ligand (FASL) und der TNF-abhängige Apoptose-induzierende Ligand (TRAIL) exprimiert, die durch Bindung an Todesrezeptoren den

Zelltod in Tumorzellen einleiten [116]. In der vorliegenden Arbeit konnten wir beobachten, dass entzündungsfördernde Zytokine wie Interferon-gamma (IFN-γ), Interleukin (IL)-6, IL-8 und Tumornekrosefaktor (TNF) sowie der Inhalt der zytotoxischen Granula (Granzym B) unter dem Einfluss von Kaltplasma vermehrt ausgeschüttet werden.

Zudem konnten wir zeigen, dass eine Plasma-Behandlung der Tumorzellen in einer Ko-Kultur von Tumorzellen und NK-Zellen aus peripherem Blut (PBMC) die zytotoxische Wirkung der NK-Zellen steigert. Durch die Präsenz von NK-Zellen wurden die metabolische Aktivität der Tumorzellen herabgesetzt, mehr Zelltod in Tumorzellen gemessen sowie eine erhöhte Sekretion von Granzym B nachgewiesen. Dieser Effekt konnte in beiden Typen von Hautkrebszellen, jedoch nicht in nicht-malignen Keratinozyten beobachtet werden. Dies verdeutlicht, dass Plasma auf maligne Zellen toxisch wirkt, ohne gesunde Zellen zu beeinträchtigen. Eine erhöhte Sekretion der entzündungsfördernden Zytokine IL-6 und IL-8 in einer Ko-Kultur von NK-Zellen mit Plasma-behandelten Tumorzellen lässt eine verstärkte Immunogenität mit der Fähigkeit zur Induktion einer adaptiven Immunantwort vermuten. Zuvor wurde gezeigt, dass erhöhte Konzentrationen von IL-6 und IL-8 mit einer besseren Prognose im Patienten einhergehen [117]. Die Rekrutierung von Immunzellen durch die Sekretion proinflammatorischer Zytokine führt zu einer vermehrten Einwanderung von Immunzellen in das Tumormikromilieu. Neben anderen Immunzellen werden adaptive Immunzellen wie T-Helferzellen und zytotoxische $CD8^+$ T-Zellen stimuliert. Um die Immunogenität von mit Plasma-behandelten Tumorzellen und die Infiltration von Immunzellen zu untersuchen, sind Studien im lebenden Organismus essenziell, da es nicht möglich ist, eine Immunantwort in einer Zellkultur nachzuahmen. Daher haben wir in einer weiteren Arbeit die Immunogenität von Plasma-behandelten Melanomzellen in einem syngenen Tumormodell in der Maus untersucht.

2.2. Kaltplasma erhöht die Immunogenität von Tumoren

Abhängig von der Dichte der infiltrierenden Immunzellen kann ein Tumor als „heiß“ oder „kalt“ eingestuft werden [118, 119]. Ein „heißer“ Tumor ist durch eine erhöhte Dichte von Immunzellen im Tumorgewebe charakterisiert, welche eine Antitumor-Immunantwort auslösen können. Zu diesen Immunzellen zählen neben

Zytokin-ausschüttenden innaten Immunzellen auch aktivierte CTLs. Insbesondere Typ I-Interferon (IFN-I) sezernierende Zellen sind zur Rekrutierung von T-Zellen wichtig und tragen zu einem immunogenen Mikromilieu bei. Bei „kalten Tumoren“ fehlen die Infiltration von Immunzellen, Zytokinsekretion und T-Zellrekrutierung. Diese werden vom Immunsystem aufgrund ihrer geringen Immunogenität ignoriert und sprechen nur wenig auf Immuntherapien an. Einige Therapien zielen darauf, die Infiltration von Immunzellen zu fördern, um einen „kalten“ Tumor in einen „heißen“ Tumor zu transformieren. Die dafür erforderliche erhöhte Immunogenität wird zum Beispiel durch die Induktion des ICD geschaffen. Der immunogene Zelltod ist durch eine erhöhte Expression, Sekretion oder Translokation von Calreticulin (CRT), Hitzeschock-Proteinen (HSPs), HMGB1, MHC-I und weiteren Molekülen charakterisiert [120-122]. Da bereits gezeigt wurde, dass eine Behandlung mit Kaltplasma ICD auslöst [70, 71, 91], liegt die Vermutung nahe, dass Kaltplasma *in vivo* Entzündungsreaktionen und adaptive Antitumor-Immunantworten induziert.

Wir konnten zeigen, dass eine Kaltplasma-Behandlung des murinen Melanoms (B16F10) *in vivo* zu einer Reduktion der Tumormasse führt, die von einer vermehrten Einwanderung von Immunzellen begleitet ist (Kapitel 6.2, [123]). Die Verwendung verschiedener Gaszumischungen zur Optimierung der Behandlung zeigte in unser Arbeit unterschiedlich starke Effekte, was durch die Produktion unterschiedlicher RONS begründet ist [124, 125]. Eine Behandlung mit Helium-Sauerstoff-Plasma ($pHeO_2$) führte zu einer nahezu vollständigen Tumorreduktion, während Argon-Sauerstoff-Plasma ($pArO_2$), Helium-Plasma (pHe) und Argon-Plasma (pAr) geringere Effekte zeigten. Interessanterweise wird der klinisch zugelassene kINPen MED mit pAr verwendet, obwohl in der vorliegenden Arbeit eine stärkere Regression mit $pHeO_2$ beobachtet wurde. Dies sollte in zukünftigen Studien weiter evaluiert werden. Der Fokus in der vorliegenden Arbeit lag neben der Optimierung einer Behandlung außerdem auf dem immunologischen Effekt einer Plasma-Behandlung. Daher wurden die Tumore isoliert und die Infiltration von Immunzellen untersucht. In $pHeO_2$ und pAr behandelten Tumoren konnte, neben der Reduktion der Tumormasse, mehr infiltrierende $CD8^+$ und $CD4^+$ T-Zellen, Makrophagen und DCs beobachtet werden. Eine Behandlung mit der Positivkontrolle Imiquimod (immunstimulatorischer Agonist für den Toll-like-Rezeptor 7 und 8 [126, 127]), war im Vergleich weniger wirksam. Das Stroma enthielt weniger

tumorinfiltrierende $CD4^+$ T-Zellen. Zudem konnten wir im Vergleich zu mit Plasma behandelten Tumoren nach Imiquimod-Applikation weniger Makrophagen und DCs im Gewebe messen, obwohl die Behandlung zu einer Reduktion der Tumormasse führte. Imiquimod wird durch seinen immunstimulatorische Effekt vorwiegend als adjuvante Tumortherapie in Kombination mit anderen Therapeutika empfohlen. Der Einsatz von Imiquimod in Kombination mit einer Plasma-Behandlung zeigte in unserer Arbeit neben einer verstärkten Tumorreduktion eine erhöhte Dichte von infiltrierenden Immunzellen.

Die von sterbenden Tumorzellen freigesetzten Moleküle können durch APCs aufgenommen und präsentiert werden, um T-Zell Priming einzuleiten und Gedächtniszellen zu generieren (Kapitel 1.3). In unserer Arbeit haben wir den immunisierten Mäusen die Milzen entnommen, um Immunzellen zu isolieren. Anschließend haben wir die Splenozyten *in vitro* mit Tumorfragmenten stimuliert, um die Aktivität von Gedächtniszellen zu messen und dadurch Aufschluss über die systemische Wirkung nach einer lokalen Plasma-Behandlung zu erhalten. Die Aktivität der Lymphozyten wurde durch die Inkubation mit Hitze-inaktivierten Tumorzellen erhöht, besonders die von Gedächtniszellen. Diese Zellen besitzen Antigen-spezifische Rezeptoren und sind für die Erkennung von MHC-Peptid-Komplexen auf Tumorzellen unerlässlich. Sie werden als Antwort auf eine Tumor-Immunisierung gebildet werden und bieten dann Schutz vor Tumorwachstum. In vorherigen Studien konnte gezeigt werden, dass eine Immunisierung mit Tumorlysat oder Lysat-beladenen APCs einen tendenziellen, jedoch keinen vollständigen Schutz bietet [128-130]. In darauf aufbauenden Studien konnte hingegen gezeigt werden, dass durch HOCl modifizierte Lysate wirksamer sind [131, 132]. Im Vergleich mit HOCl allein, enthält Kaltplasma ein breites Spektrum an RONS und ermöglicht eine Vielfalt weiterer Modifikationen der Tumorantigene. Unsere Arbeit befasste sich mit der Effizienz einer Vakzinierung mit durch Kaltplasma getöteten und oxidativ modifizierten Tumorzellen (oxLysaten). Wir konnten zeigen, dass solche Immunisierung mit oxLysaten das Tumorwachstum stärker beeinträchtige als eine nicht ICD-induzierende Behandlung (MitomycinC). In vorherigen Studien wurde verdeutlicht, dass die stärkere Aktivierung Antigen-spezifischer $CD8^+$ T-Zellen bei der ICD-vermittelten Immunantwort durch eine verbesserte Antigenerkennung begründet ist [133, 134]. Dies konnte in unserer Studie ebenfalls

beobachtet werden, da eine vermehrte $CD8^+$ T-Zellaktivierung in stimulierten Immunzellen nach einer Vakzinierung mit oxLysat vorlag.

Die erhöhte Immunogenität des oxLysats könnte durch einen adjuvanten Effekt begründet sein, d. h. auf eine Aktivierung innater Immunfunktionen, die zur Stimulation und Rekrutierung der adaptiven Immunzellen beiträgt. Alternativ kann das oxLysat neben oxidativ modifizierten Antigenen auch native Antigene enthalten. Die modifizierten Antigene könnten eine höhere Affinität zu MHC-Molekülen besitzen und zu einer verstärkten T-Zellantwort führen (Antigenität). Da zudem die TCR-Überlagerung zur Aktivierung der T-Zellen beiträgt, kann diese durch die Orientierung und Lage der Peptide in der MHC-Peptidbindungstasche oder durch Modifikationen an Aminosäuren beeinflusst werden [135]. Durch die Aufnahme der im oxLysat enthaltenen Proteine durch APCs könnten also zusätzliche Epitope präsentiert werden, welche durch ein unbehandeltes, natives Protein nicht entstehen. Die neuen Epitope würden zu einer Erweiterung des TCR-Repertoires führen. In einigen Studien konnte zuvor gezeigt werden, dass eine Erweiterung des T-Zell-Pools zu einer stärkeren Antitumor-Immunantwort führt [136, 137]. Die spezifische Erkennung von Antigenen und RONS-modifizierten Antigenen durch T-Zellen mit spezifischen TCR wurde in der nachfolgenden Arbeit untersucht.

2.3. Immunisierung durch Vakzinierung eines oxidierten Antigens

Tumorantigene sind in der klinischen Praxis sowohl als Tumormarker für die initiale Diagnostik, als auch therapeutisch z.B. für die Entwicklung von monoklonalen Antikörpern hilfreich. Spezifische, körpereigene Antikörper die gegen ein Tumorantigen gerichtet sind, können auch durch eine Immunisierung mit dem entsprechenden TA im Organismus gebildet werden. Diese führt jedoch nicht nur zu einer Bildung von Antikörpern, sondern ermöglicht zudem, dass sich Antigen-spezifische CTLs, Helferzellen und Gedächtniszellen entwickeln. Eine erfolgreiche Immunisierung durch die Injektion von Peptiden oder DNA lässt sich an der reduzierten Tumorprogression ablesen, welche auf der Aktivierung von Antigen-spezifischen T-Zellen basiert [17, 18, 138]. In einigen Modellsystemen konnte zudem gezeigt werden, dass eine Immunisierung mit HOCl-modifizierten TA, oder TA mit Aminosäureaustausch den Krankheitsverlauf deutlicher verbessert, als eine Immunisierung mit nativem Protein oder Peptid [139, 140]. Obwohl

sich Tumorzellen durch die Präsentation von TA und Neoantigenen von gesunden Zellen unterscheiden, reagieren T-Zellen nicht zwangsläufig auf diese Unterschiede. Ob naive T-Zellen aktiviert werden, hängt von der Stärke der TCR-pMHC-Interaktion ab, welche durch Modifikationen an Epitopen variieren kann. Diese Bindungsstärke ist davon abhängig, wie gut ein Antigen in der MHC-Bindungstasche liegt und wie der TCR an das pMHC Molekül bindet. Durch verschiedene Bindungsaffinitäten zwischen Antigen und MHC, sowie zwischen TCR und pMHC, kann das Epitop stärker oder schwächer immunogen sein [141, 142]. In vorherigen Studien konnte gezeigt werden, dass ein Austausch einzelner Aminosäuren des Epitops in der Ankerregion und an mittleren Positionen zu unterschiedlichen Bindungsaffinitäten führen, wodurch die T-Zellaktivität variiert [143, 144]. Die Aktivierung der T-Zellen korreliert typischerweise mit allgemeinen Parametern der TCR-pMHC-Interaktion, wie Andockwinkel, Cofaktor-Anforderung, Assoziation Raten, Dissoziationsraten, Halbwertszeit oder Verweilzeiten [145]. Eine starke TCR-pMHC Bindung durch einen hochaffinen $CD4^+$ TCR korreliert interessanterweise mit einem reduzierten Tumorwachstum [146, 147].

Daraus resultiert die Frage, ob durch eine Plasma-Behandlung entstehende RONS-modifizierte Antigene stärker oder schwächer immunogen sind als nicht-modifizierte. In unserer Studie wurden die durch Plasma-induzierten Veränderungen an einem Modellantigen untersucht und deren Effekte auf die T-Zellaktivierung *ex vivo* und *in vivo* analysiert (Kapitel 6.3, [148]). Zudem haben wir die Antitumor-Immunantwort nach einer Immunisierung von wildtypischen Mäusen mit Plasma-behandeltem Protein eruiert. In unserer Arbeit haben wir das Hühnereiweißprotein (Ovalbumin, Ova) als Modellantigen gewählt, welches auch von Melanomzellen exprimiert wurde (B16F10-Ova). Eine Antigen-spezifische T-Zellantwort konnte mit hoher Sensitivität in TCR-transgenen Mäusen (OT-II) untersucht werden, welche angereicherte $CD4^+$ T-Zellen mit spezifischen TCR für Ova besitzen. Unter Verwendung des kINPen mit verschiedenen Gasen und Gaszumischungen (pAr und $pHeO_2$) konnten wir strukturelle Veränderungen und oxidative Modifikationen an Ova (oxOva) beobachten. In vorherigen Veröffentlichungen wurden verschiedene Modifikationen an Aminosäuren, Peptiden und Proteinen durch verschiedene Plasma-Konditionen gezeigt [125, 149], jedoch wurde die Immunogenität nicht berücksichtigt. Zudem wurde beobachtet, dass eine Behandlung mit Plasma zu strukturellen Veränderungen in Proteinen führt, welche teils

die Aktivität oder Funktion verändern [150-156]. Strukturelle Veränderungen von Proteinen können immunogene Effekte aufweisen und zu Immunzellpolarisationen führen [157, 158]. Außerdem können RONS-modifizierte Proteine die Aufnahmeaktivität von APCs steigern [159]. In unserer Arbeit konnten wir bestätigen, dass oxOva von APCs besser aufgenommen wird als unbehandeltes OVA. Dazu wurden die Zellen mit einem Tracer-Protein (DQ-Ova), welches bei einem intrazellulären Abbau fluoresziert, stimuliert. Zeitgleich wurde Ova oder oxOva zugegeben, um den APCs die Wahl zwischen DQ-Ova oder Ova/oxOva zu gewähren. Das gemessene DQ-Ova Signal war in Präsenz von oxOva schwächer, als in Gegenwart des nativen Proteins und zeigt daher die bevorzugte Aufnahme von oxOva oder dessen induzierte Signaltransduktion. Durch den Verdau von Ova und oxOva werden Peptide auf MHC-Komplexen für T-Zellen präsentiert. In isolierten Immunzellen von OT-II Tieren konnten wir nach einer Stimulation mit oxOva eine stärkere Aktivierung und Proliferation von Antigen-spezifischen $CD4^+$ T-Zellen, sowie eine erhöhte Zytokinsekretion messen. Diese Effekte konnten jedoch nicht durch eine Behandlung mit äquimolaren RONS Konzentrationen (H_2O_2, NO_2^-, NO_3^-, HOCl; alle eingesetzt in der genau der Konzentration, wie sie durch eine Kaltplasma-Behandlung in Flüssigkeiten generiert werden) rekapituliert werden. Da H_2O_2, NO_2^-, NO_3^-, HOCl jeweils langlebige Spezies sind, wurde der beobachtete Effekt vermutlich durch kurzlebige reaktive Spezies induziert. Die Entstehung von kurzlebigen RONS macht die Verwendung des Kaltplasmas einzigartig, da diese kommerziell nicht erhältlich sind. Trotz RONS-Modifikationen wird eine Antigen-spezifische Aktivierung ermöglicht und wurde durch eine ausbleibende T-Zellantwort in unspezifischen $CD4^+$ T-Zellen aus wildtypischen C57BL6 und SKH-1 Mäusen nach der Stimulation mit oxOva bestätigt. Durch die intraperitoneale Injektion von oxOva in OT-II Tieren konnten wir *in vivo* ebenfalls eine erhöhte T-Zellaktivierung und vermehrte Sekretion von entzündungsfördernden Zytokinen nachweisen.

In einem *proof-of-concept* Experiment konnten wir zeigen, dass in wildtypischen Mäusen (C57BL6) eine Immunisierung mit oxOva einen besseren Schutz vor einem Melanom (B16F10-Ova) bietet, als eine Vakzinierung mit Ova. Die wildtypischen Tiere besitzen keine genetisch codierten Antigen-spezifischen T-Zellen für Ova und konnten erfolgreich immunisiert werden. Eine Differenzierung von Gedächtniszellen wurde in Ova und oxOva-vakzinierten Tieren durch eine Stimulation der Immunzellen mit

unbehandelten Protein bestätigt. Mit oxOva vakzinierte Tiere zeigten eine stärkere T-Zellaktivierung durch Ova als mit Ova vakzinierte Tiere. Da es in oxOva-vakzinierten Tieren theoretisch keine für Ova spezifischen T-Zellen geben sollte, können die beobachteten Effekte *ex vitro* nur durch eine veränderte TCR-pMHC Bindungsaffinität oder einen erweiterten T-Zell-Pool begründet sein.

Zusammenfassend wurde gezeigt, dass Ovalbumin nach einer Behandlung mit Kaltplasma eine erhöhte Immunogenität besitzt und einen Schutz vor dem Wachstum von Ovalbumin-exprimierenden Melanomzellen bietet.

2.4. Oxidierte Antigene als therapeutische Vakzinen

Die oxidativ modifizierten Antigene können, wie zuvor gezeigt, zu einer vermehrten T-Zellaktivierung führen und als präventive Vakzinen eine Antitumor-Immunantwort fördern (Kapitel 2.2, 2.3). Während einer Immunantwort und des Priming-Prozesses proliferieren T-Zellen, welche einen spezifischen TCR besitzen und gegen das Antigen gerichtet sind. Durch die in unseren Studien durchgeführten Stimulationsassays konnten wir zeigen, dass eine Vakzinierung mit oxidativ modifizierten Lysat und Antigen auch zu einer Aktivierung von T-Zellen nach Stimulation mit unbehandelten Proteine führt. Die erhöhte Immunogenität und erfolgreiche Immunisierung kann durch eine Erweiterung des TCR Repertoires, eine veränderte Bindungsaffinität der Antigene oder durch eine Stimulation der innaten Immunzellen begründet sein. Während der Immunisierung differenzieren Antigen-spezifische T-Zellen, welche jedoch nicht nur durch eine präventive Vakzinierung, sondern auch durch eine therapeutische Vakzinierung entstehen. Beide Anwendungen dienen der Bekämpfung von Tumorzellen, und beugen der Tumorprogression und rezidivierendem Tumorwachstum vor. Die Verwendung von RONS-modifizierten Antigenen oder Tumorlysaten als therapeutisches Vakzin ist aufgrund der gezeigten verstärkten Immunogenität naheliegend. In der vorliegenden Literaturarbeit wurde eine mögliche personalisierte Therapie durch eine Tumorbiopsie mit anschließender Kaltplasma-Behandlung und Vakzinierung erörtert (Kapitel 6.4, [160]). Ziel dieser Anwendung ist die Aktivierung des Immunsystems, um die körpereigene Antitumor-Immunantwort bei Krebspatienten durch die Gabe von RONS-modifizierten Antigenen zu stärken.

Verschiedene Antigen- oder Tumorzell-basierte Vakzinen wurden bereits 2014 mit verschiedenen Adjuvanzien oder Immunmodulatoren in Studien mit bis zu 1349 Probanden getestet [161]. In weiteren Studien wurde gezeigt, dass eine Immunisierung mit MART, gp100 und anderen Antigenen, sowie Multipeptid-Vakzinen zu einer Aktivierung und Vermehrung von Antigen-spezifischen T-Zellen führt [162-165]. Da Tumore eine starke Heterogenität aufweisen und die Präsentation einzelner TA eher unwahrscheinlich ist, ist eine Immunisierung durch eine Kombination mehrerer Antigene ein vielversprechender Ansatz. Um vorhandene Peptide im Tumorgewebe zu identifizieren und zu sequenzieren, werden Biopsien aufgrund der verschiedenen Antigenen und Neoantigenen entnommen [166]. Mit Hilfe der daraus resultierenden Erkenntnis können personalisierte Therapien mit individuellen Antigenen entwickelt und verabreicht werden (aktuelle Patientenstudie: NCT03633110). Neoantigene sind durch ihre Abweichung von natürlichen Proteinen stärker immunogen, wodurch ihre Präsenz in Tumoren mit einem besseren klinischen Verlauf im Pankreaskarzinom und Melanom korreliert [16, 167]. Dennoch besteht weiterer Optimierungsbedarf der Vakzinen aus Biopsien, da einige Studien aufgrund ausbleibender Tumorreduktion abgebrochen wurden [168-171]. Verschiedene Strategien zur Optimierung von Antigenvakzinen durch Adjuvanzien, oxidative Modifikationen oder Einkapseln wurden bereits vorgeschlagen [172-175]. Eine weitere Strategie ist die Verwendung von Kaltplasma, welches durch reaktive Spezies individuelle oxidative Modifikationen an Antigenen oder Tumorlysaten induziert. Oxidative Modifikationen dienen als intrinsisches Adjuvans und mechanistisch wird ihnen eine Funktion zugeschrieben, die den DAMPs ähnelt [176, 177]. Die Injektion von mit RONS behandelten Lysaten führt zur Aktivierung und Vermehrung von T-Zellen mit TCRs für native und auch für oxidierte Antigene. Methodisch sollen Biopsien aus dem Tumorgewebe des Patienten entnommen, *ex vivo* unter sterilen Bedingungen mit Kaltplasma behandelt und in den Patienten injiziert werden. Ziel dieses therapeutischen Ansatzes ist die Stimulation des Immunsystems durch die Gabe von RONS-modifizierten Antigenen.

3. Zusammenfassung und Ausblick

In den vorliegenden Arbeiten wurde gezeigt, dass **(1)** eine Behandlung von Hautkrebszellen mit Kaltplasma einen stimulatorischen Effekt auf natürliche Killerzellen *in vitro* erzielt, **(2)** die Behandlung von Melanomen *in vivo* zu einer erhöhten Infiltration von Immunzellen in das Tumorgewebe und zur Reduktion des Tumorwachstums führt. **(3)** Eine Vakzinierung mit RONS-modifizierten Tumorlysat und Tumorantigen aktiviert T-Zellen stärker und verringert das Tumorwachstum.

Die genannten *proof-of-concept*-Experimente wurden durchgeführt, um die immunologischen Konsequenzen einer Kaltplasma-Behandlung im Tumorkontext zu untersuchen. Zusammenfassend führt eine Behandlung von Hautkrebszellen mit Kaltplasma zu einer Veränderung der Oberflächenrezeptoren, welche auf einen immunogenen Zelltod hinweisen und innate Immunzellen stimuliert. Zeitgleich verändert Plasma die Immunogenität von sezernierten Molekülen, da das Plasma-behandelte Ovalbumin bevorzugt von innaten Zellen aufgenommen wird und zu einer erhöhten Aktivierung von Antigen-spezifischen T-Zellen führt. *In vivo* führt die Kaltplasma-Behandlung zu einer reduzierten Tumormasse und fördert die Migration von Immunzellen in das Tumorgewebe. Zuletzt konnte gezeigt werden, dass eine präventive Vakzinierung mit RONS modifizierten Lysat und Antigen zu einem reduzierten Melanom Wachstum führt.

Zukünftig sollten Studien zu der therapeutischen Vakzinierung mit oxidativ modifizierten Lysaten und Antigenen erfolgen. Zudem sollte die durch Plasma-behandeltes Antigen verstärkte T-Zellaktivierung durch die Verwendung eines relevanten Tumor-Antigen analysiert und bekräftigt werden. Um grundlegende Mechanismen zu verstehen, sollten (I) Prozesse der Erkennung, Prozessierung und Präsentation von oxAntigenen in Antigen-präsentierenden Zellen und (II) Epitope, T-Zellrezeptorsequenzen und Bindungsaffinitäten in nachfolgenden Studien untersucht werden.

4. Abkürzungsverzeichnis

APC	Antigen-präsentierende Zelle
CTL	Zytotoxische T-Zelle
DAMPS	Schädenassoziierte Moleküle*; damage-associated molecular patterns*
DC	Dendritische Zelle; *dendritic cell*
ICD	Immunogener Zelltod; *immunogenic cell death*
H_2O_2	Wasserstoffperoxid
HO•	Hydroxyl-Radikal
HOCl	Hypochlorige Säure
MHC	*major histocompatibility complex*
NK(-Zellen)	Natürliche Killerzellen
NO	Stickstoffmonoxid
O2-•	Superoxid Anion
OCl-	Hypochlorid
ONOO-	Peroxynitrit
Ova	Ovalbumin
oxOva	Plasma-behandeltes Ovalbumin
pAr	Argon Plasma
$pArO_2$	Argon 2% Sauerstoff Plasma
$pHeO_2$	Helium 2% Sauerstoff Plasma
PDT	photodynamische Therapie; *photodynamic therapy*
pMHC	Mit einem Peptid beladenes MHC-Moleküle
TA	Tumorantigen
TCR	T-Zellrezeptor
RONS	Reaktive Sauerstoff- und Stickstoffspezies

5. Literaturverzeichnis

1. Burton, K.A., K.A. Ashack, and A. Khachemoune, *Cutaneous Squamous Cell Carcinoma: A Review of High-Risk and Metastatic Disease.* Am J Clin Dermatol, 2016. **17**(5): p. 491-508.
2. Jilaveanu, L.B., S.A. Aziz, and H.M. Kluger, *Chemotherapy and biologic therapies for melanoma: do they work?* Clin Dermatol, 2009. **27**(6): p. 614-25.
3. Forastiere, A.A., et al., *Final report of a phase II evaluation of paclitaxel in patients with advanced squamous cell carcinoma of the head and neck: an Eastern Cooperative Oncology Group trial (PA390).* Cancer, 1998. **82**(11): p. 2270-4.
4. Rao, R.D., et al., *Combination of paclitaxel and carboplatin as second-line therapy for patients with metastatic melanoma.* Cancer, 2006. **106**(2): p. 375-82.
5. Flaherty, K.T., et al., *Inhibition of mutated, activated BRAF in metastatic melanoma.* N Engl J Med, 2010. **363**(9): p. 809-19.
6. Flaherty, K.T., et al., *Improved survival with MEK inhibition in BRAF-mutated melanoma.* N Engl J Med, 2012. **367**(2): p. 107-14.
7. Cascinelli, N., et al., *Effect of long-term adjuvant therapy with interferon alpha-2a in patients with regional node metastases from cutaneous melanoma: a randomised trial.* The Lancet, 2001. **358**(9285): p. 866-869.
8. Kirkwood, J.M., et al., *High- and low-dose interferon alfa-2b in high-risk melanoma: first analysis of intergroup trial E1690/S9111/C9190.* J Clin Oncol, 2000. **18**(12): p. 2444-58.
9. Gogas, H., et al., *Prognostic significance of autoimmunity during treatment of melanoma with interferon.* N Engl J Med, 2006. **354**(7): p. 709-18.
10. Kirkwood, J.M., et al., *Interferon alfa-2b adjuvant therapy of high-risk resected cutaneous melanoma: the Eastern Cooperative Oncology Group Trial EST 1684.* J Clin Oncol, 1996. **14**(1): p. 7-17.
11. Hugo, W., et al., *Genomic and Transcriptomic Features of Response to Anti-PD-1 Therapy in Metastatic Melanoma.* Cell, 2016. **165**(1): p. 35-44.
12. Oba, T., et al., *Overcoming primary and acquired resistance to anti-PD-L1 therapy by induction and activation of tumor-residing cDC1s.* Nat Commun, 2020. **11**(1): p. 5415.
13. Peng, M., et al., *Neoantigen vaccine: an emerging tumor immunotherapy.* Mol Cancer, 2019. **18**(1): p. 128.
14. Gaugler, B., et al., *Human gene MAGE-3 codes for an antigen recognized on a melanoma by autologous cytolytic T lymphocytes.* J Exp Med, 1994. **179**(3): p. 921-30.
15. Traversari, C., et al., *A nonapeptide encoded by human gene MAGE-1 is recognized on HLA-A1 by cytolytic T lymphocytes directed against tumor antigen MZ2-E.* J Exp Med, 1992. **176**(5): p. 1453-7.
16. Ott, P.A., et al., *An immunogenic personal neoantigen vaccine for patients with melanoma.* Nature, 2017. **547**(7662): p. 217-221.
17. Schwartzentruber, D.J., et al., *gp100 peptide vaccine and interleukin-2 in patients with advanced melanoma.* N Engl J Med, 2011. **364**(22): p. 2119-27.
18. Patel, P.M., et al., *Targeting gp100 and TRP-2 with a DNA vaccine: Incorporating T cell epitopes with a human IgG1 antibody induces potent T cell responses that are associated with favourable clinical outcome in a phase I/II trial.* Oncoimmunology, 2018. **7**(6): p. e1433516.
19. Cecic, I., C.S. Parkins, and M. Korbelik, *Induction of Systemic Neutrophil Response in Mice by Photodynamic Therapy of Solid Tumors¶.* Photochemistry and Photobiology, 2007. **74**(5): p. 712-720.

20. Panzarini, E., V. Inguscio, and L. Dini, *Immunogenic cell death: can it be exploited in PhotoDynamic Therapy for cancer?* Biomed Res Int, 2013. **2013**: p. 482160.
21. Shen, Z., et al., *Strategies to improve photodynamic therapy efficacy by relieving the tumor hypoxia environment.* NPG Asia Materials, 2021. **13**(1).
22. Larue, L., et al., *Fighting Hypoxia to Improve PDT.* Pharmaceuticals (Basel), 2019. **12**(4).
23. von Woedtke, T., et al., *Plasma Medicine: A Field of Applied Redox Biology.* In Vivo, 2019. **33**(4): p. 1011-1026.
24. Mashayekh, S., et al., *Atmospheric-pressure plasma jet characterization and applications on melanoma cancer treatment (B/16-F10).* Physics of Plasmas, 2015. **22**(9): p. 093508.
25. Keidar, M., et al., *Cold plasma selectivity and the possibility of a paradigm shift in cancer therapy.* Br J Cancer, 2011. **105**(9): p. 1295-301.
26. Saadati, F., et al., *Comparison of Direct and Indirect cold atmospheric-pressure plasma methods in the B16F10 melanoma cancer cells treatment.* Sci Rep, 2018. **8**(1): p. 7689.
27. Pasqual-Melo, G., et al., *Plasma Treatment Limits Cutaneous Squamous Cell Carcinoma Development In Vitro and In Vivo.* Cancers (Basel), 2020. **12**(7): p. 1993.
28. Metelmann, H.-R., et al., *Clinical experience with cold plasma in the treatment of locally advanced head and neck cancer.* Clinical Plasma Medicine, 2018. **9**: p. 6-13.
29. Mahdikia, H., et al., *Gas plasma irradiation of breast cancers promotes immunogenicity, tumor reduction, and an abscopal effect in vivo.* Oncoimmunology, 2021. **10**(1): p. 1859731.
30. Chen, G., et al., *Transdermal cold atmospheric plasma-mediated immune checkpoint blockade therapy.* Proc Natl Acad Sci U S A, 2020. **117**(7): p. 3687-3692.
31. Khalili, M., et al., *Non-Thermal Plasma-Induced Immunogenic Cell Death in Cancer: A Topical Review.* J Phys D Appl Phys, 2019. **52**(42).
32. Moritz, J., H.-R. Metelmann, and S. Bekeschus, *Physical Plasma Treatment of Eight Human Cancer Cell Lines Demarcates Upregulation of CD112 as a Common Immunomodulatory Response Element.* IEEE Transactions on Radiation and Plasma Medical Sciences, 2020. **4**(3): p. 343-349.
33. Bekeschus, S., et al., *Ex Vivo Exposure of Human Melanoma Tissue to Cold Physical Plasma Elicits Apoptosis and Modulates Inflammation.* Applied Sciences, 2020. **10**(6).
34. Gandhirajan, R.K., et al., *The amino acid metabolism is essential for evading physical plasma-induced tumour cell death.* Br J Cancer, 2021. **124**(11): p. 1854-1863.
35. Bekeschus, S., et al., *Physical Plasma Elicits Immunogenic Cancer Cell Death and Mitochondrial Singlet Oxygen.* IEEE Transactions on Radiation and Plasma Medical Sciences, 2018. **2**(2): p. 138-146.
36. Nijdam, S., et al., *An Introduction to Nonequilibrium Plasmas at Atmospheric Pressure*, in *Plasma Chemistry and Catalysis in Gases and Liquids*. 2012. p. 1-44.
37. von Woedtke, T., et al., *Plasmas for medicine.* Physics Reports, 2013. **530**(4): p. 291-320.
38. Adamovich, I., et al., *The 2017 Plasma Roadmap: Low temperature plasma science and technology.* Journal of Physics D-Applied Physics, 2017. **50**(32): p. 323001.
39. Bruggeman, P.J., et al., *Plasma-liquid interactions: a review and roadmap.* Plasma Sources Science & Technology, 2016. **25**(5): p. 053002.
40. Gorbanev, et al., *Applications of the COST Plasma Jet: More than a Reference Standard.* Plasma, 2019. **2**(3): p. 316-327.
41. Reuter, S., T. von Woedtke, and K.D. Weltmann, *The kINPen-a review on physics and chemistry of the atmospheric pressure plasma jet and its applications.* Journal of Physics D-Applied Physics, 2018. **51**(23).
42. Khlyustova, A., et al., *Important parameters in plasma jets for the production of RONS in liquids for plasma medicine: A brief review.* Front. Chem. Sci. Eng., 2019. **13**(2): p. 238-252.

43. Lin, L. and M. Keidar, *A map of control for cold atmospheric plasma jets: From physical mechanisms to optimizations.* Applied Physics Reviews, 2021. **8**(1).
44. Sies, H., *Hydrogen peroxide as a central redox signaling molecule in physiological oxidative stress: Oxidative eustress.* Redox Biol, 2017. **11**: p. 613-619.
45. Van Loenhout, J., et al., *Oxidative Stress-Inducing Anticancer Therapies: Taking a Closer Look at Their Immunomodulating Effects.* Antioxidants (Basel), 2020. **9**(12).
46. Boeckmann, L., et al., *Cold Atmospheric Pressure Plasma in Wound Healing and Cancer Treatment.* Applied Sciences, 2020. **10**(19).
47. Bernhardt, T., et al., *Plasma Medicine: Applications of Cold Atmospheric Pressure Plasma in Dermatology.* Oxid Med Cell Longev, 2019. **2019**: p. 3873928.
48. Eming, S.A., T. Krieg, and J.M. Davidson, *Inflammation in wound repair: molecular and cellular mechanisms.* J Invest Dermatol, 2007. **127**(3): p. 514-25.
49. Dunnill, C., et al., *Reactive oxygen species (ROS) and wound healing: the functional role of ROS and emerging ROS-modulating technologies for augmentation of the healing process.* Int Wound J, 2017. **14**(1): p. 89-96.
50. Bekeschus, S., et al., *Medical gas plasma-stimulated wound healing: Evidence and mechanisms.* Redox Biol, 2021. **46**: p. 102116.
51. Haertel, B., et al., *Non-thermal atmospheric-pressure plasma possible application in wound healing.* Biomol Ther (Seoul), 2014. **22**(6): p. 477-90.
52. Stratmann, B., et al., *Effect of Cold Atmospheric Plasma Therapy vs Standard Therapy Placebo on Wound Healing in Patients With Diabetic Foot Ulcers: A Randomized Clinical Trial.* JAMA Netw Open, 2020. **3**(7): p. e2010411.
53. Daeschlein, G., et al., *Hyperspectral imaging: innovative diagnostics to visualize hemodynamic effects of cold plasma in wound therapy.* Biomed Tech (Berl), 2018. **63**(5): p. 603-608.
54. Kubinova, S., et al., *Non-thermal air plasma promotes the healing of acute skin wounds in rats.* Sci Rep, 2017. **7**: p. 45183.
55. Lee, Y.S., et al., *Non-thermal atmospheric plasma ameliorates imiquimod-induced psoriasis-like skin inflammation in mice through inhibition of immune responses and up-regulation of PD-L1 expression.* Sci Rep, 2017. **7**(1): p. 15564.
56. Hasse, S., et al., *Induction of proliferation of basal epidermal keratinocytes by cold atmospheric-pressure plasma.* Clin Exp Dermatol, 2016. **41**(2): p. 202-9.
57. Liu, J.R., et al., *Low temperature plasma promoting fibroblast proliferation by activating the NF-kappaB pathway and increasing cyclinD1 expression.* Sci Rep, 2017. **7**(1): p. 11698.
58. Schmidt, A., et al., *Gas plasma-spurred wound healing is accompanied by regulation of focal adhesion, matrix remodeling, and tissue oxygenation.* Redox Biol, 2021. **38**: p. 101809.
59. Lou, B.S., et al., *Helium/Argon-Generated Cold Atmospheric Plasma Facilitates Cutaneous Wound Healing.* Front Bioeng Biotechnol, 2020. **8**: p. 683.
60. Daeschlein, G., et al., *Skin and wound decontamination of multidrug-resistant bacteria by cold atmospheric plasma coagulation.* J Dtsch Dermatol Ges, 2015. **13**(2): p. 143-50.
61. Schmidt, A., et al., *Nrf2 signaling and inflammation are key events in physical plasma-spurred wound healing.* Theranostics, 2019. **9**(4): p. 1066-1084.
62. Mittal, M., et al., *Reactive oxygen species in inflammation and tissue injury.* Antioxid Redox Signal, 2014. **20**(7): p. 1126-67.
63. Hampton, M.B., A.J. Kettle, and C.C. Winterbourn, *Inside the neutrophil phagosome: oxidants, myeloperoxidase, and bacterial killing.* Blood, 1998. **92**(9): p. 3007-17.
64. Winterbourn, C.C., A.J. Kettle, and M.B. Hampton, *Reactive Oxygen Species and Neutrophil Function.* Annu Rev Biochem, 2016. **85**: p. 765-92.
65. Franchina, D.G., C. Dostert, and D. Brenner, *Reactive Oxygen Species: Involvement in T Cell Signaling and Metabolism.* Trends Immunol, 2018. **39**(6): p. 489-502.

66. Winterbourn, C.C., et al., *Modeling the reactions of superoxide and myeloperoxidase in the neutrophil phagosome: implications for microbial killing.* J Biol Chem, 2006. **281**(52): p. 39860-9.
67. Krysko, D.V., et al., *Immunogenic cell death and DAMPs in cancer therapy.* Nat Rev Cancer, 2012. **12**(12): p. 860-75.
68. Galluzzi, L., et al., *Consensus guidelines for the definition, detection and interpretation of immunogenic cell death.* J Immunother Cancer, 2020. **8**(1).
69. Galluzzi, L., et al., *Immunogenic cell death in cancer and infectious disease.* Nat Rev Immunol, 2017. **17**(2): p. 97-111.
70. Lin, A.G., et al., *Non-thermal plasma induces immunogenic cell death in vivo in murine CT26 colorectal tumors.* Oncoimmunology, 2018. **7**(9): p. e1484978.
71. Freund, E., et al., *Physical plasma-treated saline promotes an immunogenic phenotype in CT26 colon cancer cells in vitro and in vivo.* Sci Rep, 2019. **9**(1): p. 634.
72. Gajewski, T.F., H. Schreiber, and Y.X. Fu, *Innate and adaptive immune cells in the tumor microenvironment.* Nat Immunol, 2013. **14**(10): p. 1014-22.
73. Lanzavecchia, A. and F. Sallusto, *Regulation of T cell immunity by dendritic cells.* Cell, 2001. **106**(3): p. 263-6.
74. Addou-Klouche, L., *NK Cells in Cancer Immunotherapy*, in *Natural Killer Cells*. 2017.
75. Del Zotto, G., et al., *Markers and function of human NK cells in normal and pathological conditions.* Cytometry B Clin Cytom, 2017. **92**(2): p. 100-114.
76. Morvan, M.G. and L.L. Lanier, *NK cells and cancer: you can teach innate cells new tricks.* Nat Rev Cancer, 2016. **16**(1): p. 7-19.
77. Klein, L., et al., *Positive and negative selection of the T cell repertoire: what thymocytes see (and don't see).* Nat Rev Immunol, 2014. **14**(6): p. 377-91.
78. Chen, D.S. and I. Mellman, *Oncology meets immunology: the cancer-immunity cycle.* Immunity, 2013. **39**(1): p. 1-10.
79. Duray, A., et al., *Immune Suppression in Head and Neck Cancers: AReview.* Clinical and Developmental Immunology, 2010.
80. Rabinovich, G.A., D. Gabrilovich, and E.M. Sotomayor, *Immunosuppressive strategies that are mediated by tumor cells.* Annual Review of Immunology, 2007. **25**: p. 267-296.
81. Witzke, K., et al., *Plasma medical oncology: Immunological interpretation of head and neck squamous cell carcinoma.* Plasma Processes and Polymers, 2020. **17**(10): p. e1900258.
82. Bekeschus, S., R. Clemen, and H.-R. Metelmann, *Potentiating anti-tumor immunity with physical plasma.* Clinical Plasma Medicine, 2018. **12**: p. 17-22.
83. Miller, V., A. Lin, and A. Fridman, *Why Target Immune Cells for Plasma Treatment of Cancer.* Plasma Chemistry and Plasma Processing, 2015. **36**(1): p. 259-268.
84. Tanaka, M., et al., *Immunogenic cell death due to a new photodynamic therapy (PDT) with glycoconjugated chlorin (G-chlorin).* Oncotarget, 2016. **7**(30): p. 47242-47251.
85. Lin, A., et al., *Nanosecond-Pulsed DBD Plasma-Generated Reactive Oxygen Species Trigger Immunogenic Cell Death in A549 Lung Carcinoma Cells through Intracellular Oxidative Stress.* Int J Mol Sci, 2017. **18**(5): p. 966.
86. Troitskaya, O., et al., *Non-Thermal Plasma Application in Tumor-Bearing Mice Induces Increase of Serum HMGB1.* Int J Mol Sci, 2020. **21**(14).
87. Yoon, Y., et al., *Cold Atmospheric Plasma Induces HMGB1 Expression in Cancer Cells.* Anticancer Res, 2019. **39**(5): p. 2405-2413.
88. Pasqual-Melo, G., et al., *Combination of Gas Plasma and Radiotherapy Has Immunostimulatory Potential and Additive Toxicity in Murine Melanoma Cells In Vitro.* International Journal of Molecular Sciences, 2020. **21**(4): p. 1379.
89. Bekeschus, S., et al., *Toxicity and Immunogenicity in Murine Melanoma following Exposure to Physical Plasma-Derived Oxidants.* Oxid Med Cell Longev, 2017. **2017**: p. 4396467.

90. Weiss, M., et al., *Cold Atmospheric Plasma Treatment Induces Anti-Proliferative Effects in Prostate Cancer Cells by Redox and Apoptotic Signaling Pathways.* PLoS One, 2015. **10**(7): p. e0130350.
91. Van Loenhout, J., et al., *Cold Atmospheric Plasma-Treated PBS Eliminates Immunosuppressive Pancreatic Stellate Cells and Induces Immunogenic Cell Death of Pancreatic Cancer Cells.* Cancers (Basel), 2019. **11**(10).
92. Khabipov, A., et al., *RAW 264.7 Macrophage Polarization by Pancreatic Cancer Cells - A Model for Studying Tumour-promoting Macrophages.* Anticancer Res, 2019. **39**(6): p. 2871-2882.
93. Bekeschus, S., et al., *Argon Plasma Exposure Augments Costimulatory Ligands and Cytokine Release in Human Monocyte-Derived Dendritic Cells.* Int J Mol Sci, 2021. **22**(7): p. 3790.
94. Kaushik, N.K., et al., *Cytotoxic macrophage-released tumour necrosis factor-alpha (TNF-alpha) as a killing mechanism for cancer cell death after cold plasma activation.* Journal of Physics D-Applied Physics, 2016. **49**(8): p. 084001.
95. Freund, E., et al., *Plasma-Derived Reactive Species Shape a Differentiation Profile in Human Monocytes.* Applied Sciences-Basel, 2019. **9**(12).
96. Bundscherer, L., et al., *Non-thermal plasma treatment induces MAPK signaling in human monocytes.* Open Chemistry, 2015. **13**(1): p. 606-613.
97. Frostegard, J., et al., *Oxidized Low-Density Lipoprotein (OxLDL)-Treated Dendritic Cells Promote Activation of T Cells in Human Atherosclerotic Plaque and Blood, Which Is Repressed by Statins: microRNA let-7c Is Integral to the Effect.* J Am Heart Assoc, 2016. **5**(9).
98. Strollo, R., et al., *Antibodies to post-translationally modified insulin in type 1 diabetes.* Diabetologia, 2015. **58**(12): p. 2851-60.
99. Nybo, T., et al., *Chlorination and oxidation of the extracellular matrix protein laminin and basement membrane extracts by hypochlorous acid and myeloperoxidase.* Redox Biol, 2019. **20**: p. 496-513.
100. Clemen, R. and S. Bekeschus, *Oxidatively Modified Proteins: Cause and Control of Diseases.* Applied Sciences, 2020. **10**(18): p. 6419.
101. Viola, A. and A. Lanzavecchia, *T cell activation determined by T cell receptor number and tunable thresholds.* Science, 1996. **273**(5271): p. 104-6.
102. Manz, B.N., et al., *T-cell triggering thresholds are modulated by the number of antigen within individual T-cell receptor clusters.* Proc Natl Acad Sci U S A, 2011. **108**(22): p. 9089-94.
103. Lanzavecchia, A., G. Iezzi, and A. Viola, *From TCR Engagement to T Cell Activation.* Cell, 1999. **96**(1): p. 1-4.
104. Tan, M.P., et al., *T cell receptor binding affinity governs the functional profile of cancer-specific CD8+ T cells.* Clin Exp Immunol, 2015. **180**(2): p. 255-70.
105. Chan, K.F., et al., *Divergent T-cell receptor recognition modes of a HLA-I restricted extended tumour-associated peptide.* Nat Commun, 2018. **9**(1): p. 1026.
106. Vivier, E., et al., *Functions of natural killer cells.* Nat Immunol, 2008. **9**(5): p. 503-10.
107. Poggi, A., et al., *Mechanisms of tumor escape from immune system: role of mesenchymal stromal cells.* Immunol Lett, 2014. **159**(1-2): p. 55-72.
108. Menier, C., et al., *MICA triggering signal for NK cell tumor lysis is counteracted by HLA-G1-mediated inhibitory signal.* Int J Cancer, 2002. **100**(1): p. 63-70.
109. Guillerey, C. and M.J. Smyth, *NK Cells and Cancer Immunoediting.* Curr Top Microbiol Immunol, 2016. **395**: p. 115-45.
110. Rosental, B., et al., *The effect of chemotherapy/radiotherapy on cancerous pattern recognition by NK cells.* Curr Med Chem, 2012. **19**(12): p. 1780-91.
111. Markasz, L., et al., *Effect of frequently used chemotherapeutic drugs on the cytotoxic activity of human natural killer cells.* Mol Cancer Ther, 2007. **6**(2): p. 644-54.

112. Clemen, R., et al., *Physical Plasma-Treated Skin Cancer Cells Amplify Tumor Cytotoxicity of Human Natural Killer (NK) Cells.* Cancers (Basel), 2020. **12**(12): p. 3575.
113. Yamamoto, K., et al., *Oxidative stress increases MICA and MICB gene expression in the human colon carcinoma cell line (CaCo-2).* Biochim Biophys Acta, 2001. **1526**(1): p. 10-2.
114. Soriani, A., et al., *Reactive oxygen species- and DNA damage response-dependent NK cell activating ligand upregulation occurs at transcriptional levels and requires the transcriptional factor E2F1.* J Immunol, 2014. **193**(2): p. 950-60.
115. Meza Guzman, L.G., N. Keating, and S.E. Nicholson, *Natural Killer Cells: Tumor Surveillance and Signaling.* Cancers (Basel), 2020. **12**(4).
116. Backes, C.S., et al., *Natural killer cells induce distinct modes of cancer cell death: Discrimination, quantification, and modulation of apoptosis, necrosis, and mixed forms.* J Biol Chem, 2018. **293**(42): p. 16348-16363.
117. Chen, Z., et al., *Expression of proinflammatory and proangiogenic cytokines in patients with head and neck cancer.* Clin Cancer Res, 1999. **5**(6): p. 1369-79.
118. Galon, J. and D. Bruni, *Approaches to treat immune hot, altered and cold tumours with combination immunotherapies.* Nat Rev Drug Discov, 2019. **18**(3): p. 197-218.
119. Duan, Q., et al., *Turning Cold into Hot: Firing up the Tumor Microenvironment.* Trends Cancer, 2020. **6**(7): p. 605-618.
120. Panaretakis, T., et al., *Mechanisms of pre-apoptotic calreticulin exposure in immunogenic cell death.* EMBO J, 2009. **28**(5): p. 578-90.
121. Zhou, J., et al., *Immunogenic cell death in cancer therapy: Present and emerging inducers.* J Cell Mol Med, 2019. **23**(8): p. 4854-4865.
122. Garg, A.D., et al., *Immunogenic cell death, DAMPs and anticancer therapeutics: an emerging amalgamation.* Biochim Biophys Acta, 2010. **1805**(1): p. 53-71.
123. Bekeschus, S., et al., *Medical Gas Plasma Jet Technology Targets Murine Melanoma in an Immunogenic Fashion.* Adv Sci (Weinh), 2020. **7**(10): p. 1903438.
124. Reuter, S., et al., *From RONS to ROS: Tailoring Plasma Jet Treatment of Skin Cells.* Ieee Transactions on Plasma Science, 2012. **40**(11): p. 2986-2993.
125. Wenske, S., et al., *Reactive species driven oxidative modifications of peptides-Tracing physical plasma liquid chemistry.* Journal of Applied Physics, 2021. **129**(19).
126. Scarfi, F., et al., *The role of topical imiquimod in melanoma cutaneous metastases: A critical review of the literature.* Dermatol Ther, 2020. **33**(6): p. e14165.
127. Miller, R.L., et al., *Review Article Imiquimod applied topically: a novel immune response modifier and new class of drug.* International Journal of Immunopharmacology, 1999. **21**(1): p. 1-14.
128. Herbert, G.S., et al., *Initial phase I/IIa trial results of an autologous tumor lysate, particle-loaded, dendritic cell (TLPLDC) vaccine in patients with solid tumors.* Vaccine, 2018. **36**(23): p. 3247-3253.
129. Lee, W.C., et al., *Vaccination of advanced hepatocellular carcinoma patients with tumor lysate-pulsed dendritic cells: a clinical trial.* J Immunother, 2005. **28**(5): p. 496-504.
130. Yu, J.S., et al., *Vaccination with tumor lysate-pulsed dendritic cells elicits antigen-specific, cytotoxic T-cells in patients with malignant glioma.* Cancer Res, 2004. **64**(14): p. 4973-9.
131. Tanyi, J.L., et al., *Personalized cancer vaccine effectively mobilizes antitumor T cell immunity in ovarian cancer.* Sci Transl Med, 2018. **10**(436).
132. Chiang, C.L., et al., *A dendritic cell vaccine pulsed with autologous hypochlorous acid-oxidized ovarian cancer lysate primes effective broad antitumor immunity: from bench to bedside.* Clin Cancer Res, 2013. **19**(17): p. 4801-15.
133. Jiang, Q., et al., *Mitochondria-Targeting Immunogenic Cell Death Inducer Improves the Adoptive T-Cell Therapy Against Solid Tumor.* Front Oncol, 2019. **9**: p. 1196.

134. Adkins, I., et al., *Severe, but not mild heat-shock treatment induces immunogenic cell death in cancer cells.* Oncoimmunology, 2017. **6**(5): p. e1311433.
135. Armstrong, K.M., K.H. Piepenbrink, and B.M. Baker, *Conformational changes and flexibility in T-cell receptor recognition of peptide-MHC complexes.* Biochem J, 2008. **415**(2): p. 183-96.
136. Tanyi, J.L., et al., *Personalized cancer vaccine strategy elicits polyfunctional T cells and demonstrates clinical benefits in ovarian cancer.* NPJ Vaccines, 2021. **6**(1): p. 36.
137. Chiang, C.L., et al., *Hypochlorous acid enhances immunogenicity and uptake of allogeneic ovarian tumor cells by dendritic cells to cross-prime tumor-specific T cells.* Cancer Immunol Immunother, 2006. **55**(11): p. 1384-95.
138. Weber, J., et al., *Phase 1 trial of intranodal injection of a Melan-A/MART-1 DNA plasmid vaccine in patients with stage IV melanoma.* J Immunother, 2008. **31**(2): p. 215-23.
139. Marcinkiewicz, J., et al., *Enhancement of Immunogenic Properties of Ovalbumin as a Result of Its Chlorination.* International Journal of Biochemistry, 1991. **23**(12): p. 1393-1395.
140. Mansour, M., et al., *Therapy of established B16-F10 melanoma tumors by a single vaccination of CTL/T helper peptides in VacciMax.* J Transl Med, 2007. **5**: p. 20.
141. Baumgartner, C.K., H. Yagita, and L.P. Malherbe, *A TCR affinity threshold regulates memory CD4 T cell differentiation following vaccination.* J Immunol, 2012. **189**(5): p. 2309-17.
142. Snook, J.P., C. Kim, and M.A. Williams, *TCR signal strength controls the differentiation of CD4(+) effector and memory T cells.* Sci Immunol, 2018. **3**(25).
143. Cole, D.K., et al., *Modification of MHC anchor residues generates heteroclitic peptides that alter TCR binding and T cell recognition.* J Immunol, 2010. **185**(4): p. 2600-10.
144. Capasso, C., et al., *A novel in silico framework to improve MHC-I epitopes and break the tolerance to melanoma.* Oncoimmunology, 2017. **6**(9): p. e1319028.
145. Szeto, C., et al., *TCR Recognition of Peptide-MHC-I: Rule Makers and Breakers.* Int J Mol Sci, 2020. **22**(1).
146. Soto, C.M., et al., *MHC-class I-restricted CD4 T cells: a nanomolar affinity TCR has improved anti-tumor efficacy in vivo compared to the micromolar wild-type TCR.* Cancer Immunol Immunother, 2013. **62**(2): p. 359-69.
147. Frankel, T.L., et al., *Both CD4 and CD8 T cells mediate equally effective in vivo tumor treatment when engineered with a highly avid TCR targeting tyrosinase.* J Immunol, 2010. **184**(11): p. 5988-98.
148. Clemen, R., et al., *Gas Plasma Technology Augments Ovalbumin Immunogenicity and OT-II T Cell Activation Conferring Tumor Protection in Mice.* Adv Sci (Weinh), 2021. **8**(10): p. 2003395.
149. Lackmann, J.W., et al., *Nitrosylation vs. oxidation - How to modulate cold physical plasmas for biological applications.* PLoS One, 2019. **14**(5): p. e0216606.
150. Laroussi, M., *Effects of Low Temperature Plasmas on Proteins.* IEEE Transactions on Radiation and Plasma Medical Sciences, 2018. **2**(3): p. 229-234.
151. Attri, P., et al., *CAP modifies the structure of a model protein from thermophilic bacteria: mechanisms of CAP-mediated inactivation.* Sci Rep, 2018. **8**(1): p. 10218.
152. Krewing, M., et al., *The molecular chaperone Hsp33 is activated by atmospheric-pressure plasma protecting proteins from aggregation.* J R Soc Interface, 2019. **16**(155): p. 20180966.
153. Yusupov, M., et al., *Impact of plasma oxidation on structural features of human epidermal growth factor.* Plasma Processes and Polymers, 2018. **15**(8).
154. De Backer, J., et al., *The effect of reactive oxygen and nitrogen species on the structure of cytoglobin: A potential tumor suppressor.* Redox Biol, 2018. **19**: p. 1-10.

155. Nasri, Z., et al., *Singlet Oxygen-Induced Phospholipase A2 Inhibition: a Major Role for Interfacial Tryptophan Dioxidation.* Chemistry, 2021.
156. Peng, S., et al., *Oxidative modifications and structural changes of human serum albumin in response to air dielectric barrier discharge plasma.* High Voltage, 2021. **6**(5): p. 813-821.
157. Scheiblhofer, S., et al., *Influence of protein fold stability on immunogenicity and its implications for vaccine design.* Expert Rev Vaccines, 2017. **16**(5): p. 479-489.
158. Winter, P., et al., *In silico Design of Phl p 6 Variants With Altered Fold-Stability Significantly Impacts Antigen Processing, Immunogenicity and Immune Polarization.* Front Immunol, 2020. **11**: p. 1824.
159. Prokopowicz, Z.M., et al., *Hypochlorous acid: a natural adjuvant that facilitates antigen processing, cross-priming, and the induction of adaptive immunity.* J Immunol, 2010. **184**(2): p. 824-35.
160. Clemen, R. and S. Bekeschus, *ROS Cocktails as an Adjuvant for Personalized Antitumor Vaccination?* Vaccines (Basel), 2021. **9**(5).
161. Melero, I., et al., *Therapeutic vaccines for cancer: an overview of clinical trials.* Nat Rev Clin Oncol, 2014. **11**(9): p. 509-24.
162. Speiser, D.E., et al., *Rapid and strong human CD8+ T cell responses to vaccination with peptide, IFA, and CpG oligodeoxynucleotide 7909.* J Clin Invest, 2005. **115**(3): p. 739-46.
163. Weber, J., et al., *Granulocyte-macrophage-colony-stimulating factor added to a multipeptide vaccine for resected Stage II melanoma.* Cancer, 2003. **97**(1): p. 186-200.
164. Baumgaertner, P., et al., *Vaccination of stage III/IV melanoma patients with long NY-ESO-1 peptide and CpG-B elicits robust CD8(+) and CD4(+) T-cell responses with multiple specificities including a novel DR7-restricted epitope.* Oncoimmunology, 2016. **5**(10): p. e1216290.
165. Qian, J., et al., *CD204 suppresses large heat shock protein-facilitated priming of tumor antigen gp100-specific T cells and chaperone vaccine activity against mouse melanoma.* J Immunol, 2011. **187**(6): p. 2905-14.
166. Yarchoan, M., et al., *Targeting neoantigens to augment antitumour immunity.* Nat Rev Cancer, 2017. **17**(4): p. 209-222.
167. Balachandran, V.P., et al., *Identification of unique neoantigen qualities in long-term survivors of pancreatic cancer.* Nature, 2017. **551**(7681): p. 512-516.
168. Pilla, L., et al., *A phase II trial of vaccination with autologous, tumor-derived heat-shock protein peptide complexes Gp96, in combination with GM-CSF and interferon-alpha in metastatic melanoma patients.* Cancer Immunol Immunother, 2006. **55**(8): p. 958-68.
169. Belli, F., et al., *Vaccination of metastatic melanoma patients with autologous tumor-derived heat shock protein gp96-peptide complexes: clinical and immunologic findings.* J Clin Oncol, 2002. **20**(20): p. 4169-80.
170. Wood, C.G. and P. Mulders, *Vitespen: a preclinical and clinical review.* Future Oncol, 2009. **5**(6): p. 763-74.
171. Dreno, B., et al., *MAGE-A3 immunotherapeutic as adjuvant therapy for patients with resected, MAGE-A3-positive, stage III melanoma (DERMA): a double-blind, randomised, placebo-controlled, phase 3 trial.* The Lancet Oncology, 2018. **19**(7): p. 916-929.
172. Wang, T., et al., *A cancer vaccine-mediated postoperative immunotherapy for recurrent and metastatic tumors.* Nat Commun, 2018. **9**(1): p. 1532.
173. Kotsakis, A., et al., *Clinical outcome of patients with various advanced cancer types vaccinated with an optimized cryptic human telomerase reverse transcriptase (TERT) peptide: results of an expanded phase II study.* Ann Oncol, 2012. **23**(2): p. 442-9.
174. Goldinger, S.M., et al., *Nano-particle vaccination combined with TLR-7 and -9 ligands triggers memory and effector CD8(+) T-cell responses in melanoma patients.* Eur J Immunol, 2012. **42**(11): p. 3049-61.

175. Slingluff, C.L., Jr., et al., *Clinical and immunologic results of a randomized phase II trial of vaccination using four melanoma peptides either administered in granulocyte-macrophage colony-stimulating factor in adjuvant or pulsed on dendritic cells.* J Clin Oncol, 2003. **21**(21): p. 4016-26.
176. Gong, T., et al., *DAMP-sensing receptors in sterile inflammation and inflammatory diseases.* Nat Rev Immunol, 2020. **20**(2): p. 95-112.
177. Carta, S., et al., *DAMPs and inflammatory processes: the role of redox in the different outcomes.* J Leukoc Biol, 2009. **86**(3): p. 549-55.

6. Publikationen

6.1. *Physical plasma-treated skin cancer cells amplify tumor cytotoxicity of human natural killer cells*

Authors: Clemen, R.; Heirman, P.; Lin, A.; Bogaerts, A. and Bekeschus, S.

Journal: Cancers (Basel) 2020, Volume 12, Start Page 3575, ISSN: 2072-6694 (Print)/ 2072-6694 (Linking)

doi: 10.3390/cancers12123575

Author Contributions: Conceptualization, S.B.; Methodology, R.C. and P.H.; Software, R.C., P.H., and S.B.; Validation, R.C. and P.H.; Formal Analysis, P.H.; Investigation, R.C. and P.H.; Resources, S.B.; Data Curation, R.C. and P.H.; Writing—Original Draft Preparation, R.C. and S.B.; Writing—Review & Editing, R.C., P.H., A.L., A.B., and S.B.; Visualization, R.C. and P.H.; Supervision, A.B. and S.B.; Project Administration, R.C., A.L., and S.B.; Funding Acquisition, S.B.

Ausweis der Eigenanteile:

Ramona Clemen hat in Kooperation mit Sander Bekeschus die Experimente geplant und zusammen mit Pepijn Heirman durchgeführt, sowie die Daten analysiert und interpretiert. Sie hat die Abbildungen erstellt und das Manuskript geschrieben.

6.2. *Medical gas plasma jet technology targets murine melanoma in an immunogenic fashion*

Authors: Bekeschus, S.; **Clemen, R.;** Niessner, F.; Sagwal, S.K.; Freund, E. and Schmidt, A.

Journal: Advanced Science 2020, Volume 7, Start Page 1903438, ISSN: 2198-3844 (Print)/ 2198-3844 (Linking)

doi: 10.1002/advs.201903438

Author Contributions: E.F. and A.S. contributed equally to this work. S.B. designed the study, analyzed the data, and wrote the manuscript. R.C., F.N., S.K.S., E.F., and A.S. performed the experiments, analyzed the data, and reviewed the manuscript.

Ausweis der Eigenanteile:

Ramona Clemen hat die Experimente durchgeführt (*in vivo*, *ex vivo* & Revision), sowie in Zusammenarbeit mit Sander Bekeschus die Daten analysiert und interpretiert.

6.3. *Gas plasma technology augments ovalbumin immunogenicity and OT-II T cells*

Authors: Clemen, R.; Freund, E.; Mrochen, D.; Miebach, L.; Schmidt, A.; Rauch, B.H.; Lackmann, J.W.; Martens, U.; Wende, K.; Lalk, M.; Delcea, M.; Bröker, B.M. and Bekeschus, S.

Journal: Advanced Science 2021, Volume 8, Start Page 2003395, ISSN: 2198-3844 (Electronic)/ 2198-3844 (Linking)

doi: 10.1002/advs.202003395

Author Contributions: S.B. and R.C. designed the study, analyzed the data, and wrote the manuscript. R.C., L.M., D.M., J.-W.L., U.M., E.F. and A.S. performed the experiments, R.C., L.M., D.M., J.-W.L., U.M., K.W. and S.B. analyzed the data, and reviewed the manuscript.

Ausweis der Eigenanteile:

Ramona Clemen hat die Experimente designt, geplant und durchgeführt. Sie hat in Kooperation mit Sander Bekeschus die Daten analysiert und interpretiert sowie das Manuskript geschrieben.

6.4. *ROS Cocktails as an Adjuvant for Personalized Antitumor Vaccination?*

Authors: Clemen, R. [1]; Bekeschus, S.[1]

Journal: Vaccines 2021, Volume 9, Start Page 527, ISSN: 2076-393X

doi: 10.3390/vaccines9050527

Author Contributions: Conceptualization, S.B. and R.C.; methodology, S.B. and R.C.; resources, S.B.; writing—original draft preparation, S.B. and R.C.; writing—review and editing, S.B. and R.C.; visualization, S.B. and R.C.; supervision, S.B.; project administration, S.B.

Ausweis der Eigenanteile:

Ramona Clemen wirkte bei der Erstellung dem Konzept des Übersichtsartikels und beim Schreiben des Manuskripts in Form von Rezension und Editierung mit.

_____	_____
Ramona Clemen	Michael Lalk

cancers

MDPI

Article

Physical Plasma-Treated Skin Cancer Cells Amplify Tumor Cytotoxicity of Human Natural Killer (NK) Cells

Ramona Clemen [1,†], Pepijn Heirman [1,2,†], Abraham Lin [2,3], Annemie Bogaerts [2] and Sander Bekeschus [1,*]

1 ZIK plasmatis, Leibniz Institute for Plasma Science and Technology (INP), Felix-Hausdorff-Str. 2, 17489 Greifswald, Germany; ramona.clemen@inp-greifswald.de (R.C.); pepijn.Heirman@student.uantwerpen.be (P.H.)
2 Research group PLASMANT, Department of Chemistry, University of Antwerp, Universiteitsplein 1, 2610 Antwerpen-Wilrijk, Belgium; abraham.lin@uantwerpen.be (A.L.); annemie.bogaerts@uantwerpen.be (A.B.)
3 Center for Oncological Research (CORE)–Integrated Personalized & Precision Oncology Network (IPPON), University of Antwerp, Universiteitsplein 1, 2610 Antwerpen-Wilrijk, Belgium
* Correspondence: sander.bekeschus@inp-greifswald.de
† These authors contributed equally to this paper as first authors.

Received: 9 October 2020; Accepted: 26 November 2020; Published: 30 November 2020

check for updates

Simple Summary: Natural killer (NK)-cells are known to have antitumor potential. Cold physical plasma generates ROS exogenously to be utilized as a novel anticancer agent, especially in skin cancer. However, it is unknown whether plasma-treated skin cancer cells promote or inhibit NK-cell-mediated toxicity. To this end, we analyzed NK-cell-activating receptors on plasma-treated skin cancer cells and demonstrated an enhanced NK-cell activity augmenting tumor cell death upon plasma treatment.

Abstract: Skin cancers have the highest prevalence of all human cancers, with the most lethal forms being squamous cell carcinoma and malignant melanoma. Besides the conventional local treatment approaches like surgery and radiotherapy, cold physical plasmas are emerging anticancer tools. Plasma technology is used as a therapeutic agent by generating reactive oxygen species (ROS). Evidence shows that inflammation and adaptive immunity are involved in cancer-reducing effects of plasma treatment, but the role of innate immune cells is still unclear. Natural killer (NK)-cells interact with target cells via activating and inhibiting surface receptors and kill in case of dominating activating signals. In this study, we investigated the effect of cold physical plasma (kINPen) on two skin cancer cell lines (A375 and A431), with non-malignant HaCaT keratinocytes as control, and identified a plasma treatment time-dependent toxicity that was more pronounced in the cancer cells. Plasma treatment also modulated the expression of activating and inhibiting receptors more profoundly in skin cancer cells compared to HaCaT cells, leading to significantly higher NK-cell killing rates in the tumor cells. Together with increased pro-inflammatory mediators such as IL-6 and IL-8, we conclude that plasma treatment spurs stress responses in skin cancer cells, eventually augmenting NK-cell activity.

Keywords: kINPen; NK-cells; plasma medicine; reactive oxygen species; ROS

1. Introduction

The immune system protects the body from pathogens and the damage they inflict. It is classically divided into innate immunity and adaptive immunity. The local inflammatory reaction of myeloid cells

carries out an early, innate immune response. They secret cytokines and chemokines to recruit immune cells such as natural killer cells (NK-cells) circulating in the blood. Evidence has shown that reactive oxygen species (ROS) are involved in inflammation, immune cell activation, and the modulation of the tissue microenvironment [1]. Similar findings were made in the tumor microenvironment [2], making ROS a putative target and treatment strategy in oncology [3].

Several technologies exploit the generation of ROS as anticancer agents, such as photodynamic therapy [4]. Another potent ROS-generating technology emerging as an anticancer tool is cold physical plasma [5]. This partially ionized gas is operated at body temperature and therefore does not inflict thermal damage within the target tissue. Several plasma technologies are accredited as medical products in Europe [6]. One type of plasma source is the atmospheric pressure plasma jet. Here, the working principle includes using a noble gas ionized within a high-frequency electrode shielded by a dielectric barrier [7]. The highly energetic noble gas molecules are subsequently expelled to the ambient air, reacting with oxygen and nitrogen to form reactive oxygen and nitrogen species, respectively [8]. With hundreds of chemical reactions taking place in the millisecond range, the redox chemistry in those plasma systems is highly complex and still subject to investigation [9,10]. Physical plasma treatment was shown to promote cell death in several tumor cell types, including skin cancer [11–14]. Additionally, we have previously shown an increased surface expression or release of calreticulin, ATP, and heat-shock proteins in plasma-treated tumor cells [15–17]. These molecules are important for triggering the activation of innate immune cells and the immunogenic cancer cell death (ICD) [18]. Subsequently, this can lead to enhanced immuno-protection upon plasma treatment in vivo [19–21]. However, the consequences of plasma-induced cancer cell death perceived by other types of innate immune cells, such as NK-cells, is unexplored.

NK-cells are lymphocytes and part of the innate immune system [22]. They can recognize virus-infected cells, tumor cells, and immunoglobulin-labeled cells [23] that are subsequently either ignored or lysed [24,25]. Unlike T-cells, which have specific receptors to interact with peptide-antigens presented by major histocompatibility complexes (MHC), NK-cells express germline-encoded receptors. Those receptors recognize evolutionary-conserved target structures expressed on the surface of infected, stressed, and malignantly transformed cells. To circumvent T-cell mediated tumor cell removal, cancer cells can downregulate MHC class I ("missing self"). This, however, leads to the activation of NK-cells since regular MHC-I expression inhibits NK-cell activity. Another hallmark of malignant transformation is the expression of stress-induced ligands ("stress-induced self") on the cell surface, which also activates NK-cells by binding to receptors on the NK-cell surface [22,24]. These include NKG2D that binds to stress-induced ligands of the MHC class I chain-related proteins (MIC A and MIC B; MIC A,B). Inhibiting NK-cell receptors recognize different types of MHC class I, i.e., various kinds of the killer immunoglobulin-like receptor (KIR) and the heterodimer of CD94 (NKG2A) [26,27]. Finally, the immune checkpoint receptor PD-1 is also expressed by NK-cells, resulting in a robust inhibitory signal upon binding to its ligand CD274 (PD-L1), frequently overexpressed on cancer cells [28]. Thus, NK-cell activation is triggered upon tipping the balance of inhibitory to activating signals on the target cell surface. Once NK-cells are activated, they secrete cytokines and release cytotoxic granule enzymes to initiate tumor cell killing [29].

In this study, we investigated the cytotoxic effects of cold physical plasma on two human skin cancer cell lines that were subsequently co-cultured with human peripheral blood-derived NK-cells. Using HaCaT keratinocytes as a non-malignant control cell line, we identified plasma treatment to potentiate NK-cell-mediated inactivation of tumor cells and to spur the release of inflammatory mediators.

2. Results

2.1. Plasma Treatment Inactivated Skin Cancer Cells and Modulated NK-Cell Ligand-Receptor Expression

We aimed at investigating the consequences of plasma-inactivated tumor cells on NK-cell activity. To this end, the effect of plasma treatment (Figure 1a) on the skin cancer cells (Figure 1b) alone was investigated first to identify suitable dose regimens using the kINPen plasma jet. Plasma treatment decreased the metabolic activity of the skin cancer cell lines A431 (Figure 1c) and A375 (Figure 1d) in a treatment time-dependent manner. To analyze the percentage of dead cells, flow cytometry was used (Figure 1e), which confirmed the cytotoxic effects in A431 (Figure 1f) and A375 (Figure 1g) cells 24 h after plasma treatment. Importantly, plasma-induced cytotoxicity in non-malignant HaCaT cells (Figure 1h) was much less pronounced when compared to results observed in the skin cancer cells (Figure 1f,g).

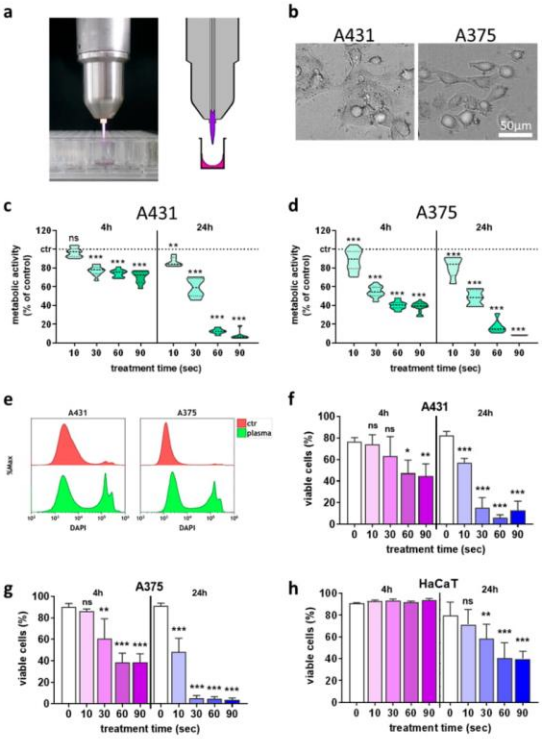

Figure 1. Plasma treatment inactivated skin cancer cells in a treatment time-dependent fashion. (**a**) atmospheric pressure argon plasma jet kINPen; (**b**) representative brightfield image of the two cancer cell types used in this study; (**c**,**d**) normalized metabolic activity 4 h and 24 h after plasma treatment in A431 (**c**) and A375 (**d**) cells; (**e**) representative overlay flow cytometry histograms of the terminal cell death dye DAPI in cells with and without plasma treatment at 24 h; (**f**–**h**) quantification of viable A431 (**f**), A375 (**g**), and HaCaT (**h**) cells using flow cytometry. Data are the mean of three independent experiments. Statistical analysis was performed using one-way ANOVA (* = $p < 0.01$, ** = $p < 0.01$, *** = $p < 0.001$). ns = not significant, ctr = control.

Next, the surface expression of several NK-cell-relevant ligands was investigated at 4 h and 24 h after plasma treatment using multi-color flow cytometry. The analysis of MIC A,B (Figure 2a) and HLA-A,B,C (Figure 2b) revealed a significant increase of the former (Figure 2c) and the latter (Figure 2d) in both A431 and A375 cells at 24 h post plasma exposure for extended treatment times. For HLA-E (Figure 2e) and PD-L1 (Figure 2f), a significant decrease in A431 and increase in A375 was found for HLA-E expression (Figure 2g), while no change was found in A431 for PD-L1 (Figure 2h). In A375, PD-L1 was upregulated when exposed to extended plasma treatment times. Only viable ($DAPI^-$) cells were used for data analysis, and no relevant changes were found in either of the cell lines at 4 h after plasma treatment. To compare these results against a non-malignant cell line, HaCaT keratinocytes were investigated for their expression of the same molecules following plasma exposure (Figure 2i). Besides a decrease in HLA-E at 24 h, no significant changes were observed for any of the remaining targets investigated (Figure 2j).

Altogether, a plasma treatment time-dependent cytotoxicity was observed in the skin cancer cell lines A375 and A431, while non-malignant HaCaT keratinocytes were less affected. At longer plasma treatment times, a significant modulation of NK-cell-relevant ligands was observed on the tumor cells' surface. As we aimed at investigating the crosstalk of viable tumor cells with human NK-cells to allow investigating additive toxicity, a moderate plasma treatment time (10 s) was used for subsequent co-culture experiments. In plasma-killed tumor cells, increased MIC A,B expression associated with stress responses was also found for plasma treatment times shorter than 60 s in A431 (Figure S1a) and A375 (Figure S1b) cells at 24 h.

2.2. *Plasma-Treated Tumor Cells Augmented NK-Cell-Mediated Toxicity*

The question of our study was whether plasma-treated cancer cells inhibit or augment NK-cell-mediated toxicity. To this end, plasma-treated skin cancer cells were incubated for 24 h, followed by the co-culture with human NK-cells at an effector-target-ratio of 1:1. Kinetic metabolic activity assays served to investigate the cytotoxic responses. In A431 cells (Figure 3a), the addition of NK-cells caused a greater decline of A431 metabolic activity in plasma-treated cells compared to untreated tumor cells (Figure 3b). In A375 cells (Figure 3c), a similar effect was observed (Figure 3d), suggesting an enhanced NK-cell activity against the plasma-treated cancer cells. In co-cultures of NK-cells with HaCaT keratinocytes (Figure 3e), such an augmented activity was not observed upon plasma treatment (Figure 3f). Using multiparametric fluorescence microscopy, a qualitative analysis of co-cultures confirmed that the decline of metabolic activity was related to cell death, as tumor cells (stage 1, t = 5 h after addition of NK-cells) upon contact with NK-cells (stage 2, t = 6; stage 3, t = 7 h) led to rapid terminal cell death (stage 4, t = 11 h) (Figure 3g). This notion of NK-cell-enhanced cytotoxicity in plasma-treated tumor cells was supported quantitatively by calculating the tumor cell to NK-cell ratios using absolute cell counting by flow cytometry 24 h after co-culture initiation (Figure 3h). These findings collectively suggest that plasma treatment inflicted stress in A375 and A431 skin cancer cells but not non-malignant HaCaT keratinocytes, leading to the enhanced recognition and killing of the tumor cells by NK-cells.

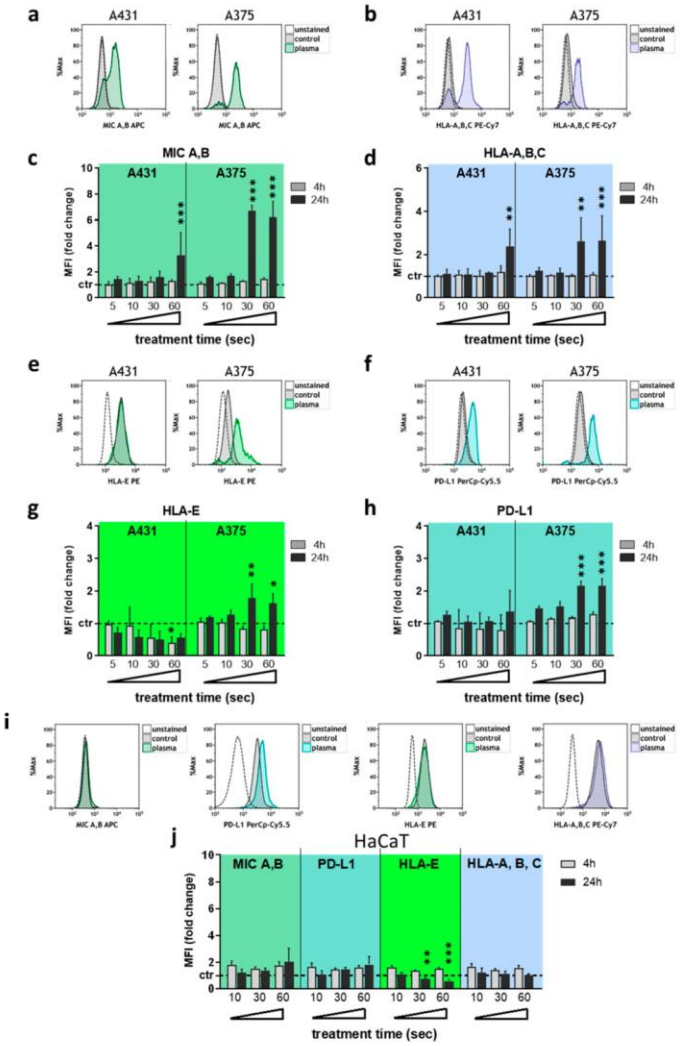

Figure 2. Plasma treatment modulated NK-cell ligand-receptor expression predominantly in malignant cells. (**a**–**d**) representative overlay flow cytometry histograms of MIC A,B (**a**) and HLA-A,B,C (**b**), and quantification and normalization of the MFI of MIC A,B (**c**) and HLA-A,B,C (**d**) in viable A431 and A375 cells at 4 h and 24 h after plasma treatment; (**e**–**h**) representative overlay flow cytometry histograms of HLA-E (**e**) and PD-L1 (**f**), and quantification and normalization of the MFI of HLA-E (**g**) and PD-L1 (**h**) in viable A431 and A375 cells at 4 h and 24 h after plasma treatment; (**i**,**j**) representative overlay flow cytometry histograms of MIC A,B, PD-L1, HLA-E, and HLA-A,B,C (**i**) and quantification and normalization of their corresponding MFI (**j**) in viable HaCaT cells at 4 h and 24 h after plasma treatment. Data are the mean of three independent experiments. Statistical analysis was performed using one-way ANOVA (* = $p < 0.01$, ** = $p < 0.01$, *** = $p < 0.001$). MFI = mean fluorescent intensity.

Cancers **2020**, *12*, 3575

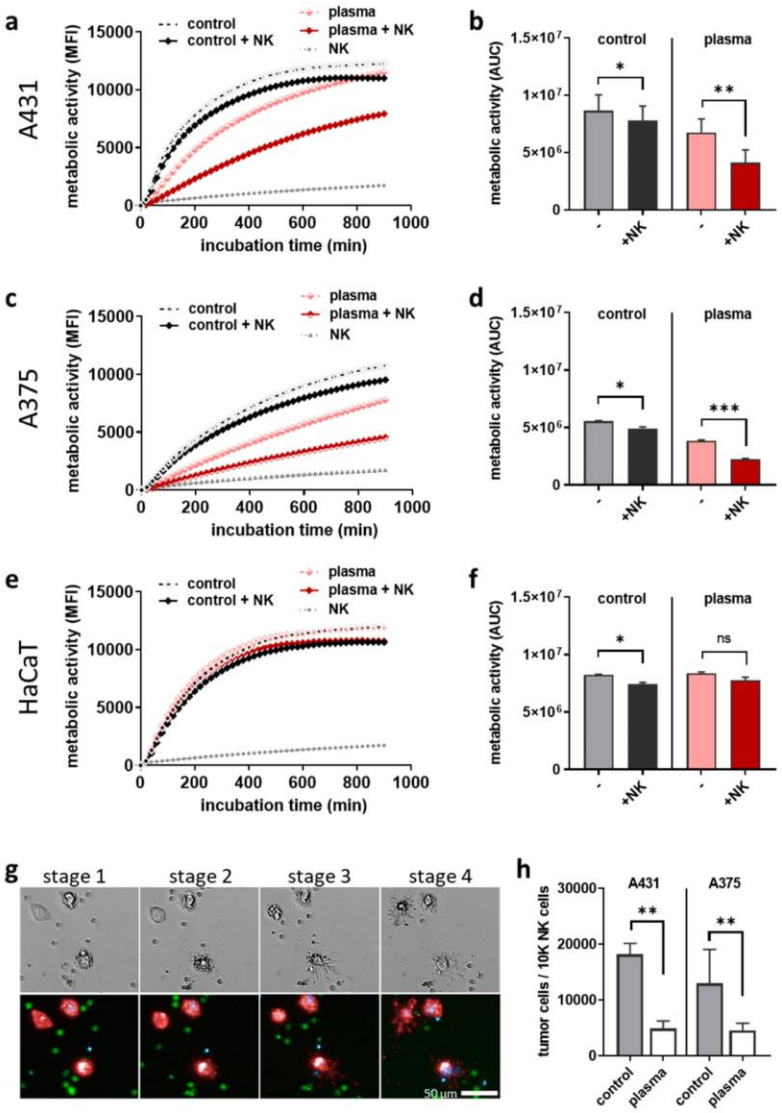

Figure 3. Plasma-treated tumor cells augmented NK-cell-mediated toxicity. (**a**–**f**) kinetic metabolic activity and the corresponding AUC in untreated and plasma-treated A431 (**a**,**b**), A375 (**c**,**d**), and HaCaT (**e**,**f**) cells in the absence or presence of NK-cells (effector-target-ratio 1:1); (**g**) representative brightfield (upper row) and fluorescence (lower row) images of co-culture with red-labeled tumor cells, green-labeled NK-cells, and blue-labeled dead cells; (**h**) tumor cell count normalized to NK-cell count at 24 h after initiation of co-cultures using flow cytometry. Data are the mean of three independent experiments. Statistical analysis was performed using one-way ANOVA (* = $p < 0.01$, ** = $p < 0.01$, *** = $p < 0.001$). ns = not significant, MFI = mean fluorescent intensity, AUC = area under the curve.

2.3. Plasma-Treated Tumor Cells Stimulated the Secretion of Inflammatory Mediators upon Co-Culture with NK-Cells

Activated NK-cells release cytotoxic granule enzymes to initiate killing and secret stimulatory cytokines to recruit immune cells (Figure 4a). To investigate NK-cell activation in co-cultures upon plasma treatment, we measured the concentration of granzyme B in supernatants at 4 h, 6 h, and 24 h (except for HaCaT only at 24 h). Granzyme B levels were increased in plasma-treated vs. untreated A431 cells, but not in A375 or HaCaT cells co-cultured with NK-cells (Figure 4b). Subsequently, we measured the secretion of several pro and anti-inflammatory cytokines 24 h after co-culture and shown as ratio of the co-culture concentration to the respective mono-culture concentration. A significant increase of interleukin (IL)-6 and IL-8 was observed for plasma treatment in A431 (Figure 4c) and A375 (Figure 4d) but not HaCaT (Figure 4e) cells. In general, plasma-treated HaCaT cells in co-culture with NK-cells did not show significant changes in the analytes' levels compared to co-cultures with untreated HaCaT cells. By contrast, significant elevation of Chemokine (C-C motif) ligands (CCL) 4 and tumor necrosis factor (TNF)-α was found in plasma conditions for A431, while in A375 co-culture supernatants, plasma treatment led to a significant increase in interferon (IFN)-γ and IL-2, whereas TNF-α levels declined. These findings suggested that plasma-treated skin cancer cells provoked a pro-inflammatory milieu when encountered by NK-cells.

2.4. H_2O_2 Treatment Did Not Replicate Results Observed with Plasma Treatment

Hydrogen peroxide (H_2O_2) is one of the most abundant ROS produced in plasma-treated liquids [30], but it is not always clear to which extent the findings with plasma treatment depend on the generation of this agent. Accordingly, the plasma generated H_2O_2 levels were quantified, and the concentration of 60 μM was equivalent to the 10 s of plasma treatment time used in the previous experiments (Figure 5a). The treatment of skin cancer cells with this concentration generated somewhat more cytotoxic responses in A431 after 24 h and A375 after 4 h (Figure 5b) compared to the corresponding plasma treatment time (solid lines). When investigating the ligand expression (Figure 5c), only MIC A,B differed significantly after H_2O_2 treatment. Kinetic metabolic activity assessment of NK-cells co-cultured with H_2O_2-treated A431 (Figure 5d) or A375 (Figure 5e) cells suggested H_2O_2 treatment to spur metabolic activity in skin cancer cells (Figure 5f), which is in stark contrast to findings with low-dose plasma treatment. The addition of NK-cells caused a reduced metabolic activity, suggesting some degree of cytotoxicity against the tumor cells. However, the amplitude of differences between samples with or without NK-cells and between untreated and H_2O_2-treated cells was smaller than in the plasma treatment regimens. These results suggested that H_2O_2 treatment yielded partially similar but not identical results in terms of cytotoxicity, surface marker expression, and consequences of co-culture in vitro with human NK-cells.

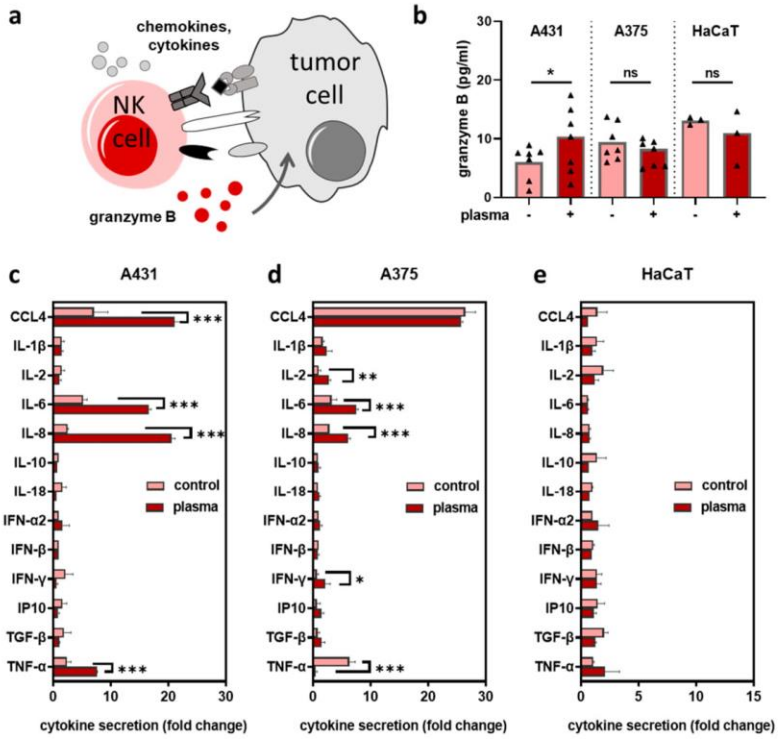

Figure 4. Plasma-treated skin tumor cells stimulated the secretion of inflammatory mediators upon co-culture with NK-cells. (**a**) simplified scheme and consequences of NK-cell-tumor cell interaction; (**b**) granzyme B quantification in supernatants of co-cultures (±plasma treatment) at 4 h, 6 h, and 24 h (A431 and A375) and 24 h (HaCaT); (**c**–**e**) quantification of cytokines in co-cultures in supernatants of untreated (vehicle) and plasma-treated A431 (**c**), A375 (**d**), and HaCaT (**e**) cells at 24 h as a ratio to the respective single tumor cell or HaCaT keratinocyte culture. Data are the mean of three independent experiments. Statistical analysis was performed using t-test or two-way ANOVA (* = $p < 0.01$, ** = $p < 0.01$, *** = $p < 0.001$, ns = not significant).

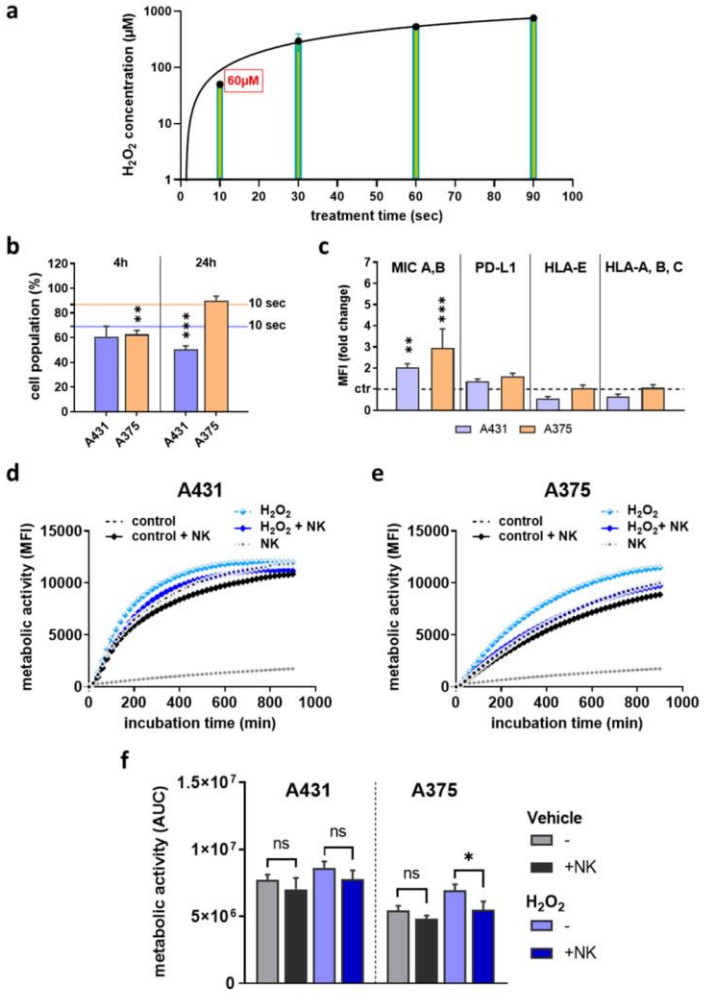

Figure 5. H_2O_2 treatment did not replicate the results observed with plasma treatment. (**a**) 10 s of plasma treatment yielded approximately 60 µM of H_2O_2 in solution, which was subsequently used as control treatment; (**b**) cell viability of A431 and A375 cells at 4 h and 24 h after H_2O_2 treatment as determined using flow cytometry; (**c**) quantification of the expression of surface markers MIC A,B, PD-L1, HLA-E, and HLA-A,B,C in viable cells 24 h after H_2O_2 treatment using flow cytometry; (**d**–**f**) H_2O_2-treated or untreated A431 (**d**) and A375 (**e**) cells in presence or absence of NK-cells, and kinetic assessment of metabolic activity as well as AUC (**f**) of the data over 15 h. Data are mean of three independent experiments. Statistical analysis was performed using one-way ANOVA or t-test (* = $p < 0.01$, ** = $p < 0.01$, *** = $p < 0.001$). ns = not significant, AUC = area under the curve, MFI = mean fluorescent intensity.

3. Discussion

In plasma medicine, oncology is a promising research field, and successful tumor reduction has already been observed in animal models and human patients suffering from endstage head and neck cancer [31,32]. Moreover, the exposure of cancer tissue to cold physical plasma was recently outlined to have an immunological dimension [33], but NK-cells have not been studied in the field of plasma medicine so far. To this end, we here investigated three human cell lines (two of malignant origin) and human peripheral blood-derived NK-cells to understand the immunomodulating consequences of plasma-treated skin cancer cells in co-culture with NK-cells

Plasma-treated skin cancer cells augmented NK-cells-mediated tumor cell inactivation. It is known that plasma jets, such as the kINPen, expel a plethora of ROS simultaneously [34] that, in an exogenous manner, subsequently target cells. Interestingly, the increase of surface marker expression, as, e.g., MIC A,B in response to extracellular ROS, has been described previously [35,36]. Investigating intracellular ROS generation using pharmacological (sulforaphane) or physical (ionizing radiation) agents was previously found to enhance NK-cell-mediated tumor cell lysis using several cancer cell lines [37]. Similar to our findings, the authors found an increase of the NKG2D ligand MIC A,B in tumor cells upon intracellular ROS increase. With plasma treatment, it is also established that extracellular ROS generation subsequently raises intracellular ROS levels [38]. Another study using sublethal doses of hematoporphyrin-based photodynamic therapy reached a similar conclusion based on elevated MIC A,B tumor cell expression in the context of ROS generation, and subsequently enhanced NK-cell-mediated killing [39]. However, it needs to be stressed that ROS severely impair NK-cell activity and survival, as IL-15-primed NK-cells upregulate thioredoxin activity to protect themselves from cytotoxic ROS in the tumor microenvironment (TME) [40]. This is in line with the notion that NK-cells are sensitive against ROS like hydrogen peroxide [41]. These aspects were incorporated in our study design by adding NK-cells to the plasma-treated tumor cells only at 24 h post-exposure, allowing the plasma-introduced ROS to deteriorate before NK-cell addition.

Besides MIC A,B, we have also investigated other effectors with a putative contribution to our findings. This includes HLA-A,B,C that can trigger NK-cell-activation when absent via KIR receptor ligation [42], but HLA-A,B,C expression was not substantially altered for the moderate plasma treatment time (10 s) investigated. HLA-E, an inhibitory ligand signaling via CD94/NKG2A, was found to be decreased upon selenite-induced oxidative stress and facilitated the enhanced NK-cell-mediated killing of tumor cells [43]. Moderate plasma treatment downregulated HLA-E in A431 but not A375 cells, which might be linked to the increased levels of granzyme B in supernatants of the co-culture with the former over the latter. For PD-L1, a potent NK-cell inhibitor upon ligation of PD-1 [44], plasma treatment showed no substantial increase at shorter treatment times, making its contribution to a more-than-average inhibition of NK-cells unlikely. In supernatants of co-cultures of NK-cells with either of the skin cancer cell lines but not HaCaT keratinocytes, we identified elevated IL-6 and IL-8 levels in plasma conditions. IL-8 was previously shown to be critical for NK-cell chemotaxis [45] and might have contributed to guide NK-cells to the tumor cells on a microscale in the co-culture conditions. Nevertheless, at least in colorectal cancer, the positive protective value of IL-8 and granzyme B levels in the TME is related to T-cells rather than NK-cells [46]. Due to multiple cell types producing IL-6 and its pleiotropic effects [47], an unambiguous role of the increased levels of IL-6 in the plasma conditions cannot be identified.

Studies using the kINPen so far have concluded that non-malignant tissue is affected only to a minor extent [48], with no adverse long-term side effects and including increased metastasis [49–51], and a lack of genotoxicity of the plasma treatment procedure [52,53]. The present study demonstrated that prolonged exposure to plasma drastically decreases viability and metabolic activity in two skin cancer cell lines. In contrast, the viability of non-malignant skin cells treated under the same conditions was far less affected. Changes in chemokine and cytokine release were observed for NK-cell co-cultures with skin cancer cells. Conversely, plasma treated non-malignant HaCaT cells showed neither an altered marker expression after plasma treatment nor an altered metabolism or cytokine profile in

co-culture with NK-cells. Both effects confirmed our hypothesis and indicated an immune-stimulating and tumor-specific impact of the plasma treatment as previously suggested and independent of NK-cells [54,55].

While we could not identify changes in one surface molecule that facilitated improved tumor surveillance, our data suggest several effectors at play. The NK-cell activation after target-cell engagement binding is determined by a balance between both activating and inhibiting signals. Our data suggest MIC A,B to be of paramount importance, as its role in NK-cell activation is well described, and its upregulation was found in our study. However, it cannot be solely responsible for the effects observed as it was also increased in plasma-treated HaCaT cells, which did not promote NK-cell activation. Besides, the fact that H_2O_2 treatment did not replicate the plasma effects supports the conclusion that other types of plasma-derived ROS or RNS [56] might be involved in explaining our findings. A likely possibility is that the plasma treatment modulated the expression of ligands other than the ones investigated in this study. A wide range of ligands and receptors contribute to the interaction between NK-cells and tumor cells [28]. This, together with exploring the role of NK-cells in plasma treatment in experimental tumor models in vivo, should be deciphered in future studies in more detail.

In our study, the epidermoid carcinoma A431 and the human melanoma cell line A375 were used, each with distinct activation pathways. A431 express abnormally high levels of the epidermal growth factor (EGF) receptor but are void of the tumor suppressor p53 [57]. The cells can differentiate through the JNK pathway [58]. As non-malignant cell line, we used HaCaT keratinocytes. The ROS treatment of those cells induced p53 and JNK phosphorylation as well as MAPK activation [59]. As for similarities, it was found that IFN-γ treatment induces MHC-I upregulation in both A431 and non-malignant keratinocytes [60]. Moreover, UVB treatment increases sestrin-1 in both HaCaT and A431 cells [61], which promotes AKT activation through a PTEN-related mechanism. The amelanotic A375 cells also harbor PTEN but differ from A431 as well as HaCaT cells in multiple ways, such as a highly aberrant expression of the putative oncogenic transcription factor NFAT [62] and the mutation profile (Figure S1c). Nevertheless, the plasma treatment showed overall similar effects in both cell lines, suggesting that their responses to oxidative stress might be related. The triad of A431, A375, and HaCaT keratinocytes has been used in multiple studies before demonstrating similar effects in A431 and A375 [63–66]. However, a limitation of our study was the lack of non-malignant primary melanocytes as a control for melanoma. Hence, the selectivity of the plasma treatment towards A375 cells could not be determined. Notwithstanding, it needs to be mentioned that the plasma therapy is a local, topical treatment. Other local treatments, such as cryoablation, photodynamic therapy, and electrochemotherapy, also come with a certain degree of collateral damage to non-malignant cells in the TME but still have been proven to be clinical efficacious in several cancer types [67–69]. Regardless, previous studies using other plasma devices have provided evidence of a selective toxicity of plasma treatment in malignant melanoma cells over non-malignant melanocytes [70,71], underlining the findings for non-melanoma skin cancer and HaCaT keratinocytes in the present study.

4. Experimental Section

4.1. Cell Culture and NK-Cell Isolation

The human epidermoid carcinoma cell line A431 (ATCC CRL-1555), the malignant melanoma cell line A375 (ATCC CRL-1619), and the non-malignant HaCaT keratinocyte cell line (CVCL-0038) were cultured in Roswell Park Memorial Institute (RPMI 1640; Corning, Kaiserslautern, Germany) medium containing 10% fetal bovine serum (Sigma-Aldrich, Hamburg, Germany), 1% glutamine (Corning), and 1% penicillin/streptomycin (Corning). The cells were grown in tissue-culture treated cell culture flasks (Sarstedt, Sarstedt, Germany) at 37 °C, 95% humidity, and 5% CO_2, and subcultured twice a week. Peripheral blood was obtained with informed consent from healthy donors as approved by the local ethics committee (approval number BB166/17). Peripheral blood mononuclear cells were isolated

as described before [72] via the Ficoll-Paque density gradient centrifugation method. Erythrocytes were lysed (RBC lysis buffer; BioLegend, Amsterdam, The Netherlands), and $CD56^+$ NK-cells were negatively selected via magnetic bead separation (BioLegend). The cells were washed and resuspended in fully supplemented cell culture medium.

4.2. Plasma Jet Treatment

Plasma treatment was performed using the atmospheric pressure plasma jet kINPen (neoplas, Greifswald, Germany) and argon (purity 99.9999%; Air Liquide, Paris, France) as carrier gas at a flow rate of two standard liters per min. The jet is extensively characterized [8], and the pin-type powered electrode was operated in a dielectric ceramic tube (inner diameter: 1.6 mm; outer diameter: 2.0 mm) with a grounded electrode at a frequency of 1 MHz. The distance from the exit to the nozzle tip is 3.5 mm. It has a dissipated power of 3.5 W. For the plasma treatment, 1×10^4 cells in 100 µL of fully supplemented cell culture medium were seeded in 96-well plates (Eppendorf, Hamburg, Germany) and treated with plasma in a standardized manner as described before [73]. For co-culture experiments, the medium of plasma-treated tumor cells was removed at 24 h, and 100 µL suspension containing 10^4 NK-cells was added to each well.

4.3. Metabolic Activity

Metabolic activity was measured in a multimode plate reader (Tecan, Männedorf, Switzerland) at λ_{ex} 535 nm and λ_{em} 590 nm, 4 h after resazurin (Alfa Aesar, Haverhill, MA, USA) was added to the cells at a final concentration of 100 µM. Resazurin was added directly after plasma treatment to determine metabolic activity at 4 h, or after 20 h to determine metabolic activity at 24 h. For co-culture experiments, resazurin was added, and kinetic measurements were performed in a multiplate plate reader heated to 37 °C and continuously flushed with 5% CO_2. Fluorescence was measured every 20 min over 15 h. To avoid excessive evaporation during this period, the outer cavity in the 96-well plate was filled with 6 mL of deionized water.

4.4. Flow Cytometry

Flow cytometry experiments were performed using a CytoFLEX LX device (Beckman-Coulter, Krefeld, Germany). Cell viability was determined using *CellEvent* Caspase 3/7 green detection agent (Thermo Fisher Scientific, Bremen, Germany) and 4',6-diamidino-2-phenylindole dihydrochloride (DAPI; BioLegend). Surface marker expression was investigated by incubating the cells with fluorochrome-conjugated antibodies (Table 1). Data analysis was performed using Kaluza 2.1 (Beckman-Coulter).

Table 1. Antibodies used in this study.

Ligand	Fluorochrome	Clone	Supplier
MIC A,B	APC	6D4	BioLegend
HLA-A,B,C	PE-Cy7	G46-2.6	BD Biosciences
HLA-E	PE	3D12	BioLegend
PD-L1	PerCP/Cyanine5.5	29E2A3	BioLegend

4.5. High Content Imaging

The imaging of co-cultures was performed using a high content imaging system (Operetta CLS; PerkinElmer, Hamburg, Germany) equipped with a 16-bit 4.7MP sCMOS camera and a 785 nm laser autofocus. After plasma treatment, skin cancer cells were stained with the red cell labeling dye Vybrant DiD (Invitrogen; Carlsbad, CA, USA) for 90 min at 37 °C and washed with PBS. The NK-cells were stained green by incubation in RPMI containing 100 nM Calcein AM (Invitrogen) for 30 min. A washing step was done before adding the NK-cells to the cancer cells with an effector-target-ratio of 1:1. Sytox blue dead cell stain (final concentration 0.5 µM; Invitrogen) was added to each well. 96-well

plates (Eppendorf) were used to facilitate imaging via a 20× water immersion objective (NA 1.0; Zeiss, Jena, Germany). Excitation and emission settings were λ_{ex} 475 nm and λ_{em} 548 ± 32 for Calcein AM, λ_{ex} 550 nm and λ_{em} 610 ± 40 for DiD red, and λ_{ex} 405 nm and λ_{em} 493 ± 23 for Sytox blue, respectively.

4.6. H_2O_2 Measurements

The concentration of H_2O_2 in plasma-treated medium without cells was measured using the Amplex Ultra Red reagent kit (Thermo Fisher Scientific) as described before [74].

4.7. Cytokine Measurement

Supernatants of single and co-cultured cells were collected after 24 h. Granzyme B secretion was measured using ELISA according to the manufacturer's instructions (BioLegend). Parallel quantification of a set of cytokines and chemokines was done using flow cytometry (CytoFLEX S; Beckman-Coulter) and LegendPlex technology (BioLegend) as described before [75].

4.8. Statistical Analysis

Graphing and statistical analysis were performed using *Prism* 9.0 (GraphPad Software, San Diego, CA, USA). Comparison of two groups was made using Student's t-test. The comparison of more than two groups was made using one-way analysis of variances (ANOVA). The comparison of more than two groups across different data sets was made using two-way ANOVA. Levels of significance were indicated as follows: $\alpha = 0.05$ (*), $\alpha = 0.01$ (**), $\alpha = 0.001$ (***).

5. Conclusions

Plasma-treated tumor cells augment NK-cell activity through the modulated expression of activating and inhibiting receptors. In comparison, plasma-treated HaCaT keratinocytes also showed altered expression but did not increase NK-cell activity.

Supplementary Materials: The following are available online at http://www.mdpi.com/2072-6694/12/12/3575/s1, Figure S1: (a,b) surface marker expression on dead A431 (a) and A375 (b) cells 4 h and 24 h after exposure to plasma as determined using flow cytometry; (c) VENN diagram of mutations in A431 cells as compared to A375 cells as retrieved from https://portals.broadinstitute.org/ccle. Data are mean of three independent experiments. Statistical analysis was performed using one-way ANOVA (* = $p < 0.01$, ** = $p < 0.01$, *** = $p < 0.001$). MFI = mean fluorescent intensity.

Author Contributions: Conceptualization, S.B.; Methodology, R.C. and P.H.; Software, R.C., P.H., and S.B.; Validation, R.C. and P.H.; Formal Analysis, P.H.; Investigation, R.C. and P.H.; Resources, S.B.; Data Curation, R.C. and P.H.; Writing—Original Draft Preparation, R.C. and S.B.; Writing—Review & Editing, R.C., P.H., A.L., A.B., and S.B.; Visualization, R.C. and P.H.; Supervision, A.B. and S.B.; Project Administration, R.C., A.L., and S.B.; Funding Acquisition, S.B. All authors have read and agreed to the published version of the manuscript.

Funding: This work was funded by the German Federal Ministry of Education and Research (BMBF), grant numbers 03Z22DN11 and 03Z22Di1. The funding source had no role in the design of this study or its execution, analyses, interpretation of the data, or decision to publish the results.

Acknowledgments: The authors acknowledge the technical assistance of Eric Freund, Julia Berner, Sanjeev Kumar Sagwal, Christina Wolff, Felix Niessner, Walison Brito, and Lea Miebach.

Conflicts of Interest: The authors declare no conflict of interest.

References

1. Mittal, M.; Siddiqui, M.R.; Tran, K.; Reddy, S.P.; Malik, A.B. Reactive oxygen species in inflammation and tissue injury. *Antioxid. Redox Signal.* **2014**, *20*, 1126–1167. [CrossRef] [PubMed]
2. Helfinger, V.; Schroder, K. Redox control in cancer development and progression. *Mol. Aspects Med.* **2018**, *63*, 88–98. [CrossRef] [PubMed]
3. Trachootham, D.; Alexandre, J.; Huang, P. Targeting cancer cells by ros-mediated mechanisms: A radical therapeutic approach? *Nat. Rev. Drug Discov.* **2009**, *8*, 579–591. [CrossRef] [PubMed]

4. Agostinis, P.; Berg, K.; Cengel, K.A.; Foster, T.H.; Girotti, A.W.; Gollnick, S.O.; Hahn, S.M.; Hamblin, M.R.; Juzeniene, A.; Kessel, D.; et al. Photodynamic therapy of cancer: An update. *CA Cancer J. Clin.* **2011**, *61*, 250–281. [CrossRef]
5. Dai, X.; Bazaka, K.; Richard, D.J.; Thompson, E.R.W.; Ostrikov, K.K. The emerging role of gas plasma in oncotherapy. *Trends Biotechnol.* **2018**, *36*, 1183–1198. [CrossRef]
6. Bekeschus, S.; Schmidt, A.; Weltmann, K.-D.; von Woedtke, T. The plasma jet kinpen—A powerful tool for wound healing. *Clin. Plas. Med.* **2016**, *4*, 19–28. [CrossRef]
7. Winter, J.; Brandenburg, R.; Weltmann, K.D. Atmospheric pressure plasma jets: An overview of devices and new directions. *Plasma Sources Sci. Technol.* **2015**, *24*, 064001. [CrossRef]
8. Reuter, S.; von Woedtke, T.; Weltmann, K.D. The kinpen-a review on physics and chemistry of the atmospheric pressure plasma jet and its applications. *J. Phys. D Appl. Phys.* **2018**, *51*. [CrossRef]
9. Viegas, P.; Bourdon, A. Numerical study of jet–target interaction: Influence of dielectric permittivity on the electric field experienced by the target. *Plasma Chem. Plasma Process.* **2019**, *40*, 661–683. [CrossRef]
10. Liu, Z.; Xu, D.; Zhou, C.; Cui, Q.; He, T.; Chen, Z.; Liu, D.; Chen, H.; Kong, M.G. Effects of the pulse polarity on helium plasma jets: Discharge characteristics, key reactive species, and inactivation of myeloma cell. *Plasma Chem. Plasma Process.* **2018**, *38*, 953–968. [CrossRef]
11. Binenbaum, Y.; Ben-David, G.; Gil, Z.; Slutsker, Y.Z.; Ryzhkov, M.A.; Felsteiner, J.; Krasik, Y.E.; Cohen, J.T. Cold atmospheric plasma, created at the tip of an elongated flexible capillary using low electric current, can slow the progression of melanoma. *PLoS ONE* **2017**, *12*, e0169457. [CrossRef] [PubMed]
12. Bekeschus, S.; Eisenmann, S.; Sagwal, S.K.; Bodnar, Y.; Moritz, J.; Poschkamp, B.; Stoffels, I.; Emmert, S.; Madesh, M.; Weltmann, K.D.; et al. Xct (slc7a11) expression confers intrinsic resistance to physical plasma treatment in tumor cells. *Redox Biol.* **2020**, *30*, 101423. [CrossRef] [PubMed]
13. Guerrero-Preston, R.; Ogawa, T.; Uemura, M.; Shumulinsky, G.; Valle, B.L.; Pirini, F.; Ravi, R.; Sidransky, D.; Keidar, M.; Trink, B. Cold atmospheric plasma treatment selectively targets head and neck squamous cell carcinoma cells. *Int. J. Mol. Med.* **2014**, *34*, 941–946. [CrossRef]
14. Welz, C.; Emmert, S.; Canis, M.; Becker, S.; Baumeister, P.; Shimizu, T.; Morfill, G.E.; Harreus, U.; Zimmermann, J.L. Cold atmospheric plasma: A promising complementary therapy for squamous head and neck cancer. *PLoS ONE* **2015**, *10*, e0141827. [CrossRef]
15. Bekeschus, S.; Rodder, K.; Fregin, B.; Otto, O.; Lippert, M.; Weltmann, K.D.; Wende, K.; Schmidt, A.; Gandhirajan, R.K. Toxicity and immunogenicity in murine melanoma following exposure to physical plasma-derived oxidants. *Oxid. Med. Cell. Longev.* **2017**, *2017*, 4396467. [CrossRef]
16. Lin, A.; Truong, B.; Patel, S.; Kaushik, N.; Choi, E.H.; Fridman, G.; Fridman, A.; Miller, V. Nanosecond-pulsed dbd plasma-generated reactive oxygen species trigger immunogenic cell death in a549 lung carcinoma cells through intracellular oxidative stress. *Int. J. Mol. Sci.* **2017**, *18*, 966. [CrossRef]
17. Pasqual-Melo, G.; Sagwal, S.K.; Freund, E.; Gandhirajan, R.K.; Frey, B.; von Woedtke, T.; Gaipl, U.; Bekeschus, S. Combination of gas plasma and radiotherapy has immunostimulatory potential and additive toxicity in murine melanoma cells in vitro. *Int. J. Mol. Sci.* **2020**, *21*, 1379. [CrossRef]
18. Galluzzi, L.; Buque, A.; Kepp, O.; Zitvogel, L.; Kroemer, G. Immunogenic cell death in cancer and infectious disease. *Nat. Rev. Immunol.* **2017**, *17*, 97–111. [CrossRef]
19. Lin, A.G.; Xiang, B.; Merlino, D.J.; Baybutt, T.R.; Sahu, J.; Fridman, A.; Snook, A.E.; Miller, V. Non-thermal plasma induces immunogenic cell death in vivo in murine ct26 colorectal tumors. *Oncoimmunology* **2018**, *7*, e1484978. [CrossRef]
20. Bekeschus, S.; Clemen, R.; Niessner, F.; Sagwal, S.K.; Freund, E.; Schmidt, A. Medical gas plasma jet technology targets murine melanoma in an immunogenic fashion. *Adv. Sci.* **2020**, *7*, 1903438. [CrossRef]
21. Lin, A.; Gorbanev, Y.; De Backer, J.; Van Loenhout, J.; Van Boxem, W.; Lemiere, F.; Cos, P.; Dewilde, S.; Smits, E.; Bogaerts, A. Non-thermal plasma as a unique delivery system of short-lived reactive oxygen and nitrogen species for immunogenic cell death in melanoma cells. *Adv. Sci.* **2019**, *6*, 1802062. [CrossRef] [PubMed]
22. Vivier, E.; Ugolini, S.; Blaise, D.; Chabannon, C.; Brossay, L. Targeting natural killer cells and natural killer t cells in cancer. *Nat. Rev. Immunol.* **2012**, *12*, 239–252. [CrossRef] [PubMed]
23. Vivier, E.; Tomasello, E.; Baratin, M.; Walzer, T.; Ugolini, S. Functions of natural killer cells. *Nat. Immunol.* **2008**, *9*, 503–510. [CrossRef] [PubMed]

24. Waldhauer, I.; Steinle, A. Nk cells and cancer immunosurveillance. *Oncogene* **2008**, *27*, 5932–5943. [CrossRef] [PubMed]
25. Vitale, M.; Cantoni, C.; Pietra, G.; Mingari, M.C.; Moretta, L. Effect of tumor cells and tumor microenvironment on nk-cell function. *Eur. J. Immunol.* **2014**, *44*, 1582–1592. [CrossRef] [PubMed]
26. Chester, C.; Fritsch, K.; Kohrt, H.E. Natural killer cell immunomodulation: Targeting activating, inhibitory, and co-stimulatory receptor signaling for cancer immunotherapy. *Front. Immunol.* **2015**, *6*, 601. [CrossRef]
27. Pegram, H.J.; Andrews, D.M.; Smyth, M.J.; Darcy, P.K.; Kershaw, M.H. Activating and inhibitory receptors of natural killer cells. *Immunol. Cell. Biol.* **2011**, *89*, 216–224. [CrossRef]
28. Del Zotto, G.; Marcenaro, E.; Vacca, P.; Sivori, S.; Pende, D.; Della Chiesa, M.; Moretta, F.; Ingegnere, T.; Mingari, M.C.; Moretta, A.; et al. Markers and function of human nk cells in normal and pathological conditions. *Cytom. B Clin. Cytom.* **2017**, *92*, 100–114. [CrossRef]
29. Guillerey, C.; Smyth, M.J. Nk cells and cancer immunoediting. *Curr. Top. Microbiol. Immunol.* **2016**, *395*, 115–145. [CrossRef]
30. Bekeschus, S.; Kolata, J.; Winterbourn, C.; Kramer, A.; Turner, R.; Weltmann, K.D.; Broker, B.; Masur, K. Hydrogen peroxide: A central player in physical plasma-induced oxidative stress in human blood cells. *Free Radic. Res.* **2014**, *48*, 542–549. [CrossRef]
31. Metelmann, H.-R.; Seebauer, C.; Miller, V.; Fridman, A.; Bauer, G.; Graves, D.B.; Pouvesle, J.-M.; Rutkowski, R.; Schuster, M.; Bekeschus, S.; et al. Clinical experience with cold plasma in the treatment of locally advanced head and neck cancer. *Clin. Plasma Med.* **2018**, *9*, 6–13. [CrossRef]
32. Metelmann, H.R.; Seebauer, C.; Rutkowski, R.; Schuster, M.; Bekeschus, S.; Metelmann, P. Treating cancer with cold physical plasma: On the way to evidence-based medicine. *Contrib. Plasma Phys.* **2018**, *58*, 415–419. [CrossRef]
33. Witzke, K.; Seebauer, C.; Jesse, K.; Kwiatek, E.; Berner, J.; Semmler, M.L.; Boeckmann, L.; Emmert, S.; Weltmann, K.D.; Metelmann, H.R.; et al. Plasma medical oncology: Immunological interpretation of head and neck squamous cell carcinoma. *Plasma Process. Polym.* **2020**, *17*, e1900258. [CrossRef]
34. Dunnbier, M.; Schmidt-Bleker, A.; Winter, J.; Wolfram, M.; Hippler, R.; Weltmann, K.D.; Reuter, S. Ambient air particle transport into the effluent of a cold atmospheric-pressure argon plasma jet investigated by molecular beam mass spectrometry. *J. Phys. D Appl. Phys.* **2013**, *46*, 435203. [CrossRef]
35. Yamamoto, K.; Fujiyama, Y.; Andoh, A.; Bamba, T.; Okabe, H. Oxidative stress increases mica and micb gene expression in the human colon carcinoma cell line (caco-2). *Biochim. Biophys. Acta* **2001**, *1526*, 10–12. [CrossRef]
36. Kotsafti, A.; Scarpa, M.; Castagliuolo, I.; Scarpa, M. Reactive oxygen species and antitumor immunity-from surveillance to evasion. *Cancers* **2020**, *12*, 1748. [CrossRef]
37. Amin, P.J.; Shankar, B.S. Sulforaphane induces ros mediated induction of nkg2d ligands in human cancer cell lines and enhances susceptibility to nk cell mediated lysis. *Life Sci.* **2015**, *126*, 19–27. [CrossRef]
38. Graves, D.B. The emerging role of reactive oxygen and nitrogen species in redox biology and some implications for plasma applications to medicine and biology. *J. Phys. D Appl. Phys.* **2012**, *45*, 263001. [CrossRef]
39. Park, M.J.; Bae, J.H.; Chung, J.S.; Kim, S.H.; Kang, C.D. Induction of nkg2d ligands and increased sensitivity of tumor cells to nk cell-mediated cytotoxicity by hematoporphyrin-based photodynamic therapy. *Immunol. Investig.* **2011**, *40*, 367–382. [CrossRef]
40. Yang, Y.; Neo, S.Y.; Chen, Z.; Cui, W.; Chen, Y.; Guo, M.; Wang, Y.; Xu, H.; Kurzay, A.; Alici, E.; et al. Thioredoxin activity confers resistance against oxidative stress in tumor-infiltrating nk cells. *J. Clin. Investig.* **2020**, *130*, 5508–5522. [CrossRef]
41. Harlin, H.; Hanson, M.; Johansson, C.C.; Sakurai, D.; Poschke, I.; Norell, H.; Malmberg, K.J.; Kiessling, R. The cd16- cd56(bright) nk cell subset is resistant to reactive oxygen species produced by activated granulocytes and has higher antioxidative capacity than the cd16+ cd56(dim) subset. *J. Immunol.* **2007**, *179*, 4513–4519. [CrossRef] [PubMed]
42. Karre, K. Nk cells, mhc class i molecules and the missing self. *Scand. J. Immunol.* **2002**, *55*, 221–228. [CrossRef] [PubMed]
43. Enqvist, M.; Nilsonne, G.; Hammarfjord, O.; Wallin, R.P.; Bjorkstrom, N.K.; Bjornstedt, M.; Hjerpe, A.; Ljunggren, H.G.; Dobra, K.; Malmberg, K.J.; et al. Selenite induces posttranscriptional blockade of hla-e expression and sensitizes tumor cells to cd94/nkg2a-positive nk cells. *J. Immunol.* **2011**, *187*, 3546–3554. [CrossRef] [PubMed]

44. Oyer, J.L.; Gitto, S.B.; Altomare, D.A.; Copik, A.J. Pd-l1 blockade enhances anti-tumor efficacy of nk cells. *Oncoimmunology* **2018**, *7*, e1509819. [CrossRef]
45. Vujanovic, L.; Ballard, W.; Thorne, S.H.; Vujanovic, N.L.; Butterfield, L.H. Adenovirus-engineered human dendritic cells induce natural killer cell chemotaxis via cxcl8/il-8 and cxcl10/ip-10. *OncoImmunology* **2014**, *1*, 448–457. [CrossRef]
46. Halama, N.; Braun, M.; Kahlert, C.; Spille, A.; Quack, C.; Rahbari, N.; Koch, M.; Weitz, J.; Kloor, M.; Zoernig, I.; et al. Natural killer cells are scarce in colorectal carcinoma tissue despite high levels of chemokines and cytokines. *Clin. Cancer Res.* **2011**, *17*, 678–689. [CrossRef]
47. Johnson, D.E.; O'Keefe, R.A.; Grandis, J.R. Targeting the il-6/jak/stat3 signalling axis in cancer. *Nat. Rev. Clin. Oncol.* **2018**, *15*, 234–248. [CrossRef]
48. Hasse, S.; Seebauer, C.; Wende, K.; Schmidt, A.; Metelmann, H.R.; von Woedtke, T.; Bekeschus, S. Cold argon plasma as adjuvant tumour therapy on progressive head and neck cancer: A preclinical study. *Appl. Sci.* **2019**, *9*, 2061. [CrossRef]
49. Schmidt, A.; Woedtke, T.V.; Stenzel, J.; Lindner, T.; Polei, S.; Vollmar, B.; Bekeschus, S. One year follow-up risk assessment in skh-1 mice and wounds treated with an argon plasma jet. *Int. J. Mol. Sci.* **2017**, *18*, 868. [CrossRef]
50. Hasse, S.; Meder, T.; Freund, E.; von Woedtke, T.; Bekeschus, S. Plasma treatment limits human melanoma spheroid growth and metastasis independent of the ambient gas composition. *Cancers* **2020**, *12*, 2570. [CrossRef]
51. Bekeschus, S.; Freund, E.; Spadola, C.; Privat-Maldonado, A.; Hackbarth, C.; Bogaerts, A.; Schmidt, A.; Wende, K.; Weltmann, K.D.; von Woedtke, T.; et al. Risk assessment of kinpen plasma treatment of four human pancreatic cancer cell lines with respect to metastasis. *Cancers* **2019**, *11*, 1237. [CrossRef] [PubMed]
52. Bekeschus, S.; Schmidt, A.; Kramer, A.; Metelmann, H.R.; Adler, F.; von Woedtke, T.; Niessner, F.; Weltmann, K.D.; Wende, K. High throughput image cytometry micronucleus assay to investigate the presence or absence of mutagenic effects of cold physical plasma. *Environ. Mol. Mutagen.* **2018**, *59*, 268–277. [CrossRef] [PubMed]
53. Kluge, S.; Bekeschus, S.; Bender, C.; Benkhai, H.; Sckell, A.; Below, H.; Stope, M.B.; Kramer, A. Investigating the mutagenicity of a cold argon-plasma jet in an het-mn model. *PLoS ONE* **2016**, *11*, e0160667. [CrossRef] [PubMed]
54. Khalili, M.; Daniels, L.; Lin, A.; Krebs, F.C.; Snook, A.E.; Bekeschus, S.; Bowne, W.B.; Miller, V. Non-thermal plasma-induced immunogenic cell death in cancer: A topical review. *J. Phys. D Appl. Phys.* **2019**, *52*. [CrossRef]
55. Privat-Maldonado, A.; Schmidt, A.; Lin, A.; Weltmann, K.D.; Wende, K.; Bogaerts, A.; Bekeschus, S. Ros from physical plasmas: Redox chemistry for biomedical therapy. *Oxid. Med. Cell. Longev.* **2019**, *2019*, 9062098. [CrossRef]
56. Wende, K.; von Woedtke, T.; Weltmann, K.D.; Bekeschus, S. Chemistry and biochemistry of cold physical plasma derived reactive species in liquids. *Biol. Chem.* **2018**, *400*, 19–38. [CrossRef]
57. Graness, A.; Hanke, S.; Boehmer, F.D.; Presek, P.; Liebmann, C. Protein-tyrosine-phosphatase-mediated epidermal growth factor (egf) receptor transinactivation and egf receptor-independent stimulation of mitogen-activated protein kinase by bradykinin in a431 cells. *Biochem. J.* **2000**, *347*, 441–447. [CrossRef]
58. Alameda, J.P.; Fernandez-Acenero, M.J.; Moreno-Maldonado, R.; Navarro, M.; Quintana, R.; Page, A.; Ramirez, A.; Bravo, A.; Casanova, M.L. Cyld regulates keratinocyte differentiation and skin cancer progression in humans. *Cell Death Dis.* **2011**, *2*, e208. [CrossRef]
59. Schmidt, A.; Bekeschus, S.; Jarick, K.; Hasse, S.; von Woedtke, T.; Wende, K. Cold physical plasma modulates p53 and mitogen-activated protein kinase signaling in keratinocytes. *Oxid. Med. Cell. Longev.* **2019**, *2019*, 1–16. [CrossRef]
60. Pollack, B.P.; Sapkota, B.; Cartee, T.V. Epidermal growth factor receptor inhibition augments the expression of mhc class i and ii genes. *Clin. Cancer Res.* **2011**, *17*, 4400–4413. [CrossRef]
61. Zhao, B.; Shah, P.; Budanov, A.V.; Qiang, L.; Ming, M.; Aplin, A.; Sims, D.M.; He, Y.Y. Sestrin2 protein positively regulates akt enzyme signaling and survival in human squamous cell carcinoma and melanoma cells. *J. Biol. Chem.* **2014**, *289*, 35806–35814. [CrossRef] [PubMed]

62. Xiao, T.; Zhu, J.J.; Huang, S.; Peng, C.; He, S.; Du, J.; Hong, R.; Chen, X.; Bode, A.M.; Jiang, W.; et al. Phosphorylation of nfat3 by cdk3 induces cell transformation and promotes tumor growth in skin cancer. *Oncogene* **2017**, *36*, 2835–2845. [CrossRef] [PubMed]
63. Mantso, T.; Trafalis, D.T.; Botaitis, S.; Franco, R.; Pappa, A.; Rupasinghe, H.P.V.; Panayiotidis, M.I. Novel docosahexaenoic acid ester of phloridzin inhibits proliferation and triggers apoptosis in an in vitro model of skin cancer. *Antioxidants* **2018**, *7*. 188. [CrossRef]
64. Hopkins, S.L.; Siewert, B.; Askes, S.H.; Veldhuizen, P.; Zwier, R.; Heger, M.; Bonnet, S. An in vitro cell irradiation protocol for testing photopharmaceuticals and the effect of blue, green, and red light on human cancer cell lines. *Photochem. Photobiol. Sci.* **2016**, *15*, 644–653. [CrossRef]
65. Mantso, T.; Vasileiadis, S.; Anestopoulos, I.; Voulgaridou, G.P.; Lampri, E.; Botaitis, S.; Kontomanolis, E.N.; Simopoulos, C.; Goussetis, G.; Franco, R.; et al. Hyperthermia induces therapeutic effectiveness and potentiates adjuvant therapy with non-targeted and targeted drugs in an in vitro model of human malignant melanoma. *Sci. Rep.* **2018**, *8*, 10724. [CrossRef]
66. Kang, T.H.; Yoon, G.; Kang, I.A.; Oh, H.N.; Chae, J.I.; Shim, J.H. Natural compound licochalcone b induced extrinsic and intrinsic apoptosis in human skin melanoma (a375) and squamous cell carcinoma (a431) cells. *Phytother. Res.* **2017**, *31*, 1858–1867. [CrossRef]
67. Haen, S.P.; Pereira, P.L.; Salih, H.R.; Rammensee, H.G.; Gouttefangeas, C. More than just tumor destruction: Immunomodulation by thermal ablation of cancer. *Clin. Dev. Immunol.* **2011**, *2011*, 160250. [CrossRef]
68. Castano, A.P.; Mroz, P.; Hamblin, M.R. Photodynamic therapy and anti-tumour immunity. *Nat. Rev. Cancer* **2006**, *6*, 535–545. [CrossRef]
69. Kreuter, A.; van Eijk, T.; Lehmann, P.; Fischer, M.; Horn, T.; Assaf, C.; Schley, G.; Herbst, R.; Kellner, I.; Weisbrich, C.; et al. Electrochemotherapy in advanced skin tumors and cutaneous metastases—A retrospective multicenter analysis. *J. Dtsch. Dermatol. Ges.* **2015**, *13*, 308–315. [CrossRef]
70. Arndt, S.; Wacker, E.; Li, Y.F.; Shimizu, T.; Thomas, H.M.; Morfill, G.E.; Karrer, S.; Zimmermann, J.L.; Bosserhoff, A.K. Cold atmospheric plasma, a new strategy to induce senescence in melanoma cells. *Exp. Dermatol.* **2013**, *22*, 284–289. [CrossRef]
71. Biscop, E.; Lin, A.; Boxem, W.V.; Loenhout, J.V.; Backer, J.; Deben, C.; Dewilde, S.; Smits, E.; Bogaerts, A.A. Influence of cell type and culture medium on determining cancer selectivity of cold atmospheric plasma treatment. *Cancers* **2019**, *11*. 1287. [CrossRef] [PubMed]
72. Bekeschus, S.; Masur, K.; Kolata, J.; Wende, K.; Schmidt, A.; Bundscherer, L.; Barton, A.; Kramer, A.; Broker, B.; Weltmann, K.D. Human mononuclear cell survival and proliferation is modulated by cold atmospheric plasma jet. *Plasma Process. Polym.* **2013**, *10*, 706–713. [CrossRef]
73. Bekeschus, S.; Schmidt, A.; Niessner, F.; Gerling, T.; Weltmann, K.D.; Wende, K. Basic research in plasma medicine—A throughput approach from liquids to cells. *J. Vis. Exp.* **2017**, e56331. [CrossRef] [PubMed]
74. Freund, E.; Liedtke, K.R.; Gebbe, R.; Heidecke, A.K.; Partecke, L.-I.; Bekeschus, S. In vitro anticancer efficacy of six different clinically approved types of liquids exposed to physical plasma. *IEEE Trans. Rad. Plas. Med. Sc.* **2019**, *3*, 588–596. [CrossRef]
75. Freund, E.; Moritz, J.; Stope, M.; Seebauer, C.; Schmidt, A.; Bekeschus, S. Plasma-derived reactive species shape a differentiation profile in human monocytes. *Appl. Sci.* **2019**, *9*. 2530. [CrossRef]

FULL PAPER

ADVANCED SCIENCE Open Access

www.advancedscience.com

Medical Gas Plasma Jet Technology Targets Murine Melanoma in an Immunogenic Fashion

Sander Bekeschus, Ramona Clemen, Felix Nießner, Sanjeev Kumar Sagwal, Eric Freund, and Anke Schmidt*

Medical technologies from physics are imperative in the diagnosis and therapy of many types of diseases. In 2013, a novel cold physical plasma treatment concept was accredited for clinical therapy. This gas plasma jet technology generates large amounts of different reactive oxygen and nitrogen species (ROS). Using a melanoma model, gas plasma technology is tested as a novel anticancer agent. Plasma technology derived ROS diminish tumor growth in vitro and in vivo. Varying the feed gas mixture modifies the composition of ROS. Conditions rich in atomic oxygen correlate with killing activity and elevate intratumoral immune-infiltrates of $CD8^+$ cytotoxic T-cells and dendritic cells. T-cells from secondary lymphoid organs of these mice stimulated with B16 melanoma cells ex vivo show higher activation levels as well. This correlates with immunogenic cancer cell death and higher calreticulin and heat-shock protein 90 expressions induced by gas plasma treatment in melanoma cells. To test the immunogenicity of gas plasma treated melanoma cells, 50% of mice vaccinated with these cells are protected from tumor growth compared to 1/6 and 5/6 mice negative control (mitomycin C) and positive control (mitoxantrone), respectively. Gas plasma jet technology is concluded to provide immunoprotection against malignant melanoma both in vitro and in vivo.

1. Introduction

Medical technologies from physics are irreplaceable for both diagnosis and therapy of many types of diseases. For instance, ionizing radiation still is the first-line treatment in several types of cancers.[1] Similarly, the concept of photodynamic therapy that is based mainly on the local production of singlet delta oxygen is used for the treatment of several malignant disorders.[2] In 2013, a novel physics-based therapy was added to the array of accredited therapies based on physics: medical plasma technology.[3] This technology mainly acts via deposition of a plethora of different reactive oxygen and nitrogen species (ROS) deposited locally into the target tissue[4] without causing thermal damage.[5] The current indication of medical plasma therapy is to promote beneficial effects on the healing of chronic wounds and ulcers, apart from other dermatological indications.[6] Strikingly, antitumor efficacy in head and neck cancer patients suggested plasma treatment to have a role in oncology as well.[7] The concept linking these seemingly unrelated effects of stimulation of healing in non-healing wounds on the one hand, and killing of tumor cells on the other hand is termed hormesis. ROS are a prime class of hormetically acting molecules that are stimulating molecules in intracellular signaling at low concentrations while having cytotoxic effects at higher concentrations.[8] However, the species that are produced via gas plasmas are not necessarily the species that directly act on cells on tissues directly.[4] Instead, secondary products and ROS derived from the primary ROS generated by plasmas are more likely to be the biological effectors[8] that may also have immunological consequences.[9]

It is known not only since the Nobel Prize for Medicine or Physiology awarded in 2018 to checkpoint immunotherapy that the immune system plays a pivotal role in antitumor responses in patients.[10] In particular, T-cells are critical in selectively targeting malignant over non-malignant cells.[11] A prerequisite of antitumor T-cell immunity is the availability of tumor antigens as well as a pro-immunogenic context in which these antigens are displayed. Already, a decade ago, Obeid and colleagues discovered calreticulin (CRT) exposure to be vital in dictating the immunogenicity of tumor cell death.[12] Accordingly, the recently reviewed paradigm of immunogenic cancer cell death (ICD) postulates that not only the event of cell death but also its inflammatory context is decisive for the immune system responding to dying tumor cells in a tolerogenic or immunogenic fashion.[13]

The first tumor entity showing the importance of anticancer immunity and checkpoint therapy is malignant melanoma.[14] Melanoma is particularly stimulating to the immune system due to its extraordinary high mutation rate, which leads to the formation of several cancer-neoantigens.[15] Melanoma is therefore considered as model tumor when investigating novel

Dr. S. Bekeschus, R. Clemen, F. Nießner, S. K. Sagwal, E. Freund, Dr. A. Schmidt
ZIK plasmatis
Leibniz Institute for Plasma Science and Technology (INP Greifswald)
Felix-Hausdorff-Str. 3, Greifswald 17489, Germany
E-mail: sander.bekeschus@inp-greifswald.de

The ORCID identification number(s) for the author(s) of this article can be found under https://doi.org/10.1002/advs.201903438.

DOI: 10.1002/advs.201903438

therapeutic concepts linked to anticancer immunity.[16] To this end, we investigated and confirmed both the efficacy and the immunogenicity of medical gas plasma treatment in an experimental model of syngeneic melanoma. To provide a measure of the degree of immunogenicity of the gas plasma treatment, we used a poorly immunogenic drug (mitomycin C) and a highly immunogenic drug (mitoxantrone) as reference treatments as outlined in a previous study.[12]

2. Results

2.1. Plasma Jet Treatment Oxidized and Killed Melanoma Cells by Gas Phase Derived ROS

Medical gas plasma jet technology generates different types of ROS simultaneously (**Figure 1**a). These ROS were capable of oxidizing murine B16F10 melanoma cells (Figure 1b) to a significant extent when compared to that of untreated cells (Figure 1c). Analyzing the metabolic activity of gas plasma jet treated melanoma cells (Figure 1d), a treatment time dependent decrease was observed that differed significantly from that of the untreated cells (Figure 1e). This decline was associated with terminal cell death (Figure 1f). The feed gas composition of a plasma jet determines its mixture of ROS in the plasma gas phase. Utilizing four different feed gas composition to ignite the medical gas plasma jet, namely, argon (Ar), argon/oxygen (Ar/O_2), helium (He), and helium/oxygen (He/O_2), a differential impact of each feed gas composition on the viability of plasma-treated melanomas was observed (Figure 1g). An indirect measure of analyzing the reactive species composition of the plasma gas phase is determining the generation of long-lived end products in the liquids exposed to plasma. While Ar plasma generates significant amounts of hydrogen peroxide (H_2O_2) in the liquid phase, primarily via hydroxyl radical ($HO\cdot$) production, the He/O_2 but not the He or Ar plasma setting was capable of producing hypochlorous acid (HOCl) in liquids (Figure 1i). Vice versa, the He/O_2 condition did not generate H_2O_2 while the Ar condition did not generate HOCl. The Ar/O_2 and He condition produced some H_2O_2 but not HOCl. The latter was dependent on the amount of O_2 added to the He and was close to maximum at 1%. A direct measure of analyzing some types of ROS in the plasma gas phase is using optical emission spectroscopy. This technique captures the unique emission spectra of discharge plasmas with characteristic emission spectral lines for different types of atoms or molecules. For instance, the Ar plasma generates a visible peak for $OH\cdot$ at 307 nm and the second positive system of nitrogen for the bands immediately right of that line (Figure 1j). The bands above 700 nm mostly relate to Ar-derived species and atomic oxygen (O) at 777 nm. Comparing the area under the curve of O for Ar (Figure 1j), Ar/O_2 (Figure 1k), He (Figure 1l), and He/O_2 (Figure 1m), O was present mainly in the Ar and He/O_2 setups (Figure 1n). O_2 addition was 1%. Altogether, plasma treatment oxidized and subsequently inactivated murine melanoma cells, and the degree of this inactivation was dependent on the feed gas composition and its resulting ROS mixture in the plasma gas phase.

2.2. Plasma Treatment of Syngeneic Melanoma Reduced Tumor Mass and Increased Leukocyte Tumor Infiltrates In Vivo

To investigate the antitumor efficacy of the four different gas plasma setups, C57BL/6 mice were inoculated with 1×10^5 B16F10 melanoma cells on the left flank (**Figure 2**a). Treatment of the tumor with gas plasma or the positive control (pos. ctrl; imiquimod) was performed four times before the sacrifice of animals and tissue collection (Figure 2b). Analysis of the tumor weight showed a reduction of tumor growth, which was significant for He/O_2, positive control, and positive control plus Ar plasma (Figure 2c). After sacrifice, tumors were collected and digested using GentleMacs technology to retrieve viable, single-cell tumor suspensions. Cell suspensions were labeled with fluorescently conjugated monoclonal antibodies targeting several immune cell subsets of the tumor microenvironment prior to performing multicolor flow cytometry. Leukocyte quantification was done by gating on single cells and the viable (Sytox Blue-negative) leukocyte ($CD45^+$) fraction among them (Figure 2d). The major histocompatibility class II (MHCII) negative cells were mostly T-cells ($CD3^+$), with the majority being cytotoxic $CD8^+$ over helper $CD4^+$ T-cells. $MHCII^+$ myeloid cells were gated for $F4/80^+$ macrophages and $CD11c^+$ dendritic cells (DCs). In our melanoma model, the majority of intratumoral T-cells were of a memory ($CD62L^-$) phenotype, which is consistent with findings in patients.[17] This is because $CD62L^+$ T-cells preferentially home to secondary lymphoid organs that are lined with high endothelial venues, while $CD62L^-$ T-cells primarily prime into tissues such as tumors, where they patrol in search for their cognate antigen.[18] Quantification of different intratumoral leukocyte subsets revealed a non-significant increase of $CD4^+$ T-cells in all groups but Ar/O_2, with the number of $CD4^+$ cells in the positive control plus Ar plasma differing significantly from that in the untreated control tumors (Figure 2e). By contrast, $CD8^+$ cytotoxic T-cells were significantly increased in the groups showing the best tumor control (Figure 2c), namely Ar, He/O_2, positive control, and positive control plus argon plasma (Figure 2f). A similar trend was observed for intratumoral macrophages, with the exception of a significant increase of macrophages in the He but not the positive control group tumors (Figure 2g). DCs, the prime cell type launching antitumor T-cell responses, were significantly elevated in the Ar, He/O_2, and positive control plus Ar plasma group, while in the Ar/O_2 condition, they were significantly decreased (Figure 2h). In summary, medical gas plasma jet treatment reduced melanoma burden in vivo and stimulated intratumoral leukocyte infiltration, with the feed gas setting being decisive for both antitumor efficacy and immune infiltration.

2.3. Plasma Treatment of Murine Syngeneic Melanomas Increased T-Cell Activation

Plasma-treated tumors showed an enhanced immuno-infiltration, and the next question was to assess activation levels of T-cells, a subset of leukocytes known to mediate antitumor immune responses. Secondary lymphoid organs (lymph nodes, spleens) were collected, digested using GentleMacs technology, and viable $CD4^+$ and $CD8^+$ T-cells were analyzed by multicolor flow cytometry (**Figure 3**a). CD127, the interleukin

ADVANCED SCIENCE NEWS
www.advancedsciencenews.com

ADVANCED SCIENCE Open Access
www.advancedscience.com

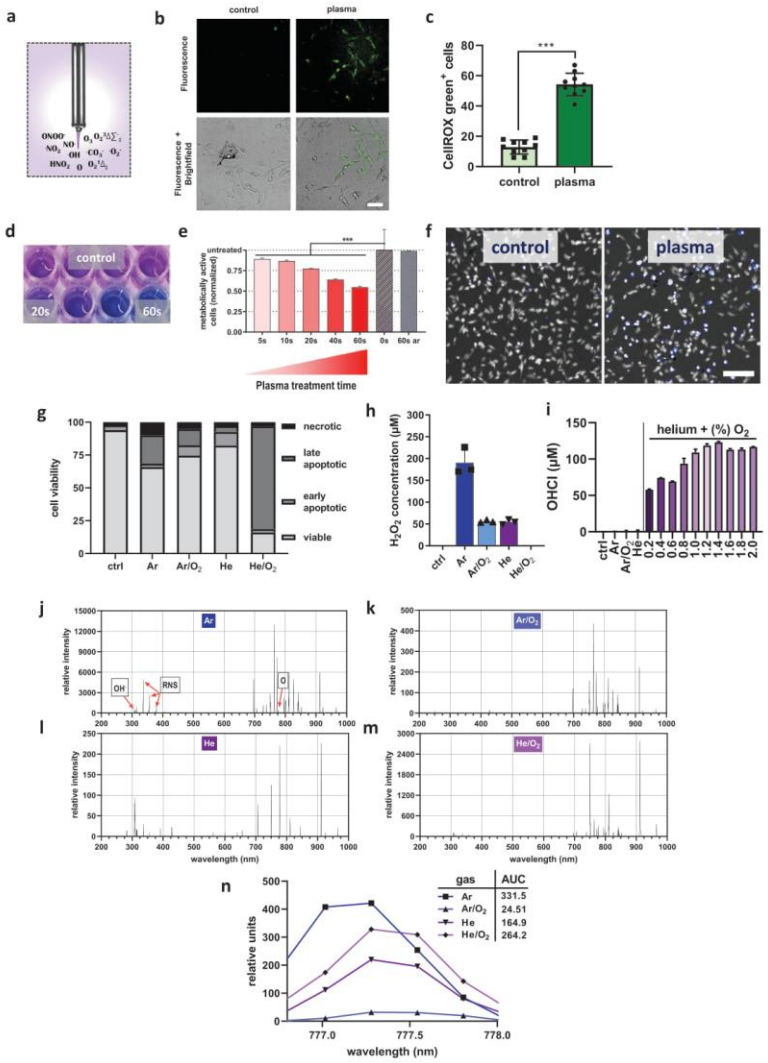

Figure 1. Plasma jet treatment oxidized and killed melanoma cells by gas phase-derived ROS. a) Scheme of the medical plasma jet technology generating a multitude of ROS simultaneously. b) Representative brightfield and DCF fluorescence images of control and plasma-treated B16F10 melanoma cells as well as c) quantification of fluorescence. d) Representative image of resazurin to resorufin turnover of cells in microplates and e) quantification of metabolic activity of melanoma cells exposed to plasma or left untreated (60 s ar = 60 s argon gas treatment alone with plasma off). f) Representative overlay images of digital phase contrast (white) and DAPI (blue) in control and plasma-treated cells and g) flow cytometric viability analysis for each plasma gas setup. h,i) Quantification of H_2O_2 (h) and HOCl (i) in liquid with argon (Ar), argon/oxygen (Ar/O_2), helium (He), and helium/oxygen (He/O_2) plasma treatment. Optical emission spectroscopy (OES) spectra of j) argon (Ar), k) argon/oxygen (Ar/O_2), l) helium (He), and m) helium/oxygen (He/O_2) plasmas. n) Comparison of intensities at about 777 nm indicative for atomic oxygen and area under the curve (AUC) calculation (inlet). Data are mean ± SEM. Statistical comparison was performed using *t*-test (c) and ANOVA against control cells (e). Scale bar is 20 µm (b) and 100 µm (f).

ADVANCED SCIENCE NEWS
www.advancedsciencenews.com

ADVANCED SCIENCE Open Access
www.advancedscience.com

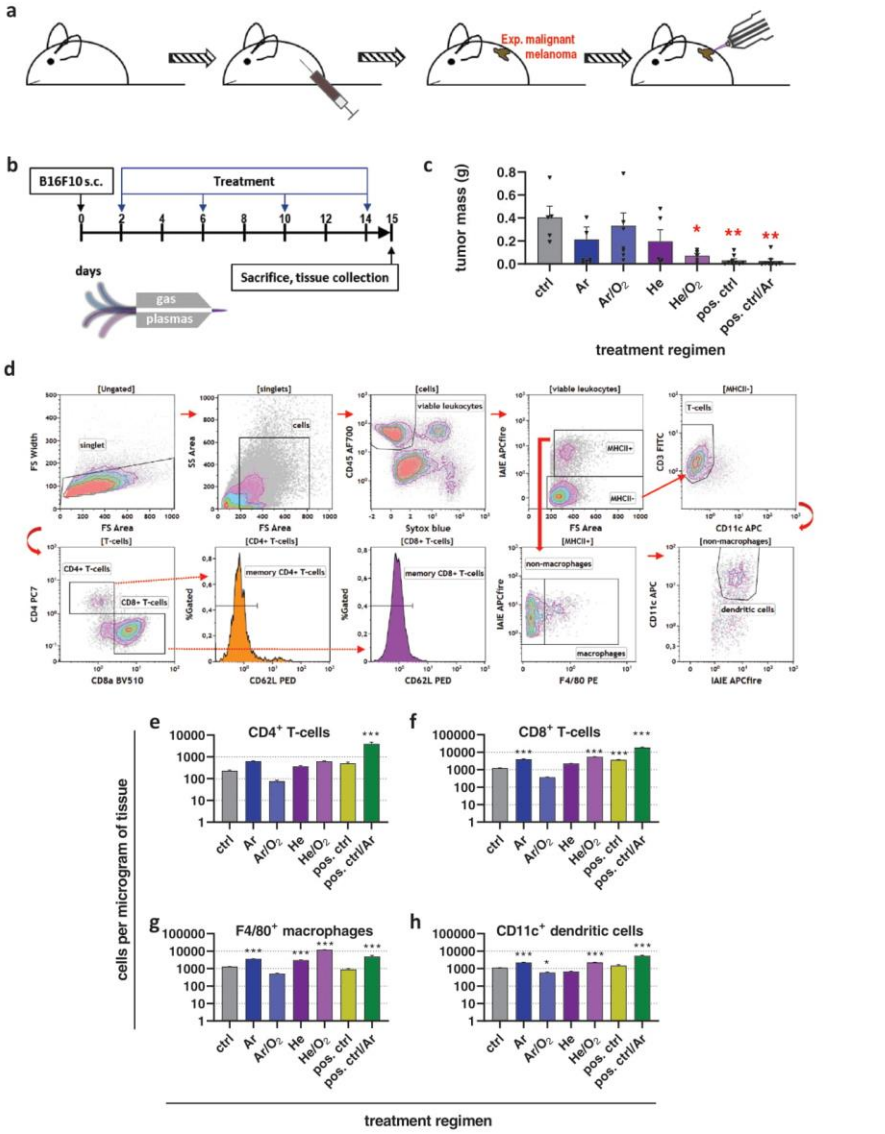

Figure 2. Plasma treatment of syngeneic melanoma reduced tumor mass and increased leukocyte tumor infiltrates in vivo. a) Workflow of in vivo experiment and b) treatment schedule; c) tumor mass of control and treatment groups; d) flow cytometry gating strategy to determine intratumoral leukocyte subpopulations; e–h) quantification intratumoral of $CD4^+$ T-helper cells (e), $CD8^+$ cytotoxic T-cells (f), $F4/80^+$ macrophages (g), and $CD11c^+$ dendritic cells (h) per microgram of tumor tissue. Data are mean ± SEM from two independent experiments. Statistical comparison was performed using ANOVA against the control group.

ADVANCED SCIENCE NEWS
www.advancedsciencenews.com

ADVANCED SCIENCE Open Access
www.advancedscience.com

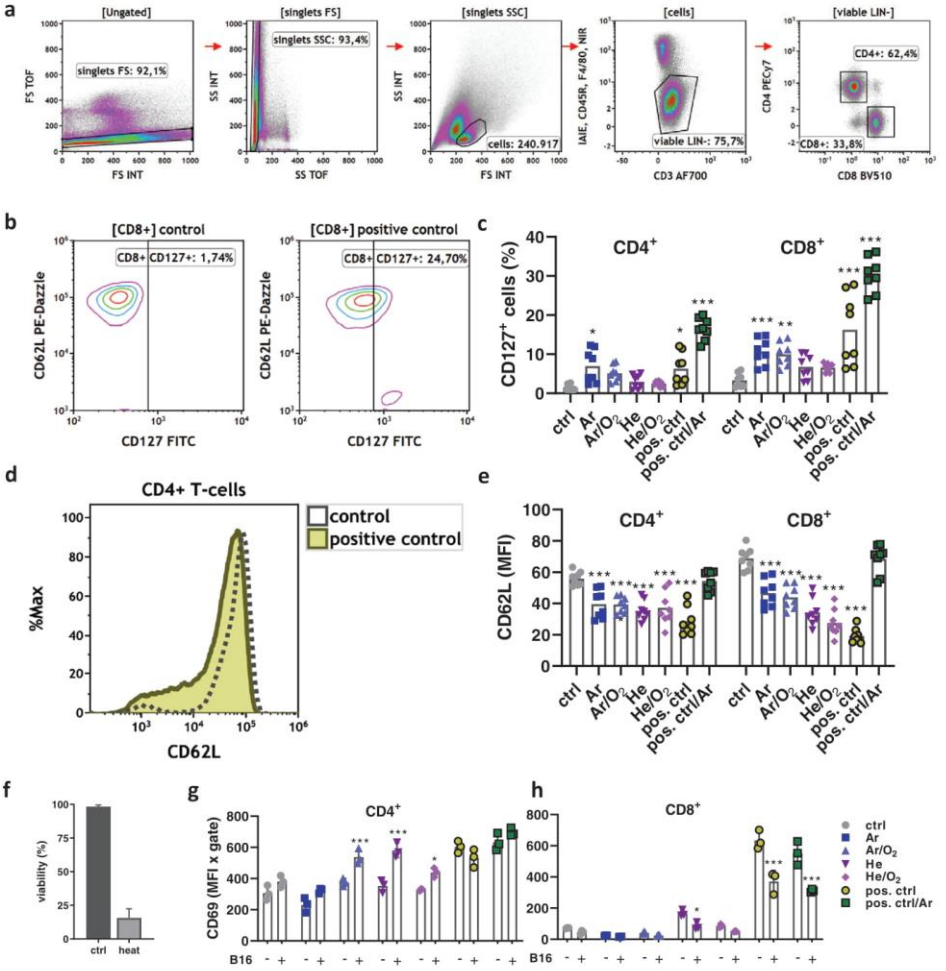

Figure 3. Plasma treatment of murine syngeneic melanomas increased T-cell activation. a) Flow cytometry gating strategy to investigate $CD4^+$ and $CD8^+$ T-cells from secondary lymphoid organs of tumor-bearing mice; b) representative contour plots for CD62L and CD127 in $CD8^+$ T-cells from control and positive control animals; c) quantification of CD127 in $CD4^+$ and $CD8^+$ T-cells from lymph nodes and splenocytes of tumor-bearing mice; d) representative overlay histogram of CD62L expression on $CD4^+$ T-cells from control and positive control of tumor-bearing mice; e) quantification of CD62L in $CD4^+$ and $CD8^+$ T-cells from lymph nodes and splenocytes; f) viability of B16F10 cells in control conditions or after heat inactivation (65 °C for 3 min) as determined by flow cytometry; g,h) quantification of CD69 expression on $CD4^+$ (f) and $CD8^+$ (g) T-cells from splenocytes of tumor-bearing mice in presence or absence of B16F10 melanoma cells for 18 h. Data are mean ± SEM from secondary lymphoid organs extracted from animal experiments shown in Figure 2. Statistical comparison was performed using ANOVA against control (ctrl) group (c,e) or multiple *t*-tests of cells in the presence (+) and absence (–) of melanoma cells (g,h).

(IL) 7 receptor, is a marker for T-cell activation and differentiation. This marker was enhanced in T-cells from lymph nodes of the animals receiving imiquimod antitumor therapy (Figure 3b). The quantification revealed a significant upregulation of CD127 in both $CD4^+$ and $CD8^+$ T-cells in the Ar plasma, positive control, and positive control plus Ar plasma groups

when compared to untreated controls (Figure 3c). Notably, all types of treatment increased CD127 expression. At the same time, a decrease of CD62L expression of T-cells (Figure 3d) was observed in all mice receiving plasma or imiquimod anti-melanoma therapy. A decrease of CD62L is known to be associated with T-cell activation, and a significant decrease was observed in both $CD4^+$ and $CD8^+$ T-cells in all groups except positive control plus Ar plasma (Figure 3e). It is unclear why the latter group receiving combination therapy did not show any decline in CD62L while the monotherapy did. To investigate whether T-cells of tumor-bearing mice were responsive to B16F10-derived tumor antigen, splenocytes of tumor-bearing mice were co-cultured ex vivo with partially heat-inactivated melanoma cells to free up antigen while at the same allowing the live-cell fraction (Figure 3f) to provide for T-cell stimulation. Analyzing the expression of the early activation marker of T-cells, CD69, a significant increase was observed for the Ar/O_2, He, and He/O_2 conditions when comparing splenic $CD4^+$ T-cells cultured in the presence or absence of melanoma cells (Figure 3g). For $CD8^+$ T-cells, a significant decrease was observed in the He plasma and positive control groups (Figure 3h). Taken together, T-cells of secondary lymphoid organs showed a higher baseline activation with therapy groups compared to controls, while the re-stimulation of splenocytes with tumor cells ex vivo only partially led to enhanced T-cell activation.

2.4. Gas Plasma Treatment Induced Immunogenic Cancer Cell Death in Melanoma Cells

Medical gas plasma jet treatment of syngeneic murine melanomas led to an increased immuno-infiltration and an enhanced T-cell activation profile. To analyze the immunogenic nature of gas plasma treatment of tumor cells, melanoma cells were exposed in vitro to argon gas plasma treatment or drugs known to have a low (mitomycin C, MMC) or high (mitoxantrone) immunogenic profile.[12] The toxic action of the drugs was confirmed by the assessment of the metabolic activity melanoma cells (**Figure 4**a). To investigate the ICD-nature of the drugs and plasma treatment, multicolor flow cytometry was performed after 24 h of incubation to quantify the levels of the anti-phagocytic molecule CD47, the eat-me signal calreticulin (CRT), the ICD marker heat-shock protein 90 (HSP90), and MHCI (Figure 4b). CD47 was significantly enhanced with plasma and MTX treatment (Figure 4c), suggesting a putative decrease of phagocytosis. At the same time, however, the pro-phagocytic and immunogenic markers CRT (Figure 4d) and HSP90 (Figure 4e) were significantly increased with both the plasma and MTX treatment. MHCI, on the other hand, was significantly increased only with MMC treatment (Figure 4f). To analyze the transcription factors involved with the plasma and drug exposure, quantitative high content image analysis was performed for analyzing the nuclear translocation of the nuclear factor of activated T-cells (NFAT), nuclear factor E2-related factor 2 (Nrf2), and nuclear factor "kappa-light-chain-enhancer" of activated B-cells (NFκB). This was done by segmenting the nuclear ($DAPI^+$) and cytosolic ($DAPI^-$ and digital phase contrast$^+$) region of each individual cell of an image. The nuclear over the cytosolic mean fluorescent intensity was calculated for each of the transcription factors as an indicator of their nuclear translocation and activation of downstream genes (Figure 4g). For each condition, about 20 000 individual cells were analyzed. For NFAT, algorithm-driven quantification revealed a modest but significant increase for MTX but not for plasma and MMC (Figure 4h). For Nrf2, a significant increase was found with MTX and MMC (Figure 4i). MTX also facilitated a substantial and significant increase of NFκB, while that of MMC and plasma treatment was lower but still significantly enhanced compared to that of the untreated control cells (Figure 4j). In sum, plasma treatment increased immunogenic cancer cell death in melanoma cells, which was concomitant with elevated nuclear translocation of NFκB.

2.5. Vaccination with Plasma-Treated Cells Protected from Melanoma Growth

To investigate the in vivo relevance of plasma-induced ICD identified in vitro, the "gold-standard" assay of tumor cell vaccination was employed.[19] Mice were injected with a supposedly preventive vaccine of either argon gas plasma treated or drug-treated melanoma cells. Seven days later, animals were re-challenged with live untreated cells, and the number of animals developing tumors was assessed (**Figure 5**a). While one out of six animals receiving cells treated with the low-immunogenic drug MMC were protected from tumor growth, it was three out of six for the plasma group and five out of six for the group receiving cells exposed to highly immunogenic drug MTX (Figure 5b). None of the animals developed tumors at the vaccination site. Re-stimulation of splenocytes isolated from these mice with B16F10 melanoma cells revealed a significant increase of the early activation marker CD69 in $CD8^+$ (Figure 5c) but not in $CD4^+$ (Figure 5d) T-cells. To analyze the inflammatory changes associated with the co-culture of splenocytes or lymph node-derived cells from the vaccinated animals with melanoma cells ex vivo, 12-plex bead-based cytokine and chemokine quantification of the supernatants was performed at 24 h (Figure 5d). Statistical comparison was made by analyzing the *p*-values of the MMC versus the plasma group and the MTX versus the plasma group. Most significant differences were observed for splenocytes, while for lymph node derived cells, only IL12p70 was significantly elevated in the MTX group. With splenocytes, the plasma group showed significantly enhanced levels of (C-X-C motif) ligand 1 (CXCL1), CXCL10, interferon-gamma (IFNγ), IL1α, IL6, and tumor necrosis factor-alpha (TNFα) as well as significantly decreased levels of granulocyte-macrophage colony-stimulating factor (GM-CSF) and the chemokine (C-C motif) ligand 17 (CCL17, also known as TARC) when compared to either MMC, MTX, or both. In total, the chemokine and cytokine expression profile was pro-inflammatory. It can be concluded that vaccination with plasma-treated melanoma cells provided immunoprotection from melanoma growth in 50% of mice, and leukocytes from these mice cultured with melanoma cells showed enhanced activation and inflammatory activity that may have supported antitumor immunity in vivo.

ADVANCED SCIENCE NEWS
www.advancedsciencenews.com

ADVANCED SCIENCE Open Access
www.advancedscience.com

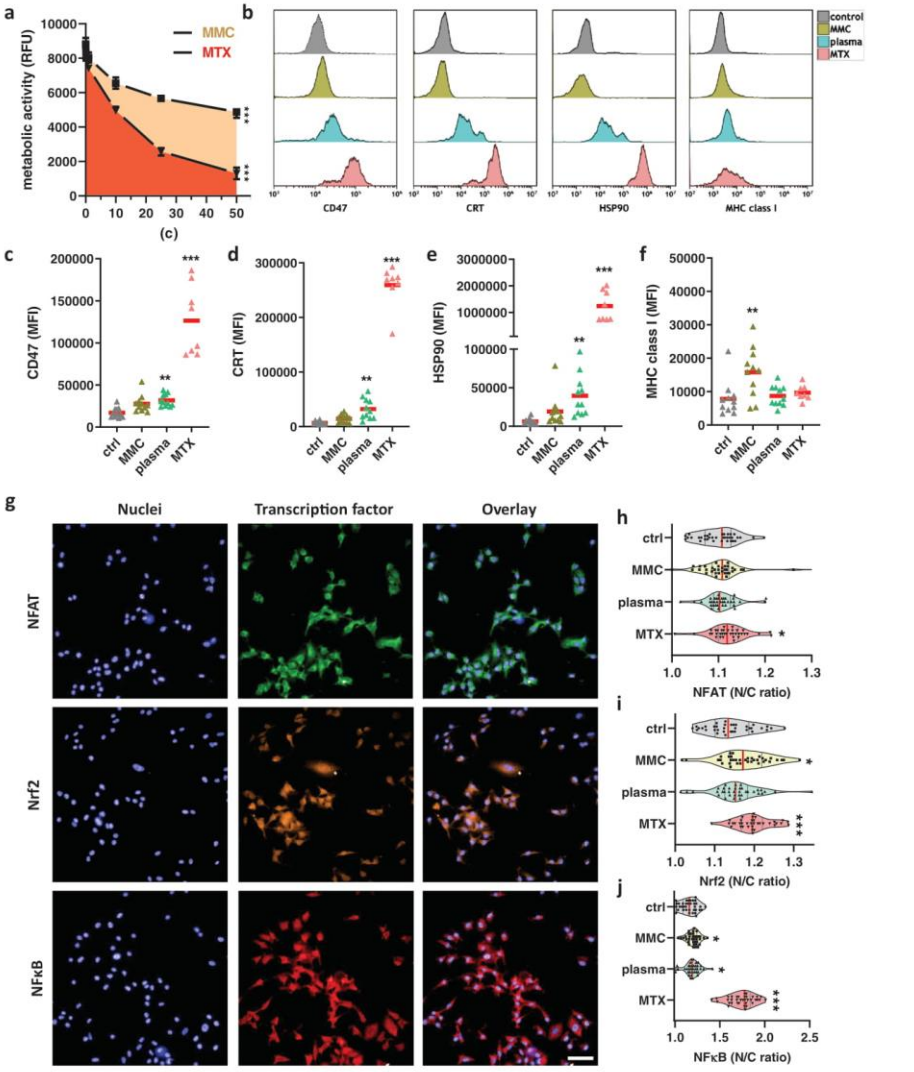

Figure 4. Argon gas plasma treatment induced immunogenic cancer cell death in melanoma cells. a) Metabolic activity of B16F10 melanoma cells incubated with varying concentrations of mitomycin C (MMC) or mitoxantrone (MTX) at 24 h; b) representative overlay histograms of expression intensities of CD47, calreticulin (CRT), heat-shock protein 90 (HSP90), and major histocompatibility complex I (MHCI) on B16F10 melanoma cells at 24 h; c–f) quantitative comparison of mean fluorescent intensity (MFI) of cells at 24 h for CD47 (c), CRT (d), HSP90 (e), and MHCI (f); g) representative images of one field of view of nuclei (DAPI) and transcription factors (NFAT, Nrf2, NFκB) labeled with fluorescent antibodies as well as overlays in B16F10 melanoma cells; h–j) quantification of the nuclear to cytoplasmic (N/C) fluorescence intensity ratio for NFAT (h), Nrf2 (i), and NFκB (j), each dot represents data from four fields of view. Data from three experiments show mean ± SEM (a), mean (c–f), and violin plots and mean (h–j). Statistical analysis was performed using ANOVA against control cells. Scale bar is 50 µm. RFU = Relative fluorescence units.

ADVANCED SCIENCE NEWS
www.advancedsciencenews.com

ADVANCED SCIENCE Open Access
www.advancedscience.com

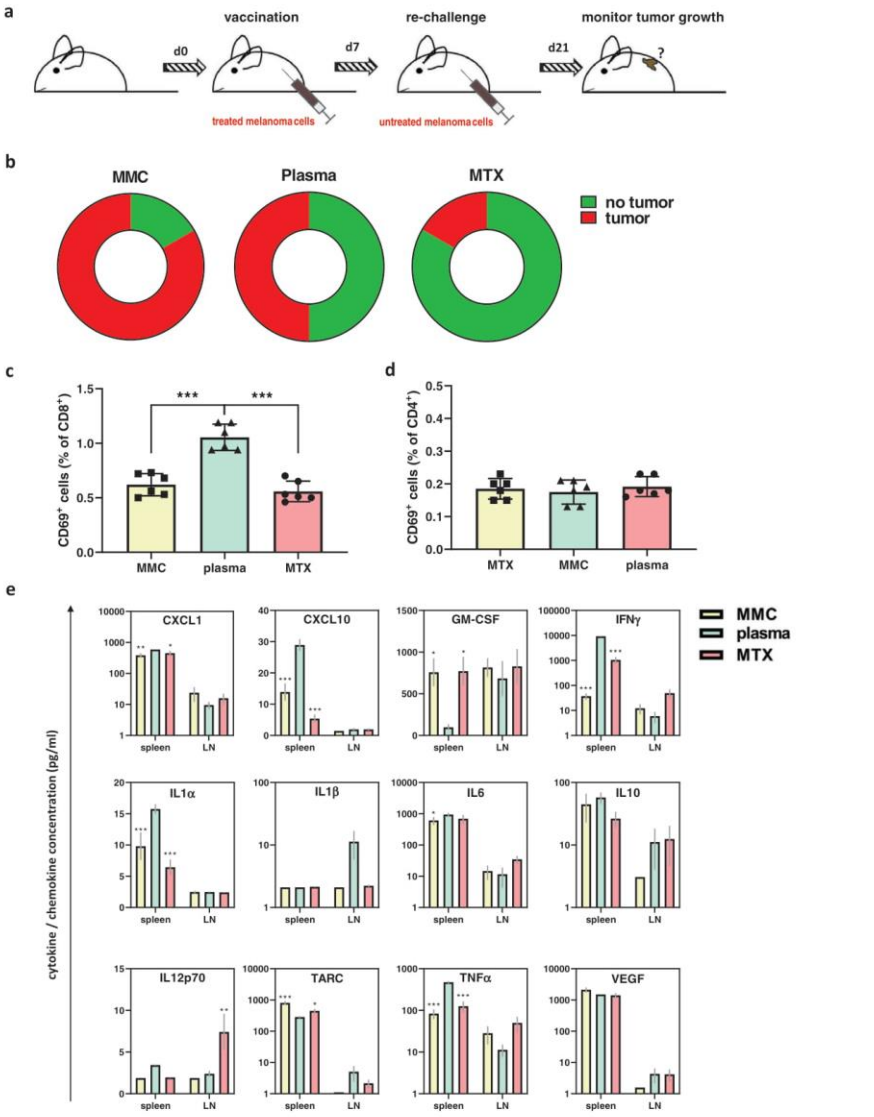

Figure 5. Vaccination with plasma-treated cells protected from melanoma growth. a) Workflow of the vaccination animal experiment; b) quantification of the fraction of tumor-bearing animals for each of the groups receiving cells exposed to either mitomycin C (MMC), plasma, or mitoxantrone (MTX)-treated B16F10 melanoma cells prior to re-challenge with viable cells; c,d) quantification of CD69 expression in $CD8^+$ (c) and $CD4^+$ (d) splenic T-cells from vaccinated animals cultured with melanoma cells in vitro at 24 h; e) 12-plex quantification of cytokines and chemokines in supernatant retrieved of splenocytes (spleen) or lymph node-derived cells (LN) from vaccinated animals cultured with B16F10 melanoma cells at 24 h. Data are mean ± SEM from six animals per group. Statistical comparison was performed using ANOVA against the plasma group.

3. Discussion

Despite improvements in therapy, cancer still ranks first among causes of death in the western world and people younger than 80 years old.[20] At the same time, the importance of the immune system to target cancer cells becomes increasingly evident.[21] Novel anticancer therapies are hence urgently needed that target cancer cells while fostering antitumor immunity. We investigated a novel anticancer treatment modality, medical gas plasma, in a murine syngeneic model of malignant melanoma and tested its ability to promote antitumor efficacy and immuno-stimulation.

Gas plasma treatment was effective in inactivating melanoma cells in vitro and reducing tumor mass in vivo. This is in line with previous reports on melanoma using experimental plasma prototypes.[9,22,23] However, the translational relevance of these plasma sources is low while it is high for the atmospheric pressure plasma jet kINPen used in this study that is similar to the jet accredited as a medical device in Europe.[3] The evidence in the field of medical gas plasma research points to the importance of ROS in mediating plasma-induced tumor cell death.[8] The current concept is that these plasma-derived ROS generate secondary ROS and oxidation products that accumulate inside tumor cells, leading to mitochondrial damage[24] and pro-apoptotic signaling.[25] Exposure of tumor cells to plasma-derived ROS is accompanied by changes in the release of chemokines and cytokines,[26] several immunomodulatory receptors,[27] and upregulation of markers of the immunogenic cancer cell death (ICD)[28] and cellular senescence.[29] While many reports point to a selectivity of gas plasma treatment to induce toxic effects in tumor cells over non-malignant cells,[30–33] more comprehensive studies revealed that selectivity depended on the type of tumor cell investigated and the cell line used for comparison.[34–37] Notwithstanding, increased expression of pro-immunogenic surface markers in ROS-treated cells was observed in malignant over non-malignant cells.[38]

With millions of non-malignant cells dying within the human body each day, apoptosis is per definition an immunologically silent form of cell death. This way, immunological tolerance is maintained toward self-antigens,[39] a mechanism being exploited by tumor cells to evade anticancer immune responses.[40] If apoptosis, however, occurs in a highly pro-inflammatory context, T-cell co-stimulation by activated DCs drive antitumor responses critical in the inactivation of cancer cells.[41] CRT and heat-shock proteins are two key immunological determinates in this context,[42–44] and our results underline their increased surface expression in the immunogenic treatment regimens mitoxantrone (MTX) and gas plasma treatment. This corroborates previous results using another plasma source.[9] By contrast, mitomycin C (MMC) induced a tolerogenic form of cell death in both our's and other studies.[45–47] For this reason, the immunosuppressive capacity of MMC is exploited to reduce graft versus host disease.[48] In our study, MMC was the only drug that enhanced the expression of MHC class I molecules on B16F10 cells while other treatment regimens did not. This suggests that antitumor immunity was efficient even at baseline MHCI levels on melanoma cells presenting tumor-specific peptides. Vice versa, CD47 was markedly increased with gas plasma and—to an even greater extent—MTX treatment. CD47 is a prominent inhibitor of phagocytosis, and its therapeutic blockage has been shown in clinical trials.[49] Nonetheless, sufficient immunogenic signaling was shown to overcome CD47-mediated "don't-eat-me" signaling,[50] exemplifying the delicate balance of a number of surface molecules determining the efficacy of anticancer responses via immune cells. Along similar lines, our study showed an increased nuclear translocation and hence activation of NFκB, a transcription factor known to promote malignant progression and invasiveness.[51] For MTX, however, it is established that such NFκB activation is a consequence of drug-induced DNA double-strand breaks and apoptosis.[52] With regard to ICD, HSP90 can also inhibit cell death[53] through interaction with Akt via NFκB-mediated apoptosis inhibition.[54] In DCs, phosphorylation of NFκB through DAMPs and TLR4 is a critical mechanism of antitumor activity of these cells.[55] Necrotic cells, which are pro-inflammatory and immunogenic per se, can trigger pro-inflammatory cytokine release through activation of NFκB.[56] Gas plasma treatment releases ROS. Another physical clue generating therapeutic ROS is photodynamic therapy, which was shown to stimulate antitumor inflammation via phosphorylation of NFκB.[57] Nrf2 is another transcription factor discussed being a tumor promotor and suppressor at the same time.[58] Nrf2 translocation to the nucleus was increased with MMC and MTX as well as plasma treatment in tendency and regulates the transcription of antioxidant and anti-apoptotic genes.[59] The increased translocation of Nrf2 was likely due to its redox-sensitive activation upstream.[60] With gas plasma exposure and subsequent ROS deposition onto cells and tissues, Nrf2 activation seems to be a frequently observed process as we recently found its phosphorylation in plasma-treated wounds in mice.[61] Garg and colleagues previously postulated that ICD shares key danger signaling pathways with viral infection,[62] in which Nrf2 plays a critical role[63] besides its part in the unfolded protein response.[64] However, Nrf2 activation can also promote autophagy that counteracts ER stress and ICD.[65] As it protects from oxidative stress, it is also thought that excessive phosphorylation of Nrf2 protects cells from dying in an immunogenic manner, even at high cytotoxic dosages of a given ICD inducer.[66] In this regard, it is interesting to note that plasma only poorly activated Nrf2 but was highly immunogenic, while MMC and MTX activated Nrf2 to a significantly greater extent. Clearly, the link between oxidative stress and ICD has not been fully elucidated yet. For NFAT, only MTX gave a small but significant increase of nuclear translocation. Hence, its role in ICD, which was clearly elicited in response to gas plasma and MTX treatment, was presumingly little in our model. NFAT activation is involved in TNFα release,[67] known to target tumor apoptosis in a T-cell dependent manner.[67,68] Like with the other two transcription factors investigated, however, NFAT was also previously linked to immunosuppressive effects,[69] making tissue–environmental factors likely to tip the balance of these pathways toward either tumor promotion or tumor regression.[70]

Targeting tumor cells with pharmacologically generated ROS has been proposed to be an effective anticancer strategy already a decade ago.[71] However, clinical success has so far been limited,[72] mainly because of difficulties in targeting therapies in a tumor-specific way when administered systemically.

By contrast, physical methods such as light-induced photodynamic therapy (PDT),[73] ionizing radiation,[74] UV-treatment,[75] pulsed-electric fields,[76] and gas plasmas[77] generate tumor-toxic ROS in a localized manner that can moreover then contribute to ICD. However, while the physical modalities mentioned generate ROS in the interior of cells, gas plasma treatment adds ROS from the outside with mechanisms and redox-chemical reaction pathways only starting to be understood as of now.[78–80] Due to the mechanism of action, gas plasma produced ROS may only act in a localized manner but not systemically.

The benefit of gas plasma therapy, especially with the jet used in this study, is its multimodal production of a plethora of ROS types simultaneously.[81] The two most effective gas plasma settings in our current study, argon and helium/oxygen, were the conditions with most atomic oxygen generation. Hence, we here show for the first time that changing the ROS composition of a gas plasma jet changes the antitumor efficacy against melanoma in a syngeneic animal model. This is a significant step toward the proof-of-concept that gas plasma jets can be optimized toward a tumor entity with the potential to serve a novel tool in precision oncology in the future. To identify the ideal gas mixture yielding a maximum antitumor efficacy, however, extensive comparative studies in vivo are needed whose screening nature would not qualify for ethical approval in Germany, at the moment. Not only many more feed gas combinations could be tested (e.g., argon-oxygen-nitrogen, argon with nitrogen shielding gas) but also several increments of the additives (e.g., 0.2%, 0.5%, 1%, and 2%). Investigating more iterations will likely optimize antitumor efficacy further, while in this study, we have provided a good starting point suggesting the ·OH-rich argon gas plasmas and the atomic oxygen-rich He/O_2-gas plasma of a redox-chemistry having potent tumoricidal effects.

It has also been established with this plasma jet technology that changing the feed gas condition has a significant impact on the ROS composition and its subsequent post-translational modifications of biomolecules.[82] As a functional consequence, some ROS mixtures are associated with a potent cell kill, while others are not.[83] We recently identified atomic oxygen, and possibly singlet delta oxygen, to be an essential mediator of toxicity in a leukemia model.[84] This was especially evident when oxygen was added to helium, which efficiently generates atomic oxygen at a high concentration as measured before using molecular beam mass spectrometry (MBMS) and two-photon absorption laser-induced fluorescence (TALIF).[85] Atomic oxygen then is able to generate HOCl in the presence of chloride and liquids, which—at least in tissue cultures—is present at excess. It is crucial to note that this process is highly dependent on the distance of the jet to the liquid as atomic oxygen levels quickly drop with increasing distance from the nozzle.[86] Such an effect can also be noticed when analyzing HOCl production as a function of the treatment distance to a target, for example, a liquid.[83] This is because ambient air oxygen scavenges atomic oxygen to react to ozone. One question might be why this process is less evident with He/O_2 while all other conditions (Ar, Ar/O_2, and He) have higher scavenging rates as seen by the lack of HOCl production in the liquid. First, it needs to be mentioned that the argon and helium settings generate atomic oxygen as well but at concentrations several orders of magnitude lower compared to the respective addition of oxygen.[87,88] Second, argon plasma (regardless of addition of 1% O_2 or not) has high turbulences that lead to intense influx of ambient air into the active plasma zone already at short axial distances from the nozzle.[89] Such effect is less pronounced with helium and its lower diffusion coefficient,[90] which has a more laminar and not turbulent flow[91] as compared to argon. Argon also has a higher diffusion coefficient that exponentially adds to the on-axis density of the ambient air. This is vice versa suggested by the fact that when the kINPen plasma is shielded with a gas not containing oxygen (e.g., nitrogen or argon), large amounts of atomic oxygen but not ozone are measureable.[92] Third, there are many ways of generating atomic oxygen in the complex plasma chemistry that is partly related to molecular gas admixture but also its effects on metastable and electron densities.[93]

He/O_2 was the most potent gas mixture for inactivating melanoma cells. In vitro, this might have been due to its high atomic oxygen levels, leading to HOCl production in vitro in the presence of excess liquid and chloride, underlining previous findings.[83,84] In a groundbreaking recent study, HOCl was used to prepare autologous tumor material for cell killing and increasing its immunogenicity, which enhanced the antitumor immuno-protection in patients suffering from ovarian cancer.[94] However, also the argon condition was very potent, leading to a significant decline of melanoma growth in vitro and in vivo. The argon plasma is very rich in hydroxyl radical (·OH) generation,[95] the most reactive and destructive type of ROS in nature.[96] However, ·OH radicals have very short diffusion distances, and quickly deteriorate to H_2O_2 in liquids.[97] It is vital to note the knowledge gap in redox biology and medicine regarding the spatio-temporal profiles of different types of ROS, generated via drugs or physico-chemical means, in tissues. The gas plasma treated tumors in this study were rich in keratins and matrix as well as lipids, with the biomass to liquid ratio being much higher compared to in vitro systems. This means that while laboratory analysis of ROS in the plasma gas phase and liquids might be somewhat accurate, they may not reflect ROS levels in the tissue. As a consequence, the ·OH of the argon gas plasma may promote lipid peroxidation in vivo,[98] while in vitro the molecule fails to do so and quickly deteriorates to H_2O_2 in the excess liquid. Resolving the trajectories of individual gas plasma-derived types of ROS in tissues is one of the main technical advances needed at the moment.

Novel treatment modalities require both efficacy and safety. Despite reports with other plasma sources suggesting that antitumor effects of gas plasmas are facilitated via DNA damage,[99–101] we have no indication of our plasma jet being genotoxic. Our previous studies established that plasma treatment did not cause micronucleus formation in vitro[102] regardless of the feed gas settings[103] as well as in vivo.[104] We also identified that in response to gas plasma exposure, the DNA-damage indicator γH2AX is a consequence of pro-apoptotic signaling rather than plasma-derived ROS directly inducing DNA double-strand breaks.[105] Moreover, a 1-year follow-up study in gas plasma-treated mice confirmed a lack of plasma-induced tumor formation in vivo.[106] Besides the ICD-inducing nature of

plasma-mediated tumor cell death shown in our present work, gas plasma treatment but not a positive control failed to induce autoimmune events in a previous study in vivo[107] that would have occurred in case of an overshooting immune reaction after plasma exposure. In addition, we recently established tumor-toxic gas plasma treatment[108] to be void of pro-metastatic effects in four human pancreatic cancer cell lines.[109]

In conclusion, our study suggests medical gas plasma technology to effectively control tumor growth in a syngeneic mouse model of melanoma. Concomitant with enhanced immune cell tumor infiltration and leukocyte activation, we have shown gas plasma treatment to induce immunogenic cancer cell death that protected mice from subsequent tumor growth. Together with previous data on the safety of the medical gas plasma jet system, we propose this technology to be a promising anticancer agent as first reports in patients already suggest. However, the detailed mechanisms of how exactly gas plasma derived ROS penetrate and act on tumor tissue remain to be elucidated in future studies.

4. Experimental Section

Cell Culture: Highly malignant and metastatic B16F10 murine melanoma cells (ATCC: CRL-6475) were cultured in Roswell Park Memorial Institute (RPMI) medium containing 10% fetal bovine serum, 2% glutamine, and 1% penicillin/streptomycin (all Sigma). Cells were grown at 37 °C, 95% humidity, and 5% CO_2, and subcultured twice a week.

Medical Gas Plasma Jet Technology: For plasma treatment, an atmospheric pressure argon plasma jet (kINPen) was employed. The device technically is similar to the kINPen MED that has received accreditation as medical device class IIa in Europe and is frequently used in dermatology.[3] In standard mode, it is operated using a flow of argon gas (purity 99.9999%; Air Liquide) at three standard liters per minute and a visible plum of about 1 cm. Other feed gas settings were argon plus oxygen, helium, and helium plus oxygen. In the electrode configuration contained within the head of the plasma jet, the noble gas was excited at a frequency of 1 MHz, generating power of about 1 W of the plasma, while total input power was 20 W. For the plasma treatment in vitro, 1×10^4 cells were seeded in 96-well plates (Eppendorf) having a rim that was filled with double distilled water to minimize edge effects during culture. After adherence overnight, cells were exposed to plasma by guiding the jet's plume over the center of each well for the indicated time in an automated manner. To achieve this, the jet was installed on a *xyz* motorized table (CNC step) controlled via software written to attain sub-millimeter precision to maximize the reproducibility of the plasma treatment.

ROS Detection: For investigating plasma-derived products, the plasma jet was positioned in front of a UV-sensitive optical emission spectrometer (Aventes AvaSpec-2048-USB2) with a spectral resolution of 0.7 nm and end-on the plasma jet at a distance of 50 mm from the jet nozzle. The computer-driven *xyz* motorized table ensured the exact positioning of the plasma jet in this setup. In plasma-treated liquid, H_2O_2 was quantified using the Amplex Ultra Red assay (Thermo) according to the manufacturer's instruction. Fluorescence was determined using a multiplate reader (Tecan F200) at λ_{ex} 560 nm and λ_{em} 590 nm, and absolute concentrations were calculated against a standard curve of H_2O_2. Hypochlorous acid was quantified using the taurine chloramine assay. To generate the standard curve, 50 µL of hypochlorite was added to 950 µL of water. 100 µL of this solution was then added to 900 µL of 200 mM KOH (pH 12), and the absorbance was measured at 292 nm using a microplate reader (Tecan M200). The concentration of HOCl was determined using the extinction coefficient of hypochlorite anion. A standard curve was prepared by mixing HOCl with equal volumes of taurine (Sigma) buffer and adding developer solution. The latter consisted of sodium acetate (pH 5.4), sodium iodide, tetramethylbenzidine, and dimethylformamide. The absorbance was measured at 645 nm using a multiplate reader. HOCl concentrations of samples were measured against this standard by adding both taurine buffer and developer.

Metabolic Activity and Viability: To analyze the metabolic activity of plasma-treated B16F10 murine melanoma cells, cells were incubated with resazurin (Alfar Aesar) at a final concentration of 100 µM at 20 h. Resazurin (7-hydroxy-3H-phenoxazin-3-one 10-oxide) is a nontoxic and cell-permeable dye that is reduced to highly fluorescent resorufin by intracellular enzymes of metabolically active cells. Fluorescence was determined by the utilization of a multiplate reader (Tecan F200) at λ_{ex} 560 nm and λ_{em} 590 nm. Viability was determined microscopically but analyzing terminally dead cells with compromised membranes through which the DNA-binding dye 4′,6-diamidino-2-phenylindole (DAPI; Sigma) can enter. DAPI was excited at 365 nm using an LED of a fluorescence microscope, and dye-dependent light emission was captured through a 493 ± 23 nm bandpass filter.

Flow Cytometry: Flow cytometry was performed using a 4-laser (405, 488, 561, and 633 nm) flow cytometer (CytoFLEX S; Beckman-Coulter) equipped with an autosampler to acquire from 96-well plates and a three-laser (405 nm, 488 nm, 638 nm) device (Gallios; Beckman-Coulter) equipped with an autosampler to acquire from 12 × 75 mm FACS tubes (Sarstedt). Cell suspensions were incubated with a master mix prepared from several monoclonal antibodies conjugated to fluorophores (**Table 1**). For labeling tumor cell suspensions, antibodies targeting CD3 and labeled with fluorescein isothiocyanate (FITC), F4/80 phycoerythrin (PE), CD62L PE-dazzle, CD4 PE-cyanine 7 (PC7), CD11c allophycocyanin (APC), CD45 Alexa Fluor (AF) 700, IAIE APC-fire, and CD8a brilliant violet (BV) 510 were added together with Sytox Blue (Thermo) to exclude terminally dead cells. After incubation for 30 min on ice, cells were washed twice with running buffer (Miltenyi Biotec) and resuspended in running buffer prior to the acquisition by flow cytometry. To label leukocytes derived from secondary lymphoid organs, the antibody master mix was adjusted to incorporate CD127 FITC and CD69 BV421.

Table 1. Antibodies used in this study.

Target	Clone	Vendor
CD3	17A2	BioLegend
CD4	L3T4	BioLegend
CD8	53-6.7	BioLegend
CD11c	HL3	Thermo
CD127	A7R34	BioLegend
CD25	PC61	BioLegend
CD45	30-F11	BioLegend
CD45R	RA3-6B2	BioLegend
CD47	miap301	BioLegend
CD62L	MEL-14	BioLegend
CD69	H1.2F3	BioLegend
CRT	1G6A7	Novus Biologicals
F4/80	BM8	BioLegend
MHCI	28-14-8	Invitrogen
HSP90	AC88	Novus Biologicals
IAIE (MHCII)	Sca-1	BioLegend
NFAT	D43B1	Cell Signaling
NFκB	K10-895.12.50	BD biosciences
Nrf2	A-10	Santa Cruz

Cells of interest were gated from the LIN (lineage)-negative population labeled with IAIE APC-fire, CD45R APC-fire, F4/80 APC-fire (to gate out myeloid cells, B-cells, and macrophages), and Zombie (BioLegend) NIR to gate out dead cells in a single dump channel. To assess immuno-relevant markers on B16F10 melanoma cells, the cells were stained with fluorescently labeled antibodies targeting CD47 PerCP-Cy5.5, CRT AF647, HSP90 AF700, and MHCI PE. For analysis of viability, B16F10 cells were gas plasma treated and incubated for 24 h at 37 °C. Cells were collected using accutase and washed and stained in annexin V binding buffer (AVBB) containing annexin V-FITC (both BioLegend) and DAPI (final concentration: 1 µM) for 15 min in the dark. After washing and resuspending in AVBB, the fluorescence per cell was acquired using flow cytometry. Data analysis and display of gating, dot plots, and histograms were performed using Kaluza analysis 2.1.1 software (Beckman-Coulter). Since a total of more than 250 Mio single cells acquired by flow cytometry were analyzed in this study, high-performance computing was required using a dedicated Tesla K40 graphics (Nvidia) that utilizes 2880 CUDA cores for parallel computing.

High Content Imaging: A high content/high throughput imaging system (Operetta CLS; PerkinElmer) equipped with a 16-bit 4.7MP sCMOS camera and a 785 nm laser autofocus was used for quantitative image analysis of transcription factor translocation in B16F10 melanoma cells. After plasma treatment or incubation with either mitomycin C (MMC, final concentration 50 µM) or mitoxantrone (MTX, final concentration 50 µM), cells were fixed and permeabilized, and stained with antibodies for 1 h at 37 °C. DAPI was used as a counterstain for nuclei. 96-well glass-bottom plates (PerkinElmer) were used to facilitate the use of a 20× water immersion objective (NA 1.0; Zeiss) for maximum photon counts on the photomultiplier. Excitation and emission settings were λ_{ex} 475 nm and λ_{em} 525 ± 25 for AF488, λ_{ex} 550 nm and λ_{em} 610 ± 40 for AF594, and λ_{ex} 630 nm and λ_{em} 708 ± 52 for AF647, respectively. For each condition, about 50 000 individual cells were analyzed using algorithm-driven quantitative image analysis facilitated using Harmony 4.9 software (PerkinElmer). The analysis sequenced included segmentation of nuclei via DAPI and finding of the cytosolic region of each cell using the digital phase contrast (DPC) channel of the system in a label-free manner. Subsequently, the mean fluorescence intensity (MFI) of each transcription factor in the nucleus was calculated over that of the cytosol and given as N/C ratio.

In Vivo Anti-Melanoma Plasma Jet Therapy: The ethical implications of the experiment were reviewed and approved by the local authority *Landesamt für Landwirtschaft, Lebensmittelsicherheit und Fischerei* (LALLF) *Mecklenburg-Vorpommern* (approval number M-V 7221.3-1-023/17). Wildtype C57BL/6 mice were shaved on the flank and inoculated with 1×10^5 syngeneic murine B16F10 melanoma cells in 50 µL of phosphate-buffered saline (PBS). For plasma treatment, the tumors were exposed to the gas plasma for 4 min during each intervention cycle. Feed gas settings were argon, argon plus 1% oxygen helium, and helium + 1% oxygen. As a positive control, imiquimod (Aldara) was applied via creaming the inoculation area. This small molecule is used to treat human metastatic melanoma in the skin of patients,[110–112] and its clinical relevance makes this drug an excellent positive control. Its mechanism of action is that it acts as toll-like-receptor 7 (TLR7) agonist, which leads to the recruitment of myeloid cells, such as dendritic cells, into the tumor microenvironment (TME),[113] which potentiates antitumor immunity. The second mode of action is its potent inhibition of complex I in the mitochondrial membrane, which is being discussed as an additional antitumor mechanism.[114] In another animal group in our experiments, imiquimod was added, followed by argon plasma treatment. This combination was chosen because both imiquimod and the argon-driven plasma jet are accredited clinical procedures already. Compelling evidence of our and future studies may, therefore, motivate an investigator-initiated clinical trial. Feed gas combinations other than argon alone may need accreditation according to the medical device regulation in Europe first before its clinical use could be envisaged. In the control group, tumors were left untreated. After sacrifice, tumors and secondary lymphoid organs (spleens, lymph nodes) were explanted. Tumors were weighed. Single-cell suspensions of tumors were retrieved using the GentleMacs tumor dissociation kit mouse (Miltenyi) and the OctaMacs device (Miltenyi) and subjected to analysis by flow cytometry. Viable cell suspensions of spleens and lymph nodes were retrieved using the spleen dissociation kit (Miltenyi) and the OctaMacs device, prior to the flow cytometric analysis. In addition, 1×10^6 splenocytes were cultured for 18 h in the presence or absence of 1×10^5 heat-inactivated (3 min, 65 °C) B16F10 cells in 24-well plates (Eppendorf), and investigated by flow cytometry thereafter.

In Vivo Anti-Melanoma Vaccination: The ethical implications of the experiment were reviewed and approved by the local authority *Landesamt für Landwirtschaft, Lebensmittelsicherheit und Fischerei* (LALLF) *Mecklenburg-Vorpommern* (approval number M-V 7221.3-1-023/17). Seven-hundred thousand melanoma cells were exposed to argon plasma or drugs. The latter were either the positive control MTX (final concentration 10 µM) or the negative control MMC (final concentration 50 µM). The cells were cultured in a flask for 24 h, before dislodgement using accutase (BioLegend), and resuspension in 700 µL of PBS; 100 µL of this suspension was injected into the left flank (vaccination) of wildtype C57BL/6 mice (six mice per group). Seven days later, 1×10^5 syngeneic murine B16F10 melanoma cells in 50 µL of PBS were inoculated in the right flank of the animals (re-challenge). On the day of sacrifice, tumor growth was inspected at the re-challenge injection site. Secondary lymphoid organs were harvested, and single-cell suspensions were retrieved as described above. Cell suspensions were cultured in the presence of B16F10 melanoma cells for 18 h. Flow cytometric analysis of splenocytes was performed. In addition, supernatants were collected and stored at −20 °C prior to analysis by multiplex bead based quantification of chemokines and cytokines (LEGENDPlex; BioLegend). Quantification of the 12 analytes was performed according to the manufacturer's instructions and analyzed using the LEGENDplex data analysis software utilizing an *R*-package.

Statistical Analysis: Graphing and statistical analysis were performed using prism 8.3 (Graphpad software). Comparison of two groups was made using unpaired student's *t*-test. The comparison of more than two groups was made using a one-way analysis of variances (ANOVA). The comparison of more than two groups across different immune cell subpopulations was made using two-way ANOVA. Level of significance is indicated as follows: $\alpha = 0.05$ (*), $\alpha = 0.01$ (**), $\alpha = 0.001$ (***).

Acknowledgements

This work was funded by the German Federal Ministry of Education and Research (BMBF), grant number 03Z22DN11. This funding source had no role in the design of this study and will not have any role during its execution, analyses, interpretation of the data, or decision to submit results. The technical assistance of Broder Poschkamp and Juliane Moritz, as well as the discussion with Jörn Winter and Ansgar Schmidt-Bleker, is appreciated. The authors acknowledge Bernhard Rauch and Markus Grube for their support with animal housing. S.B. acknowledges the support of the ZIK plasmatis internal steering board members Klaus-Dieter Weltmann, Thomas von Woedtke, Hans-Robert Metelmann, and Wolfgang Motz.

Note: A tense mistake was corrected in the abstract on 20 May 2020 after original online publication.

Conflict of Interest

The authors declare no conflict of interest.

Author Contributions

E.F. and A.S. contributed equally to this work. S.B. designed the study, analyzed the data, and wrote the manuscript. R.C., F.N., S.K.S., E.F., and A.S. performed the experiments, analyzed the data, and reviewed the manuscript.

Keywords

B16F10, kINPen, plasma medicine, reactive oxygen species, reactive nitrogen species

Received: November 29, 2019
Revised: February 25, 2020
Published online: March 30, 2020

[1] M. Durante, R. Orecchia, J. S. Loeffler, *Nat. Rev. Clin. Oncol.* **2017**, *14*, 483.
[2] A. P. Castano, P. Mroz, M. R. Hamblin, *Nat. Rev. Cancer* **2006**, *6*, 535.
[3] S. Bekeschus, A. Schmidt, K.-D. Weltmann, T. von Woedtke, *Clin. Plas. Med.* **2016**, *4*, 19.
[4] K. Wende, T. von Woedtke, K. D. Weltmann, S. Bekeschus, *Biol. Chem.* **2018**, *400*, 19.
[5] S. Bekeschus, J. Brüggemeier, C. Hackbarth, T. von Woedtke, L.-I. Partecke, J. van der Linde, *Clin. Plas. Med.* **2017**, *7–8*, 58.
[6] T. von Woedtke, A. Schmidt, S. Bekeschus, K. Wende, K. D. Weltmann, *In Vivo* **2019**, *33*, 1011.
[7] H.-R. Metelmann, C. Seebauer, V. Miller, A. Fridman, G. Bauer, D. B. Graves, J.-M. Pouvesle, R. Rutkowski, M. Schuster, S. Bekeschus, K. Wende, K. Masur, S. Hasse, T. Gerling, M. Hori, H. Tanaka, E. Ha Choi, K.-D. Weltmann, P. H. Metelmann, D. D. Von Hoff, T. v. Woedtke, *Clin. Plas. Med.* **2018**, *9*, 6.
[8] A. Privat-Maldonado, A. Schmidt, A. Lin, K. D. Weltmann, K. Wende, A. Bogaerts, S. Bekeschus, *Oxid. Med. Cell. Longev.* **2019**, *2019*, 9062098.
[9] A. Lin, Y. Gorbanev, J. De Backer, J. Van Loenhout, W. Van Boxem, F. Lemiere, P. Cos, S. Dewilde, E. Smits, A. Bogaerts, *Adv. Sci.* **2019**, *6*, 6.
[10] J. Galon, D. Bruni, *Nat. Rev. Drug Discovery* **2019**, *18*, 197.
[11] M. J. Smyth, S. F. Ngiow, A. Ribas, M. W. Teng, *Nat. Rev. Clin. Oncol.* **2016**, *13*, 143.
[12] M. Obeid, A. Tesniere, F. Ghiringhelli, G. M. Fimia, L. Apetoh, J. L. Perfettini, M. Castedo, G. Mignot, T. Panaretakis, N. Casares, D. Metivier, N. Larochette, P. van Endert, F. Ciccosanti, M. Piacentini, L. Zitvogel, G. Kroemer, *Nat. Med.* **2007**, *13*, 54.
[13] L. Galluzzi, A. Buque, O. Kepp, L. Zitvogel, G. Kroemer, *Nat. Rev. Immunol.* **2017**, *17*, 2.
[14] J. B. Haanen, *Eur. J. Cancer Suppl.* **2013**, *11*, 97.
[15] T. N. Schumacher, R. D. Schreiber, *Science* **2015**, *348*, 69.
[16] T. C. Longoria, K. S. Tewari, *Expert Opin. Drug Metab. Toxicol.* **2016**, *12*, 1247.
[17] A. Ribas, D. S. Shin, J. Zaretsky, J. Frederiksen, A. Cornish, E. Avramis, E. Seja, C. Kivork, J. Siebert, P. Kaplan-Lefko, X. Wang, B. Chmielowski, J. A. Glaspy, P. C. Tumeh, T. Chodon, D. Pe'er, B. Comin-Anduix, *Cancer Immunol. Res.* **2016**, *4*, 194.
[18] S. K. Bromley, T. R. Mempel, A. D. Luster, *Nat. Immunol.* **2008**, *9*, 970.
[19] G. Kroemer, L. Galluzzi, O. Kepp, L. Zitvogel, *Annu. Rev. Immunol.* **2013**, *31*, 51.
[20] R. L. Siegel, K. D. Miller, A. Jemal, *Ca-Cancer J. Clin.* **2019**, *69*, 7.
[21] M. D. Wellenstein, K. E. de Visser, *Immunity* **2018**, *48*, 399.
[22] S. Mashayekh, H. Rajaee, M. Akhlaghi, B. Shokri, Z. M. Hassan, *Phys. Plasmas* **2015**, *22*, 093508.
[23] Y. Binenbaum, G. Ben-David, Z. Gil, Y. Z. Slutsker, M. A. Ryzhkov, J. Felsteiner, Y. E. Krasik, J. T. Cohen, *PLoS One* **2017**, *12*, e0169457.
[24] R. K. Gandhirajan, K. Rodder, Y. Bodnar, G. Pasqual-Melo, S. Emmert, C. E. Griguer, K. D. Weltmann, S. Bekeschus, *Sci. Rep.* **2018**, *8*, 12734.
[25] M. Ishaq, S. Kumar, H. Varinli, Z. J. Han, A. E. Rider, M. D. Evans, A. B. Murphy, K. Ostrikov, *Mol. Biol. Cell* **2014**, *25*, 1523.
[26] K. Rödder, J. Moritz, V. Miller, K.-D. Weltmann, H.-R. Metelmann, R. Gandhirajan, S. Bekeschus, *Appl. Sci.* **2019**, *9*, 660.
[27] J. Moritz, H.-R. Metelmann, S. Bekeschus, *IEEE Trans. Radiat. Plasma Med. Sci.* **2019**.
[28] A. Lin, B. Truong, S. Patel, N. Kaushik, E. H. Choi, G. Fridman, A. Fridman, V. Miller, *Int. J. Mol. Sci.* **2017**, *18*, 5.
[29] C. Schneider, L. Gebhardt, S. Arndt, S. Karrer, J. L. Zimmermann, M. J. M. Fischer, A. K. Bosserhoff, *Sci. Rep.* **2018**, *8*, 10048.
[30] C. Canal, R. Fontelo, I. Hamouda, J. Guillem-Marti, U. Cvelbar, M. P. Ginebra, *Free Radical Biol. Med.* **2017**, *110*, 72.
[31] R. Guerrero-Preston, T. Ogawa, M. Uemura, G. Shumulinsky, B. L. Valle, F. Pirini, R. Ravi, D. Sidransky, M. Keidar, B. Trink, *Int. J. Mol. Med.* **2014**, *34*, 941.
[32] B. S. Kwon, E. H. Choi, B. Chang, J. H. Choi, K. S. Kim, H. K. Park, *Phys. Biol.* **2016**, *13*, 056001.
[33] K. R. Liedtke, S. Diedrich, O. Pati, E. Freund, R. Flieger, C. D. Heidecke, L. I. Partecke, S. Bekeschus, *Anticancer Res.* **2018**, *38*, 5655.
[34] P. M. Girard, A. Arbabian, M. Fleury, G. Bauville, V. Puech, M. Dutreix, J. S. Sousa, *Sci. Rep.* **2016**, *6*, 29098.
[35] K. Wende, S. Reuter, T. von Woedtke, K. D. Weltmann, K. Masur, *Plasma Processes Polym.* **2014**, *11*, 655.
[36] L. Bundscherer, S. Bekeschus, H. Tresp, S. Hasse, S. Reuter, K.-D. Weltmann, U. Lindequist, K. Masur, *Plasma Med.* **2013**, *3*, 71.
[37] E. Biscop, A. Lin, W. V. Boxem, J. V. Loenhout, J. Backer, C. Deben, S. Dewilde, E. Smits, A. A. Bogaerts, *Cancers* **2019**, *11*, 1287.
[38] E. Freund, K. R. Liedtke, J. van der Linde, H. R. Metelmann, C. D. Heidecke, L. I. Partecke, S. Bekeschus, *Sci. Rep.* **2019**, *9*, 634.
[39] F. Osorio, C. Fuentes, M. N. Lopez, F. Salazar-Onfray, F. E. Gonzalez, *Front. Immunol.* **2015**, *6*, 535.
[40] I. Poschke, D. Mougiakakos, R. Kiessling, *Cancer Immunol. Immunother.* **2011**, *60*, 1161.
[41] A. D. Garg, P. Agostinis, *Immunol. Rev.* **2017**, *280*, 126.
[42] I. Adkins, L. Sadilkova, N. Hradilova, J. Tomala, M. Kovar, R. Spisek, *OncoImmunology* **2017**, *6*, e1311433.
[43] A. D. Garg, E. Romano, N. Rufo, P. Agostinis, *Cell Death Differ.* **2016**, *23*, 938.
[44] J. Fucikova, L. Kasikova, I. Truxova, J. Laco, P. Skapa, A. Ryska, R. Spisek, *Immunol. Lett.* **2018**, *193*, 25.
[45] H. J. Ko, Y. J. Kim, Y. S. Kim, W. S. Chang, S. Y. Ko, S. Y. Chang, S. Sakaguchi, C. Y. Kang, *Cancer Res.* **2007**, *67*, 15.
[46] M. Tongu, N. Harashima, T. Yamada, T. Harada, M. Harada, *Cancer Immunol. Immunother.* **2010**, *59*, 769.
[47] K. Youlin, Z. Li, W. Xiaodong, L. Xiuheng, Z. Hengchen, *Clin. Dev. Immunol.* **2012**, *2012*, 439235.
[48] C. Morath, A. Schmitt, M. Zeier, M. Schmitt, F. Sandra-Petrescu, G. Opelz, P. Terness, M. Schaier, C. Kleist, *Langenbeck's Arch. Surg.* **2015**, *400*, 541.
[49] M. Ngo, A. Han, A. Lakatos, D. Sahoo, S. J. Hachey, K. Weiskopf, A. H. Beck, I. L. Weissman, A. D. Boiko, *Cell Rep.* **2016**, *16*, 1701.
[50] M. Liu, R. S. O'Connor, S. Trefely, K. Graham, N. W. Snyder, G. L. Beatty, *Nat. Immunol.* **2019**, *20*, 3.
[51] M. Tafani, B. Pucci, A. Russo, L. Schito, L. Pellegrini, G. A. Perrone, L. Villanova, L. Salvatori, L. Ravenna, E. Petrangeli, M. A. Russo, *Front. Pharmacol.* **2013**, *4*, 13.
[52] Y. Habraken, J. Piette, *Biochem. Pharmacol.* **2006**, *72*, 1132.
[53] S. Bekeschus, M. Lippert, K. Diepold, G. Chiosis, T. Seufferlein, N. Azoitei, *Sci. Rep.* **2019**, *9*, 4112.
[54] O. N. Ozes, L. D. Mayo, J. A. Gustin, S. R. Pfeffer, L. M. Pfeffer, D. B. Donner, *Nature* **1999**, *401*, 6748.
[55] A. Asea, S. K. Kraeft, E. A. Kurt-Jones, M. A. Stevenson, L. B. Chen, R. W. Finberg, G. C. Koo, S. K. Calderwood, *Nat. Med.* **2000**, *6*, 435.
[56] T. Vanden Berghe, M. Kalai, G. Denecker, A. Meeus, X. Saelens, P. Vandenabeele, *Cell. Signalling* **2006**, *18*, 328.
[57] S. O. Gollnick, C. M. Brackett, *Immunol. Res.* **2010**, *46*, 216.
[58] L. Milkovic, N. Zarkovic, L. Saso, *Redox Biol.* **2017**, *12*, 727.
[59] P. Shelton, A. K. Jaiswal, *FASEB J.* **2013**, *27*, 414.
[60] S. K. Niture, R. Khatri, A. K. Jaiswal, *Free Radical Biol. Med.* **2014**, *66*, 36.

[61] A. Schmidt, T. von Woedtke, B. Vollmar, S. Hasse, S. Bekeschus, *Theranostics* **2019**, *9*, 1066.
[62] A. D. Garg, A. M. Dudek-Peric, E. Romano, P. Agostinis, *Int. J. Dev. Biol.* **2015**, *59*, 131.
[63] H. M. Zhang, H. Dai, P. J. Hanson, H. Li, H. Guo, X. Ye, M. G. Hemida, L. Wang, Y. Tong, Y. Qiu, S. Liu, F. Wang, F. Song, B. Zhang, J. G. Wang, L. X. Zhang, D. Yang, *ACS Chem. Biol.* **2014**, *9*, 4.
[64] N. Rufo, A. D. Garg, P. Agostinis, *Trends Cancer* **2017**, *3*, 643.
[65] A. D. Garg, H. Maes, E. Romano, P. Agostinis, *Photochem. Photobiol. Sci.* **2015**, *14*, 1410.
[66] A. Showalter, A. Limaye, J. L. Oyer, R. Igarashi, C. Kittipatarin, A. J. Copik, A. R. Khaled, *Cytokine* **2017**, *97*, 123.
[67] J. Ding, Y. Huang, B. Ning, W. Gong, J. Li, H. Wang, C. Y. Chen, C. Huang, *Curr. Cancer Drug Targets* **2009**, *9*, 81.
[68] C. López-Rodríguez, J. Aramburu, L. Jin, A. S. Rakeman, M. Michino, A. Rao, *Immunity* **2001**, *15*, 47.
[69] K. Lee, X. Shen, R. König, *Toxicology* **2001**, *169*, 53.
[70] B. Englinger, C. Pirker, P. Heffeter, A. Terenzi, C. R. Kowol, B. K. Keppler, W. Berger, *Chem. Rev.* **2018**, *119*, 1519.
[71] D. Trachootham, J. Alexandre, P. Huang, *Nat. Rev. Drug Discovery* **2009**, *8*, 579.
[72] M. H. Raza, S. Siraj, A. Arshad, U. Waheed, F. Aldakheel, S. Alduraywish, M. Arshad, *J. Cancer Res. Clin. Oncol.* **2017**, *143*, 1789.
[73] S. M. Gondivkar, A. R. Gadbail, M. G. Choudhary, P. R. Vedpathak, M. S. Likhitkar, *J. Investig. Clin. Dent.* **2018**, *9*, e12270.
[74] I. Adkins, J. Fucikova, A. D. Garg, P. Agostinis, R. Spisek, *OncoImmunology* **2014**, *3*, e968434.
[75] M. Obeid, T. Panaretakis, N. Joza, R. Tufi, A. Tesniere, P. van Endert, L. Zitvogel, G. Kroemer, *Cell Death Differ.* **2007**, *14*, 1848.
[76] C. Y. Calvet, D. Famin, F. M. Andre, L. M. Mir, *Oncoimmunology* **2014**, *3*, e28131.
[77] M. Weiss, J. Barz, M. Ackermann, R. Utz, A. Ghoul, K. D. Weltmann, M. B. Stope, D. Wallwiener, K. Schenke-Layland, C. Oehr, S. Brucker, P. Loskill, *ACS Appl. Mater. Interfaces* **2019**, *11*, 22.
[78] S. Bekeschus, S. Eisenmann, S. K. Sagwal, Y. Bodnar, J. Moritz, B. Poschkamp, I. Stoffels, S. Emmert, M. Madesh, K.-D. Weltmann, T. von Woedtke, R. K. Gandhirajan, *Redox Biol.* **2020**, *30*, 101423.
[79] T. Heusler, G. Bruno, S. Bekeschus, J.-W. Lackmann, T. von Woedtke, K. Wende, *Clin. Plas. Med.* **2019**, *14*, 100086.
[80] S. Bekeschus, E. Freund, K. Wende, R. K. Gandhirajan, A. Schmidt, *Antioxidants* **2018**, *7*, 11.
[81] S. Reuter, T. von Woedtke, K. D. Weltmann, *J. Phys. D: Appl. Phys.* **2018**, *51*, 233001.
[82] J. W. Lackmann, K. Wende, C. Verlackt, J. Golda, J. Volzke, F. Kogelheide, J. Held, S. Bekeschus, A. Bogaerts, V. Schulz-von der Gathen, K. Stapelmann, *Sci. Rep.* **2018**, *8*, 7736.
[83] K. Wende, P. Williams, J. Dalluge, W. V. Gaens, H. Aboubakr, J. Bischof, T. von Woedtke, S. M. Goyal, K. D. Weltmann, A. Bogaerts, K. Masur, P. J. Bruggeman, *Biointerphases* **2015**, *10*, 029518.
[84] S. Bekeschus, K. Wende, M. M. Hefny, K. Rodder, H. Jablonowski, A. Schmidt, T. V. Woedtke, K. D. Weltmann, J. Benedikt, *Sci. Rep.* **2017**, *7*, 2791.
[85] D. Ellerweg, J. Benedikt, A. von Keudell, N. Knake, V. Schulz-von der Gathen, *New J. Phys.* **2010**, *12*, 013021.
[86] D. Ellerweg, A. von Keudell, J. Benedikt, *Plasma Sources Sci. Technol.* **2012**, *21*, 034019.
[87] N. Knake, S. Reuter, K. Niemi, V. Schulz-von der Gathen, J. Winter, *J. Phys. D: Appl. Phys.* **2008**, *41*, 194006.
[88] S. Reuter, J. Winter, A. Schmidt-Bleker, D. Schroeder, H. Lange, N. Knake, V. Schulz-von der Gathen, K. D. Weltmann, *Plasma Sources Sci. T.* **2012**, *21*, 2.
[89] S. Iseni, A. Schmidt-Bleker, J. Winter, K. D. Weltmann, S. Reuter, *J. Phys. D: Appl. Phys.* **2014**, *47*, 15.
[90] E. Karakas, M. Koklu, M. Laroussi, *J. Phys. D: Appl. Phys.* **2010**, *43*, 155202.
[91] S. A. Norberg, E. Johnsen, M. J. Kushner, *Plasma Sources Sci. Technol.* **2015**, *24*, 035026.
[92] A. Schmidt-Bleker, J. Winter, S. Iseni, M. Dunnbier, K. D. Weltmann, S. Reuter, *J. Phys. D: Appl. Phys.* **2014**, *47*, 145201.
[93] A. Schmidt-Bleker, J. Winter, A. Bosel, S. Reuter, K. D. Weltmann, *Plasma Sources Sci. Technol.* **2016**, *25*, 015005.
[94] J. L. Tanyi, S. Bobisse, E. Ophir, S. Tuyaerts, A. Roberti, R. Genolet, P. Baumgartner, B. J. Stevenson, C. Iseli, D. Dangaj, B. Czerniecki, A. Semilietof, J. Racle, A. Michel, I. Xenarios, C. Chiang, D. S. Monos, D. A. Torigian, H. L. Nisenbaum, O. Michielin, C. H. June, B. L. Levine, D. J. Powell Jr., D. Gfeller, R. Mick, U. Dafni, V. Zoete, A. Harari, G. Coukos, L. E. Kandalaft, *Sci. Transl. Med.* **2018**, *10*, eaao5931.
[95] S. Bekeschus, A. Schmidt, F. Niessner, T. Gerling, K. D. Weltmann, K. Wende, *J Vis Exp* **2017**, e56331.
[96] C. C. Winterbourn, *Nat. Chem. Biol.* **2008**, *4*, 278.
[97] J. Winter, K. Wende, K. Masur, S. Iseni, M. Dunnbier, M. U. Hammer, H. Tresp, K. D. Weltmann, S. Reuter, *J. Phys. D: Appl. Phys.* **2013**, *46*, 29.
[98] M. M. Gaschler, B. R. Stockwell, *Biochem. Biophys. Res. Commun.* **2017**, *482*, 419.
[99] J. W. Chang, S. U. Kang, Y. S. Shin, K. I. Kim, S. J. Seo, S. S. Yang, J.-S. Lee, E. Moon, S. J. Baek, K. Lee, *Arch. Biochem. Biophys.* **2014**, *545*, 133.
[100] N. Kaushik, N. Kumar, C. H. Kim, N. K. Kaushik, E. H. Choi, *Plasma Processes Polym.* **2014**, *11*, 1175.
[101] M. Adhikari, N. Kaushik, B. Ghimire, B. Adhikari, S. Baboota, A. A. Al-Khedhairy, R. Wahab, S. J. Lee, N. K. Kaushik, E. H. Choi, *Cell Commun. Signaling* **2019**, *17*, 52.
[102] K. Wende, S. Bekeschus, A. Schmidt, L. Jatsch, S. Hasse, K. D. Weltmann, K. Masur, T. von Woedtke, *Mutat. Res./Genet. Toxicol. Environ. Mutagen.* **2016**, *798–799*, 48
[103] S. Bekeschus, J. Bruggemeier, C. Hackbarth, K. D. Weltmann, T. von Woedtke, L. I. Partecke, J. van der Linde, *Plasma Sources Sci. Technol.* **2018**, *27*, 034001.
[104] S. Kluge, S. Bekeschus, C. Bender, H. Benkhai, A. Sckell, H. Below, M. B. Stope, A. Kramer, *PLoS One* **2016**, *11*, 9.
[105] S. Bekeschus, C. S. Schütz, F. Niessner, K. Wende, K.-D. Weltmann, N. Gelbrich, T. von Woedtke, A. Schmidt, M. B. Stope, *Oxid. Med. Cell. Longevity* **2019**, *2019*, 8535163.
[106] A. Schmidt, T. V. Woedtke, J. Stenzel, T. Lindner, S. Polei, B. Vollmar, S. Bekeschus, *Int. J. Mol. Sci.* **2017**, *18*, 4.
[107] J. van der Linde, K. R. Liedtke, R. Matthes, A. Kramer, C.-D. Heidecke, L. I. Partecke, *Plasma Med.* **2017**, *7*, 383.
[108] S. Bekeschus, A. Kading, T. Schroder, K. Wende, C. Hackbarth, K. R. Liedtke, J. van der Linde, T. von Woedtke, C. D. Heidecke, L. I. Partecke, *Anti-Cancer Agents Med. Chem.* **2018**, *18*, 824.
[109] S. Bekeschus, E. Freund, C. Spadola, A. Privat-Maldonado, C. Hackbarth, A. Bogaerts, A. Schmidt, K. Wende, K. D. Weltmann, T. von Woedtke, C. D. Heidecke, L. I. Partecke, A. Kading, *Cancers* **2019**, *11*, 1237.
[110] I. H. Wolf, J. Smolle, B. Binder, L. Cerroni, E. Richtig, H. Kerl, *Arch. Dermatol.* **2003**, *139*, 273.
[111] A. B. Bong, B. Bonnekoh, I. Franke, M. Schon, J. Ulrich, H. Gollnick, *Dermatology* **2002**, *205*, 135.
[112] L. Z. Ellis, J. L. Cohen, W. High, L. Stewart, *Dermatol. Surg.* **2012**, *38*, 6.
[113] S. Adams, D. W. O'Neill, D. Nonaka, E. Hardin, L. Chiriboga, K. Siu, C. M. Cruz, A. Angiulli, F. Angiulli, E. Ritter, R. M. Holman, R. L. Shapiro, R. S. Berman, N. Berner, Y. Shao, O. Manches, L. Pan, R. R. Venhaus, E. W. Hoffman, A. Jungbluth, S. Gnjatic, L. Old, A. C. Pavlick, N. Bhardwaj, *J. Immunol.* **2008**, *181*, 776.
[114] C. J. Gross, R. Mishra, K. S. Schneider, G. Medard, J. Wettmarshausen, D. C. Dittlein, H. Shi, O. Gorka, P. A. Koenig, S. Fromm, G. Magnani, T. Cikovic, L. Hartjes, J. Smollich, A. A. B. Robertson, M. A. Cooper, M. Schmidt-Supprian, M. Schuster, K. Schroder, P. Broz, C. Traidl-Hoffmann, B. Beutler, B. Kuster, J. Ruland, S. Schneider, F. Perocchi, O. Gross, *Immunity* **2016**, *45*, 4.

Check for updates

FULL PAPER

ADVANCED SCIENCE Open Access

www.advancedscience.com

Gas Plasma Technology Augments Ovalbumin Immunogenicity and OT-II T Cell Activation Conferring Tumor Protection in Mice

*Ramona Clemen, Eric Freund, Daniel Mrochen, Lea Miebach, Anke Schmidt, Bernhard H. Rauch, Jan-Wilm Lackmann, Ulrike Martens, Kristian Wende, Michael Lalk, Mihaela Delcea, Barbara M. Bröker, and Sander Bekeschus**

Reactive oxygen species (ROS/RNS) are produced during inflammation and elicit protein modifications, but the immunological consequences are largely unknown. Gas plasma technology capable of generating an unmatched variety of ROS/RNS is deployed to mimic inflammation and study the significance of ROS/RNS modifications using the model protein chicken ovalbumin (Ova vs oxOva). Dynamic light scattering and circular dichroism spectroscopy reveal structural modifications in oxOva compared to Ova. T cells from Ova-specific OT-II but not from C57BL/6 or SKH-1 wild type mice presents enhanced activation after Ova addition. OxOva exacerbates this activation when administered ex vivo or in vivo, along with an increased interferon-gamma production, a known anti-melanoma agent. OxOva vaccination of wild type mice followed by inoculation of syngeneic B16F10 Ova-expressing melanoma cells shows enhanced T cell number and activation, decreased tumor burden, and elevated numbers of antigen-presenting cells when compared to their Ova-vaccinated counterparts. Analysis of oxOva using mass spectrometry identifies three hot spots regions rich in oxidative modifications that are associated with the increased T cell activation. Using Ova as a model protein, the findings suggest an immunomodulating role of multi-ROS/RNS modifications that may spur novel research lines in inflammation research and for vaccination strategies in oncology.

1. Introduction

Reactive oxygen and nitrogen species (ROS/RNS) play a multifaceted role in biology.[1] They are part of the ancient immune defense mechanisms to protect from infection. At homeostatic levels, ROS/RNS also are versatile signaling molecules involved in antioxidant defense pathways, cell differentiation, and migration.[2] At supraphysiological levels during inflammation, however, ROS/RNS damage cells and tissues. Chronic inflammation and ROS/RNS generation is associated with several common diseases, such as autoimmunity, cardiovascular disease, and carcinogenesis.[3,4] While the unleashed activity of ROS-generating cells and immunopathological mechanisms in inflammation-associated diseases has been widely investigated in the past decades,[5–7] the specific roles of ROS/RNS-modified protein antigens are underexplored. Evidence for their significance is gained from reports on, for instance, oxidized low-density lipoprotein as a

R. Clemen, E. Freund, D. Mrochen, L. Miebach, A. Schmidt, K. Wende, S. Bekeschus
ZIK plasmatis
Leibniz Institute for Plasma Science and Technology (INP)
Felix-Hausdorff-Str. 2, Greifswald 17489, Germany
E-mail: sander.bekeschus@inp-greifswald.de

E. Freund, L. Miebach
Department of General
Visceral
Thoracic
and Vascular Surgery
University Medicine Greifswald
Sauerbruchstr. DZ7 Greifswald 17475, Germany

The ORCID identification number(s) for the author(s) of this article can be found under https://doi.org/10.1002/advs.202003395

DOI: 10.1002/advs.202003395

D. Mrochen, B. M. Bröker
Department of Immunology
University Medicine Greifswald
Sauerbruchstr. DZ7 Greifswald 17475, Germany

B. H. Rauch
Institute of Pharmacology (C_Dat)
University Medicine Greifswald
Felix-Hausdorff-Str. 1 Greifswald 17489, Germany

J.-W. Lackmann
CECAD proteomics facility
University of Cologne
Joseph-Stelzmann-Str. 26 Cologne 50931, Germany

U. Martens, M. Delcea
ZIK HIKE
University of Greifswald
Fleischmannstr. 42–44 Greifswald 17489, Germany

U. Martens, M. Lalk, M. Delcea
Institute of Biochemistry
University of Greifswald
Felix-Hausdorff-Str. 4 Greifswald 17489, Germany

putative biomarker in diabetes and cardiovascular disease.[8,9] A similar suggestion was made for oxidatively modified laminin in atherosclerosis.[10] In these conditions, it is hypothesized that ROS/RNS-mediated protein modifications may generate novel immunoepitopes or break tolerance against existing epitopes, which contributes to autoinflammation and autoimmunity.[11,12] While current therapeutic strategies aim to decrease ROS/RNS levels to avoid misguided immunity, the same is encouraged in some research lines in oncology. This seeming contradiction relates to the fact that tumors actively suppress immune responses targeted against tumor antigens, and ROS/RNS may revert this action as recently suggested in a vaccination study showing increased protection in ovarian cancer patients.[13]

The ROS/RNS chemistry and reaction pathways are complex as myeloid cells and partially also stromal cells release a plethora of different enzymatically generated ROS/RNS during inflammation. For instance, the nitric oxide synthase (NOS) produces nitric oxide (NO), while NADPH oxidases (NOX) generate superoxide (O_2^-), and both agents can combine to yield peroxynitrite ($^-$ONOO). Superoxide can also spontaneously disproportionate to hydrogen peroxide (H_2O_2), a process amplified by the enzyme superoxide dismutase (SOD). The enzyme myeloperoxidase (MPO) is known to generate hypobromous acid, hypochlorous acid, and hypothiocyanite.[14] Hypochlorite, in turn, contributes to the generation of atomic and singlet oxygen (O) and hydroxyl radicals (OH),[15] while the latter is predominantly generated via the Fenton reaction of H_2O_2 with ferrous iron as catalyst. Some or even the complete selection of mentioned agents are present during inflammation. However, it is challenging to produce them simultaneously by chemical means to model the inflammatory environment.

Gas plasma, an electron-impact and photon-driven technology, bridges this gap. This partially ionized gas generates diverse ROS/RNS concurrently and in a spatially controlled manner.[16] In physics, the term gas plasma generally includes also hot plasmas not suitable for biomedical applications. Hence, we here use the term gas plasma as a synonym for physical plasmas that operate at about body temperature and do not cause thermal harm to cells and tissues. Other synonyms of the term gas plasma used in applied plasma physics in biomedical fields are cold (physical) plasma, nonthermal plasma, (cold) atmospheric (pressure) plasma, tissue-tolerable plasma, discharge plasma, and low-temperature plasma. In gas plasma jets, a noble gas is excited by a high-frequency electrode, and the excited noble gas species transfer their chemical energy to oxygen and nitrogen in the ambient air, generating reactive oxygen and nitrogen species, respectively. Recent leap innovations facilitated this technology to generate highly reactive gas plasmas at body temperature, allowing the study of ROS/RNS without thermal effects in the medical field.[17] Not only due to its antibacterial properties,[18] this technology is successfully applied for studying the promotion of ROS/RNS-related wound healing in animal models [19] as well as in patients.[20] As ROS/RNS have hormetic properties, being stimulating at low and toxic at high doses,[21] the technology is increasingly investigated to treat cancer, especially of the skin.[22–27] We have recently provided evidence in mice that gas plasma treatment reduces skin cancer [26] and first patients suffering from actinic keratosis [28] and end-stage head and neck cancer have benefited from gas plasma therapy.[29] Strikingly, we and others identified gas plasma treatment to have an immunological dimension [30,31] by inducing the immunogenic cancer cell death (ICD [32]) in vitro [33,34] and in vivo.[35,36] Several reports have moreover suggested using gas plasma technology as anticancer agent against internal tumors [37] originating from, for instance, breast,[38–40] pancreatic,[41–43] colon,[44–46] liver,[47–49] central nervous,[50–52] ovarian,[53–55] and prostate[56–58] tissue. These and other studies also clearly demonstrated the importance of short-lived ROS/RNS in the induction of ICD. Although unambiguously identifying every single type of ROS/RNS in the gas plasma is currently limited by the lack of technical tools, the composition of gas plasma-derived ROS/RNS landscapes and subsequent biological responses can be controlled by modifying the gas composition fed into a gas plasma jet.[59,60] The different landscapes allow identifying sets of effector ROS/RNS linked to the effects observed.

We here aimed to understand the immunological consequences of a ROS/RNS-modified model protein, chicken ovalbumin (Ova), using preformed anti-Ova T cells from OT-II mice. To generate a versatile array of inflammation-related ROS/RNS, gas plasma technology was used for Ova oxidation (oxOva). We identified enhanced T cell activity towards oxOva ex vivo and in vivo and found a tumor-protective action of oxOva when given as a vaccine to mice challenged with Ova-expressing melanoma cells. Two different gas plasmas setups were used, one operated with argon (ox I) and another operating with helium/oxygen (ox II) gas. Each generated a distinct pattern of ROS/RNS as analyzed in the plasma gas phase, treated liquids, and modified proteins using mass spectrometry. By finding that ox II was superior to ox I in amplifying T cell responses and linking this to the physicochemical analysis of both gas plasma setups, singlet delta oxygen and atomic oxygen reaching the target are components suggested to be held responsible for promoting the immunogenicity of ovalbumin in our model systems.

2. Results

2.1. Gas Plasma-Generated ROS/RNS Chemistry and Protein Modification

We aimed to investigate the immunological consequences of ROS/RNS-derived protein modifications using chicken ovalbumin (Ova) as a model protein. To mimic a multi-ROS/RNS environment, gas plasma, an electron-impact and photon-driven technology, was employed using an atmospheric pressure plasma jet. As feed gas, either argon (ox I) or helium/oxygen (ox II) was used (**Figure 1**a, left panel), and the gas plasma, as well as the gas plasma-treated liquid, was analyzed (Figure 1a, right panel). To distinguish distinct ROS/RNS fingerprints in these two modes, optical emission spectroscopy (OES) identified the ox I set up to be rich in the lines of the second positive system of nitrogen that are responsible for RNS formation as well as hydroxyl radical (OH). In contrast, the ox II setup showed enrichment of atomic oxygen (O) (Figure 1b). These two modes were subsequently used to treat a liquid (PBS) spiked with Ova or not. Alternatively, mock gas treatment alone (with the plasma being switched off) served as control. Only one mock condition was used as both were shown to not have an effect in pilot experiments. The gas plasma treatment did not affect the pH of a

ADVANCED SCIENCE NEWS
www.advancedsciencenews.com

ADVANCED SCIENCE Open Access
www.advancedscience.com

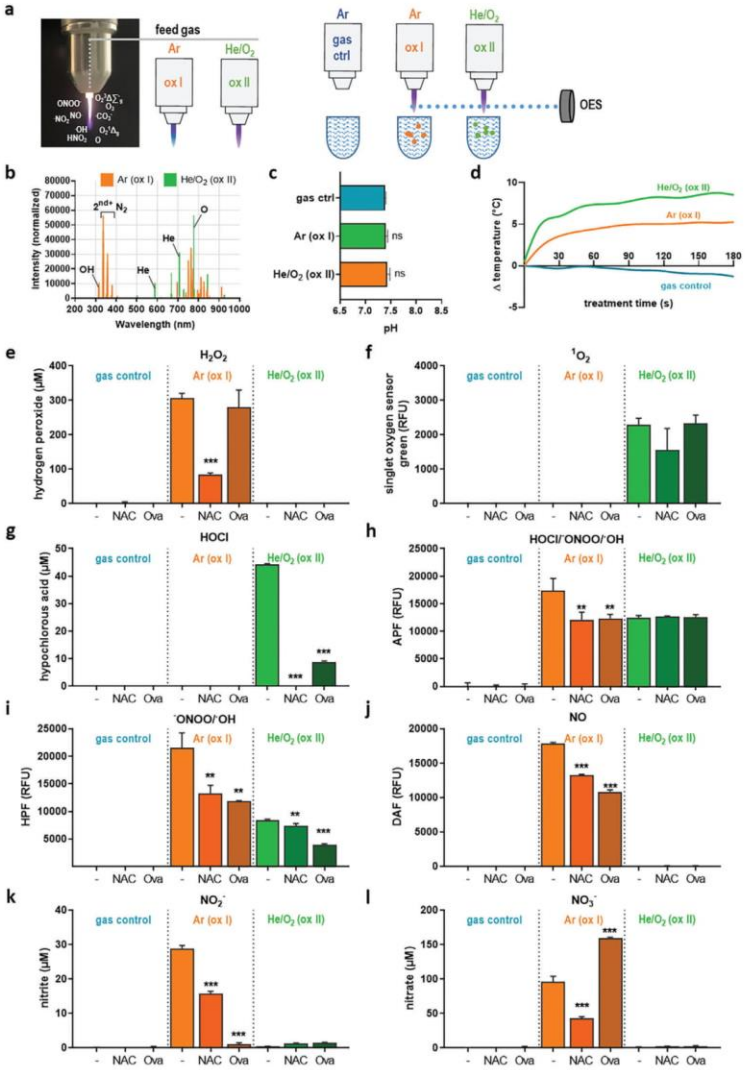

Figure 1. ROS/RNS fingerprint of two distinct gas plasma modes. a) Image of the atmospheric pressure plasma jet kINPen used in this study, and schematic of the two gas modes employed to generate different types of plasma; b) optical emission spectroscopy (OES) of the two plasma modes showing distinct peak characteristics representing different types of reactive atoms and molecules such as reactive nitrogen species (RNS), hydroxyl radicals (OH), and atomic oxygen (O); c) pH of PBS measured after gas plasma treatment; d) temperature kinetic of PBS during gas plasma exposure; e–l) major reactive species analyzed in control and gas plasma-treated PBS in the presence or absence of ovalbumin (Ova) or *n*-acetylcysteine (NAC), showing levels of e) hydrogen peroxide (H_2O_2), f) singlet oxygen ($^1O_2$), g) hypochlorous acid (HOCl), h) APF, i) HPF, j) DAF, k) nitrite (NO_2^-), and l) nitrate (NO_3^-), Data are representative of several experiments; statistical analysis was performed using one-way anova (* $p < 0.05$; ** $p < 0.01$; *** $p < 0.001$); Ar = argon; He = helium; ctrl = control.

phosphate-saline solution (Figure 1c), while modest changes in the temperature of this solution (baseline temperature: 15 °C) were observed (Figure 1d). Subsequently, the analysis of a selection of primary and secondary reactive species in the liquid was performed in the absence or presence of Ova or *n*-acetylcysteine (NAC). For hydrogen peroxide (H_2O_2), only ox I but not ox II conditions yielded this secondary oxidant mostly derived from hydroxyl radicals, and the presence of NAC but not Ova reduced significant amounts of H_2O_2 (Figure 1e). For singlet delta oxygen ($^1O_2$), a marked elevation in the ox II but not the ox I condition was revealed with negligible scavenging ability of Ova (Figure 1f). By contrast, both Ova and NAC scavenged significant amounts of hypochlorous acid (HOCl) generated in the ox II but not ox I mode (Figure 1g). Aminophenyl fluorescein (APF) and hydroxyphenyl fluorescein (HPF) sense peroxynitrite ($^-$ONOO) and hydroxyl radicals ($^\cdot$OH), while APF also senses HOCl.[61] Both ox I and ox II increased fluorescence of APF, while NAC and OVA significantly reduced signal intensities only in ox I (Figure 1h). Ova and NAC reduced HPF fluorescence following ox I and ox II treatment (Figure 1i). Therefore, the data of both APF and HPF suggested the generation of hydroxyl radicals and peroxynitrite, which was confirmed for hydroxyl radicals (Figure S1a, Supporting Information) and is in line with previous research on this jet's chemistry.[62,63] Increased fluorescence of diaminofluoresceins (DAF) indicates nitric oxide (NO).[64] Under the ox I but not ox II condition generating emission lines of the second positive nitrogen system capable of eliciting RNS (Figure 1b), ox I but not ox II treatment generated NO (Figure 1j) and the NO-related products nitrite (Figure 1k) and nitrate (Figure 1l). Interestingly, the presence of Ova during the treatment modulated the levels of nitrite (NO_2^-) and nitrate (NO_3^-) levels in both ox I and ox II conditions. Moreover, NAC significantly scavenged NO, NO_2^-, and NO_3^-, while the presence of Ova led to a significant increase of the latter. These data pointed to two distinct ROS/RNS chemistries of the ox I and ox II condition and the Ova protein interfering with the decay kinetics of the reactive species deposited by the plasma jet. Subsequently, Ova treated with either the ox I (oxOva I) or ox II (oxOva II) gas plasma setting was analyzed (**Figure 2**a). Although treatment with ox I and ox II seemingly decreased the presence of native Ova in nonreducing SDS-PAGE (Figure 2b, left panel), Western Blot analysis confirmed the presence of the protein (Figure 2b, right panel). To analyze possible protein degradation or aggregation, dynamic light scattering was performed. The correlogram of oxOva II showed a shorter light scatter decay time, and the one of oxOva I was longer (Figure 2c), both being significantly different from native Ova (Figure 2d). In the presence of NAC, correlograms of Ova, oxOva I, and oxOva II were similar (Figure S1b, Supporting Information), suggesting a ROS/RNS dependent mechanism of the changes observed without NAC. Moreover, these findings indicated changes in the reflective properties of the protein solution following gas plasma treatment. Diameter measurements confirmed these findings, and especially oxOva II showed a small but distinguishable second peak (Figure 2e), which area under the curve (AUC) was significantly larger compared to that of native Ova (Figure 2f). Collectively, this pointed to an overall subtle increase in protein aggregation in the ox II condition. The notion of a more diverse protein population in ox II was supported by calculating the polydispersity index (PDI) from the correlograms (Figure 2g). To characterize the gas plasma-derived ROS/RNS and subsequently induced changes to Ova in terms of protein structure and folding, circular dichroism (CD) spectroscopy was performed. In CD spectroscopy measurement, α-helical structures are indicated by a minimum signal at 209 nm and a shoulder at 222 nm.[65] Characteristic for β-sheets are peaks at 195 nm and a negative minimum at 217 nm.[66] Gas plasma treatment of Ova led to a shift in the signal for minima and maxima as well as ellipticity (Figure 2h). This was pronounced in oxOva II, in which an increase of α-helical structures and a reduction in β-sheets were observed. Again, the presence of NAC abrogated these changes and showed similar CD spectra (Figure S1c, Supporting Information). In summary, we found both gas plasma modes to generate a distinct set of reactive species that subsequently affected the monomeric form and secondary structure of Ova, especially in the ox II condition being rich in atomic and singlet oxygen production.

2.2. Oxidized Ova Changes Antigen Uptake but not Activation in APCs Being Relevant for Mounting Activation of OT-II T Cells

ROS/RNS are agents plentifully released during inflammation, but the immunological consequences of ROS/RNS-induced modifications are underexplored. To this end, we used gas plasma technology to oxidatively modify Ova (oxOva), and to incubate Ova-specific T cells of splenocytes with Ova or oxOva before assessing their activity (**Figure 3**a). Genetically engineered OT-II mice harbor this specific set of $CD4^+$ T helper cells that encode anti-Ova T cell receptors. Splenocytes of OT-II mice are a suitable model system to study the immunogenicity of Ova modifications. The hypothesis was that oxOva modulates the uptake, processing, and/or presentation of antigen by professional antigen-presenting cells (APCs) such as macrophages and dendritic cells (DCs) via major histocompatibility complex (MHC) II to $CD4^+$ T cells. Initially, the activation of viable macrophages ($CD11b^+/CD11c^+/CD64^+$) and DCs ($CD11b^+/CD11c^+/CD24^+$) being incubated with either Ova or oxOva was measured using flow cytometry analysis of the murine MHC II molecule I-A/I-E (Figure 3b). No significant I-A/I-E expression changes were found (Figure 3c), discouraging the idea of oxOva acting as an immediate danger-signaling molecule in these cells. This was supported by western blot data bone marrow-derived dendritic cells from wildtype C57BL/6 mice incubated with either Ova or oxOva II, and harvested 15, 30, and 60 min later for analyzing protein phosphorylation within MAPK-related signaling pathways (Figure S1f, Supporting Information). None of the targets (Akt, Erk1/2, MSK2/3, RSK1/2) showed a significant change in oxOva II when compared against native Ova (Figure S1g, Supporting Information). To understand the specificity of T cell activation and the role of professional antigen-presenting cells (APCs) in augmenting T cell activation, fluorescently labeled APC subtypes were initially investigated. Bodipy-conjugated Ova (DQ-Ova), an Ova-aggregate, shows only background fluorescence since the fluorescence moieties quench each other when being in close vicinity. Upon uptake, however, DQ-Ova is degraded, increasing its fluorescence intensity.[67] We confirmed the uptake and degradation of this protein into $CD11b^+$ myeloid cells in general (Figure 3d) and $F4/80^+$ macrophages, specifically (Figure 3e). We

ADVANCED SCIENCE NEWS
www.advancedsciencenews.com

ADVANCED SCIENCE Open Access
www.advancedscience.com

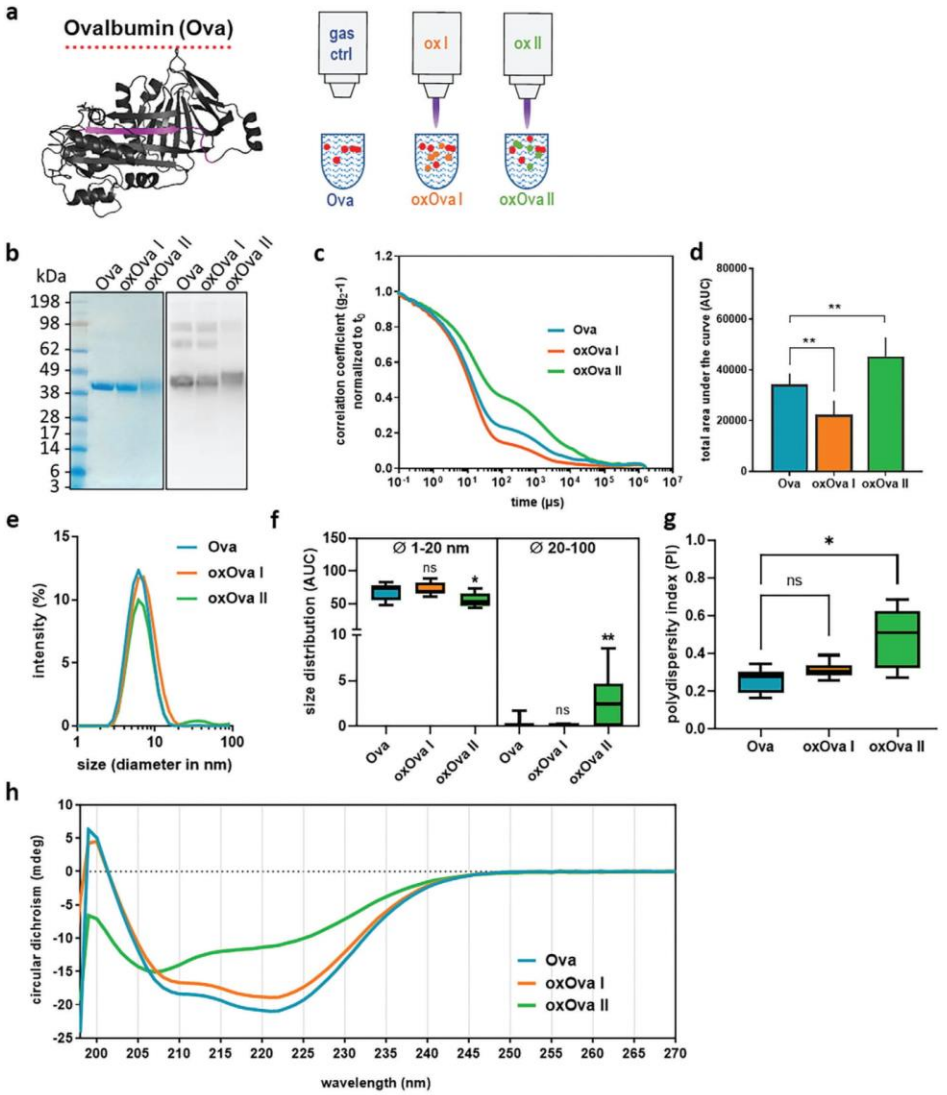

Figure 2. Gas plasmas-derived modifications of Ova protein morphology. a) Crystal structure of Ova and schematic indicating the gas plasma treatment of Ova; b) representative coomassie-stained gel and western blot of Ova and oxOva showing different staining patterns. c,d) photon correlation spectroscopy and correlation coefficients c) showing smaller and larger Ova structures for d) oxOva I and oxOva II ($n = 4$), respectively; e) intensity-weighted hydrodynamic diameter and f) area under the curve (AUC) quantification of this parameter suggesting modest but significant aggregation with oxOva II ($n = 3$); g) polydispersity index (PDI) of correlogram showing more diverse particles with oxOva II ($n = 3$); h) structural properties and secondary folding measured using circular dichroism spectroscopy ($n = 2$). Statistical analysis was performed using one-way anova (* $p < 0.05$; ** $p < 0.01$; *** $p < 0.001$); ns = not significant.

ADVANCED SCIENCE NEWS
www.advancedsciencenews.com

ADVANCED SCIENCE Open Access
www.advancedscience.com

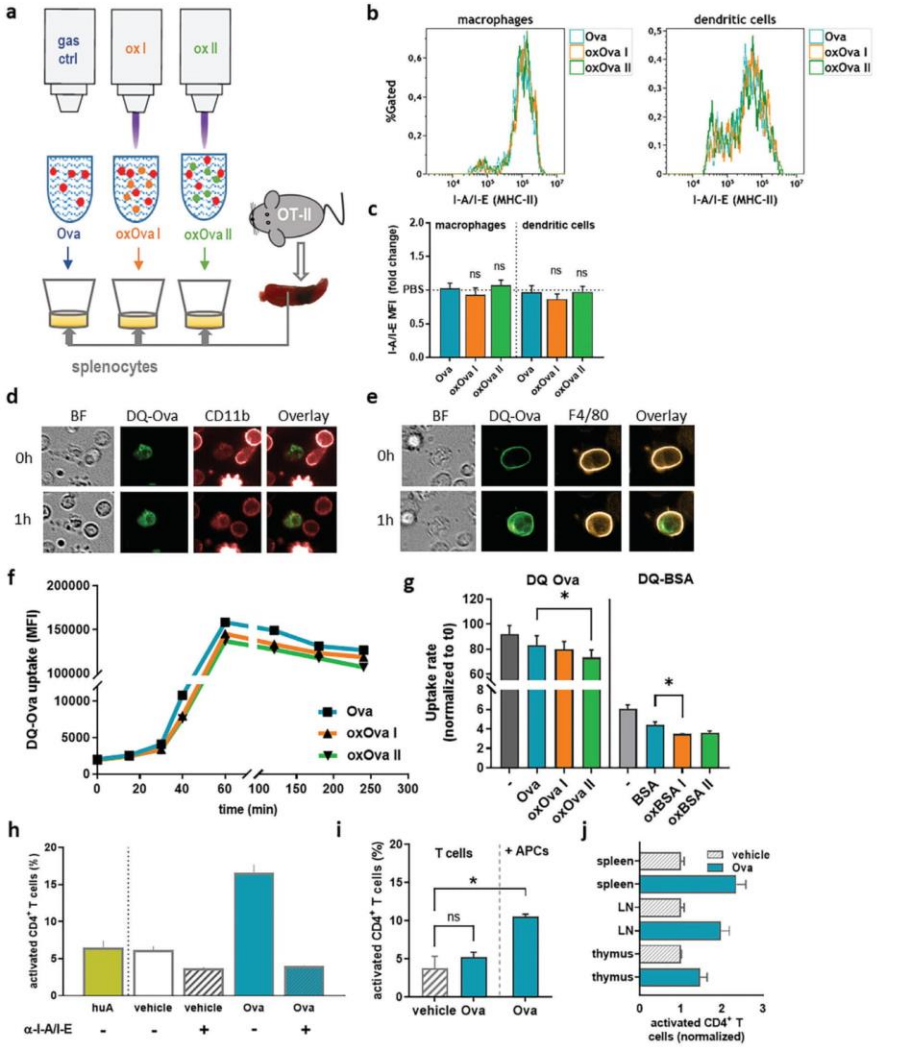

Figure 3. Oxidized Ova changes antigen uptake but not activation in APCs being relevant for mounting activation of OT-II T cells. a) Setup of the gas plasma treatment of Ova and incubation with OT-II derived splenocytes; b,c) representative flow cytometry intensity histograms of I-A/I-E (MHC-II) expression on live macrophages and dendritic cells from splenocytes pulsed with either b) Ova, oxOVA I, or oxOVA II, and c) quantification thereof; d,e) visualization of DQ-Ova (green) uptake and degradation in d) CD11b+ myeloid cells and e) F4/80$^+$ macrophages; f,g) representative kinetic of the mean fluorescence intensity of DQ-Ova fluorescing only upon uptake in I-A/I-E (MHC II)-positive cells in presence of Ova, oxOva I, or oxOva II as determined using multicolor flow cytometry, and quantification thereof of DQ-Ova (+Ova) or DQ-BSA (+BSA) at g) 120 min; h) preincubation of splenocytes anti-I-A/I-E antibodies abolished Ova-induced activation of CD4$^+$ T cells activation that was specific to chicken Ova but not to human albumin; i) activation of magnetically sorted CD4$^+$ T cells in the presence of Ova or Ova+APCs; j) CD4$^+$ T cell activation from different tissues after pulsing with Ova. Data representative of three independent experiments; statistical analysis was performed using one-way anova (* $p < 0.05$); ns = not significant; scale bar = 20 µm.

then asked whether the uptake kinetics of DQ-Ova in murine professional antigen-presenting cells changed in the presence of Ova compared to oxOva I or oxOva II (Figure 3f). Interestingly, the uptake or processing of DQ-Ova significantly declined in the presence of ox Ova II, suggesting competing uptake kinetics or preferential uptake via a specific route in APCs (Figure 3g). We were also able to recapitulate this finding in a second model protein, bovine serum albumin (BSA) compared to oxBSA I or oxBSA II in the presence of DQ-BSA, and observed a less pronounced but still significant effect in ox I conditions (Figure 3g). To next ascertain the specificity of OT-II $CD4^+$ T cells to Ova-derived peptides presented by APCs, the interaction between T cells and APCs was prohibited by using MHC-II (I-A/I-E) blocking antibodies (Figure 3h). OT-II T cell activation (% of $CD69^+/CD25^+$ cells) in splenocytes was observed only against chicken Ova but not human albumin (huA), and only in the absence of blocking antibody. Vice versa, magnetically isolated $CD4^+$ T cells were not activated by Ova in the absence of APCs (Figure 3i). Investigating several lymphatic organs, T cell activation to Ova was maximal in splenocytes (Figure 3j). These data emphasized the suitability of the model and the specificity of OT-II derived splenocytes for studying the effect of Ova modifications on $CD4^+$ T cell activation.

2.3. Oxidation of Ova Augments Activation of OT-II T Cells

Several concentrations of Ova, oxOva I, and oxOva II were tested for their inherent toxicity to $CD4^+$ T cells in terms of caspase 3/7 activation indicative of apoptosis (**Figure 4**a). The quantification revealed a consistent but mild reduction of viability for oxOva I but not oxOva II (Figure 4b). Subsequently, the percentage of $CD69^+/CD25^+$ activated $CD4^+$ T cells among all $CD4^+$ T cells was analyzed ex vivo in splenocytes derived from OT-II mice (Figure 4c). A significant fold-change increase of T cell activation was observed for both ox Ova I and oxOva II when compared to Ova, which was specific for $CD4^+$ OT-II cells but not found in $CD8^+$ T cells of OT-I mice (Figure 4d). The effect of oxOva was identified only in T cells from OT-II mice (harboring Ova-specific $CD4^+$ T cells) but not C57BL/6 or SKH-1 wild type mice (Figure 4e). This suggested the oxPTM-enhanced T cell activation ex vivo to take place preferentially in antigen-specific cells. This striking finding suggested a role of oxidative protein modifications in T cell cross-talk with APCs, as it was not observed in the presence of I-A/I-E (MHC II) blocking antibodies interfering with T cell-APC interaction (Figure 4f) and in magnetically isolated T cells alone (absence of APCs) incubated with oxOva (Figure 4g). To underline the dominating role of oxidative protein modifications, we exposed Ova to pulsed electric fields, a physical property of gas plasma jets.[68] The treatment could not increase the activation of $CD4^+$ T cells among splenocytes above the level of native Ova alone (Figure S1d, Supporting Information), suggesting this physical parameter to not play a role in the effects observed. To further confirm T cell activation, proliferation studies were performed by labeling splenocytes with the cell-tracer CFSE and analyzing the fluorescence distribution three days later (Figure 4h). The quantification of proliferated cells revealed a marked increase for oxOva I and oxOva II when compared to Ova (Figure 4i, left panel). Importantly, $CD4^+$ OT-II cells failed to proliferate not only in PBS (vehicle) controls but also in response to human albumin (huAlb) or gas plasma-modified huAlb (oxhuAlb I and oxhuAlb II) (Figure 4j, right panel). Analysis of the expression of CD44, a marker of memory T cells, in all T cells exposed to either Ova, oxOva I, or oxOva II, the latter two showed significantly amplified CD44 intensities as determined at day 3 by flow cytometry (Figure 4j). Of note, quantifying the intensity of CD69, a T cell activation marker, in the nonproliferating portion of $CD4^+$ OT-II cells three days after challenge with either Ova, oxOva I, or oxOva II, a significant increase was observed (Figure 4k). This suggested that oxidative modifications of Ova not only spurred the proliferation of T cells but also led to the activation of T cells that did not proliferate. To provide evidence of the dominant role of ROS/RNS in these findings, the addition of the antioxidant NAC in plasma treated protein solution significantly decreased oxOva I and oxOva II-induced T cell activation in OT-II splenocytes (Figure 4l). To additionally ascertain that direct gas plasma treatment of Ova and its subsequent modifications via short-lived ROS/RNS and not the mere presence of long-lived ROS/RNS was a requirement for augmented T cell activation among splenocytes of OT-II mice, two experiments were set up. In the first experiment, splenocytes were pulsed with Ova, oxOva I, oxOva II, or Ova treated with those concentrations of hydrogen peroxide (H_2O_2, only generated in ox I), nitrite (NO_2^-, only generated in ox I), nitrate (NO_3^-, only generated in ox I), and hypochlorous acid (HOCl, only generated in ox II) that exactly matched the concentrations yielded by gas plasma treatment in PBS alone, to disguise the effects of individual, long-lived components. None of the agents recapitulated the increase in T cell activation as observed with ox I or ox II, except for a modest increased for HOCl (Figure 4m). In the second experiment, PBS without Ova was exposed to gas plasma or left untreated (PBS, oxPBS I, and oxPBS II). Incubation of splenocytes with oxPBS I or oxPBS II alone (in the absence of Ova) did not yield elevated T cell activation (Figure 4n, left panel). This underlined that the ROS/RNS alone did not promote T cell activation and only the Ova antigen or its oxidized counterpart oxOva did so. This important notion was underlined by gas plasma-treating PBS first and adding Ova second before the Ova-PBS or Ova-oxPBS was added to splenocytes. No increase in T cell activation was observed (Figure 4n, right panel). These results strongly suggested that the direct gas plasma oxidation of Ova via short-lived ROS/RNS, and not individual and well known long-lived ROS/RNS alone, were required to achieve the strong stimulatory effects observed in OT-II Ova-specific T cells. Additionally, the finding of increased CD69 activation in nonproliferating T cells following exposure to oxOva (Figure 4k) indicated differential responses of $CD4^+$ T cell subpopulations to oxOva-derived peptides presented by APC, possibly being reflected in changes in the cytokine profile. To this end, we performed multiplex arrays to map the cytokine profiles that were accompanied by Ova or oxOva stimulation. In supernatants of splenocytes incubated with Ova or oxOva ex vivo for 24 h, a significant increase in interferon-gamma (IFNγ) and interleukin (IL) 13 was identified (Figure 4o). T_H17 cytokines, such as IL-17F and IL-22, were elevated as well. In general, it was the notion that oxOva II exerted more potent effects on cytokine release compared to oxOva I.

ADVANCED SCIENCE NEWS
www.advancedsciencenews.com

ADVANCED SCIENCE Open Access
www.advancedscience.com

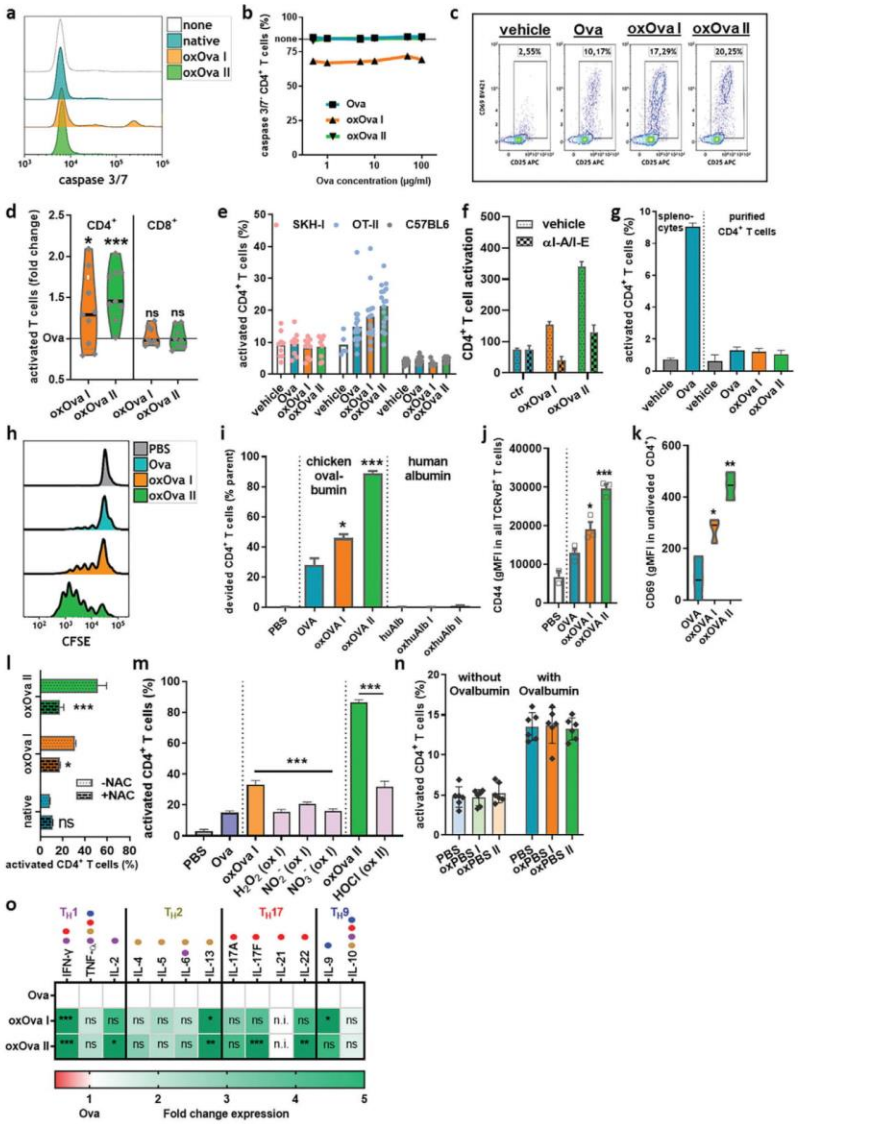

Figure 4. Oxidation of Ova augments the activation of OT-II T cells. a) Representative overlay histograms and b) percentage of caspase 3/7⁻ cells 24 h after incubation (with either Ova, oxOva I, or oxOva II across a range of Ova concentrations; c) representative flow cytometry dot plots of OT-II splenocytes-derived CD4⁺ T cells and their activation (CD69⁺/CD25⁺) after stimulation with either Ova, oxOva I, or oxOva II at 24 h; d) quantification of activation of T cells from OT-II (CD4⁺) or OT-I (CD8⁺) splenocytes in response to either Ova, oxOva I, or oxOva II at 24 h, and shown as fold-change of oxOva I and oxOva II to Ova; e) T cell activation of Ova-specific CD4⁺ T cells from OT-II mice-derived splenocytes, wild type C57BL/6 mice-derived

2.4. T Cell Response to Vaccination of OT-II Mice with Ova or Oxidized Ova

Up to this point, we used two different ROS/RNS environments generated by gas plasma to differentially oxidize Ova (oxOva I and oxOva II), and tested the consequences of incubation with either Ova or oxOva I or II in OT-II derived splenocytes and T cell activation and proliferation ex vivo. To next analyze the ability of oxOva to exacerbate T cell activation in vivo (**Figure 5**a), we rechallenged OT-II mice with either Ova, oxOva I, or oxOva II, and three days later analyzed $CD4^+$ T cell activity in the draining lymph nodes (Figure 5b). Both oxOva II and especially oxOva I vaccination but not oxOva + NAC (Figure S1e, Supporting Information) yielded significantly elevated numbers of activated T cells when compared to native Ova (Figure 5c), pointing to increased immunogenicity of the gas plasma-treated protein ovalbumin. Among all activated $CD4^+$ T cells, effector (oxOva II) and memory T cells (oxOva I) were found to a greater extent when compared to native activated T cells of animals vaccinated with Ova (Figure 5d). Similar to the results seen ex vivo, this pointed to a differential role of the T cell subpopulations, leading us to investigate the T_H cytokine profile in the minced draining lymph nodes of vaccinated animals in more detail (Figure 5e). For oxOva II, there was an increase in IL-2 and IL-17F as well as IL-22. These results were strikingly similar to those obtained in the ex vivo experiments (Figure 4o). For all other targets investigated, oxOva I administered in vivo did not give any changes, while oxOva II additionally spurred the release of tumor necrosis factor (TNF) α and several other T_H2 and T_H17-related cytokines. However, the most apparent congruency was found for IFNγ secretion being sharply elevated in both lymph nodes from oxOva I / ox Ova II vaccinated mice splenocytes incubated ex vivo with oxOva I / ox Ova II.

2.5. OxOva Vaccination of C57BL/6 Wild Type Reduced Melanoma Growth In Vivo

Vaccination of OT-II mice with oxOva generated a marked increase in IFNγ release, a molecule known for its antitumor effects. To test the functional consequences of gas plasma-oxidized Ova in wild type mice with no pre-existing anti-Ova adaptive immunity, C57BL/6 mice were vaccinated two times with either Ova or oxOva, followed by subcutaneous inoculation of Ova-expressing B16F10 syngeneic melanoma cells (**Figure 6**a). OxOva II but not oxOva I immunization led to a significantly impaired tumor growth (Figure 6b), pointing to an enhanced adaptive antitumor immune response mediated by the oxidized compared to the native form of Ova. The analysis of tumor-infiltrating T cells showed increased numbers of $CD4^+$ and $CD8^+$ T cells in the tumor microenvironment (Figure 6c). OxOva vaccination also was accompanied by significantly elevated numbers of intratumoral dendritic cells and macrophages (Figure 6d). Additionally, in $CD8^+$ cytotoxic T cells, the expression of the memory T cell marker CD44 (Figure 6e) was found to be increased in tumors of mice that had received oxOva II vaccination (Figure 6f). This corroborated our analysis of the T cell activation profile, which was found to be enhanced in both $CD4^+$ and $CD8^+$ T cells but only for oxOva II and not oxOva I vaccination (Figure 6g). These findings suggested that oxOva II led to a more pronounced generation of Ova-specific T cells that, in turn, contributed to decelerated growth of Ova-expressing melanoma cells in wild type mice in vivo. Finally, to confirm the improved generation and activation of novel anti-Ova T cell entities, splenocytes of tumor-bearing wild type mice receiving oxOva vaccination were restimulated with Ova ex vivo. The analysis of the percentage of activated T cells 24 h later showed a significantly increased activation in the $CD4^+$ helper cell subpopulation for both oxOva I and oxOva II vaccinated mice (Figure 6h). In contrast, a more pronounced activation within the $CD8^+$ cytotoxic subpopulation was observed for oxOva II only (Figure 6i). Interestingly, a modest but significant enhancement of T cell activation was also observed upon restimulation with the melanoma antigen MART-1 (data not shown), a finding that warrants further investigation in future studies. Collectively, these results suggest that gas plasma-derived ROS/RNS increased the immunogenicity of Ova, leading to enhanced activation of existing adaptive immunity as well as a greater quantity or quality of newly generated Ova-specific T cells, which possibly contributed to effective antitumor immunity.

2.6. Modification Mapping Unraveled Three Distinct Hyperoxidized Regions in oxOva

The altered immunological perception of oxOva compared to native Ova prompted us to analyze the gas plasma-introduced

splenocytes, or SKH-1 mice-derived splenocytes in response to either Ova, oxOva I, or oxOva II at 24 h; f) OT-II splenocytes were cultured incubated with vehicle or I-A/I-E blocking antibodies prior to addition of Ova, oxOva I, and oxOva II, showing that $CD4^+$ T cell activation was dependent on binding I-A/I-E on APCs; g) magnetically isolated $CD4^+$ T cells alone (in absence of APCs) fail to show increased activation in response to oxOva I or oxOva II compared to $CD4^+$ T cells within splenocytes, confirming the need of APCs to be present for the enhanced immunogenicity of oxOva in terms of T cell activation; h) 3d incubation of CFSE-labeled OT-II splenocytes with either h) Ova, oxOval, or oxOva II, and representative CFSE overlay, i) quantification of proliferating ($CFSE^{low}$) cells including appropriate human albumin (huAlb) control, j) the intensity of the memory T cell marker CD44 in all $TCR\nu B^+$ T cells, and k) staining intensity of the T cell activation marker CD69 in the nonproliferating ($CFSE^{hi}$) T cell population; l) addition of NAC prior to gas plasma treatment of Ova abrogated the ability of oxOva I and oxOva II to augment $CD4^+$ T cell activation in OT-II splenocytes ex vivo; m) experimentally added (chemical) ROS/RNS such as hydrogen peroxide (H_2O_2, only generated in ox I), hypochlorous acid (HOCl, only generated in ox II), nitrite (NO_2^-, only generated in ox I), and nitrate (NO_3^-, only generated in ox I) supplied at the concentration matched to what gas plasma treatment generated in PBS alone failed to promote T cell activation to a similar extent compared to gas plasma-derived mixtures of short-lived ROS/RNS; n) PBS was left untreated or exposed to ox I (oxPBS I) or ox II (oxPBS II) gas plasma, added to OT-II splenocytes, followed by addition of vehicle (-ovalbumin) or Ova (+ovalbumin) 1 h later, and $CD4^+$ T cell activation was measured 24 h later, showing the prerequisite of short-lived ROS/RNS from the direct gas plasma treatment of Ova oxidation for augmented $CD4^+$ T cell activation in OT-II splenocytes ex vivo; o) T_H cell cytokine profile of Ova/oxOva I/oxOva II-pulsed OT-II-splenocytes at 24 h with dominating cytokine signatures ($T_H1/T_H2/T_H17/T_H9$ segmentation) and annotated possible cytokine production (color code and dots). Data are representative of three independent experiments; statistical analysis was performed using one-way or two-way anova (* $p < 0.05$; ** $p < 0.01$; *** $p < 0.001$).

ADVANCED SCIENCE NEWS
www.advancedsciencenews.com

ADVANCED SCIENCE Open Access
www.advancedscience.com

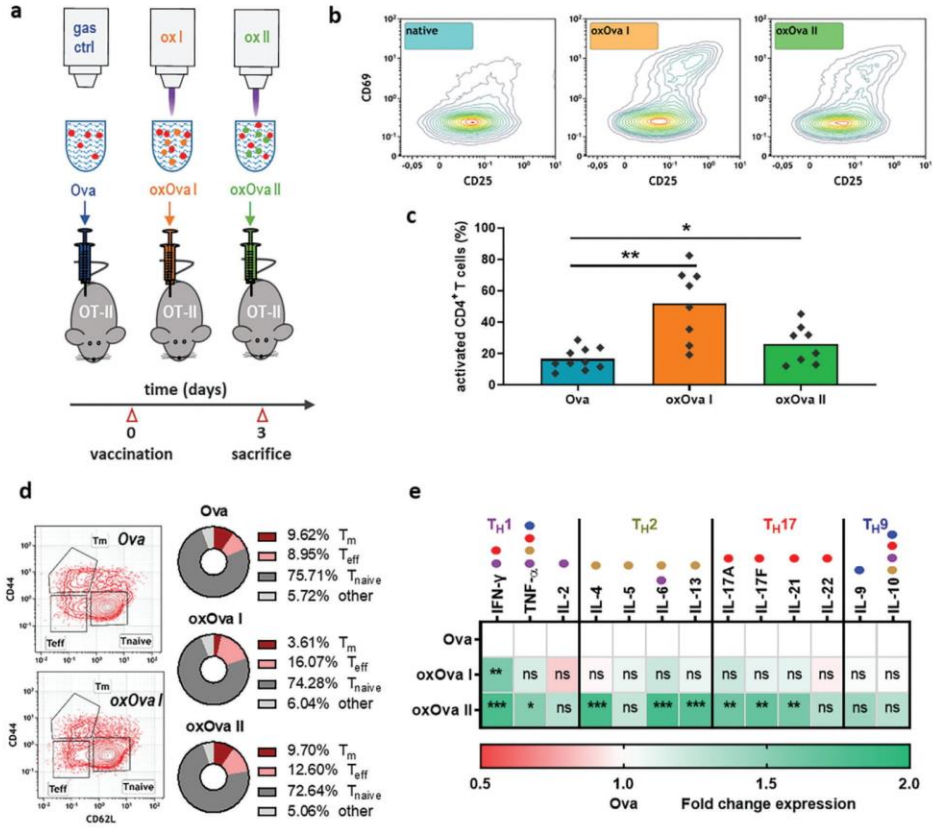

Figure 5. T cell response to vaccination of OT-II mice with Ova or oxidized Ova. a) Setup of the gas plasma treatment of Ova and repeated injection of either Ova, oxOva I, or oxOva II into OT-II mice; b) Representative CD69/CD25 expression and c) quantification of activated T cells from draining lymph nodes at d3; d) $CD4^+$ T cell subpopulation analysis via CD44 and CD62L within the activated $CD4^+$ parent population; e) T_H cell cytokine profile of cells of the draining lymph nodes of vaccinated OT-II animals at 3d with dominating cytokine signatures ($T_H1/T_H2/T_H17/T_H9$ segmentation) and annotated possible cytokine production (color code and dots). Data are representative of at least 4 mice per group; statistical analysis was performed using one-way or two-way anova (* $p < 0.05$; ** $p < 0.01$; *** $p < 0.001$).

post-translational modifications (PTMs) of the protein using mass spectrometry. The comparison of the chromatograms already revealed major differences in the peak distribution between Ova, oxOva I, and oxOva II (**Figure 7**a). Subsequent mapping of several types of PTMs to the amino acid sequence of Ova showed several distinct PTM-hot spot regions (Figure 7b) that appeared at amino acids at the exterior of the protein (Figure 7c). A detailed view of the cumulative number of PTMs in oxOva I and oxOva II was set up next. For each type of PTM, the total number of PTMs in Ova was subtracted from those identified for oxOva I and oxOva II, respectively, and put into relation (percentage of oxOva I or oxOva II of the sum of modifications from oxOva I and oxOva II; Figure 7d). These data were generated based on the assumption that the location and the total number of modifications are possibly relevant to the immunological perception of a protein. oxOva II vaccination showed superior protection from melanoma growth in vivo compared to oxOva I. This correlated with exclusive PTMs for oxOva II (chlorination, quinones, and double didehydro) as well as the majority of total PTMs identified in oxOva I and II together being attributed mostly to oxOva II (>75% for amidation, carbonylation, didehydro, and nitro-o). Another apparent hallmark of oxOva II was its substantial hyperoxidation (oxidation, dioxidation, and trioxidation) at several regions of the protein sequence (Figure 7e), which was greater in

ADVANCED SCIENCE NEWS
www.advancedsciencenews.com

ADVANCED SCIENCE Open Access
www.advancedscience.com

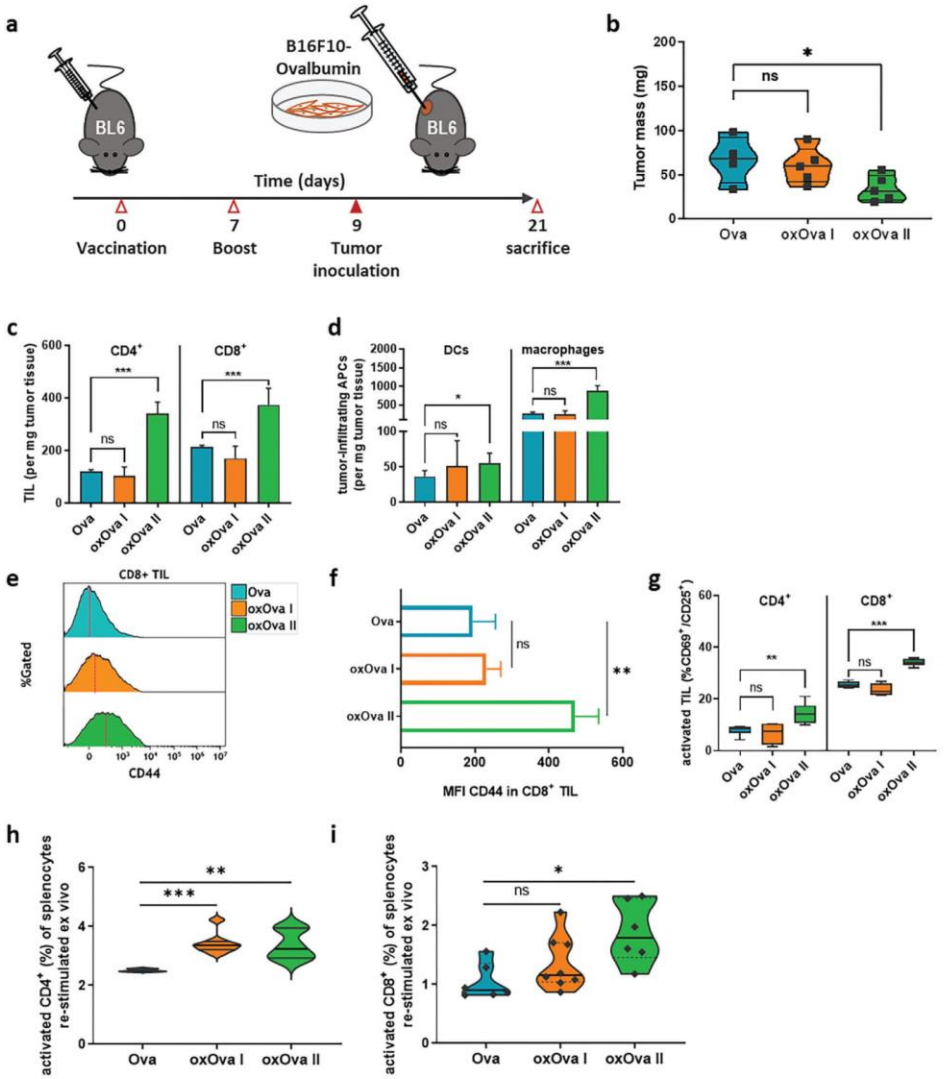

Figure 6. oxOva vaccination confers superior protection again B16F10-Ova melanoma growth in vivo. a) Wild type C57BL/6 were vaccinated twice i.p. with 10 µg of either Ova, oxOva I, or oxOva II followed by subcutaneous inoculation of Ova-expressing B16F10; b) tumor weights of individual animals in each group; c) tumor-infiltrating lymphocytes (TIL) were elevated for $CD4^+$ and $CD8^+$ cells in the oxOva II vaccination regimen; d) number of tumor-infiltrating APCs showed an increase of dendritic cells (DCs) and macrophages in the oxOva II vaccination regimen; e) representative flow cytometry intensity histograms of CD44 in $CD8^+$ TIL and f) quantification; g) activation of $CD4^+$ and $CD8^+$ TIL was enhanced in the oxOva II vaccination regimen; h,i) splenocytes of tumor-bearing animals receiving the respective Ova, oxOva I, or oxOva II vaccination were isolated and restimulated ex vivo with Ova and h) $CD4^+$ and i) $CD8^+$ T cell activation was analyzed 24 h later. Data are representative of three independent experiments and 6–8 mice per group; statistical analysis was performed using one-way anova (* $p < 0.05$; ** $p < 0.01$; *** $p < 0.001$).

ADVANCED SCIENCE NEWS
www.advancedsciencenews.com

ADVANCED SCIENCE Open Access
www.advancedscience.com

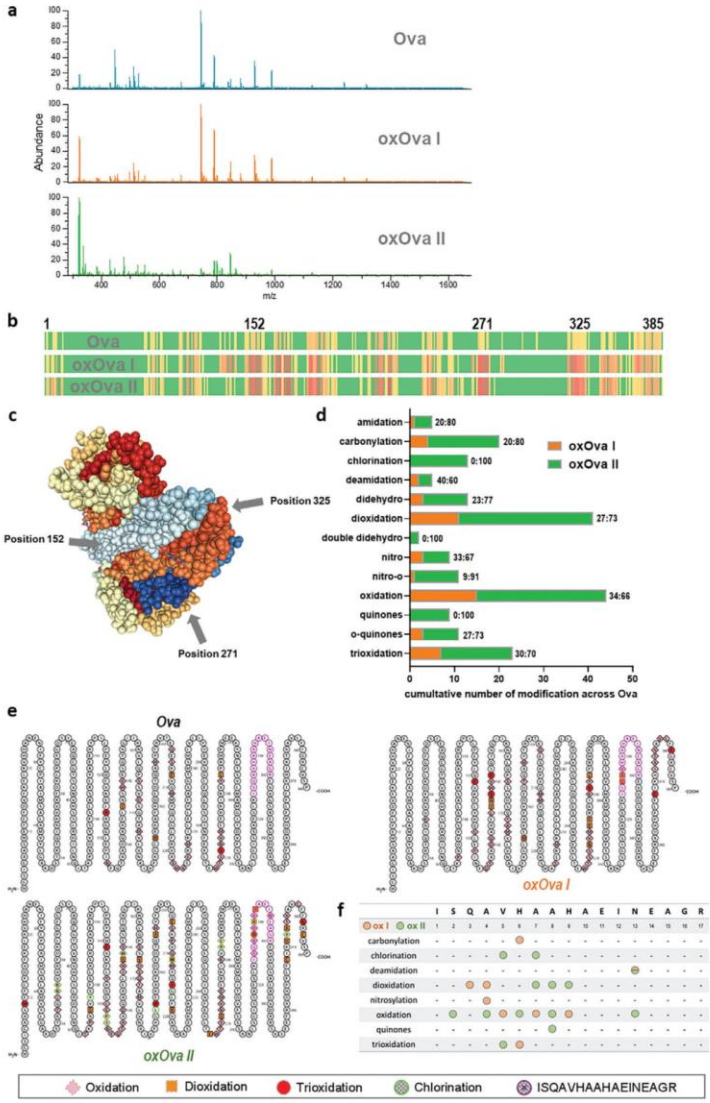

Figure 7. Modification mapping unraveled three distinct hyperoxidized regions in oxOva. a) Mass spectrometry peak distribution of Ova, oxOva I, and oxOva II; b) sum of modifications across the amino acid sequence of Ova, oxOva I, and oxOva II; c) rendering of Ova protein showing the three distinct hyperoxidized positions at outward-pointed regions of the protein; d) cumulative numbers of different types of post-translational modifications (PTMs) of oxOva I and oxOva II that were subtracted by the number of background PTMs of native Ova, and relations (%) of oxOva I to oxOva II among the sum of PTMs observed in both oxOva I and II; e) hyperoxidation (oxidation, dioxidation, and trioxidation) in oxOva I and II compared to Ova across its amino acid sequence; f) oxPTMs along the antigenic peptide sequence of Ova. Data are representative of three independent experiments.

oxOva II as compared to Ova and oxOva I. Subsequently, we performed a more detailed analysis of the 17 amino acid-long antigenic peptide region of Ova responsible for activating the majority of Ova-specific $CD4^+$ T-helper cells in OT-II mice (Figure 7f). Among the modifications mapped out, the amino acids at positions 4 to 9 seemed especially vulnerable to oxidative modifications introduced via the ox I or ox II gas plasma treatment. It was also interesting to note that except for the deamidation at position 13, there was no overlap of modifications in this antigenic sequence between the ox I and ox II condition. This underlined the notion of the different chemistries observed in the ox I versus ox II gas plasma condition (Figure 1) and might relate to the differences observed in the functional consequences of oxOva I and oxOva II in the preventive vaccination experiments (Figure 6). In general, we have investigated only nonenzymatic but not enzymatic PTMs in gas plasma-treated Ova using mass spectrometry analysis.

3. Discussion

The multi-ROS/RNS environment in chronic inflammation is linked to autoimmunity and cancerogenesis. While the cellular pathobiology in these conditions has been studied extensively during the past decades, the role of ROS/RNS-derived oxidative modifications received considerably less attention. Using gas plasma, an electron-impact and photon-driven technology, we mimicked the multi-ROS/RNS inflammatory environment and tested the immunological consequences of oxidatively modified ovalbumin (oxOva). This model protein is frequently used for testing the activation of anti-Ova T cells from genetically engineered mice, and oxOva showed superior T cell activation compared to native Ova. According to the sequential T cell memory model,[69] the oxidation might affect the differentiation velocity of T cells, as in the OT-II model, all cells should be naïve in the beginning. In wild type mice, oxOva vaccination gave enhanced protection from B16F10-Ova melanoma growth, and mass spectrometry attributed a specific set of oxidative post-translational modifications to our findings.

Transgenic OT-II and OT-I mice are particularly useful for immunological studies of Ova, as these mice harbor Ova-specific $CD4^+$ and $CD8^+$ T cells, respectively. Their activation is not dependent on the NOX-derived production of ROS/RNS, at least with B cells as APCs.[70] We noted that oxOva markedly increased $CD4^+$ T cell activation in OT-II splenocytes but not $CD8^+$ T cell activation in OT-I splenocytes. This, in turn, might be due to differences in processing routes being less sensitive to protein oxPTM-induced alterations, as a link between ROS/RNS, autophagy and immune response had been recently established.[71] Exogenously supplied Ova needs to be endocytosed via the mannose-receptor in dendritic cells (DCs) and additionally the scavenger receptor in macrophages before cross-presentation via MHC I eliciting $CD8^+$ T cell activation. By contrast, pinocytosis is the primary mechanism for MHC II peptide presentation, having a more efficient antigen processing activity, at least in DCs.[72,73] Along similar lines, it is also conceivable that the effect of oxPTMs is conserved through lysosomal or endosomal compartments. OT-II-derived $CD4^+$ T cells recognize Ova peptide at position 323–339 in the context of $H\text{-}2A^b$, while OT-I-derived $CD8^+$ T cells recognize Ova peptide at 257–264 in the context of $H\text{-}2K^b$. Gas-plasma-mediated oxidative modifications occurred primarily in the amino acid sequence cognate to $CD4^+$ but not in that cognate to $CD8^+$ T cells, suggesting that oxPTMs might be able to alter the MHC-peptide-TCR binding affinity, a crucial factor in T cell activation.[74]

The binding affinity of amino acids between antigenic peptides and the MHC binding groove is relevant regarding the threshold activation between the TCR and MHC.[75,76] Based on the mentioned observations, an altered binding affinity to MHC loaded with oxidatively modified peptides might be suggested due to oxPTMs in the TCR specific sequence ISQAVHAAHAEINEAGR ($Ova_{323\text{-}339}$) that we determined via mass spectrometry and were associated with an increased T cell activation. The oxidation occurs prototypically at thiols, which respond vastly to gas plasma-derived ROS and RNS,[77] as do other amino acids.[78,79] In a previous study, the immunogenicity of an antigenic peptide in its reduced and oxidized state was investigated. The reduced peptide elicited T cell activation, while the oxidized form failed to do so,[80] which would contrast our results. In our case, however, there was no cysteine in the antigenic peptide sequence of Ova. In another study, the antigenic peptide for insulin was found to dimerize upon oxidation of cysteine, changing its secondary structure, and directly leading to activation of $\gamma\delta$ but not $\alpha\beta$ T cell hybridomas in the case of dimers but not monomers.[81] Nevertheless, in our study, we oxidized the entire protein that included the peptide sequence, ruling out the peptide sequence's dimerization upon oxidation as a mechanism of action. However, it is possible that upon Ova cleavage during intracellular antigen processing, dimerization occurred, but it is unclear how this might have contributed to the elevated T cell activation observed. Other reports suggested methionine oxidation for abrogating $CD4^+$ T cell activation [82] as well as $CD8^+$ T cell activation,[83] but our peptide sequence neither contained methionine nor was its oxidation associated with less T cell activity. Interestingly, APCs actively and intracellularly reduce cystines in oxidized antigenic peptides 2–4 h after internalization, leading to enhanced T cell activity,[84] as indicated by another report also.[85] The importance of cysteine oxidation and its detrimental effects on T cell activation has been recently reported for tumor-reactive $CD8^+$ T cells as well.[86] In addition, oxidation was shown to lead to conformational changes in a malaria-related antigen and reduced T cell activity.[87] The studies mentioned above focused on cysteine residues in peptide sequences that were partially oxidized through various (not gas plasma) methods, which might have also oxidized other amino acids in the antigenic peptides, being associated with decreased T cell activation. This suggests that oxidation was less important in explaining our results when considering the 15 oxidations at different amino acids identified in oxOva I or oxOva II. Alternatively, nitrosylation of antigen was reported many times to elicit autoimmunity.[88–91] In our work, gas plasmas produced ^-ONOO and other RNS might have contributed to the 3-nitrotyrosine formation. Nevertheless, nitrosylation was only observed in oxOva I but not oxOva II exposure in the antigenic Ova peptide sequences, failing to explain our results fully. This is also the case for chlorination, which was previously shown to enhance antigen immunogenicity,[92] but was only found in the ox II treatment that generated HOCl, while ox I did not. However, also deamidation was associated with increased binding affinity of self-epitopes to HLA,[92] and both gas plasma regimens induced

this modification at asparagine. This suggests the possibility of oxPTMs in the antigenic peptide sequence to contribute to the enhanced T cell activation observed in our study. In addition, many other oxPTMs were observed across the entire protein that might have led to changes in T cell activation, as previously reported for chlorinated ovalbumin.[93,94] At the same time, it is known that peptides with substituted amino acids change the conformational plasticity, leading to altered affinity in MHC-TCR interaction.[95–97] Yet, our mass spectrometry analysis did not identify amino acid substitution with gas plasma treatment, ruling out changes in the MHC-TCR binding via this mechanism.

The presence of APCs was necessary for enhanced T cell activation with oxOva, as magnetically sorted $CD4^+$ T cells without APCs failed to be activated in response to Ova or oxOva. Together with a lack of increased activation in DCs and macrophages, this led us to conclude that the gas-plasma hyperoxidized Ova did not pertain to an inherent DAMP (damage-associated molecular pattern) activity, at least in our model. This is in contrast to other modifications such as advanced glycosylation endproducts (AGE) on naturally occurring carbohydrates of Ova that are capable of increasing DC activation in a scavenger and mannose receptor-dependent and RAGE and galectin-3 independent manner.[98] Protein aggregation, observed to a minor extent in our study, also affects protein immunogenicity.[99] Aggregation in vaccination development is associated with decreased immunogenicity [100] while protein-protein-aggregates (e.g., Ova and TLR agonist) mount markedly elevated DC activation and T cell responses in experimental models.[101] Protein aggregation also can lead to autoantibody formation due to the formation of neoepitopes.[102,103] For oxidative modifications, previous reports pointed to a pivotal role of Ova chlorination in enhancing its immunogenicity and endocytic uptake as well as intracellular degradation.[94,104] However, our oxOva I condition was void of chlorination but still facilitated enhanced $CD4^+$ T cell activation in OT-II mice, pointing to chlorination being one of several factors of elevated gas plasma-induced protein immunogenicity that involved other types of oxidative modifications.

OxOva II vaccination led to enhanced T cell activation in OT-II mice and showed superior protection from B16F10-Ova melanoma growth in wild type mice compared to vaccination with native Ova. This suggested oxOva II to mount a more pronounced antitumor adaptive immune response in terms of either quantity (amplified T cell responses) or quality (broadened anti-Ova TCR repertoire) or both. Such finding was also reported in a previous study using oxidized whole-tumor-lysates fed to DCs used as an autologous vaccine in ovarian cancer patients that strengthened existing T cell responses and led to the generation of T cells targeting cancer neoepitopes.[13] Alternatively, it is conceivable that our results emerged from an inflammatory self-amplification loop initiated by T_H17 cells that, in turn, aided in the generation of additional antitumor $CD8^+$ T cell entities.[105] This is supported by our findings that i) oxOva II but not oxOva I vaccination dampened tumor growth in vivo and ii) oxOva II but not oxOva I elicited a T_H17 cytokine signature both ex vivo and in vivo in OT-II mice. Noteworthy, also AGE pyrraline-modified Ova was found to increase IL17A release in Ova-specific T cells, while – similar to our results – failed to increase DC activation per se.[106] IFNγ is a molecule known to upregulate MHC I expression in B16F10 melanoma cells,[107] and elevated numbers of $CD4^+$ TILs were reported to be essential promotors of cancer immunotherapies.[108] Our observed increase of IFNγ secretion in oxOva conditions hence suggested a stronger immunorecognition of oxOva II compared to native Ova, which possibly altered the tumor microenvironment (TME) in favor of anticancer immunity. In the light of Ova peptide-MHC complexes being present for at least 16 h on the surface of DCs,[109] sustained anti-Ova T cell generation with oxOva II vaccination might have also contributed to improved antitumor immunity. Vice versa, B16F10-Ova melanomas are capable of conditioning cancer-associated fibroblasts to repress $CD8^+$ responses within TME T cell zones,[110] a mechanism not explored in our study. However, the increased presence of intratumoral DCs in oxOva II vaccinated mice suggested beneficial conditioning of the TME.[111,112]

Another mechanism that might contribute to the enhanced antitumor effect of oxOva vaccination is intracellular ROS/RNS of tumor cells.[113] It is established that cancer cells display elevated ROS/RNS levels due to exacerbated metabolic activity and dysregulated redox balance.[114] We hypothesized these ROS/RNS to introduce a more diverse set of modifications in intracellular protein antigens,[115] leading to more a diverse set of cognate MHC I peptides than generated with regular unmodified protein vaccines, which elicit a presumably smaller TCR repertoire in the host. Using gas plasma technology, we aimed to bridge this "oxidation gap" by supplying antigen with a maximal diverse set of oxidative modifications capable of mimicking both intracellular and extracellular inflammation-derived ROS/RNS.[116–120] Using cysteine as a model biomolecule, we previously established unique gas plasma-derived oxidative/nitrosative fingerprints otherwise not yielded with conventional chemical oxidation/nitration methods and the vital role of the plasma feed gas compositions governing and tuning the multi-ROS/RNS compositions expelled by the plasma jet.[77,121] A summary of the many types of ROS/RNS identified in the plasma gas phase and treated liquids was given recently.[122,123] Nevertheless, the multi-ROS/RNS nature of plasma technology poses technical challenges in identifying single agents responsible for the effects observed. This is exemplified in the diverse quality and quantity of oxidative modifications that we identified to be introduced in a protein-based on a custom-engineered mass spec oxPTM library generated in-house.[60] However, the identification and exploitation of this angle of protein immunogenicity still is in its infancy. Dramatic differences were observed, e.g., for gas plasma-treated Ova oxidation/dioxidation/trioxidation in amino acids across the entire protein – types of modifications, a recent autoimmunity ligandomic study, for instance, excluded explicitly in its mass spectrometry peptide analysis workflow.[124] We found these types of oxidations to align in the $Ova_{323-339}$ ($CD4^+$) but not the $Ova_{257-264}$ ($CD8^+$) peptide-binding region, apart from other oxidation hot spots located at three distinct hyperoxidized regions of Ova. A previous report also established that such an oxidation pattern observed in distinct sets of MHC-peptides not only is a product of random oxidative stress but also serves dedicated redox signaling functions,[125] underlining the notion of our oxPTMs signatures related to eliciting distinct immunobiological consequences as observed in vivo. The importance of oxidation and chlorination, as outlined above, has also been pinpointed in a cohort of autoimmune type I diabetic patients that was

demonstrated to have autoantibodies targeting experimentally oxidized or chlorinated insulin in vitro.[126]

A role of RNS-derived PTMs was implemented as well since we observed nitro and nitro-o modifications. For instance, nitro fatty acids were identified as bioactive lipids being part of physiological homeostasis as well as metabolic and inflammatory disease,[127] exerting signaling functions in cells,[128] and promoting the formation of protein PTMs.[129] The RNS $^{-}$ONOO is known to oxidize target molecules and nitrate, e.g., tyrosine and tryptophan efficiently,[130] and nitrated protein PTMs have been linked to several inflammatory diseases.[131] $^{-}$ONOO, a species suggested to be generated in previous gas plasma-related studies,[36,62,132–134] can also form S-nitrosothiols [135] exhibiting biological functions such as inhibition of NADPH oxidases [136] and release of NO.[137] The poor oxidant NO, a species also generated by the gas plasma jet kINPen,[138] can be oxidized to the radical nitrogen dioxide [139] that efficiently nitrates proteins relevant in autoimmunity and cardiovascular disease.[140,141] These data emphasize the importance of ROS/RNS-derived PTMs in health and disease and suggest more findings to come if the multi-ROS/RNS nature of inflammation would be recapitulated using gas plasma systems. However, and owing to both a large number of targets on proteins and the complexity of antigen uptake and presentation, a direct and causative link between an individual or a set of oxPTMs and immunorecognition remains to be established.

4. Conclusion

Gas plasma, an electron-impact and photon-driven technology, was employed to generate a diverse range of ROS/RNS simultaneously for testing their effect on protein oxidative post-translational modifications (oxPTMs) and immunogenicity. Using ovalbumin (Ova) as a model protein, we confirmed increased immunogenicity of oxOva by detecting higher amounts of activated T cells correlating with decreased tumor burden and a broad set of nonenzymatic Ova-oxPTMs with oxidation and chlorination suggested to be of prime importance. Our proof-of-concept study has expansive implications for further research in autoimmunity and vaccine research.

5. Experimental Section

Plasma Treatment: Lyophilized EndoGrade ovalbumin (Ova; Hyglos, Germany) was solved in double-distilled water (ddH_2O) and diluted in PBS (100 µg mL^{-1}). In the setup, the protein does not exert a specific function, such as enzymatic activity. Instead, it serves as immunostimulant once taken up by antigen-presenting cells and presented to antigen-specific T cells. In some experiments, *n*-acetylcysteine (NAC, 2×10^{-3} M, Thermo Fisher, USA) was added before gas plasma treatment of 500 µl suspensions in a 24-well plate (Sarstedt, Germany). In additional control experiments, the Ova suspension was exposed to four pulses of electric fields (ECM 830, BTX, USA) at 1.5 kV cm^{-2}. For gas plasma treatment, the kINPen plasma jet (neoplas, Germany) was used, which is accredited as a biomedical device in Europe. The atmospheric pressure gas plasma jet requires a DC power unit. A ceramic capillary with an inner diameter of 1.6 mm has mounted at its center a pin-type electrode with a diameter of 1.0 mm diameter. A radiofrequency generator produces a sinusoidal voltage waveform, ranging from 2 to 3 kV amplitude peak at a frequency of 1 MHz. The gas plasma is generated at the tip of the central electrode and expands into the ambient air. The UV irradiation of the gas plasma jet is 105 µJ cm^{-2}. A more detailed description of the chemistry and physics of the device was recently provided.[122] In our study, the gas plasma jet was operated at two standard liters per minute of either pure argon gas (3 min treatment time) or helium gas containing 2% oxygen (1 min treatment time). Gases were 99.999% pure and from Air liquid, France. For investigating plasma-derived products, the plasma jet was positioned at a distance of 0.8 cm and perpendicular to the front of a UV-sensitive optical emission spectrometer (AvaSpec-2048-USB2; Avantes, Germany) with a spectral resolution of 0.7 nm. The OES lens center was aligned to the visible tip of the plasma, which was 0.8 cm for the argon condition and 0.6 cm for the helium/oxygen condition. A computer-controlled *xyz* motorized table ensured the plasma jet's exact positioning in this setup (CNC step, Germany). This setup was also used to attain sub-millimeter precision to maximize the reproducibility of the gas plasma treatment of samples residing in multiwell plates. Gas flux-mediated evaporation of treated liquids was compensated for by adding a predetermined amount of ddH_2O.

ROS/RNS and Liquid Analysis: During plasma treatment, the temperature of the liquid was analyzed using a PIX infrared camera (Optrix, Germany). PBS was supplemented either with or without Ova or *n*-acetylcysteine (NAC, 2×10^{-3} M; Thermo Fisher, USA) before plasma treatment. Singlet oxygen was measured using singlet oxygen sensor green (Thermo Fisher, USA), and its fluorescence was analyzed at λ_{ex} 485 nm and λ_{em} 535 nm using a plate reader as described before.[142] Nitrite and nitrate were determined by performing the Griess-assay (Cayman Chemical, Germany) as previously outlined,[41] and absorbance was measured at λ_{ex} 548 nm. Hydrogen peroxide was quantified using the Amplex Ultra Red detection reagent (Thermo Fisher, USA) according to previous protocols,[143] and measured at λ_{ex} 535 nm and λ_{em} 590 nm using a plate reader. Hypochlorous acid generated via the gas plasma was measured using the taurine chloramine assay at an absorption of 645 nm, as outlined before.[35] Aminophenyl fluorescein (APF) and hydroxyphenyl fluorescein (HPF; both Thermo Fisher, USA) sense HOCl, peroxynitrite ($^{-}$ONOO), and hydroxyl radicals ($^{\cdot}$OH), and $^{-}$ONOO and $^{\cdot}$OH, respectively.[61] The dyes were used at a final concentration of 5×10^{-6} M, and their fluorescence was analyzed at λ_{ex} 485 nm and λ_{em} 535 nm. Also, diaminofluorescein (DAF, final concentration 5×10^{-6} M; Thermo Fisher) was analyzed this way. Hydroxyl radicals were measured using the terephtalic acid assay as described before.[146]

Circular Dichroism (CD) Spectroscopy: Native and plasma-treated ovalbumin in PBS (100 µg mL^{-1}) with or without NAC (2×10^{-3} M) was measured via CD-spectroscopy using a Chirascan V100 CD Spectrometer (Applied Photophysics, UK). Samples were loaded in 5 mm-pathlength cuvettes (Hellma Analytics, Germany). Spectra were recorded at 20 °C over a wavelength range from 190 nm to 270 nm with a bandwidth of 1.0 nm and a scanning time of 1.5 s per point. Measurements were repeated five times. All spectra are blank corrected.

Photon Correlation Spectroscopy: Photon correlation spectroscopy measurements of native or gas plasma-treated Ova (100 µg mL^{-1}) using a ZS90 dynamic light scattering (DLS) device (Malvern instruments, USA) equipped with a helium-neon laser light source (632 nm). Proteins (Material RI = 1.45, absorption = 0.001) in PBS similar to water (Dispersant RI = 1.33, viscosity = 0.954) were measured in low-volume disposable cuvettes (ZEN0040). DLS measurements were done at a set angle of 90° and attenuator at 11. The size was measured at 22 °C, with an equilibration time of 120 sec and cuvette position at 3 mm. Backscatter angled detection was performed at 173° with a scattering collection angle of 147.7°. Each biological replicate was measured in several replicates with minimal time between repeats. Data analysis was carried out from three independent experiments.

B16F10-Ova: Ova-expressing murine melanoma cells (B16F10-Ova) were a kind gift of Karl Sebastian Lang (Institute of Immunology, University Hospital Essen, Germany). Cells were cultured in Roswell Park Memorial Institute (RPMI) 1640 medium (PanBioTech, Germany) containing 10% fetal bovine serum, 2% glutamine, 1% penicillin/streptomycin (all Sigma, Germany), and 0.5 µg mL^{-1} puromycin (StemCell Technologies, Germany). Cells were grown at 37 °C, 95% humidity, and 5% CO_2, and subcultured three times a week.

In Vivo Experiments and Cell Isolation: Ethical approval was received from the local authority (*Landesamt für Landwirtschaft, Lebensmittelsicherheit und Fischerei* in the state of Mecklenburg-Vorpommern, Germany; approval number M-V 7221.3-1-022/19). C57BL/6N, C57BL/6-Tg(TcraTcrb)1100Mjb/Crl (OT-I), and C57BL/6-Tg(TcraTcrb)425Cbn/Crl (OT-II), all female at 6–8 weeks of age, were purchased (Charles River Laboratories, Germany). Transgenic OT-II mice harbor T cells with specific receptors for the Ova peptide ISQAVHAAHAEINEAGR ($Ova_{323-339}$) restricted by MHC-II (I-Ab).[144] and transgenic OT-I mice harbor $CD8^+$ T cells specific for the Ova peptide SIINFEKL ($Ova_{257-264}$) restricted by MHC-I (H_2D_b).[145] Animals were kept in cages with a maximum of six animals per cage. OT-II and C57BL/6N mice received intraperitoneal injections of 100 µl of PBS with or without 10 µg of Ova or gas plasma-treated Ova (oxOva I for Ar plasma; oxOva II for He/O_2 plasma). C57BL/6N received a boost vaccination (without adjuvant) seven days later. On day 10, animals were challenged with a subcutaneous inoculation of 1×10^4 B16F10-Ova melanoma cells. After sacrifice, lymphoid organs and tumors of tumor-bearing C57BL/6 animals were removed. Splenocyte isolation and tumor digestion were performed using the splenocytes isolation kit and tumor dissociation kit, respectively, in an OctaMACS Dissociator device (Miltenyi Biotec, Germany). $CD4^+$ were separated from untouched splenocytes via a negative selection kit containing antibodies against CD8a, CD11b, CD11c, CD19, CD24, CD45R/B220, CD49b, CD105, I-A/I-E (MHC II), TER-119/Erythroid, and TCR-$\gamma\delta$ (BioLegend, UK). MojoSort cell separation was performed according to the manufacturer's instructions.

Restimulation Assay: Isolated splenocytes were resuspended in fully supplemented culture medium. For experiments, 1.5×10^6 cells in 500 µl of medium were incubated for 24 h with PBS or PBS containing Ova, oxOva I, or oxOva II. In control experiments, only PBS was plasma-treated and added to splenocytes, followed by the addition of vehicle (PBS) or Ova immediately afterwards. For MHC-II blocking experiments, isolated splenocytes were preincubated for 1 h with 1 µg mL^{-1} of purified I-A/I-E monoclonal antibodies (clone M5/114.15.2; BioLegend, UK).

Ovalbumin Uptake: Splenocytes were labeled with fluorescently conjugated antibodies targeted against F4/80 (phycoerythrin, PE; clone BM8; BioLegend, UK) and CD11b (alexa fluor 700; clone M170; BioLegend, UK). DQ-Ova (5 µg mL^{-1}; Thermo Scientific, Germany) was added. The dye exhibits a green fluorescence, which is quenched by aggregation. Upon uptake, aggregation is reduced, enhancing fluorescence emission, which was monitored using fluorescence microscopy (Operetta CLS; Perkin Elmer, Germany). Measurement was performed with a 20x (NA 0.4) objective (Zeiss, Germany) in the brightfield (BF), digital phase contrast (DPC), and fluorescence (λ_{ex} 475 nm, 550 nm, and 630 nm) channel. Flow cytometry was performed to analyze DQ-Ova or DQ-BSA (both 20 µg mL^{-1}; Thermo Scientific, Germany) in previously separated APCs of splenocytes or differentiated monocytes isolated from PBMCs. This study was approved by the local ethics committee (approval number: BB166/17). Whole blood was drawn from volunteers with informed consent. Human cells were labeled with fluorescently conjugated antibodies targeting CD11c (Brilliant Violet 510, clone 3.9), HLA-DR (APC-Cy7) and ZOMBIE NIR for dead cell exclusion (all BioLegend, Netherlands), and incubated with DQ alone or in combination with native or plasma-treated proteins (10 µg mL^{-1}).

Multiplex Cytokine Analysis: Cytokines were measured in supernatants of minced lymph nodes from in vivo experiments with OT-II mice and supernatants of OT-II-derived splenocytes cultured ex vivo with Ova or oxOva for 24 h, using multiplex cytokine detection technology (LegendPlex; BioLegend, UK) according to the manufacturer's instructions. This plex is a bead-based sandwich immunoassay and was measured using flow cytometry (CytoFLEX S; Beckman-Coulter, USA) targeting interferon-gamma (IFNγ), tumor necrosis factor-alpha (TNFα), and eleven interleukins (IL-2, IL-4, IL-5, IL-6, IL-13, IL17A, IL-17F, IL-21, IL-22, IL-9, and IL-10). For quantification, data analysis software (Vigene Tech, France) was utilized. A separate standard curve was calculated using fifth-degree polynomials for each analyte, with attention to the analytes' specific detection limits.

Flow Cytometry: Cells were collected in FACS tubes and washed three times with cold FACS washing buffer (Miltenyi Biotec, Germany). For live/dead discrimination and T cell analysis, cells were stained with activated Caspase 3/7 detection reagent (Thermo Scientific, USA) and fc block (BioLegend, UK) at room temperature for 10 min followed by incubation with fluorescently conjugated monoclonal antibodies targeting CD62L (PE-Dazzle, clone MEL-14), CD44 (PerCP-Cy5.5, clone IM7), CD4 (PE-Cy7, clone L3T4), CD25 (APC, clone PC61), CD3 (Alexa Fluor 700, clone 17A2), CD69 (brilliant violet 421, clone H1.2F3), and CD8 (brilliant violet 510, clone 53–6.7) (all BioLegend, UK) for 30 min at 4 °C. For T cell analysis, unwanted cells were gated out using a dump channel containing zombie-NIR as well as CD45R and I-A/I-E APC-fire 750 (BioLegend, UK). For macrophage analysis, leftover suspension cells were transferred into a tube, and attached cells were scratched-off and added to FACS tubes. All cells were washed as described above and stained for 30 min at 4 °C with fluorescently conjugated monoclonal antibodies targeting F4/80 (PE, cone BM8), CD11b (PE-Dazzle, clone M1/70), CD86 (PE-Cy7, clone PO3), CD64 (APC, clone X54-5/7.1), I-A/I-E (AF700, clone M5/114.15.2), CD45.2 (APC-Cy7, clone 104), Ly6G (APC-Cy7, clone HK1.4), CD24 (BV421, clone M1/69), and CD11c (BV605, N418). Dead cells were excluded using Sytox green dye (Thermo Scientific, Germany). After washing with cold FACS washing buffer, samples were measured using flow cytometry (CytoFLEX S and CytoFLEX LX; Beckman-Coulter, USA). Data analysis was performed using Kaluza analysis software 2.1 (Beckman-Coulter, USA).

Proliferation Assay: For cell proliferation experiments, cells were labeled with carboxyfluorescein succinimidyl ester (CFSE, 2.5×10^{-6} M; ThermoFisher, Germany), and exposed ex vivo to either Ova, oxOva I, or oxOva II, or to native human albumin, argon gas plasma-oxidized human albumin (oxhuAlb I), or helium/oxygen gas plasma-oxidized human albumin (oxhuAlb II) as controls. Three days later, cells were collected, washed, and labeled with antibodies to identify proliferating $CD4^+$ T cells as well as their activation and differentiation status (CD69, CD25, CD44) among all $TCRvB^+$ cells. Sample acquisition was performed using an LSR II flow cytometer (Becton-Dickinson, USA) and analyzed using Flow Jo (TreeStar Software, USA).

Gel Electrophoresis and Western Blot: All reagents, buffers, and devices were supplied by ThermoFisher Scientific unless otherwise stated. 30µl of PBS containing native or gas plasma-treated Ova (30 µg for coomassie, 15 µg for western blot) were mixed with 4x NuPAGE LDS sample buffer and loaded without denaturation on a 10-well 4–12% Bis-Tris Gel. SeeBlue prestained standard was loaded, and gel electrophoresis was performed in a chamber filled with 1x MES SDS running buffer and connected to a power supply (Biometra Analytik-Jena, Germany). For coomassie, gels were stained with 4% coomassie brilliant blue R250 in 80% methanol, 20% acetic acid (both Carl Roth, Germany), and washed with a de-staining solution (20% methanol, 10% acetic acid, 70% ddH_2O). For western blot, proteins were blotted on an activated PDVF membrane, blocked with Rotifix (Carl Roth, Germany), and stained with anti-Ova polyclonal primary antibody (Biozol, Germany) followed by secondary horse-radish peroxidase-coupled antibodies (Rockland Immunochemicals). Signals were acquired after adding ECL reagent super signal WestPicoPlus in a chemiluminescence detection system (GE Healthcare, USA).

Mass Spectrometry and Data Analysis: Gas plasma-mediated protein modifications were investigated using high-resolution mass spectrometry coupled to liquid chromatography (LC/MS). Samples were prepared for LC/MS analysis by adding four volumes of acetone (Sigma, all chemicals of MS grade). After overnight incubation at −20 °C, samples were centrifuged at 12.000 x *g* for 20 min, the supernatants were removed, and the dried pellet was solved in ddH_2O. After the determination of protein concentration using the Bradford assay (RCDC assay, BioRad), 100 µg of protein was reduced in 50×10^{-3} M TEAB buffer (Sigma, Germany) by adding Tris(2-carboxyethyl)phosphine (Merck, Germany) at a final concentration of 5.7×10^{-3} M. After incubation at 60 °C for 45 min, 0.5×10^{-3} M iodoacetamide (Merck, Germany) was added, and samples were incubated for 20 min at 22 °C. Proteins were digested by trypsinization for 18 h at room temperature and loaded on STAGE-tips (Thermo Fisher, USA) filled with 30 µg of Luna C18-Material (Phenomex, Germany), which were washed and equilibrated beforehand with acetonitrile and water, respectively (both ChemSolv, USA). Desalting was performed by washing twice with 0.1% acetic acid (Merck, Germany) and centrifugation (8000 x g, 1 min). To elute peptides from the STAGE-tip, 30 µl acetonitrile containing 0.1% acetic acid were added and pressed through the tip using

pressurized nitrogen. Acetonitrile was removed by adding 20 µl of 0.1% acetic acid and vacuum centrifugation to a final volume of 10 µl. LC/MS measurements were performed using a Q-Exactive Orbitrap coupled to an UltiMate 3000 nano HPLC (both Thermo Scientific, USA). Samples were concentrated on a PepMap C18 precolumn (20 mm x 100 µm inner diameter, 5 µm particle size) before peptides were separated on a PepMap C18 column (150 mm x 75 µm inner diameter, 3 µm particle size) running water (eluent A) against acetonitrile (eluent B). Both eluents had 0.1% acetic acid added as a modifier. The gradient was as follows: initial conditions 250 nL min^{-1} flow of 2% B, in 4 min to 10% B, in 20 min to 35% B, in 1 min to 50% B, in 2 min to 80% B. Following the gradient, washing of the column at 80% B for 8 min, followed by equilibration at 2% B for 8 min were performed. Flow for washing and equilibration was ramped to 500 nL min^{-1}. The Q-Exactive was fitted with a Nanospray flex source (Thermo Scientific, USA) and was running in data-dependent acquisition mode (Top25) with tune parameters adjusted for optimal signal intensities. Data analysis was performed in Proteom Discoverer 2.3 (Thermo Scientific, USA). The initial quality of measured spectra was assessed by searching against a chimeric database containing the ovalbumin sequence as well as the full human proteome as a control for possible contaminants using SequestHT and MS Amanda 2.0 search engines. An in-depth analysis of modifications was performed using Byonic software (Proteinmetrics, USA) as a plug-in into Proteom Discoverer running against an in-house designed database for oxidative and post-translational modifications.

Statistical Analysis: Data are from several independent experiments and show mean and standard error if not indicated otherwise. Statistical analysis was performed using t-test, one-way anova, or two-way anova, as indicated. Asterisks indicate the level of significance as follows: *, **, or *** for the *p*-values <0.05, <0.01, or <0.001, respectively. Statistical analysis was carried out using prism 8.4 (GraphPad Software, USA).

Supporting Information

Supporting Information is available from the Wiley Online Library or from the author.

Acknowledgements

E.F., D.M., and L.M. contributed equally to this work. This work was funded by the German Federal Ministry of Education and Research (BMBF), grant numbers 03Z22DN11 (R.C., E.F., and S.B.), 03Z22DN12 (K.W. and J.W.L.), 03Z22Di1 (S.B.), 03Z22C51 (U.M. and M.D.), and 03ZZ0806A (D.M. and B.M.B.). S.B. is further supported by the European Social Fund (ESF), grant number ESF/14-BM-A55-0001/18, and the German Head and Neck Cancer Research Foundation. L.M. received support from the Gerhard-Domagk-Foundation Greifswald, Germany. B.M.B. received support from the German Research Council (DFG; CRC-TRR34, RTG-1870) as well as from the EU (IMI-COMBACTE, 115523). The funding sources had no role in the design of this study and will not have any role during its execution, analysis, interpretation of the data, or decision to submit results. The authors acknowledge Markus Grube, Antje Janetzko, Tobias Schulze, and Jens van den Brandt for support with animal housing and experiments. The technical assistance of Felix Niessner, Vincent Peton, Torben Kewitz, and Christina Wolff is highly appreciated. The authors thank Karl Sebastian Lang (Institute of Immunology, Essen University Medical Center, Germany) and Diana Dudziak (Institute of Dermatology, Erlangen University Medical Center, Germany) for contributing B16F10-Ova cells, as well as Stephen Buttler for providing reagents.

Conflict of Interest

The authors declare no conflict of interest.

Data Availability Statement

Research data are not shared.

Keywords

kINPen, ovalbumin, oxPTM, ROS, vaccines

Received: September 4, 2020
Revised: January 22, 2021
Published online: March 8, 2021

[1] H. Sies, D. P. Jones, *Nat. Rev. Mol. Cell Biol.* **2020**, *21*, 363.
[2] C. C. Winterbourn, M. B. Hampton, *Nat. Chem. Biol.* **2015**, *11*, 5.
[3] C. Lood, L. P. Blanco, M. M. Purmalek, C. Carmona-Rivera, S. S. De Ravin, C. K. Smith, H. L. Malech, J. A. Ledbetter, K. B. Elkon, M. J. Kaplan, *Nat. Med.* **2016**, *22*, 146.
[4] Z. Liao, D. Chua, N. S. Tan, *Mol. Cancer* **2019**, *18*, 65.
[5] G. Schett, M. F. Neurath, *Nat. Commun.* **2018**, *9*, 3261.
[6] T. Gong, L. Liu, W. Jiang, R. Zhou, *Nat. Rev. Immunol.* **2020**, *20*, 95.
[7] J. Grootjans, A. Kaser, R. J. Kaufman, R. S. Blumberg, *Nat. Rev. Immunol.* **2016**, *16*, 469.
[8] A. Rivas-Urbina, S. Benitez, A. Perez, J. L. Sanchez-Quesada, *Front. Biosci.* **2018**, *23*, 1220.
[9] A. Trpkovic, I. Resanovic, J. Stanimirovic, D. Radak, S. A. Mousa, D. Cenic-Milosevic, D. Jevremovic, E. R. Isenovic, *Crit. Rev. Clin. Lab. Sci.* **2015**, *52*, 70.
[10] T. Nybo, S. Dieterich, L. F. Gamon, C. Y. Chuang, A. Hammer, G. Hoefler, E. Malle, A. Rogowska-Wrzesinska, M. J. Davies, *Redox Biol.* **2019**, *20*, 496.
[11] B. J. Ryan, A. Nissim, P. G. Winyard, *Redox Biol.* **2014**, *2*, 715.
[12] S. M. Anderton, *Curr. Opin. Immunol.* **2004**, *16*, 753.
[13] J. L. Tanyi, S. Bobisse, E. Ophir, S. Tuyaerts, A. Roberti, R. Genolet, P. Baumgartner, B. J. Stevenson, C. Iseli, D. Dangaj, B. Czerniecki, A. Semilietof, J. Racle, A. Michel, I. Xenarios, C. Chiang, D. S. Monos, D. A. Torigian, H. L. Nisenbaum, O. Michielin, C. H. June, B. L. Levine, D. J. Powell, Jr., D. Gfeller, R. Mick, U. Dafni, V. Zoete, A. Harari, G. Coukos, L. E. Kandalaft, *Sci. Transl. Med.* **2018**, *10*, eaao5931.
[14] C. C. Winterbourn, A. J. Kettle, M. B. Hampton, *Annu. Rev. Biochem.* **2016**, *85*, 765.
[15] D. Bagchi, M. Bagchi, D. M. Douglas, D. K. Das, *Free Radical Res. Commun.* **1992**, *17*, 2.
[16] T. von Woedtke, A. Schmidt, S. Bekeschus, K. Wende, K. D. Weltmann, *In Vivo* **2019**, *33*, 1011.
[17] S. Bekeschus, A. Schmidt, K.-D. Weltmann, T. von Woedtke, *Clin. Plas. Med.* **2016**, *4*, 1.
[18] O. Handorf, T. Weihe, S. Bekeschus, A. C. Graf, U. Schnabel, K. Riedel, J. Ehlbeck, *Appl. Environ. Microbiol.* **2018**, *84*, 21.
[19] A. Schmidt, T. von Woedtke, B. Vollmar, S. Hasse, S. Bekeschus, *Theranostics* **2019**, *9*, 1066.
[20] B. Stratmann, T. C. Costea, C. Nolte, J. Hiller, J. Schmidt, J. Reindel, K. Masur, W. Motz, J. Timm, W. Kerner, D. Tschoepe, *JAMA Netw Open* **2020**, *3*, 2010411.
[21] A. Privat-Maldonado, A. Schmidt, A. Lin, K. D. Weltmann, K. Wende, A. Bogaerts, S. Bekeschus, *Oxid. Med. Cell. Longevity* **2019**, *2019*, 9062098.
[22] G. Pasqual-Melo, R. K. Gandhirajan, I. Stoffels, S. Bekeschus, *Clin. Plas. Med.* **2018**, *10*, 1.
[23] Y. Binenbaum, G. Ben-David, Z. Gil, Y. Z. Slutsker, M. A. Ryzhkov, J. Felsteiner, Y. E. Krasik, J. T. Cohen, *PLoS One* **2017**, *12*, 0169457.
[24] M. Alimohammadi, M. Golpur, F. Sohbatzadeh, S. Hadavi, S. Bekeschus, H. A. Niaki, R. Valadan, A. Rafiei, *Biomolecules* **2020**, *10*, 1011.
[25] N. Chernets, D. S. Kurpad, V. Alexeev, D. B. Rodrigues, T. A. Freeman, *Plasma Processes Polym.* **2015**, *12*, 1400.

[26] G. Pasqual-Melo, T. Nascimento, L. J. Sanches, F. P. Blegniski, J. K. Bianchi, S. K. Sagwal, J. Berner, A. Schmidt, S. Emmert, K. D. Weltmann, T. von Woedtke, R. K. Gandhirajan, A. L. Cecchini, S. Bekeschus, *Cancers* **2020**, *12*, 1993.
[27] M. Ishaq, S. Kumar, H. Varinli, Z. J. Han, A. E. Rider, M. D. Evans, A. B. Murphy, K. Ostrikov, *Mol. Biol. Cell* **2014**, *25*, 1523.
[28] M. Wirtz, I. Stoffels, J. Dissemond, D. Schadendorf, A. Roesch, *J. Eur. Acad. Dermatol. Venereol.* **2018**, *32*, 37.
[29] H.-R. Metelmann, C. Seebauer, V. Miller, A. Fridman, G. Bauer, D. B. Graves, J.-M. Pouvesle, R. Rutkowski, M. Schuster, S. Bekeschus, K. Wende, K. Masur, S. Hasse, T. Gerling, M. Hori, H. Tanaka, E. Ha Choi, K.-D. Weltmann, P. H. Metelmann, D. D. Von Hoff, T. v. Woedtke, *Clin. Plas. Med.* **2018**, *9*, 6.
[30] K. Witzke, C. Seebauer, K. Jesse, E. Kwiatek, J. Berner, M. L. Semmler, L. Boeckmann, S. Emmert, K. D. Weltmann, H. R. Metelmann, S. Bekeschus, *Plasma Processes Polym.* **2020**, *17*, 1900258.
[31] M. Khalili, L. Daniels, A. Lin, F. C. Krebs, A. E. Snook, S. Bekeschus, W. B. Bowne, V. Miller, *J. Phys. D: Appl. Phys.* **2019**, *52*, 423001.
[32] L. Galluzzi, A. Buque, O. Kepp, L. Zitvogel, G. Kroemer, *Nat. Rev. Immunol.* **2017**, *17*, 2.
[33] S. Bekeschus, K. Rodder, B. Fregin, O. Otto, M. Lippert, K. D. Weltmann, K. Wende, A. Schmidt, R. K. Gandhirajan, *Oxid. Med. Cell. Longevity* **2017**, *2017*, 4396467.
[34] A. Lin, B. Truong, S. Patel, N. Kaushik, E. H. Choi, G. Fridman, A. Fridman, V. Miller, *Int. J. Mol. Sci.* **2017**, *18*, 5.
[35] S. Bekeschus, R. Clemen, F. Niessner, S. K. Sagwal, E. Freund, A. Schmidt, *Adv. Sci.* **2020**, *7*, 10.
[36] A. Lin, Y. Gorbanev, J. De Backer, J. Van Loenhout, W. Van Boxem, F. Lemiere, P. Cos, S. Dewilde, E. Smits, A. Bogaerts, *Adv. Sci.* **2019**, *6*, 6.
[37] X. Dai, K. Bazaka, D. J. Richard, E. R. W. Thompson, K. K. Ostrikov, *Trends Biotechnol.* **2018**, *36*, 1183.
[38] L. Xiang, X. Xu, S. Zhang, D. Cai, X. Dai, *Free Radical Biol. Med.* **2018**, *124*, 205.
[39] S. Bekeschus, M. Lippert, K. Diepold, G. Chiosis, T. Seufferlein, N. Azoitei, *Sci. Rep.* **2019**, *9*, 4112.
[40] X. Zhou, D. Cai, S. Xiao, M. Ning, R. Zhou, S. Zhang, X. Chen, K. Ostrikov, X. Dai, *J. Cancer* **2020**, *11*, 8.
[41] K. R. Liedtke, E. Freund, M. Hermes, S. Oswald, C. D. Heidecke, L. I. Partecke, S. Bekeschus, *Cancers* **2020**, *12*, 123.
[42] L. Brulle, M. Vandamme, D. Ries, E. Martel, E. Robert, S. Lerondel, V. Trichet, S. Richard, J. M. Pouvesle, A. Le Pape, *PLoS One* **2012**, *7*, 52653.
[43] L. I. Partecke, K. Evert, J. Haugk, F. Doering, L. Normann, S. Diedrich, F. U. Weiss, M. Evert, N. O. Huebner, C. Guenther, C. D. Heidecke, A. Kramer, R. Bussiahn, K. D. Weltmann, O. Pati, C. Bender, W. von Bernstorff, *BMC Cancer* **2012**, *12*,.
[44] M. Ishaq, Z. J. Han, S. Kumar, M. D. M. Evans, K. K. Ostrikov, *Plasma Processes Polym.* **2015**, *12*, 574.
[45] E. Freund, K. R. Liedtke, J. van der Linde, H. R. Metelmann, C. D. Heidecke, L. I. Partecke, S. Bekeschus, *Sci. Rep.* **2019**, *9*, 634.
[46] D. Han, J. H. Cho, R. H. Lee, W. Bang, K. Park, M. S. Kim, J. H. Shim, J. I. Chae, S. Y. Moon, *Sci. Rep.* **2017**, *7*, 43081.
[47] H. J. Ahn, K. I. Kim, N. N. Hoan, C. H. Kim, E. Moon, K. S. Choi, S. S. Yang, J. S. Lee, *PLoS One* **2014**, *9*, e86173.
[48] X. Yan, Z. L. Xiong, F. Zou, S. S. Zhao, X. P. Lu, G. X. Yang, G. Y. He, K. Ostrikov, *Plasma Processes Polym.* **2012**, *9*, 59.
[49] B. Smolkova, M. Lunova, A. Lynnyk, M. Uzhytchak, O. Churpita, M. Jirsa, S. Kubinova, O. Lunov, A. Dejneka, *Cell. Physiol. Biochem.* **2019**, *52*, 119.
[50] M. Adhikari, B. Adhikari, A. Adhikari, D. Yan, V. Soni, J. Sherman, M. Keidar, *Curr. Pharm. Des.* **2020**, *26*, 2195.
[51] Z. Chen, H. Simonyan, X. Cheng, E. Gjika, L. Lin, J. Canady, J. H. Sherman, C. Young, M. Keidar, *Cancers* **2017**, *9*, 61.
[52] E. Gjika, S. Pal-Ghosh, M. E. Kirschner, L. Lin, J. H. Sherman, M. A. Stepp, M. Keidar, *Sci. Rep.* **2020**, *10*, 16495.
[53] M. Weiss, D. Gumbel, E. M. Hanschmann, R. Mandelkow, N. Gelbrich, U. Zimmermann, R. Walther, A. Ekkernkamp, A. Sckell, A. Kramer, M. Burchardt, C. H. Lillig, M. B. Stope, *PLoS One* **2015**, *10*, 7.
[54] A. Bisag, C. Bucci, S. Coluccelli, G. Girolimetti, R. Laurita, P. De Iaco, A. M. Perrone, M. Gherardi, L. Marchio, A. M. Porcelli, V. Colombo, G. Gasparre, *Cancers* **2020**, *12*, 476.
[55] K. Nakamura, H. Kajiyama, Y. Peng, F. Utsumi, N. Yoshikawa, H. Tanaka, M. Mizuno, S. Toyokuni, M. Hori, F. Kikkawa, *Clin. Plas. Med.* **2018**, *9*, 47.
[56] A. M. Hirst, M. S. Simms, V. M. Mann, N. J. Maitland, D. O'Connell, F. M. Frame, *Br. J. Cancer* **2015**, *112*, 1536.
[57] N. Barekzi, M. Laroussi, G. Konesky, S. Roman, *Plasma Processes Polym.* **2016**, *13*, 1189.
[58] S. Bekeschus, V. Ressel, E. Freund, N. Gelbrich, A. Mustea, M. B. Stope, *Antioxidants* **2020**, *9*, 4.
[59] S. Bekeschus, J. Brüggemeier, C. Hackbarth, K.-D. Weltmann, T. von Woedtke, L.-I. Partecke, J. van der Linde, *Plasma Sources Sci. Technol.* **2018**, *27*, 034001.
[60] S. Wenske, J.-W. Lackmann, S. Bekeschus, K.-D. Weltmann, T. von Woedtke, K. Wende, *Biointerphases* **2020**, *15*, 061008.
[61] K. Setsukinai, Y. Urano, K. Kakinuma, H. J. Majima, T. Nagano, *J. Biol. Chem.* **2003**, *278*, 3170.
[62] S. Bekeschus, J. Kolata, C. Winterbourn, A. Kramer, R. Turner, K. D. Weltmann, B. Broker, K. Masur, *Free Radical Res.* **2014**, *48*, 542.
[63] C. Breen, R. Pal, M. R. J. Elsegood, S. J. Teat, F. Iza, K. Wende, B. R. Buckley, S. J. Butler, *Chem. Sci.* **2020**, *11*, 3164.
[64] N. Nakatsubo, H. Kojima, K. Kikuchi, H. Nagoshi, Y. Hirata, D. Maeda, Y. Imai, T. Irimura, T. Nagano, *FEBS Lett.* **1998**, *427*, 263.
[65] Y. Mine, T. Noutomi, N. Haga, *J. Agric. Food Chem.* **1990**, *38*, 2122.
[66] A. Kato, T. Takagi, *J. Agric. Food Chem.* **1988**, *36*, 6.
[67] D. J. Gasper, B. Neldner, E. H. Plisch, H. Rustom, E. Carrow, H. Imai, Y. Kawaoka, M. Suresh, *PLoS Pathog.* **2016**, *12*, 1006064.
[68] X. Lu, G. V. Naidis, M. Laroussi, S. Reuter, D. B. Graves, K. Ostrikov, *Phys. Rep.* **2016**, *630*, 1.
[69] D. L. Farber, N. A. Yudanin, N. P. Restifo, *Nat. Rev. Immunol.* **2014**, *14*, 24.
[70] M. L. Wheeler, A. L. Defranco, *J. Immunol.* **2012**, *189*, 4405.
[71] P. J. Vernon, D. Tang, *Antioxid. Redox Signaling* **2013**, *18*, 677.
[72] S. Burgdorf, V. Lukacs-Kornek, C. Kurts, *J. Immunol.* **2006**, *176*, 6770.
[73] S. Burgdorf, A. Kautz, V. Bohnert, P. A. Knolle, C. Kurts, *Science* **2007**, *316*, 612.
[74] J. D. Stone, A. S. Chervin, D. M. Kranz, *Immunology* **2009**, *126*, 165.
[75] J. P. Snook, C. Kim, M. A. Williams, *Sci. Immunol.* **2018**, *3*, eaas9103.
[76] C. K. Baumgartner, A. Ferrante, M. Nagaoka, J. Gorski, L. P. Malherbe, *J. Immunol.* **2010**, *184*, 573.
[77] J. W. Lackmann, K. Wende, C. Verlackt, J. Golda, J. Volzke, F. Kogelheide, J. Held, S. Bekeschus, A. Bogaerts, V. Schulz-von der Gathen, K. Stapelmann, *Sci. Rep.* **2018**, *8*, 7736.
[78] E. Takai, T. Kitamura, J. Kuwabara, S. Ikawa, S. Yoshizawa, K. Shiraki, H. Kawasaki, R. Arakawa, K. Kitano, *J. Phys. D: Appl. Phys.* **2014**, *47*, 285403.
[79] M. Yousfi, R. Zhou, R. Zhou, J. Zhuang, Z. Zong, X. Zhang, D. Liu, K. Bazaka, K. Ostrikov, *PLoS One* **2016**, *11*, 5.
[80] J. Allina, B. Hu, D. M. Sullivan, M. I. Fiel, S. N. Thung, S. F. Bronk, R. C. Huebert, J. van de Water, N. F. LaRusso, M. E. Gershwin, G. J. Gores, J. A. Odin, *J. Autoimmun.* **2006**, *27*, 232.
[81] M. K. Aydintug, L. Zhang, C. Wang, D. Liang, J. M. Wands, A. W. Michels, B. Hirsch, B. J. Day, G. Zhang, D. Sun, G. S. Eisenbarth, R. L. O'Brien, W. K. Born, *Mol. Immunol.* **2014**, *60*, 2.
[82] P. Griem, K. Panthel, H. Kalbacher, E. Gleichmann, *Eur. J. Immunol.* **1996**, *26*, 279.

[83] D. Weiskopf, A. Schwanninger, B. Weinberger, G. Almanzar, W. Parson, S. Buus, H. Lindner, B. Grubeck-Loebenstein, *J. Leukocyte Biol.* **2010**, *87*, 165.
[84] H. K. Kang, J. A. Mikszta, H. Deng, E. E. Sercarz, P. E. Jensen, B. S. Kim, *J. Immunol.* **2000**, *164*, 4.
[85] B. Maillere, J. Cotton, G. Mourier, M. Leonetti, S. Leroy, A. Menez, *J. Immunol.* **1993**, *150*, 12.
[86] A. Sachs, E. Moore, Z. Kosaloglu-Yalcin, B. Peters, J. Sidney, S. A. Rosenberg, P. F. Robbins, A. Sette, *J. Immunol.* **2020**, *205*, 539.
[87] S. Prato, J. Fleming, C. W. Schmidt, G. Corradin, J. A. Lopez, *Mol. Immunol.* **2006**, *43*, 2031.
[88] E. J. Benner, R. Banerjee, A. D. Reynolds, S. Sherman, V. M. Pisarev, V. Tsiperson, C. Nemachek, P. Ciborowski, S. Przedborski, R. L. Mosley, H. E. Gendelman, *PLoS One* **2008**, *3*, 1376.
[89] V. N. Uversky, G. Yamin, L. A. Munishkina, M. A. Karymov, I. S. Millett, S. Doniach, Y. L. Lyubchenko, A. L. Fink, *Mol. Brain Res.* **2005**, *134*, 84.
[90] H. Ohmori, N. Kanayama, *Autoimmun. Rev.* **2005**, *4*, 224.
[91] H. C. Birnboim, A. M. Lemay, D. K. Lam, R. Goldstein, J. R. Webb, *J. Immunol.* **2003**, *171*, 528.
[92] J. Sidney, J. L. Vela, D. Friedrich, R. Kolla, M. von Herrath, J. D. Wesley, A. Sette, *BMC Immunol.* **2018**, *19*, 12.
[93] R. Biedron, M. K. Konopinski, J. Marcinkiewicz, S. Jozefowski, *PLoS One* **2015**, *10*, 0123293.
[94] Z. M. Prokopowicz, F. Arce, R. Biedron, C. L. Chiang, M. Ciszek, D. R. Katz, M. Nowakowska, S. Zapotoczny, J. Marcinkiewicz, B. M. Chain, *J. Immunol.* **2010**, *184*, 824.
[95] J. E. Slansky, F. M. Rattis, L. F. Boyd, T. Fahmy, E. M. Jaffee, J. P. Schneck, D. H. Margulies, D. M. Pardoll, *Immunity* **2000**, *13*, 529.
[96] K. F. Chan, B. S. Gully, S. Gras, D. X. Beringer, L. Kjer-Nielsen, J. Cebon, J. McCluskey, W. Chen, J. Rossjohn, *Nat. Commun.* **2018**, *9*, 1026.
[97] O. Y. Borbulevych, T. K. Baxter, Z. Yu, N. P. Restifo, B. M. Baker, *J. Immunol.* **2005**, *174*, 4812.
[98] A. Ilchmann, S. Burgdorf, S. Scheurer, Z. Waibler, R. Nagai, A. Wellner, Y. Yamamoto, H. Yamamoto, T. Henle, C. Kurts, U. Kalinke, S. Vieths, M. Toda, *J. Allergy Clin. Immunol.* **2010**, *125*, 175.
[99] M. J. Pallardy, I. Turbica, A. Biola-Vidamment, *Front. Immunol.* **2017**, *8*, 544.
[100] X. Li, S. G. Thakkar, T. B. Ruwona, R. O. Williams, 3rd, Z. Cui, *J. Controlled Release* **2015**, *204*, 38.
[101] K. Kastenmuller, U. Wille-Reece, R. W. Lindsay, L. R. Trager, P. A. Darrah, B. J. Flynn, M. R. Becker, M. C. Udey, B. E. Clausen, B. Z. Igyarto, D. H. Kaplan, W. Kastenmuller, R. N. Germain, R. A. Seder, *J. Clin. Invest.* **2011**, *121*, 1782.
[102] K. D. Ratanji, J. P. Derrick, R. J. Dearman, I. Kimber, *J. Immunotoxicol.* **2014**, *11*, 99.
[103] E. M. Moussa, J. P. Panchal, B. S. Moorthy, J. S. Blum, M. K. Joubert, L. O. Narhi, E. M. Topp, *J. Pharm. Sci.* **2016**, *105*, 417.
[104] C. L. Hawkins, *Essays Biochem.* **2019**, *64*, 75.
[105] J. M. Damsker, A. M. Hansen, R. R. Caspi, *Ann. N. Y. Acad. Sci.* **2010**, *1183*, 211.
[106] M. Heilmann, A. Wellner, G. Gadermaier, A. Ilchmann, P. Briza, M. Krause, R. Nagai, S. Burgdorf, S. Scheurer, S. Vieths, T. Henle, M. Toda, *J. Biol. Chem.* **2014**, *289*, 7919.
[107] B. Li, Z. Lei, B. D. Lichty, D. Li, G. M. Zhang, Z. H. Feng, Y. Wan, B. Huang, *Cancer Immunol. Immunother.* **2010**, *59*, 313.
[108] Y. Godet, M. Dosset, C. Borg, O. Adotevi, *Oncoimmunology* **2012**, *1*, 1617.
[109] N. S. Wilson, D. El-Sukkari, J. A. Villadangos, *Blood* **2004**, *103*, 2187.
[110] M. A. Lakins, E. Ghorani, H. Munir, C. P. Martins, J. D. Shields, *Nat. Commun.* **2018**, *9*, 948.
[111] J. H. Newman, C. B. Chesson, N. L. Herzog, P. K. Bommareddy, S. M. Aspromonte, R. Pepe, R. Estupinian, M. M. Aboelatta, S. Buddhadev, S. Tarabichi, M. Lee, S. Li, D. J. Medina, E. F. Giurini, K. H. Gupta, G. Guevara-Aleman, M. Rossi, C. Nowicki, A. Abed, J. W. Goldufsky, J. R. Broucek, R. E. Redondo, D. Rotter, S. R. Jhawar, S. J. Wang, F. J. Kohlhapp, H. L. Kaufman, P. G. Thomas, V. Gupta, T. M. Kuzel, J. Reiser, J. Paras, M. P. Kane, E. A. Singer, J. Malhotra, L. K. Denzin, D. B. Sant'Angelo, A. B. Rabson, L. Y. Lee, A. Lasfar, J. Langenfeld, J. M. Schenkel, M. J. Fidler, E. S. Ruiz, A. L. Marzo, J. S. Rudra, A. W. Silk, A. Zloza, *Proc. Natl. Acad. Sci. USA* **2020**, *117*, 1119.
[112] S. Devalaraja, T. K. J. To, I. W. Folkert, R. Natesan, M. Z. Alam, M. Li, Y. Tada, K. Budagyan, M. T. Dang, L. Zhai, G. P. Lobel, G. E. Ciotti, T. S. K. Eisinger-Mathason, I. A. Asangani, K. Weber, M. C. Simon, M. Haldar, *Cell* **2020**, *180*, 1098.
[113] C. Hegedus, K. Kovacs, Z. Polgar, Z. Regdon, E. Szabo, A. Robaszkiewicz, H. J. Forman, A. Martner, L. Virag, *Redox Biol.* **2018**, *16*, 59.
[114] N. Hay, *Nat. Rev. Cancer* **2016**, *16*, 635.
[115] K. Wang, J. Jiang, Y. Lei, S. Zhou, Y. Wei, C. Huang, *Trends Biochem. Sci.* **2019**, *44*, 401.
[116] C. C. Winterbourn, M. B. Hampton, J. H. Livesey, A. J. Kettle, *J. Biol. Chem.* **2006**, *281*, 39860.
[117] C. Xu, B. Bailly-Maitre, J. C. Reed, *J. Clin. Invest.* **2005**, *115*, 10.
[118] F. Kotsias, E. Hoffmann, S. Amigorena, A. Savina, *Antioxid. Redox Signaling* **2013**, *18*, 714.
[119] I. Dingjan, D. R. Verboogen, L. M. Paardekooper, N. H. Revelo, S. P. Sittig, L. J. Visser, G. F. Mollard, S. S. Henriet, C. G. Figdor, M. Ter Beest, G. van den Bogaart, *Sci. Rep.* **2016**, *6*, 22064.
[120] H. Matsue, D. Edelbaum, D. Shalhevet, N. Mizumoto, C. Yang, M. E. Mummert, J. Oeda, H. Masayasu, A. Takashima, *J. Immunol.* **2003**, *171*, 3010.
[121] J. W. Lackmann, G. Bruno, H. Jablonowski, F. Kogelheide, B. Offerhaus, J. Held, V. Schulz-von der Gathen, K. Stapelmann, T. von Woedtke, K. Wende, *PLoS One* **2019**, *14*, 0216606.
[122] S. Reuter, T. von Woedtke, K. D. Weltmann, *J. Phys. D: Appl. Phys.* **2018**, *51*, 233001.
[123] P. J. Bruggeman, M. J. Kushner, B. R. Locke, J. G. E. Gardeniers, W. G. Graham, D. B. Graves, R. C. H. M. Hofman-Caris, D. Maric, J. P. Reid, E. Ceriani, D. F. Rivas, J. E. Foster, S. C. Garrick, Y. Gorbanev, S. Hamaguchi, F. Iza, H. Jablonowski, E. Klimova, J. Kolb, F. Krcma, P. Lukes, Z. Machala, I. Marinov, D. Mariotti, S. M. Thagard, D. Minakata, E. C. Neyts, J. Pawlat, Z. L. Petrovic, R. Pflieger, S. Reuter, D. C. Schram, S. Schroter, M. Shiraiwa, B. Tarabova, P. A. Tsai, J. R. R. Verlet, T. von Woedtke, K. R. Wilson, K. Yasui, G. Zvereva, *Plasma Sources Sci. Technol.* **2016**, *25*, 053002.
[124] X. Wan, A. N. Vomund, O. J. Peterson, A. V. Chervonsky, C. F. Lichti, E. R. Unanue, *Nat. Immunol.* **2020**, *21*, 4.
[125] J. A. Trujillo, N. P. Croft, N. L. Dudek, R. Channappanavar, A. Theodossis, A. I. Webb, M. A. Dunstone, P. T. Illing, N. S. Butler, C. Fett, D. C. Tscharke, J. Rossjohn, S. Perlman, A. W. Purcell, *J. Biol. Chem.* **2014**, *289*, 27979.
[126] R. Strollo, C. Vinci, M. H. Arshad, D. Perrett, C. Tiberti, F. Chiarelli, N. Napoli, P. Pozzilli, A. Nissim, *Diabetologia* **2015**, *58*, 2851.
[127] B. A. Freeman, V. B. O'Donnell, F. J. Schopfer, *Nitric Oxide* **2018**, *77*, 106.
[128] N. K. Khoo, V. Rudolph, M. P. Cole, F. Golin-Bisello, F. J. Schopfer, S. R. Woodcock, C. Batthyany, B. A. Freeman, *Free Radical Biol. Med.* **2010**, *48*, 2.
[129] T. Melo, J. F. Montero-Bullon, P. Domingues, M. R. Domingues, *Redox Biol.* **2019**, *23*, 101106.
[130] W. S. Yeo, Y. J. Kim, M. H. Kabir, J. W. Kang, M. Ahsan-Ul-Bari, K. P. Kim, *Mass Spectrom. Rev.* **2015**, *34*, 2.
[131] I. Verrastro, S. Pasha, K. T. Jensen, A. R. Pitt, C. M. Spickett, *Biomolecules* **2015**, *5*, 378.

[132] Y. Gorbanev, N. Stehling, D. O'Connell, V. Chechik, *Plasma Sources Sci. Technol.* **2016**, *25*, 055017.
[133] F. Girard, V. Badets, S. Blanc, K. Gazeli, L. Marlin, L. Authier, P. Svarnas, N. Sojic, F. Clement, S. Arbault, *RSC Adv.* **2016**, *6*, 78457.
[134] P. Lukes, E. Dolezalova, I. Sisrova, M. Clupek, *Plasma Sources Sci. Technol.* **2014**, *23*, 015019.
[135] P. Ferdinandy, R. Schulz, *Circ. Res.* **2001**, *88*, 2.
[136] W. G. Siems, E. Capuozzo, D. Verginelli, C. Salerno, C. Crifo, T. Grune, *Free Radical Res.* **1997**, *27*, 353.
[137] J. Rybka, D. Kupczyk, K. Kedziora-Kornatowska, J. Motyl, J. Czuczejko, K. Szewczyk-Golec, M. Kozakiewicz, H. Pawluk, L. A. Carvalho, J. Kedziora, *Cardiovasc. Toxicol.* **2011**, *11*, 1.
[138] A. V. Pipa, S. Reuter, R. Foest, K. D. Weltmann, *J. Phys. D: Appl. Phys.* **2012**, *45*, 085201.
[139] M. M. Cortese-Krott, A. Koning, G. G. C. Kuhnle, P. Nagy, C. L. Bianco, A. Pasch, D. A. Wink, J. M. Fukuto, A. A. Jackson, H. van Goor, K. R. Olson, M. Feelisch, *Antioxid. Redox Signaling* **2017**, *27*, 684.
[140] I. Mohiuddin, H. Chai, P. H. Lin, A. B. Lumsden, Q. Yao, C. Chen, *J. Surg. Res.* **2006**, *133*, 143.
[141] A. J. Czaja, *Dig. Dis. Sci.* **2016**, *61*, 10.
[142] S. Bekeschus, K. Wende, M. M. Hefny, K. Rodder, H. Jablonowski, A. Schmidt, T. V. Woedtke, K. D. Weltmann, J. Benedikt, *Sci. Rep.* **2017**, *7*, 2791.
[143] S. Bekeschus, A. Schmidt, F. Niessner, T. Gerling, K. D. Weltmann, K. Wende, *J. Visualized Exp.* **2017**, e56331.
[144] M. J. Barnden, J. Allison, W. R. Heath, F. R. Carbone, *Immunol. Cell Biol.* **1998**, *76*, 34.
[145] S. R. Clarke, M. Barnden, C. Kurts, F. R. Carbone, J. F. Miller, W. R. Heath, *Immunol. Cell Biol.* **2000**, *78*, 110.
[146] L. Linxiang, Y. Abe, Y. Nagasawa, R. Kudo, N. Usui, K. Imai, T. Mashino, M. Mochizuki, N. Miyata, *Biomed. Chromatogr.* **2004**, *18*, 470.

vaccines

MDPI

Perspective

ROS Cocktails as an Adjuvant for Personalized Antitumor Vaccination?

Ramona Clemen and Sander Bekeschus *

ZIK, Leibniz Institute for Plasma Science and Technology (INP), Felix Hausdorff Str. 2, 17489 Greifswald, Germany; ramona.clemen@inp-greifswald.de
* Correspondence: Bekeschus@inp-greifswald.de; Tel.: +49-3834-5543-948

Abstract: Cancer is the second leading cause of death worldwide. Today, the critical role of the immune system in tumor control is undisputed. Checkpoint antibody immunotherapy augments existing antitumor T cell activity with durable clinical responses in many tumor entities. Despite the presence of tumor-associated antigens and neoantigens, many patients have an insufficient repertoires of antitumor T cells. Autologous tumor vaccinations aim at alleviating this defect, but clinical success is modest. Loading tumor material into autologous dendritic cells followed by their laboratory expansion and therapeutic vaccination is promising, both conceptually and clinically. However, this process is laborious, time-consuming, costly, and hence less likely to solve the global cancer crisis. Therefore, it is proposed to re-focus on personalized anticancer vaccinations to enhance the immunogenicity of autologous therapeutic tumor vaccines. Recent work re-established the idea of using the alarming agents of the immune system, oxidative modifications, as an intrinsic adjuvant to broaden the antitumor T cell receptor repertoire in cancer patients. The key novelty is the use of gas plasma, a multi-reactive oxygen and nitrogen species-generating technology, for diversifying oxidative protein modifications in a, so far, unparalleled manner. This significant innovation has been successfully used in proof-of-concept studies and awaits broader recognition and implementation to explore its chances and limitations of providing affordable personalized anticancer vaccines in the future. Such multidisciplinary advance is timely, as the current COVID-19 crisis is inexorably reflecting the utmost importance of innovative and effective vaccinations in modern times.

Keywords: antigen; cold physical plasma; gas plasma technology; immunogenicity; oxidative post-translational modifications; oxPTM; reactive nitrogen species; reactive oxygen species

Citation: Clemen, R.; Bekeschus, S. ROS Cocktails as an Adjuvant for Personalized Antitumor Vaccination?. *Vaccines* **2021**, *9*, 527. https://doi.org/10.3390/vaccines9050527

Academic Editor: Ralph A. Tripp

Received: 23 April 2021
Accepted: 17 May 2021
Published: 19 May 2021

1. Introduction

Each year 14.1 million new cases of cancers are diagnosed that require therapeutic attention. The classic pillars in oncology are surgery, radiotherapy, and chemotherapy. These measures have markedly improved median survival in patients across all types of cancer. However, significant progress has slowed down in the past decades for several reasons, radioresistance and chemoresistance being among them [1,2]. Meanwhile, biologicals, such as cytokines and antibodies targeting growth receptors, spurred therapy success [3–5]. A paradigm shift in oncology then came with the incorporation of antitumor immune defense into the treatment concepts and repertoires of the field of oncology. Although being predicted in the 1960s already [6,7], the concept needed several decades, and a leap in life science technology innovations, along with mechanistic concepts in immunology and oncology to harness its full potential. Today, antibodies targeting immunosuppressive checkpoint receptors on T cells have provided substantial clinical responses [8]. Their success, along with the Nobel Prize Award in Physiology and Medicine in 2018 for achievements in this field, has given antitumor T cells undisputed importance across the globe for providing tumor protection [9]. Tumor protection is carried out by generating antigen-specific T cells, followed by strengthening one's immune response through a specific anti-tumor immune response. The personalized antigen vaccines have recently come to the fore [10] because

they can be efficient and have few side effects. However, there are novel ways to optimize therapeutic anti-tumor vaccines in various strategies, such as a modified tumor biopsy vaccine [11], cryptic peptide [12], nano-particle loaded [13], or a PEG-modified antigen vaccine. Here we propose a new technical approach to optimize the immunization by mimicking a relevant biological process of the inflammatory microenvironment, namely the generation of reactive species.

2. Tumor Immune Evasion and Vaccination

Cancers evolve under the constant pressure of the immune system; a process called immune evasion [14]. Tumor variants with minimal activation of immune cells have a growth advantage over clonotypes with highly immunogenic antigens. This classic view was complemented over the last two decades with the opposite scenario. Highly immunogenic tumor cells do not attempt to hide from immune recognition but counteract immune cell activation by activating immunosuppressive ligands and receptors, for example, PD-L1, PD-L2, and CD80/86 [15]. Other mechanisms of an immunosuppressive microenvironment complement this camouflage and sabotage. For instance, hypoxia [16], soluble mediators such as kynurenine [17], and the promotion of suppressive immune cell subsets including M2 macrophages and regulator T cells [18]. However, the clinical success of checkpoint antibodies targeting receptors and ligands suggests the receptor-ligand-based immunosuppression of effector T cells as being a critical determinant of the therapeutic outcome. Hence, it is clear that strengthening the activity of *existing* antitumor T cell clones is a proven therapeutic concept in cancer immunotherapy.

A second complementary approach is broadening the T cell receptor repertoire by augmenting the generation of *novel* antitumor T cell clones. Autologous tumor vaccines provide a vast array of tumor-associated antigens (TAA) and neoantigens to the host. Such antigens are present in all types of tumors, albeit to a varying degree [19]. Another limitation is that not all of these tumor antigens are presentable on major histocompatibility complex (MHC) molecules due to the preference of protein digestion and peptide cleavage in the proteasome and immunoproteasome [20,21], as well as the affinity of the MHC receptor family towards specific amino acids of the peptide to provide suitable binding affinity [22,23]. However, the critical determinant of generating T cell activation or tolerance towards such antigens is the inflammatory context in which these are presented, along with the efficacy of antigen presentation. To address these issues, dendritic cells (DCs), being professional antigen-presenting cells, have been investigated in numerous preclinical and clinical studies for their ability to promote antitumor immunity after being loaded with tumor antigens in vitro [24,25]. Undoubtedly, this elegant type of cell therapy fostered the understanding of tumor immunology in oncology and benefited many patients enrolled in clinical trials. Nevertheless, this concept also has limitations. First, there was limited success in many clinical trials. Second, DC loading and expansion require state-of-the-art facilities and are associated with high costs. Even if near-ideal protocols had been, or were to be, developed, it is still questionable whether DC therapy would become a global gold standard for cancer therapy apart from in countries with privileged income and health care systems. Third, much focus has been put on DC activation and maturation. Simultaneously, the conditioning of the tumor material has received less attention, as was recently well demonstrated in a cohort of cancer patients [26], which at least gives rise to the idea of rethinking the inevitable need of DCs in the realm of tumor vaccination.

Textbook immunology predicts that the body has an inherent interest in mounting both B cell and T cell immune responses against (non-self) antigens if presented in a sufficiently inflammatory context. Adjuvants provide the latter, being the basis of vaccinations, a process currently receiving significant interest duringthe COVID-19 pandemic. Together, with the points mentioned above, this raises the question of what is limiting the use of autologous tumor material to be directly used as a vaccine without the need for external processing by other cell types. It is understood that early and recent attempts of using a native autologous tumor vaccination to provide therapeutic efficacy [27,28] failed. Notwith-

standing, we here outline why reactive oxygen and nitrogen species might be a fascinating option to render tumor antigens more suitable for direct vaccination campaigns in oncology and possibly adjuvant to existing strategies [29–32], which are numerous and not covered here. It should be stressed that, in the tumor context, this text always refers to therapeutic vaccinations and not preventive/prophylactic vaccination.

3. Reactive Oxygen and Nitrogen Species

Reactive oxygen and nitrogen species (ROS/RNS) are molecules with great reactivity and abbreviated with ROS in this work, as most RNS contain oxygen. Besides their past underappreciation as mere metabolic byproducts, ROS are pivotal intracellular redox signaling agents [33], critical for infection control [34], and increasingly recognized as key elements of the inflammatory microenvironment. Immune cell activation and metabolic reprogramming of leukocyte subsets have been linked to endogenous ROS production as crucial to driving these processes [35–38]. Perhaps the best-known role of non-constitutive ROS is their early appearance during inflammation by immune cells and non-immune cells alike. ROS release is the very first event during tissue damage [39] and it is required for the subsequent neutrophil influx. Subsequent neutrophil priming and activation auto-amplifies ROS production, followed by another round of ROS amplification by incoming monocytes and macrophages that complement the reactive species array with several nitrogen species [40].

For instance, nitric oxide synthase (NOS) produces nitric oxide (NO), which reacts with superoxide (O_2^-), that is generated by NADPH (nicotinamide adenine dinucleotide phosphate) oxidases (NOX), to yield peroxynitrite ($^-$ONOO). The enzyme superoxide dismutase (SOD) catalyzes the reaction of superoxide to hydrogen peroxide (H_2O_2). In the presence of hydrogen peroxide, the arterial indoleamine 2,3-dioxygenase 1 (IDO-1) formates singlet oxygen ($^1O_2$) for blood pressure regulation and vascular tone during inflammation [41]. In the presence of iron, H_2O_2 promotes the generation of highly reactive hydroxyl radicals (HO$^\cdot$) in the Fenton reaction [42]. Furthermore, myeloperoxidase (MPO) is known to generate hypobromous acid, hypochlorous acid, and hypothiocyanite. The hypochlorite radicals can participate in the formation of atomic oxygen (O) and HO [34]. This is the environment in which infection-related antigens are recognized, modified, and transported to the secondary lymphatic organs to activate adaptive immunity.

Current vaccine preparation strategies almost unanimously neglect this ancient evolutionary part of antigen modification. When taking a view into other research fields, this comes as a surprise. For decades, researchers have identified a pivotal role of ROS and oxidative post-translational modifications (oxPTMs) in autoimmunity [43]. Chronic inflammation and chronic ROS release modified antigens, leading to auto-antibodies and auto-reactive T cells that are observed in numerous diseases, including rheumatoid arthritis, systemic lupus erythematosus, and diabetes [44–48], partly in a neoepitope-like fashion [49,50]. Mechanistically, oxPTMs have been ascribed a function similar to damage-associated molecular patterns (DAMPs) [51], providing pro-inflammatory stimuli in in professional antigen-presenting cells (APCs), and are decisive for the balance between antigen tolerance and immunity. Altogether, multiple ROS modify antigens, leading to a DAMP-like character to activate innate immunity and potentially neoepitopes to broaden adaptive immunity and the B cell and T cell receptor repertoire. ROS are, therefore, ideal candidates to increase the immunogenicity of autologous tumor vaccines. However, the challenges of working with ROS are numerous. First, their production, reaction kinetics, and specificity are hard to control, apart from the short half-lives associated with most species. Second, oxidative modifications are challenging to track and require sophisticated infrastructure and bioinformatics for their analysis. Third, and most notably, a simultaneous generation of several highly reactive compounds is technically impossible unless utilizing a concept from physics: gas plasma technology.

4. Gas Plasma Technology as a Significant Innovation in Generating Multi-ROS Cocktails

Gas plasma is an electron-impact and photon-driven technology. In gas plasma jets, usually, a noble gas is excited by a high-frequency electrode [52]. Excited noble gas species transfer their chemical energy to oxygen and nitrogen in the ambient air, generating vast amounts of several reactive oxygen and nitrogen species simultaneously. Compared to hot gas plasma, cold plasmas are operated at body temperatures and therefore do not denature proteins or harm cells and tissue by thermal energy transfer. Therefore, the main product is the bio-active multi-ROS cocktail [53–55]. Similar to the ROS released during inflammation, plasmas generate short-lived species (O, •NO, •NO, O_2•$^-$, •OOH, $^-$ONOO, $^1O_2$, etc.) as well as long-lived molecules that are mostly deterioration products from short-lived species such as H_2O_2, NO_2^-, NO_3^-, and HOCl [56,57]. Hundreds of chemical reactions have been identified in gas plasma jets using computer modeling, and redox biology currently does not offer the tools to identify each of the reaction products unambiguously. The degree of complexity is increased when considering the different spatio-temporal concentrations of each of the species along the axis of a plasma jet. Nevertheless, gas plasmas are unique in their ability to deliver multi-ROS cocktails onto biologically relevant targets. Strikingly, the ROS cocktail can be modified by changing the gas composition fed into the plasma jets (Figure 1). This leads to an enrichment of some types of ROS and a partial depletion of others [58,59]. This way, unique oxidative modification patterns are being generated at biological target molecules, as recently shown for the model peptide cysteine using mass spectrometry [60]. Additionally, prototypic plasma jets often allow other parameters to be tuned, for instance, the feed gas flux, the excitation frequency and wave form, and the input power. Other studies confirmed the modification of antigens and proteins by plasmas [61,62], leading to functional changes [63–65].

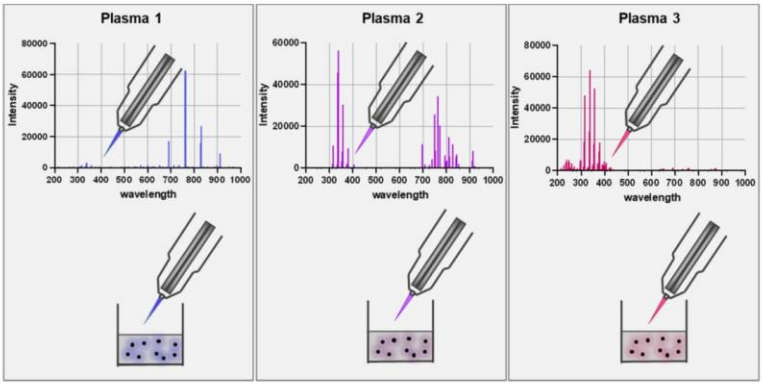

Figure 1. Scheme of using different feed gas settings to generate gas plasma with distinct ROS cocktail profiles. The upper panel represents optical emission spectroscopy (intensity: relative units; wavelength: nanometer) measurements of the visible plasma effluent leaving the jet device. The lower panel is a schematic of a biological target being exposed to the gas plasma resulting in distinct oxidative modification patterns as depicted with the color code.

5. Proof-of-Concept Study Using Multi-ROS Cocktails to Provide Vaccine Tumor Control

In a recent study, we used chicken ovalbumin (Ova) to study the immunogenicity of multi-ROS cocktails in vitro and in vivo [66]. Using transgenic OT-II mice harboring Ova-specific T cells, we found gas plasma modified Ova to elicit significantly enhanced T cell activation compared to native antigen (Ova). This effect was specific, as it could not be replicated using human albumin. Splenocytes of other mice strains also did not

show any elevated T cell activation. Strikingly, the enhanced T cell activation seen with gas plasma-treated Ova was not recapitulated when modifying Ova with equimolar amounts of long-lived reaction products from the plasma in treated liquids (H_2O_2, NO_2^-, NO_3^-, HOCl), unambiguously pointing towards a role of the unique cocktails generated by short-lived species. One plasma condition had more substantial effects than another one, which—in this specific setting—suggested a role of singlet and atomic oxygen or, possibly, lower ozone levels in providing immunogenic oxidative modifications. Using mass spectrometry, dozen of different modifications (e.g., oxidation, dioxidation, trioxidation, chlorination, and quinones) were found at many of the over 400 amino acids. This exemplifies the high degree of complexity, especially when considering the multi-ROS nature of the gas plasma system, currently making it difficult to come to a specific conclusion on which modifications have what effect. Some modifications were also in the sequence of the cognate peptide region. Moreover, it is possible (and likely, in our hands) that our observations were not based on one single type of modification or amino acid, but were rather a result of several modifications, complicating the control and understanding of this tool, as of now. We also found that oxidatively modified full Ova protein was needed, as the treatment of the oxidated immunogenic peptide alone (27 amino acids) did not elevate T cell responses. All this notwithstanding, the in vivo findings clearly showed functional consequences of the multi-ROS exposure to the antigen. In naïve mice, an increased anti-Ova T cell activity was created when using oxidized over native Ova, which was also reflected in a more inflammatory cytokine release profile. Notably, the gas plasma-derived multi-ROS Ova antigen oxidative modification led to significantly decreased tumor growth of Ova-expressing melanoma cells when given as a vaccine in a prime-boost scheme, compared to native untreated Ova. This was accompanied by the higher numbers and activation profiles of intratumoral T cells. These results emphasize the power of the multi-ROS antigen modification concept.

6. Concept and Challenges of Multi-ROS-Modified Autologous Tumor Vaccines

We propose gas plasma technology to upgrade antitumor vaccines by increasing adjuvanticity and antigenicity: the former due to the DAMP character of antigen oxPTMs promoting DC activation, as in the concept of immunogenic cell death (ICD) [67,68]. Indeed, gas plasma technology was shown to induce ICD [69], change proteomics suggesting neoepitope presentation [70], and increase the activity of antigen-presenting cells [71]. The increased immunogenicity of oxPTM and the potential formation of neoantigens was observed in autoimmunity [47,48]. However, the development of autoimmune disorders is not always based on oxidized antigens. Instead, some antigens are native [72], citrullinated [73,74] or deaminated [75]. Interestingly, Hultqvist and colleagues have shown that elevating the low oxidative burst capacity led to suppressing an autoimmune response [76,77]. With gas plasma technology, we mimic the ROS production of an oxidative burst to modify tumor-associated antigens.

We propose to homogenize collected autologous tumor tissue, followed by gas plasma exposure of the tumor lysates in a defined and pre-optimized setting (Figure 2).

The lysates may be stored frozen in several aliquots until used in multiple vaccination rounds. Next, the multi-ROS oxidized homogenates can be thawed and combined with a pre-optimized adjuvant; a process that could be performed in a quality-controlled environment, such as pharmacies. In a series of elegant studies, the team of Lana Kandalaft employed HOCl-oxidized whole tumor lysates fed to autologous DCs, followed by the therapeutic vaccination of the latter, in a cohort of ovarian cancer patients [26]. Hundreds of vaccines generated in this way were well-tolerated without serious side effects. This study, which has been preceded by a decade of research [78–86], is the clinical proof-of-concept that oxidation of autologous tumor antigen potentiates antitumor immunity. Since, in our setting, optimized gas plasma exposure was even enhanced compared to the effect of HOCl, an additional benefit of multi-ROS modification might be feasible. So far, there have been three studies using gas plasma-inactivated tumor cells as a preventive/prophylactic

vaccine that significantly decreased the tumor growth of live tumor cells given 7–9 days after vaccination [87–89]. Elevated tumor-infiltrated T cells with memory phenotypes were shown in plasma-treated tumors, and in patients, the infiltrated immune cells correlated with a better outcome [90,91]. As mechanisms of action, ICD was also recently proposed to improve DC antitumor vaccinations [92,93]. Further motivating our approach, there have been promising results with oxidized mannan-MUC1 (Mucin 1, cell surface associated; CD227) vaccination, as concluded from a 15-year follow-up study showing significantly fewer recurrences [94].

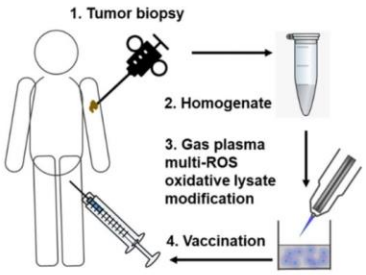

Figure 2. Simplified scheme of gas plasma technology-mediated multi-ROS-driven improvement of autologous tumor vaccines. After tumor biopsy and homogenization of the tumor material, oxidation with complex multi-ROS cocktails generated by medical gas plasma jet technology follows prior to vaccination.

It is understood that there are many degrees of freedom in this concept. The ideal ROS cocktail needs to be identified. The gas plasma technology exposure needs to be implemented in a quality-managed environment. Either the necessity of DCs or the ideal adjuvant needs to be established, along with questions on optimized absolute dosing, injection frequency, administration routes, and potential deterioration of the ROS-treated vaccine. There might also be interdependence between these parameters. For instance, it was recently reported that a sequential intravenous priming vaccination followed by a later intradermal boost vaccination showed the best effects in providing antitumor immunity in mice, while simultaneous administration significantly worsened the outcome [95]. Apart from these practical aspects, the scientific challenges lie in the mapping of the type and number of the oxidative antigen modifications, the identification of optimal ROS cocktails for maximizing immunogenicity, the elucidation of putative APC receptors needed to recognize oxidized antigen, and the clarification of the role of the proteasomal and antigen-presenting machinery activity to stimulate cognate antigen recognition optimally in the host. The T cell activation and differentiation are dependent on the binding affinity between epitope and MHC-molecules and between MHC-complex and T cell receptors [96,97]. Consequently, the presentation of oxidatively modified antigens can alter binding affinities [74], possibly resulting in an increase or even decrease in T cell activation. After all, even a presumably perfect antitumor vaccine cannot circumvent tumor microenvironments that are hostile or suppressive to T cells. Therefore, vaccination should be embedded in a treatment strategy that also addresses these challenges. Finally, augmenting antitumor immunity, especially when using whole tumor lysates containing mostly self-antigens, is always at the verge of promoting autoimmunity. However, at least in the trials performed by Kandalaft and colleagues, such adverse events were not observed [81].

7. Conclusions

Therapeutic autologous antitumor vaccination is an elegant way of providing personalized therapy in oncology. However, its efficacy and practicability are limited by different constraints, and new enhanced vaccine technologies are required. Due to the current

lack of validated biomarkers and neoantigens, upgrading a biopsy of the tumor is an intelligent, time-saving, and cost-effective way to enable personalized therapy. Oxidizing and modifying autologous tumor material with multiple reactive oxygen and nitrogen species simultaneously seems a promising avenue to increase both antigenicity (enhanced T cell receptor repertoire) and immunogenicity (increased co-stimulation and activation of adaptive antitumor immunity). Medical gas plasma jet technology is a recent innovation capable of providing multi-ROS cocktails in a unique and equivocal manner. Here, it is proposed to consider implementing this novel tool and to advocate its potential and limitations in providing efficient, fast, and affordable autologous antitumor vaccination, not just to those in privileged health care systems.

Author Contributions: Conceptualization, S.B. and R.C.; methodology, S.B. and R.C.; resources, S.B.; writing—original draft preparation, S.B. and R.C.; writing—review and editing, S.B. and R.C.; visualization, S.B. and R.C.; supervision, S.B.; project administration, S.B.; funding acquisition, S.B. All authors have read and agreed to the published version of the manuscript.

Funding: The work within the research group ZIK *plasmatis* "Plasma-Redox-Effects" is funded by the German Federal Ministry of Education and Research (BMBF, grant numbers 03Z22DN11, 03Z22Di1, 03Z22D511, 03COV06A, and 16GW0344K), the European Social Fund (ESF) conjoint with the Ministry of Education, Science, and Culture of Mecklenburg-Vorpommern, Germany (grant number ESF/14-BM-A55-0006-18), the German Research Foundation (DFG, grant number AOBJ 669606), the *Stiftung Tumorforschung Kopf-Hals*, the *Ferdinand-Eisenberger Stiftung* (grant number GeN1/FE-20), the *Gerhard-Domagk* Foundation Greifswald, and the *Comprehensive Cancer Center* Mecklenburg-Vorpommern (CCC-MV) seed funding initiative at the Greifswald University Medical Center in Greifswald, Germany. The funding sources had no role in the design of this study or its execution, analyses, interpretation of the data, or decision to publish the results.

Institutional Review Board Statement: Not applicable.

Data Availability Statement: Not applicable.

Conflicts of Interest: The authors declare no conflict of interest.

References

1. Baumann, M.; Krause, M.; Hill, R. Exploring the role of cancer stem cells in radioresistance. *Nat. Rev. Cancer* **2008**, *8*, 545–554. [CrossRef] [PubMed]
2. Zheng, H.C. The molecular mechanisms of chemoresistance in cancers. *Oncotarget* **2017**, *8*, 59950–59964. [CrossRef]
3. Ghetie, M.-A.; Ghetie, V.; Vitetta, E.S. Section Review Biologicals & Immunologicals: The use of immunoconjugates in cancer therapy. *Expert Opin. Investig. Drugs* **2008**, *5*, 309–321. [CrossRef]
4. Conlon, K.C.; Miljkovic, M.D.; Waldmann, T.A. Cytokines in the Treatment of Cancer. *J. Interferon Cytokine Res.* **2019**, *39*, 6–21. [CrossRef]
5. Lee, Y.T.; Tan, Y.J.; Oon, C.E. Molecular targeted therapy: Treating cancer with specificity. *Eur. J. Pharmacol.* **2018**, *834*, 188–196. [CrossRef]
6. Piessens, W.F. Evidence for human cancer immunity. A review. *Cancer* **1970**, *26*, 1212–1220. [CrossRef]
7. Finney, J.W.; Byers, E.H.; Wilson, R.H. Studies in Tumor Auto-Immunity. *Cancer Res.* **1960**, *20*, 351–356.
8. Azoury, S.C.; Straughan, D.M.; Shukla, V. Immune Checkpoint Inhibitors for Cancer Therapy: Clinical Efficacy and Safety. *Curr. Cancer Drug Targets* **2015**, *15*, 452–462. [CrossRef]
9. Chen, D.S.; Mellman, I. Oncology meets immunology: The cancer-immunity cycle. *Immunity* **2013**, *39*, 1–10. [CrossRef] [PubMed]
10. Hollingsworth, R.E.; Jansen, K. Turning the corner on therapeutic cancer vaccines. *NPJ Vaccines* **2019**, *4*, 7. [CrossRef]
11. Wang, T.; Wang, D.; Yu, H.; Feng, B.; Zhou, F.; Zhang, H.; Zhou, L.; Jiao, S.; Li, Y. A cancer vaccine-mediated postoperative immunotherapy for recurrent and metastatic tumors. *Nat. Commun.* **2018**, *9*, 1532. [CrossRef]
12. Kotsakis, A.; Vetsika, E.K.; Christou, S.; Hatzidaki, D.; Vardakis, N.; Aggouraki, D.; Konsolakis, G.; Georgoulias, V.; Christophyllakis, C.; Cordopatis, P.; et al. Clinical outcome of patients with various advanced cancer types vaccinated with an optimized cryptic human telomerase reverse transcriptase (TERT) peptide: Results of an expanded phase II study. *Ann. Oncol.* **2012**, *23*, 442–449. [CrossRef] [PubMed]
13. Goldinger, S.M.; Dummer, R.; Baumgaertner, P.; Mihic-Probst, D.; Schwarz, K.; Hammann-Haenni, A.; Willers, J.; Geldhof, C.; Prior, J.O.; Kundig, T.M.; et al. Nano-particle vaccination combined with TLR-7 and -9 ligands triggers memory and effector CD8(+) T-cell responses in melanoma patients. *Eur. J. Immunol.* **2012**, *42*, 3049–3061. [CrossRef]
14. Topfer, K.; Kempe, S.; Muller, N.; Schmitz, M.; Bachmann, M.; Cartellieri, M.; Schackert, G.; Temme, A. Tumor evasion from T cell surveillance. *J. Biomed. Biotechnol.* **2011**, *2011*, 918471. [CrossRef]

15. Poschke, I.; Mougiakakos, D.; Kiessling, R. Camouflage and sabotage: Tumor escape from the immune system. *Cancer Immunol. Immunother.* **2011**, *60*, 1161–1171. [CrossRef] [PubMed]
16. Balamurugan, K. HIF-1 at the crossroads of hypoxia, inflammation, and cancer. *Int. J. Cancer* **2016**, *138*, 1058–1066. [CrossRef] [PubMed]
17. Zhai, L.; Bell, A.; Ladomersky, E.; Lauing, K.L.; Bollu, L.; Sosman, J.A.; Zhang, B.; Wu, J.D.; Miller, S.D.; Meeks, J.J.; et al. Immunosuppressive IDO in Cancer: Mechanisms of Action, Animal Models, and Targeting Strategies. *Front. Immunol.* **2020**, *11*, 1185. [CrossRef] [PubMed]
18. Saleh, R.; Elkord, E. Acquired resistance to cancer immunotherapy: Role of tumor-mediated immunosuppression. *Semin. Cancer Biol.* **2020**, *65*, 13–27. [CrossRef] [PubMed]
19. Schumacher, T.N.; Schreiber, R.D. Neoantigens in cancer immunotherapy. *Science* **2015**, *348*, 69–74. [CrossRef]
20. Dalet, A.; Stroobant, V.; Vigneron, N.; Van den Eynde, B.J. Differences in the production of spliced antigenic peptides by the standard proteasome and the immunoproteasome. *Eur. J. Immunol.* **2011**, *41*, 39–46. [CrossRef]
21. Van den Eynde, B.T.J.; Morel, S. Differential processing of class-I-restricted epitopes by the standard proteasome and the immunoproteasome. *Curr. Opin. Immunol.* **2001**, *13*, 147–153. [CrossRef]
22. Neefjes, J.; Jongsma, M.L.; Paul, P.; Bakke, O. Towards a systems understanding of MHC class I and MHC class II antigen presentation. *Nat. Rev. Immunol.* **2011**, *11*, 823–836. [CrossRef]
23. Kloetzel, P.M. The proteasome and MHC class I antigen processing. *Biochim. Biophys. Acta* **2004**, *1695*, 225–233. [CrossRef] [PubMed]
24. Gu, Y.Z.; Zhao, X.; Song, X.R. Ex vivo pulsed dendritic cell vaccination against cancer. *Acta Pharmacol. Sin.* **2020**, *41*, 959–969. [CrossRef] [PubMed]
25. Nestle, F.O.; Farkas, A.; Conrad, C. Dendritic-cell-based therapeutic vaccination against cancer. *Curr. Opin. Immunol.* **2005**, *17*, 163–169. [CrossRef] [PubMed]
26. Tanyi, J.L.; Bobisse, S.; Ophir, E.; Tuyaerts, S.; Roberti, A.; Genolet, R.; Baumgartner, P.; Stevenson, B.J.; Iseli, C.; Dangaj, D.; et al. Personalized cancer vaccine effectively mobilizes antitumor T cell immunity in ovarian cancer. *Sci. Transl. Med.* **2018**, *10*. [CrossRef]
27. Cunningham, T.J.; Olson, K.B.; Laffin, R.; Horton, J.; Sullivan, J. Treatment of advanced cancer with active immunization. *Cancer* **1969**, *24*, 932–937. [CrossRef]
28. Nemunaitis, J.; Jahan, T.; Ross, H.; Sterman, D.; Richards, D.; Fox, B.; Jablons, D.; Aimi, J.; Lin, A.; Hege, K. Phase 1/2 trial of autologous tumor mixed with an allogeneic GVAX vaccine in advanced-stage non-small-cell lung cancer. *Cancer Gene Ther.* **2006**, *13*, 555–562. [CrossRef]
29. Saini, R.; Lee, N.V.; Liu, K.Y.; Poh, C.F. Prospects in the Application of Photodynamic Therapy in Oral Cancer and Premalignant Lesions. *Cancers* **2016**, *8*, 83. [CrossRef]
30. Schwaab, T.; Tretter, C.; Gibson, J.J.; Cole, B.F.; Schned, A.R.; Harris, R.; Wallen, E.M.; Fisher, J.L.; Waugh, M.G.; Truman, D.; et al. Immunological effects of granulocyte-macrophage colony-stimulating factor and autologous tumor vaccine in patients with renal cell carcinoma. *J. Urol.* **2004**, *171*, 1036–1042. [CrossRef]
31. Olin, M.R.; Pluhar, G.E.; Andersen, B.M.; Shaver, R.; Waldron, N.N.; Moertel, C.L. Victory and defeat in the induction of a therapeutic response through vaccine therapy for human and canine brain tumors: A review of the state of the art. *Crit. Rev. Immunol.* **2014**, *34*, 399–432. [CrossRef]
32. Li, L.; Ma, B.; Wang, W. Peptide-Based Nanomaterials for Tumor Immunotherapy. *Molecules* **2020**, *26*, 132. [CrossRef]
33. Hanschmann, E.M.; Godoy, J.R.; Berndt, C.; Hudemann, C.; Lillig, C.H. Thioredoxins, glutaredoxins, and peroxiredoxins—Molecular mechanisms and health significance: From cofactors to antioxidants to redox signaling. *Antioxid. Redox Signal.* **2013**, *19*, 1539–1605. [CrossRef] [PubMed]
34. Winterbourn, C.C.; Kettle, A.J. Redox reactions and microbial killing in the neutrophil phagosome. *Antioxid. Redox Signal.* **2013**, *18*, 642–660. [CrossRef] [PubMed]
35. Franchina, D.G.; Dostert, C.; Brenner, D. Reactive Oxygen Species: Involvement in T Cell Signaling and Metabolism. *Trends Immunol.* **2018**, *39*, 489–502. [CrossRef]
36. Mak, T.W.; Grusdat, M.; Duncan, G.S.; Dostert, C.; Nonnenmacher, Y.; Cox, M.; Binsfeld, C.; Hao, Z.; Brustle, A.; Itsumi, M.; et al. Glutathione Primes T Cell Metabolism for Inflammation. *Immunity* **2017**, *46*, 675–689. [CrossRef]
37. Rashida Gnanaprakasam, J.N.; Wu, R.; Wang, R. Metabolic Reprogramming in Modulating T Cell Reactive Oxygen Species Generation and Antioxidant Capacity. *Front. Immunol.* **2018**, *9*, 1075. [CrossRef] [PubMed]
38. Van den Bossche, J.; Baardman, J.; Otto, N.A.; van der Velden, S.; Neele, A.E.; van den Berg, S.M.; Luque-Martin, R.; Chen, H.J.; Boshuizen, M.C.; Ahmed, M.; et al. Mitochondrial Dysfunction Prevents Repolarization of Inflammatory Macrophages. *Cell Rep.* **2016**, *17*, 684–696. [CrossRef]
39. Niethammer, P.; Grabher, C.; Look, A.T.; Mitchison, T.J. A tissue-scale gradient of hydrogen peroxide mediates rapid wound detection in zebrafish. *Nature* **2009**, *459*, 996–999. [CrossRef]
40. Eming, S.A.; Wynn, T.A.; Martin, P. Inflammation and metabolism in tissue repair and regeneration. *Science* **2017**, *356*, 1026–1030. [CrossRef]

41. Stanley, C.P.; Maghzal, G.J.; Ayer, A.; Talib, J.; Giltrap, A.M.; Shengule, S.; Wolhuter, K.; Wang, Y.; Chadha, P.; Suarna, C.; et al. Singlet molecular oxygen regulates vascular tone and blood pressure in inflammation. *Nature* **2019**, *566*, 548–552. [CrossRef] [PubMed]
42. Winterbourn, C.C. Toxicity of iron and hydrogen peroxide: The Fenton reaction. *Toxicol. Lett.* **1995**, *82–83*, 969–974. [CrossRef]
43. Di Dalmazi, G.; Hirshberg, J.; Lyle, D.; Freij, J.B.; Caturegli, P. Reactive oxygen species in organ-specific autoimmunity. *Auto Immun Highlights* **2016**, *7*, 11. [CrossRef] [PubMed]
44. Griffiths, H.R. Is the generation of neo-antigenic determinants by free radicals central to the development of autoimmune rheumatoid disease? *Autoimmun. Rev.* **2008**, *7*, 544–549. [CrossRef]
45. Arif, Z.; Neelofar, K.; Tarannum, A.; Arfat, M.Y.; Ahmad, S.; Zaman, A.; Khan, M.A.; Badar, A.; Islam, S.N.; Iqubal, M.A. SLE autoantibodies are well recognized by peroxynitrite-modified-HSA: Its implications in the pathogenesis of SLE. *Int. J. Biol. Macromol.* **2018**, *106*, 1240–1249. [CrossRef] [PubMed]
46. Kurien, B.T.; Scofield, R.H. Autoimmunity and oxidatively modified autoantigens. *Autoimmun. Rev.* **2008**, *7*, 567–573. [CrossRef] [PubMed]
47. Nybo, T.; Dieterich, S.; Gamon, L.F.; Chuang, C.Y.; Hammer, A.; Hoefler, G.; Malle, E.; Rogowska-Wrzesinska, A.; Davies, M.J. Chlorination and oxidation of the extracellular matrix protein laminin and basement membrane extracts by hypochlorous acid and myeloperoxidase. *Redox Biol.* **2019**, *20*, 496–513. [CrossRef]
48. Strollo, R.; Vinci, C.; Arshad, M.H.; Perrett, D.; Tiberti, C.; Chiarelli, F.; Napoli, N.; Pozzilli, P.; Nissim, A. Antibodies to post-translationally modified insulin in type 1 diabetes. *Diabetologia* **2015**, *58*, 2851–2860. [CrossRef]
49. Mannering, S.I.; Di Carluccio, A.R.; Elso, C.M. Neoepitopes: A new take on beta cell autoimmunity in type 1 diabetes. *Diabetologia* **2019**, *62*, 351–356. [CrossRef]
50. Yang, M.L.; Doyle, H.A.; Clarke, S.G.; Herold, K.C.; Mamula, M.J. Oxidative Modifications in Tissue Pathology and Autoimmune Disease. *Antioxid. Redox Signal.* **2018**, *29*, 1415–1431. [CrossRef]
51. Carta, S.; Castellani, P.; Delfino, L.; Tassi, S.; Vene, R.; Rubartelli, A. DAMPs and inflammatory processes: The role of redox in the different outcomes. *J. Leukoc. Biol.* **2009**, *86*, 549–555. [CrossRef]
52. Winter, J.; Brandenburg, R.; Weltmann, K.D. Atmospheric pressure plasma jets: An overview of devices and new directions. *Plasma Sources Sci. Technol.* **2015**, *24*, 064001. [CrossRef]
53. Privat-Maldonado, A.; Schmidt, A.; Lin, A.; Weltmann, K.D.; Wende, K.; Bogaerts, A.; Bekeschus, S. ROS from Physical Plasmas: Redox Chemistry for Biomedical Therapy. *Oxid. Med. Cell. Longev.* **2019**, *2019*, 9062098. [CrossRef]
54. Graves, D.B. Mechanisms of Plasma Medicine: Coupling Plasma Physics, Biochemistry, and Biology. *IEEE Trans. Radiat. Plasma Med. Sci.* **2017**, *1*, 281–292. [CrossRef]
55. Von Woedtke, T.; Schmidt, A.; Bekeschus, S.; Wende, K.; Weltmann, K.D. Plasma Medicine: A Field of Applied Redox Biology. *In Vivo* **2019**, *33*, 1011–1026. [CrossRef]
56. Wende, K.; von Woedtke, T.; Weltmann, K.D.; Bekeschus, S. Chemistry and biochemistry of cold physical plasma derived reactive species in liquids. *Biol. Chem.* **2018**, *400*, 19–38. [CrossRef]
57. Schmidt-Bleker, A.; Winter, J.; Iseni, S.; Dunnbier, M.; Weltmann, K.D.; Reuter, S. Reactive species output of a plasma jet with a shielding gas device-combination of FTIR absorption spectroscopy and gas phase modelling. *J. Phys. D Appl. Phys.* **2014**, *47*, 145201. [CrossRef]
58. Jablonowski, H.; Santos Sousa, J.; Weltmann, K.D.; Wende, K.; Reuter, S. Quantification of the ozone and singlet delta oxygen produced in gas and liquid phases by a non-thermal atmospheric plasma with relevance for medical treatment. *Sci. Rep.* **2018**, *8*, 12195. [CrossRef]
59. Jablonowski, H.; Schmidt-Bleker, A.; Weltmann, K.D.; von Woedtke, T.; Wende, K. Non-touching plasma-liquid interaction—Where is aqueous nitric oxide generated? *Phys. Chem. Chem. Phys.* **2018**, *20*, 25387–25398. [CrossRef]
60. Lackmann, J.W.; Wende, K.; Verlackt, C.; Golda, J.; Volzke, J.; Kogelheide, F.; Held, J.; Bekeschus, S.; Bogaerts, A.; Schulz-von der Gathen, V.; et al. Chemical fingerprints of cold physical plasmas—An experimental and computational study using cysteine as tracer compound. *Sci. Rep.* **2018**, *8*, 7736. [CrossRef]
61. Wenske, S.; Lackmann, J.-W.; Bekeschus, S.; Weltmann, K.-D.; von Woedtke, T.; Wende, K. Nonenzymatic post-translational modifications in peptides by cold plasma-derived reactive oxygen and nitrogen species. *Biointerphases* **2020**, *15*. [CrossRef] [PubMed]
62. Yusupov, M.; Lackmann, J.-W.; Razzokov, J.; Kumar, S.; Stapelmann, K.; Bogaerts, A. Impact of plasma oxidation on structural features of human epidermal growth factor. *Plasma Process. Polym.* **2018**, *15*. [CrossRef]
63. Zhang, H.; Ma, J.; Shen, J.; Lan, Y.; Ding, L.; Qian, S.; Cheng, C.; Xia, W.; Chu, P.K. Comparison of the Effects Induced by Plasma Generated Reactive Species and H2O2 on Lactate Dehydrogenase (LDH) Enzyme. *IEEE Trans. Plasma Sci.* **2018**, *46*, 2742–2752. [CrossRef]
64. Krewing, M.; Stepanek, J.J.; Cremers, C.; Lackmann, J.W.; Schubert, B.; Muller, A.; Awakowicz, P.; Leichert, L.I.O.; Jakob, U.; Bandow, J.E. The molecular chaperone Hsp33 is activated by atmospheric-pressure plasma protecting proteins from aggregation. *J. R. Soc. Interface* **2019**, *16*, 20180966. [CrossRef]
65. Krewing, M.; Jung, C.T.K.; Dobbelstein, E.; Schubert, B.; Jacob, T.; Bandow, J.E. Dielectric barrier discharge plasma treatment affects stability, metal ion coordination, and enzyme activity of bacterial superoxide dismutases. *Plasma Process. Polym.* **2020**, *17*. [CrossRef]

66. Clemen, R.; Freund, E.; Mrochen, D.; Miebach, L.; Schmidt, A.; Rauch, B.H.; Lackmann, J.W.; Martens, U.; Wende, K.; Lalk, M.; et al. Gas Plasma Technology Augments Ovalbumin Immunogenicity and OT-II T Cell Activation Conferring Tumor Protection in Mice. *Adv. Sci.* **2021**. [CrossRef]
67. Zhou, J.; Wang, G.; Chen, Y.; Wang, H.; Hua, Y.; Cai, Z. Immunogenic cell death in cancer therapy: Present and emerging inducers. *J. Cell. Mol. Med.* **2019**, *23*, 4854–4865. [CrossRef]
68. Galluzzi, L.; Buque, A.; Kepp, O.; Zitvogel, L.; Kroemer, G. Immunogenic cell death in cancer and infectious disease. *Nat. Rev. Immunol.* **2017**, *17*, 97–111. [CrossRef]
69. Khalili, M.; Daniels, L.; Lin, A.; Krebs, F.C.; Snook, A.E.; Bekeschus, S.; Bowne, W.B.; Miller, V. Non-Thermal Plasma-Induced Immunogenic Cell Death in Cancer: A Topical Review. *J. Phys. D Appl. Phys.* **2019**, *52*. [CrossRef]
70. De Backer, J.; Razzokov, J.; Hammerschmid, D.; Mensch, C.; Hafideddine, Z.; Kumar, N.; van Raemdonck, G.; Yusupov, M.; Van Doorslaer, S.; Johannessen, C.; et al. The effect of reactive oxygen and nitrogen species on the structure of cytoglobin: A potential tumor suppressor. *Redox Biol.* **2018**, *19*, 1–10. [CrossRef]
71. Bekeschus, S.; Ressel, V.; Freund, E.; Gelbrich, N.; Mustea, A.; Stope, M.B. Gas Plasma-Treated Prostate Cancer Cells Augment Myeloid Cell Activity and Cytotoxicity. *Antioxidants* **2020**, *9*, 323. [CrossRef]
72. Poulsen, T.B.G.; Damgaard, D.; Jorgensen, M.M.; Senolt, L.; Blackburn, J.M.; Nielsen, C.H.; Stensballe, A. Identification of Novel Native Autoantigens in Rheumatoid Arthritis. *Biomedicines* **2020**, *8*, 141. [CrossRef] [PubMed]
73. Liang, B.; Ge, C.; Lonnblom, E.; Lin, X.; Feng, H.; Xiao, L.; Bai, J.; Ayoglu, B.; Nilsson, P.; Nandakumar, K.S.; et al. The autoantibody response to cyclic citrullinated collagen type II peptides in rheumatoid arthritis. *Rheumatology* **2019**, *58*, 1623–1633. [CrossRef]
74. Sidney, J.; Vela, J.L.; Friedrich, D.; Kolla, R.; von Herrath, M.; Wesley, J.D.; Sette, A. Low HLA binding of diabetes-associated CD8+ T-cell epitopes is increased by post translational modifications. *BMC Immunol.* **2018**, *19*, 12. [CrossRef] [PubMed]
75. Wan, X.; Vomund, A.N.; Peterson, O.J.; Chervonsky, A.V.; Lichti, C.F.; Unanue, E.R. The MHC-II peptidome of pancreatic islets identifies key features of autoimmune peptides. *Nat. Immunol.* **2020**, *21*, 455–463. [CrossRef] [PubMed]
76. Hultqvist, M.; Olofsson, P.; Gelderman, K.A.; Holmberg, J.; Holmdahl, R. A new arthritis therapy with oxidative burst inducers. *PLoS Med.* **2006**, *3*, e348. [CrossRef]
77. Hultqvist, M.; Backlund, J.; Bauer, K.; Gelderman, K.A.; Holmdahl, R. Lack of reactive oxygen species breaks T cell tolerance to collagen type II and allows development of arthritis in mice. *J. Immunol.* **2007**, *179*, 1431–1437. [CrossRef]
78. Chiang, C.L.; Coukos, G.; Kandalaft, L.E. Whole Tumor Antigen Vaccines: Where Are We? *Vaccines* **2015**, *3*, 344–372. [CrossRef]
79. Chiang, C.L.; Hagemann, A.R.; Leskowitz, R.; Mick, R.; Garrabrant, T.; Czerniecki, B.J.; Kandalaft, L.E.; Powell, D.J., Jr.; Coukos, G. Day-4 myeloid dendritic cells pulsed with whole tumor lysate are highly immunogenic and elicit potent anti-tumor responses. *PLoS ONE* **2011**, *6*, e28732. [CrossRef]
80. Chiang, C.L.; Kandalaft, L.E.; Tanyi, J.; Hagemann, A.R.; Motz, G.T.; Svoronos, N.; Montone, K.; Mantia-Smaldone, G.M.; Smith, L.; Nisenbaum, H.L.; et al. A dendritic cell vaccine pulsed with autologous hypochlorous acid-oxidized ovarian cancer lysate primes effective broad antitumor immunity: From bench to bedside. *Clin. Cancer Res.* **2013**, *19*, 4801–4815. [CrossRef]
81. Kandalaft, L.E.; Chiang, C.L.; Tanyi, J.; Motz, G.; Balint, K.; Mick, R.; Coukos, G. A Phase I vaccine trial using dendritic cells pulsed with autologous oxidized lysate for recurrent ovarian cancer. *J. Transl. Med.* **2013**, *11*, 149. [CrossRef]
82. Martin Lluesma, S.; Wolfer, A.; Harari, A.; Kandalaft, L.E. Cancer Vaccines in Ovarian Cancer: How Can We Improve? *Biomedicines* **2016**, *4*, 10. [CrossRef] [PubMed]
83. Mookerjee, A.; Graciotti, M.; Kandalaft, L.E.; Kandalaft, L. A cancer vaccine with dendritic cells differentiated with GM-CSF and IFNalpha and pulsed with a squaric acid treated cell lysate improves T cell priming and tumor growth control in a mouse model. *Bioimpacts* **2018**, *8*, 211–221. [CrossRef]
84. Ophir, E.; Bobisse, S.; Coukos, G.; Harari, A.; Kandalaft, L.E. Personalized approaches to active immunotherapy in cancer. *Biochim. Biophys. Acta* **2016**, *1865*, 72–82. [CrossRef] [PubMed]
85. Kandalaft, L.E.; Powell, D.J., Jr.; Singh, N.; Coukos, G. Immunotherapy for ovarian cancer: What's next? *J. Clin. Oncol.* **2011**, *29*, 925–933. [CrossRef] [PubMed]
86. Kandalaft, L.E.; Singh, N.; Liao, J.B.; Facciabene, A.; Berek, J.S.; Powell, D.J., Jr.; Coukos, G. The emergence of immunomodulation: Combinatorial immunochemotherapy opportunities for the next decade. *Gynecol. Oncol.* **2010**, *116*, 222–233. [CrossRef]
87. Lin, A.G.; Xiang, B.; Merlino, D.J.; Baybutt, T.R.; Sahu, J.; Fridman, A.; Snook, A.E.; Miller, V. Non-thermal plasma induces immunogenic cell death in vivo in murine CT26 colorectal tumors. *Oncoimmunology* **2018**, *7*, e1484978. [CrossRef]
88. Bekeschus, S.; Clemen, R.; Niessner, F.; Sagwal, S.K.; Freund, E.; Schmidt, A. Medical Gas Plasma Jet Technology Targets Murine Melanoma in an Immunogenic Fashion. *Adv. Sci.* **2020**, *7*, 1903438. [CrossRef]
89. Lin, A.; Gorbanev, Y.; De Backer, J.; Van Loenhout, J.; Van Boxem, W.; Lemiere, F.; Cos, P.; Dewilde, S.; Smits, E.; Bogaerts, A. Non-Thermal Plasma as a Unique Delivery System of Short-Lived Reactive Oxygen and Nitrogen Species for Immunogenic Cell Death in Melanoma Cells. *Adv. Sci.* **2019**, *6*, 1802062. [CrossRef]
90. Enomoto, K.; Sho, M.; Wakatsuki, K.; Takayama, T.; Matsumoto, S.; Nakamura, S.; Akahori, T.; Tanaka, T.; Migita, K.; Ito, M.; et al. Prognostic importance of tumour-infiltrating memory T cells in oesophageal squamous cell carcinoma. *Clin. Exp. Immunol.* **2012**, *168*, 186–191. [CrossRef]
91. Koelzer, V.H.; Lugli, A.; Dawson, H.; Hadrich, M.; Berger, M.D.; Borner, M.; Mallaev, M.; Galvan, J.A.; Amsler, J.; Schnuriger, B.; et al. CD8/CD45RO T-cell infiltration in endoscopic biopsies of colorectal cancer predicts nodal metastasis and survival. *J. Transl. Med.* **2014**, *12*, 81. [CrossRef]

92. Lamberti, M.J.; Nigro, A.; Mentucci, F.M.; Rumie Vittar, N.B.; Casolaro, V.; Dal Col, J. Dendritic Cells and Immunogenic Cancer Cell Death: A Combination for Improving Antitumor Immunity. *Pharmaceutics* **2020**, *12*, 256. [CrossRef] [PubMed]
93. Garg, A.D.; Vandenberk, L.; Koks, C.; Verschuere, T.; Boon, L.; Van Gool, S.W.; Agostinis, P. Dendritic cell vaccines based on immunogenic cell death elicit danger signals and T cell-driven rejection of high-grade glioma. *Sci. Transl. Med.* **2016**, *8*, 328ra27. [CrossRef] [PubMed]
94. Vassilaros, S.; Tsibanis, A.; Tsikkinis, A.; Pietersz, G.A.; McKenzie, I.F.; Apostolopoulos, V. Up to 15-year clinical follow-up of a pilot Phase III immunotherapy study in stage II breast cancer patients using oxidized mannan-MUC1. *Immunotherapy* **2013**, *5*, 1177–1182. [CrossRef]
95. Zhang, L.-X.; Sun, X.-M.; Jia, Y.-B.; Liu, X.-G.; Dong, M.; Xu, Z.P.; Liu, R.-T. Nanovaccine's rapid induction of anti-tumor immunity significantly improves malignant cancer immunotherapy. *Nano Today* **2020**, *35*. [CrossRef]
96. Stone, J.D.; Chervin, A.S.; Kranz, D.M. T-cell receptor binding affinities and kinetics: Impact on T-cell activity and specificity. *Immunology* **2009**, *126*, 165–176. [CrossRef]
97. Baumgartner, C.K.; Yagita, H.; Malherbe, L.P. A TCR affinity threshold regulates memory CD4 T cell differentiation following vaccination. *J. Immunol.* **2012**, *189*, 2309–2317. [CrossRef]

7. Eigenständigkeitserklärung

Hiermit erkläre ich, dass diese Arbeit bisher von mir weder an der Mathematisch-Naturwissenschaftlichen Fakultät der Universität Greifswald noch einer anderen wissenschaftlichen Einrichtung zum Zwecke der Promotion eingereicht wurde.
Ferner erkläre ich, dass ich diese Arbeit selbstständig verfasst und keine anderen als die darin angegebenen Hilfsmittel und Hilfen benutzt und keine Textabschnitte eines Dritten ohne Kennzeichnung übernommen habe.

Ramona Clemen

8. Publikationsliste

Alle bisher veröffentlichten Publikationen in *peer-reviewed* Journalen als Erst-, Zweit-, oder Mitautorin sind nachfolgend aufgeführt:

1. Bekeschus, S.; Emmert, S.; **Clemen, R.**; Boeckmann, L. Therapeutic ROS and Immunity in Cancer – the TRIC-21 Meeting, Cancers 2021, 13 (18), 4549, doi:10.3390/cancers13184549

2. Nasri, Z.; Memari, S.; Wenske, S.; **Clemen, R**.; Martens, U.; Delcea, M.; Bekeschus, S.; Weltmann, K.D.; von Woedtke, T.; Wende, K. Singlet Oxygen-Induced Phospholipase A2 Inhibition: a Major Role for Interfacial Tryptophan Dioxidation. Chemistry 2021, doi:10.1002/chem.202102306.

2. **Clemen, R.**; Bekeschus, S. ROS Cocktails as an Adjuvant for Personalized Antitumor Vaccination? Vaccines 2021, 9, doi:10.3390/vaccines9050527.

3. **Clemen, R.**; Freund, E.; Mrochen, D.; Miebach, L.; Schmidt, A.; Rauch, B.H.; Lackmann, J.W.; Martens, U.; Wende, K.; Lalk, Delcea, M.; M., Bröker, B.; Bekeschus, S. Gas Plasma Technology Augments Ovalbumin Immunogenicity and OT-II T Cell Activation Conferring Tumor Protection in Mice. Adv Sci (Weinh) 2021, 8, 2003395, doi:10.1002/advs.202003395.

4. Bekeschus, S.; Meyer, D.; Arlt, K.; von Woedtke, T.; Miebach, L.; Freund, E.; **Clemen, R.** Argon Plasma Exposure Augments Costimulatory Ligands and Cytokine Release in Human Monocyte-Derived Dendritic Cells. International journal of molecular sciences 2021, 22, 3790.

5. Mohamed, H.; **Clemen, R.**; Freund, E.; Lackmann, J.W.; Wende, K.; Connors, J.; Haddad, E.K.; Dampier, W.; Wigdahl, B.; Miller, V., Bekeschus, S.; Krebs, F. Non-thermal plasma modulates cellular markers associated with immunogenicity in a model of latent HIV-1 infection. PLoS One 2021, 16, e0247125, doi:10.1371/journal.pone.0247125.

6. Bekeschus, S.; **Clemen, R.**; Haralambiev, L.; Niessner, F.; Grabarczyk, P.; Weltmann, K.-D.; Menz, J.; Stope, M.; von Woedtke, T.; Gandhirajan, R., Schidt, A. The Plasma-Induced Leukemia Cell Death is Dictated by the ROS Chemistry and the HO-1/CXCL8 Axis. IEEE Transactions on Radiation and Plasma Medical Sciences 2021, 5, 398-411, doi:10.1109/trpms.2020.3020686.

7. Freund, E.; Miebach, L.; **Clemen, R.**; Schmidt, S.; Heidecke, A.; von Woedtke, T.; Weltmann, K.; Kersting, S.; Bekeschus, S. Large volume spark discharge and plasma jet-technology for generating plasma-oxidized saline targeting colon cancer in vitro and in vivo. Journal of Physics D - Applied Physics 2021, 129, doi:10.1063/5.0033406.

8. Miebach, L.; Freund, E.; Horn, S.; Niessner, F.; Sagwal, S.K.; von Woedtke, T.; Emmert, S.; Weltmann, K.D.; **Clemen, R.**; Schmidt, A.; Gerling, T.; Bekeschus, S. A. Tumor cytotoxicity and immunogenicity of a novel V-jet neon plasma source compared to the kINPen. Sci Rep 2021, 11, 136, doi:10.1038/s41598-020-80512-w.

9. **Clemen, R.**; Bekeschus, S. Oxidatively Modified Proteins: Cause and Control of Diseases. Applied Sciences 2020, 10, 6419, doi:10.3390/app10186419.

10. Bekeschus, S.; **Clemen, R.**; Niessner, F.; Sagwal, S.K.; Freund, E.; Schmidt, A. Medical Gas Plasma Jet Technology Targets Murine Melanoma in an Immunogenic Fashion. Adv Sci (Weinh) 2020, 7, 1903438, doi:10.1002/advs.201903438.

11. Bekeschus, S.; **Clemen, R.**; Metelmann, H.-R. Potentiating anti-tumor immunity with physical plasma. Clinical Plasma Medicine 2018, 12, 17-22, doi:10.1016/j.cpme.2018.10.001.

12. Engelowski, E.; Schneider, A.; Franke, M.; Xu, H.; **Clemen, R.**; Lang, A.; Baran, P.; Binsch, C.; Knebel, B.; Al-Hasani, H.; Moll, J.; Floß, D.; Lang, P.; Scheller, J. et al. Synthetic cytokine receptors transmit biological signals using artificial ligands. Nat Commun 2018, 9, 2034, doi:10.1038/s41467-018-04454-8.

9. Beiträge an Seminaren und Konferenzen

Vorträge

1. Ramona Clemen, Sander Bekeschus “Tumor Immunology in Plasma Cancer Treatment”. Statusseminar ZIK, Greifswald, November 2021

2. Ramona Clemen, Sander Bekeschus, „Kaltplasma erhöht die Immunogenität von Tumorspezifischen Antigenen und verstärkt eine Anti Tumor Immunantwort“. Anwenderkreis Atmosphärendruckplasma (ak-adp), Magdeburg, September 2021

3. Ramona Clemen, Sander Bekeschus „Gas plasma-medicated oxidative modifications in immunobiology and cancer treatment”. Therapeutic ROS and Immunity in Cancer (TRIC), Greifswald/Hybrid, Juli 2021

4. Ramona Clemen, Sander Bekeschus „Immunogenicity of oxidatively modified antigens”. Arbeitskreistreffen dendritische Zellen (AKDC) Deutsche Gesellschaft für Immunologie (DGfI), Online, Februar 2021

5. Ramona Clemen, Eric Freund, Anke Schmidt, Sander Bekeschus „Therapeutic ROS provide immunoprotection against malignant melanoma”. 22nd International Conference on Oxidative Stress Reduction Redox Homeostasis and Antioxidants, Online, Oktober 2020

6. Ramona Clemen, Sander Bekeschus “Plasmas as modifiers of immunogenicity”. Statusseminar ZIK, Greifswald 2019

7. Ramona Clemen, Jan-Wilm Lackmann, Kristian Wende, Sander Bekeschus „Immunogenicity of modified proteins”. Frontiers in Redox Biology and Medicine (FiRBaM) Workshop, Rostock, September 2018

8. Ramona Clemen, Jens Moll, Jürgen Scheller „Bildung von großen Proteinkomplexen durch Kombination fluoreszierender Proteine mit Nanobodies". Frontiers in Redox Biology and Chemistry (FiRBaC) Workshop, Rostock, Oktober 2017

Poster

1. Ramona Clemen, Lea Miebach, Daniel Mrochen, Eric Freund, Sander Bekeschus „Plasma treatment of Ovalbumin increases its immunogenicity". 6th International Workshop on Plasma for Cancer Therapie (IWPCT), Online, June 2021

2. Ramona Clemen, Eric Freund, Lea Miebach, Barbara M. Bröker, Sander Bekeschus „Oxidation of tumor associated antigen augments antigen-specific T cell activation providing tumor protection". Europe's Cancer Immunotherapy Meeting (CIMT), Online, May 2021

3. Ramona Clemen, Jan-Wilm Lackmann, Kristian Wende, Sander Bekeschus „Enhanced immunogenicity of modified antigens". 15th international symposium on Tumor Immunology meets Oncology (TIMO), Halle (Saale), April 2019

4. Ramona Clemen, Eric Freund, Sanjeev K. Sagwal, Sander Bekeschus „ROS-therapy increases the immunogenicity of B16F10 melanoma cells *in vitro* and *in vivo*". 6th International Workshop on Plasma for Cancer Therapie (IWPCT), Antwerpen, März 2019 **(Erhalt des "Best student poster" Preis)**

5. Ramona Clemen, Jan-Wilm Lackmann, Kristian Wende, Thomas von Woedtke, Sander Bekeschus „Vaccination approaches in plasma medicine". 7th international conference on plasma medicine (icpm), Philadelphia, June 2018 **(Erhalt des "Best student poster" Preis)**

6. Ramona Clemen, Barbara M. Bröker, Sander Bekeschus. „The MHC I peptidome of oxidatively challenged murine melanoma cells”. Akademie für Immunologie – Autumn School, Merseburg, Oktober 2018

7. Ramona Clemen, Thomas von Woedtke, Sander Bekeschus. „Regulation of antigen-presenting machinery in melanoma after plasma treatment”. 5th International Workshop on Plasma for Cancer Therapie (IWPCT), Greifswald, März 2018